JAERI 1311

JAERI 1311
NEANDC (J)-124/U
INDC (JPN)-110/L

Gamma-Ray Spectrum Data Library of Fission Product Nuclides and Its Assessment

March 1988

日 本 原 子 力 研 究 所
Japan Atomic Energy Research Institute

JAERIレポートは，日本原子力研究所が研究成果編集委員会の審査を経て不定期に公刊している研究報告書です。

入手の問合わせは，日本原子力研究所技術情報部情報資料課（〒319-11茨城県那珂郡東海村）あて，お申しこしください。なお，このほかに財団法人原子力弘済会資料センター（〒319-11 茨城県那珂郡東海村日本原子力研究所内）で複写による実費頒布をおこなっております。

JAERI reports are reviewed by the Board of Editors and issued irregularly.

Inquiries about availability of the reports should be addressed to Information Division Department of Technical Information, Japan Atomic Energy Research Institute, Tokai-mura, Naka-gun, Ibaraki-ken 319-11, Japan.

編集兼発行　日本原子力研究所
印　　刷　いばらき印刷㈱

Gamma-Ray Spectrum Data Library of Fission Product Nuclides and Its Assessment

Jun-ichi Katakura+ and Tadashi Yoshida*

Japanese Nuclear Data Committee
Tokai Research Establishment
Japan Atomic Energy Research Institute
Tokai-mura, Naka-gun, Ibaraki-ken

Received July 28, 1987

Abstract

A gamma-ray spectrum data library of fission product nuclides was prepared on the same basis as the JNDC library which is used for the decay heat prediction. The gamma-ray spectrum data were compiled with both measured and theoretically estimated spectra. For nuclides with no or insufficient gamma-ray transition data, the estimated spectra were applied to compensate the defect of the measured data. By introducing the estimated spectra, it becomes possible to calculate the gamma-ray spectra which are consistent with integral decay heat predictions by the JNDC library. By using the spectrum data library, calculations of gamma-ray spectra from aggregate fission product nuclides were carried out. The calculated spectra were compared with the measured ones performed at Oak Ridge National Laboratory and at the University of Tokyo. The spectrum calculations showed reasonable agreement with the measured data for a wide range of cooling time.

Keywords: Fission Product, Gamma-Ray Spectrum, Estimated Spectrum, Decay Heat

---

This work was performed in the eveluation work of the Working Group on Evaluation of Decay Heat, Japanese Nuclear Data Committee.

+ Department of Fuel Safety Research.

* NAIG Nuclear Research Laboratory, Nippon Atomic Industry Group Co., Ltd.

核分裂生成核種のガンマ線スペクトル・データ・ライブラリーとその評価

日本原子力研究所東海研究所シグマ研究委員会

片倉　純一[+]・吉田　　正[*]

（1987年7月28日受理）

要　　旨

核分裂生成核種のガンマ線スペクトル・データ・ライブラリーを崩壊熱予測用のJNDCファイルと同一の考えで作成した．ガンマ線スペクトル・データは測定されたものと理論的に推定したものとで編集した．ガンマ遷移のデータが測定されてない，あるいは不充分な核種に対しては，測定データの不足を補うために推定したスペクトルを適用した．この推定スペクトルを導入することにより，JNDCライブラリーで予測される積分値としての崩壊熱と矛盾しないガンマ線スペクトルを計算することが可能となった．このスペクトル・データ・ライブラリーを用いることにより，核分裂生成核種が集った時のガンマ線スペクトルの計算を実施した．計算されたスペクトルをオークリッジ研究所と東大で実施された測定スペクトルと比較した．スペクトルの計算は測定データと広い範囲の冷却時間において満足すべき一致を示した．

本報告はシグマ委員会崩壊熱ワーキング・グループにおける成果をまとめたものである．

＋燃料安全工学部

＊日本原子力事業（株）NAIG総合研究所

Contents

目　　次

1. Introduction

Nuclear data of fission product nuclides are essential to nuclear safety assessment and are indispensable for calculations of fission product build-up and depletion and of nuclear radiation source in nuclear reactors and/or fuel processing plants. In the nuclear safety assessment, the decay heat of fission product nuclides is of great important.

Decay Heat Working Group of Japanese Nuclear Data Committee (JNDC) has been continuing the evaluation work of nuclear data in order to provide a reliable nuclear data library for decay heat prediction by summation method. In the nuclear data needed for the decay heat prediction, the decay data (half life, average decay energies of beta and gamma rays, branching ratio, etc.) are essential, because the calculation of the decay heat is performed by summing up the decay energies of radioactive nuclides released in the decay process.

The working group compiled a decay data library of fission product nuclides (JNDC FP Decay Data File)[1] as the first task. The decay data adopted in this library are based on a detailed examination of experimental decay data. If the experimental decay data are not available or are deficient, theoretically estimated decay data[2),3)] by using gross theory[4)] of beta decay are adopted in the library.

In addition to the decay data, cross sections and fission yields data are needed for the decay heat prediction. The working group has released a nuclear data library including the decay data of JNDC FP Decay Data File, cross sections and fission yields of 1172 fission product nuclides as JNDC Nuclear Data Library of Fission Products (JNDC library)[5]. The decay heat calculations by using this library have shown good agreement with the measured data of important fissile nuclides from ^{235}U to ^{241}Pu.[5)]

However, it was found from the detailed comparison between the measured results and the calculated ones that there remained some problems in the decay data.[6)] In order to resolve the problems, the examination of the decay data, especially of the average decay energies, was performed and the decay data of some nuclides were revised. The library containing the revised decay data is nominary called as JNDC library 1.5. From these examination, the decay heat prediction has been improved.[6)]

These libraries, however, do not contain the spectrum data, because the primary interest of the working group is to predict an integral decay heat of fission product nuclides and not to provide spectrum data. The spectrum data, especially gamma-ray spectrum data, however, are needed not only for application field such as radiation shielding, but also for verification and improvement of the quality of the decay data. For example, the ENDF/B–IV data file[7)] contains the gamma-ray spectrum data together with the decay data, fission yields and cross sections of fission product nuclides.

However, the nuclides with short half life do not have experimental spectrum data because of the difficulty of the measurement. In the case of ENDF/B–IV, the contained spectrum data are for only about 200 nuclides in the over 800 fission product nuclides which have decay data. Therefore, the contributions from the nearly 600 nuclides, most of which have short half life, can not be treated in the calculation gamma-ray spectra from aggregate fission product nuclides.

The calculations of the gamma-ray spectra from aggregate fission product nuclides have been reported by LANL group[8),9)] and by ORNL group[10),11)] based on the data of the ENDF/B–IV data file. The calculated results showed large disagreement with the measured

ones at short cooling times after a fission event when the contributions from the nearly 600 nuclides without gamma-ray spectrum data are large.

In order to compensate the disagreement, we provided theoretically estimated gamma-ray spectra for the nuclides without experimental spectrum and for the nuclides with insufficient spectrum data.[12] For the theoretical estimation, the gross theory of beta decay and E1-cascade model for gamma-transition were used in order to keep the consistency with the average decay energies adopted in the JNDC library 1.5. By compiling the experimental spectrum data and the estimated spectra, we prepared a gamma-ray spectrum data library.

By using the library, calculations of the gamma-ray spectra from the aggregate fission product nuclides were performed and the calculated results were compared with the measured data after the thermal neutron fission of ^{235}U and ^{239}Pu performed at Oak Ridge National Laboratory[10),11)] and those after the fast neutron fission of ^{235}U, ^{239}Pu, ^{238}U and ^{232}Th and after the thermal neutron fission of ^{235}U at the University of Tokyo[13),14)].

In this report, we summarize the gamma-ray spectrum data of fission product nuclides and present the comparison between the calculated and the measured spectra from aggregate fission product nuclides. In Section2, the gamma-ray spectrum data are described with the spectrum estimation method. The calculation method of the gamma-ray spectra from aggregate fission product nuclides is given in Section 3 and the comparisons between the calculated results and the measured ones are shown in Section 4. The concluding remarks are described in Section 5.

2. Gamma-ray spectrum data

In the compilation work of nuclear data for the decay heat prediction, we have collected the experimental data concerning the decay properties of fission product nuclides. The data were examined if they are suitable for deriving the average decay energies which play an important role for the decay heat prediction by summation method. Based on the examination, the average decay energies were adopted in the library for the decay heat prediction. In our work of compiling a gamma-ray spectrum data library, it seems to be reasonable that the gamma-ray spectrum data are consistent with the average decay energies used for the decay heat prediction. Namely, the energy integrated value fo the gamma-ray spectrum should be equal to the average decay energy of the gamma ray.

In **Table 1**, the numbers of nuclides in the JNDC library used for the decay heat prediction are listed by the property of the gamma rays. Of these nuclides, 157 nuclides are stable and 37 nuclides emit no gamma rays. Other nuclides are unstable and may emit some gamma rays. It is the present work to provide the gamma-ray spectrum data for these nuclides. The average decay energies of 515 nuclides in these nuclides are calculated from the experimentally measured spectrum data. The spectrum data of these nuclides can be used for those of the gamma-ray spectrum data library. For the other 468 nuclides, the theoretically estimated average decay energies are adopted, because the experimental spectrum data are not available or are deficient for deriving the average decay energies. For these nuclides, many gamma rays may be missed in the experiment. Therefore, the experimental gamma-ray spectrum data of these nuclides are considered to be not suitable for the data of the spectrum data library.[2),3)] However, it is also considered that the gamma rays, if they are measured, should be counted in the spectrum data library. The 87 nuclides correpond to this case. In our compilation work, the spectrum data of the 87 nuclides were counted in the spectrum data library.

The experimental gamma-ray spectrum data of total 602 (515 + 87) nuclides were adopted in the gamma-ray spectrum data library. In order to compensate the difference between the average decay energies adopted in the JNDC library and the calculated ones from the spectrum data, theoretically estimated spectra were applied. The estimated spectra were also applied to the nuclides without experimental spectra.

2.1 Experimental gamma-ray spectrum

The experimental gamma-ray spectrum data of the 602 nuclides were retrieved from the data base which was used for compiling the JNDC library. The data base contains the experimental data of energies and intensities of gamma-rays, beta-rays and internal conversion electrons and other experimental decay data.

The nuclides with the experimental spectrum data of gamma rays are listed in **Table 2**. In this table, the average decay energies of nuclides denotes by asterisk are estimated theoretically. A few examples of the spectrum data are listed in **Table 3**. In this table, serial number and identification number of nuclide are listed at first. The identification number is expressed as follows:

Identification Number = $Z \times 10000 + A \times 10 + IS$,

where Z is proton number and A mass number. The IS indicates metastable state, that is, if IS is 0, the ground state is indicated and if IS is 1, the first metastable state is denoted. The next is the number of emitted gamma rays accompanied with the decay of the nuclide. After that the gamma-ray spectrum data are listed. As seen in this table, the spectrum data are given by energy and its intensity. The intensity is represented by number of photons per one disintegration of the nuclide.

The gamma-ray spectra from aggregate fission product nuclides were calculated by using only the experimental gamma-ray spectrum data, and were compared with the spectra measured at Oak Ridge National Laboratory[10),11)]. The results at 2.7 seconds after fissions are shown in **Figs. 1** and **2** for the thermal neutron fissions of ^{235}U[10)] and ^{239}Pu[11)], respectively. The detailed calculation method will be described in Section 3. As seen in these figures, the calculated results do not reproduce the measured ones. This is due to the neglect of the contrubution of the nuclides without experimental spectra. The contribution of such nuclides must be large at short cooling times after a fission event, and then become smaller as the cooling time becomes longer.

Figures 3 and **4** show the comparisons of the gamma-ray spectra between the calculations and the measurements at 500 seconds after the thermal fissions of ^{235}U[10)] and ^{239}Pu[11)], respectively. In these figures, the calculated results show considerable agreement with the measured ones.

The contribution of the nuclides without experimentally measured gamma-ray spectra is shown in **Fig. 5** for the gamma-ray component of the decay heat after the thermal neutron fission of ^{235}U. The vertical axis in this figure shows a difference of the decay heat between the calculation including all fission product nuclides and that including only the nuclides with experimental spectrum data. As seen in this figure, the nuclides without experimental spectrum data play an important role at shorter cooling times than a few hundreds seconds after a fission event. To compensate the difference, the gamma-ray spectra of the nuclides were estimated theoretically.

2.2 Estimated gamma-ray spectrum

The gamma-ray spectra of the unstable nuclides without experimental spectrum data were estimated by the calculation based on the beta strength function derived from the gross theory of beta decay and on the cascade gamma-ray transition model.[12)] In the scheme of the gross theory, the beta strength function varies slowly with mass number A and is quite sensitive to evenness and oddness of the proton number Z and the neutron number N through the pairing correlation. Therefore, the gamma-ray spectrum estimations were performed for typical 32 nuclides categolized by mass number (light, e.g., A=95 or 96 and heavy, e.g., A=139 or 140), by odd-even type of the proton and the neutron numbers (odd-odd, odd-even, even-odd and even-even) and by Q_β value (5, 7, 9 and 11 MeV). First, the beta strength function was calculated by the gross theory in accordance with the categories. By using the beta strength function $S_\beta(E)$, the beta feeding $b(E)$ per unit mega-electron-volt of final levels of daughter nucleus is obtained through the relation,

$$b(E)=S_\beta(E)\cdot f(Z,\ Q_\beta-E)\cdot T_{1/2}\ , \qquad (1)$$

where

E = excitation energy,

$T_{1/2}$ = beta decay half-life,

$f(Z,\ Q_\beta-E)$ = Fermi function.

The beta feeding function $b(E)$ is equivalent ot the initial level population density from the viewpoint of the gamma-ray cascade process that follows the beta decay. The level population $g(E')$ at the energy of E' caused by the gamma deexcitation of the higher levels and by the beta decay is written as,

$$g(E') = \int_{E'}^{E_{max}} \{b(E'') + g(E'')\} \cdot (E'' - E')^3 \times S_\gamma(E'' - E') \cdot \rho(E') dE'', \quad (2)$$

where

$S_\gamma(E'' - E')$ = gamma-ray strength function,

$\rho(E')$ = level density.

In this equation, the gamma transition is assumed to be E1-type.

The intensity of the cascade gamma-ray $I(E_\gamma)$ is written using $g(E'')$ as follows:

$$I(E_\gamma) = \int_0^{E_{max}} dE' \int_{E'}^{E_{max}} dE'' \, \delta(E'' - E' - E_\gamma) \times \{b(E'') + g(E'')\} \cdot (E'' - E')^3 \times S_\gamma(E'' - E') \cdot \rho(E'). \quad (3)$$

The integral on the right-hand side in eq.(2) can be evaluated in a numerical way from E_{max} $(= Q_\beta)$ toward the lower energy, successively.

In the calculation, the gamma-ray strength function proposed by Brink[15] and by Axel[16] was adopted. The level density was calculated following the prescription by Gilbert and Cameron[17]. Since no discrete levels were taken into account and all levels were smeared out in this gamma-ray spectrum estimation, the very low-energy component of the estimated spectrum was emphasized unrealistically. In order to avoid this situation, the intensity was assumed to be constant below a limit, which was set to be 500 keV in the estimation.

The estimated gamma-ray spectra for the typical 32 nuclides were prepared as energy spectra with energy bins of 100 keV. The energy spectra are normalized to be 1.0 if the integration is performed over the whole energy region. The normalized energy spectra are shown in **Figs. 6** through **11**. As there is little difference in the spectra between odd-even and even-odd nuclei, the results for the both cases are shown as "odd-mass nuclide". The numerical values of the normalized energy spectra are listed in **Tables 4** through **11**.

Figures 12 and **13** exemplify the calculated gamma-ray spectra from aggregate fission product nuclides compensated by the estimated spectra comparing the measured spectra at 2.7 seconds after the thermal neutron fissions of ^{235}U and ^{239}Pu. The calculations by using only the experimental spectrum data are also shown by dotted lines. The low-energy parts are shown in **Figs. 14** and **15** for the purpose of a clarity. As seen in these figures, the effect of the compensation by the estimated spectra are apparent. The detailed comparisons between the calculations and the measurements will be given in Section 4.

3. Calculation of gamma-ray spectrum from aggregate fission product nuclides

The gamma-ray spectra from aggregate fission product nuclides are calculated by using both measured and estimated gamma-ray spectrum data. The calculation flow is shown in **Fig. 16**. The nuclide concentrations of the fission product nuclides are calculated by the summation calculation with the aid of a computer code FPGS[18] and the JNDC library version 1.5[6], which is the modified version of the JNDC library[1] and contains the decay and the yield data needed in the summation calculation. Once the concentration, $N^i(t)$, of the i-th nuclide at a time t after a fission event is obtained, the gamma-ray energy spectrum from the aggregate fission product nuclides can be calculated by summing up over all the contributing nuclides as

$$D(E_\gamma, t) = \sum_i \lambda_i \cdot N^i(t) \cdot \bar{E}_\gamma^i \cdot d^i(E_\gamma), \tag{4}$$

where

$d^i(E_\gamma)$ = normalized gamma-ray energy spectrum of the i-th fission product nuclide,

λ_i = decay constant,

$\bar{E}_\gamma^i$ = average gamma-ray energy.

The nuclide, whose concentration is calculated, is examined whether it has experimental spectrum data or not. If the nuclide has the experimental spectrum data, they are applied to the nuclide.

However, there is a problem in this step. The nuclides have experimental spectrum data but the average decay energies adopted in the JNDC library 1.5 are different from the values derived from the spectrum data as mentioned in Section 2.1. In this case, it violates the consistency with the intergral decay heat calculation using the experimental spectrum data for these nuclides directly. Therefore, the calculated spectra by the method mentioned in the previous section are applied to keep the consistency. If the nuclide does not have experimental spectrum data, the calculated gamma-ray spectrum mentioned in Section 2.2 is also applied to the nuclide.

For using the experimental spectrum data, the detector resolution and the energy group structure in the gamma-ray spectrum measurement of aggregate fission product nuclides are taken into account in this step in order to compare the calculated results with the measured ones directly.

In applying the calculated spectra to the nuclide without experimental spectrum data, the type of the nuclides is determined based on the category defined in Section 2. For the nuclide that falls into each category, an appropriate spectrum from the calculated spectra is applied with renormalization constant $\bar{E}_\gamma$ taken from the JNDC library 1.5, because the calculated spectra are normalized to be 1.0 if the integration is performed over the whole energy region. For the nuclide whose average decay energy has difference between the adopted value in the JNDC library 1.5 and the derived one from the experimental spectrum data, the calculated spectrum is used to compensate the difference. Namely, if the experimental average gamma-ray energy is $\bar{E}_\gamma^e$ and the adopted one $\bar{E}_\gamma^t$, the gamma-ray spectrum of the nuclide is assumed to be

$$d^i(E_\gamma) = d^i_{ex}(E_\gamma) + (\bar{E}_\gamma^t - \bar{E}_\gamma^e) \cdot d^i_{es}(E_\gamma), \tag{5}$$

where

$d^i_{ex}(E_\gamma)$ = experimental gamma-ray spectrum,

$d^i_{es}(E_\gamma)$ = normalized estimated gamma-ray spectrum.

In this manner, we can get a gamma-ray spectrum whose energy integrated value is consistent with that adopted in the JNDC library for each nuclide as follows.

$$\begin{aligned}\int_0^\infty E_\gamma d(E_\gamma)dE_\gamma &= \int_0^\infty E_\gamma d_{ex}(E_\gamma)dE_\gamma + (\overline{E}^t_\gamma - \overline{E}^e_\gamma)\cdot\int_0^\infty E_\gamma d_{es}(E_\gamma)dE_\gamma \qquad (6)\\ &= E^e_\gamma + (\overline{E}^t_\gamma - \overline{E}^e_\gamma)\\ &= \overline{E}^t_\gamma\end{aligned}$$

In this way, we can calculate a gamma-ray spectrum consistent with the integral decay heat calculation. If the gamma-ray spectrum calculated by using the present gamma-ray spectrum data library is integrated over the whole energy range, the resulting gamma-ray energy release rate agrees with the energy release rate calculated by using the JNDC library 1.5.

4. Comparison between calculations and measurements

The calculated gamma-ray spectra from aggregate fission product nuclides were compared with the measured ones performed at Oak Ridge National Laboratory for the thermal neutron fissions of ^{235}U[10] and ^{239}Pu[11] and at the University of Tokyo[13] for the fast neutron fissions of ^{235}U, ^{238}U, ^{239}Pu and ^{232}Th and the thermal neutron fission of ^{235}U. And also the gamma-ray component of integral decay heat for those nuclides are compared between the measurements and the calculations by using the JNDC library and the JNDC library 1.5. The measured data are specified by an irradiation time t_{irrad}, a waiting time t_{wait} and a counting time t_{count}. The spectrum and the decay heat calculations, however, were performed at a cooling time t after an instantaneous fission event. The cooling time t was taken to be $t_{wait} + \frac{1}{2}(t_{irrad} + t_{count})$ for the comparison between the calculation and the measurement. Therefore, the contributions by neutron capture of fission products during the irradiation time were neglected in the calculation, because the irradiation time was considered to be too short to cause a sizable effect by the neutron capture in these measurements.

In order to adjust the calculated line width of gamma-ray to the finite energy resolution of detector in the measurement, the lines of the gamma-rays except for the calculated spectra were broadened according to the experimental condition. The energy group structure was also adjusted to that of the measurement.

In the following comparisons, the gamma-ray energy spectra are expressed by a unit of MeV/fission/bin/sec, that is, the energy release rate in each energy bin. Thus, if the integration of the spectrum over whole energy region is performed, the energy release rate at a cooling time t can be obtained. The integral decay heat is described by a unit of MeV/fission, that is, the energy release rate at a cooling time t multilied by the cooling time.

4.1 Comparison with the measurement at Oak Ridge National Labolatory

The gamma-ray spectrum data from aggregate fission product nuclides measured at Oak Ridge National Laboratory have been reported in a tabular form for thermal neutron fissions of ^{235}U and ^{239}Pu by Dickens et al.[10), 11)].

Samples of 1 to 10 μg were irradiated for 1, 10 and 100 seconds and the resulting gamma-rays were counted for 2 to 14000 seconds after fissions. The spectra were measured by an NaI detector whose full energy peak has a Gaussian width σ given by

$$\sigma = 0.01 E_\gamma (1.352 + 5.064/\sqrt{E_\gamma})/2.35482,$$

where E_γ is in MeV.

By using the width σ, the line of a gamma-ray was broadened in the present calculation as follows

$$(I_\gamma/\sqrt{2\pi}\sigma) \cdot exp\{-(E-E_\gamma)^2/(2\sigma^2)\},$$

where I_γ is an intensity of a gamma ray.

The number of energy bins in the measurement was 175 between 0 and 7.5 MeV. The calculated gamma-ray spectra were also grouped into the 175 energy bins to adjust the measured energy bins.

For the thermal neutron fission of ^{235}U, the gamma-ray component of the decay heat is shown in **Fig. 17** as a function of the cooling time. The vertical line is expressed as decay

power, that is, the energy release rate per fission multiplied by the cooling time. As seen in this figure, the calculated results by the JNDC library and the version 1.5 agree within ±10% with the measured ones at cooling times shorter than a few hundreds seconds. However, at cooling times longer than a few hundreds seconds, the calculations overpredict the decay heat by over 20%.

The gamma-ray spectra calculated at each cooling time are shown in **Figs. 18** through **54** with the measured data. The calculated spectra at cooling times shorter than a few hundreds seconds show good agreement with the measurements except for gamma rays with energy higher than 4 MeV, where the calculations do not reproduce some peaks observed in the measurements. This disagreement above 4 MeV seems to suggest that the high energy gamma rays emitted in direct transition to low-lying discrete levels are depressed in the cascade model used in the spectrum estimation, because all levels are smeared out. The calculated spectra at cooling times from a few tens seconds to a few hundreds seconds satisfactorily reproduce the measured ones. The calculated spectra at cooling times longer than a few hundreds seconds show an overestimation as indicated in the decay heat calculation. The overestimation is seen for an energy region between 1 and 3 MeV. The calculations reproduce the spectrum shapes, but the intensities of the calculated gamma-rays exceed the measured ones. About this disagreement, we will discuss later in connection with the measurements performed at the University of Tokyo.

For the thermal neutron fission of ^{239}Pu, the decay heat calculation is shown in **Fig. 55** with the measured data and the calculated gamma-ray spectra are shown in **Figs. 56** through **86** together with the measured spectra. The calculated decay heat agrees within ±10% with the measured data except for a little discrepancy seen at cooling times between 200 and 2000 seconds. For this cooling time region, the disagreement attains over 15%. The discrepancy is also seen in the gamma-ray spectra at this cooling time region.

The calculated spectra are below the measured ones for energy region between 1 and 4 MeV. The underestimation of the decay heat is in an accordance with this fact. The energy positions of the gamma-ray peaks, however, agree well each other both in the calculations and the measurements. Only the intensities are different from each other. The gamma-ray spectrum is the product of the nuclide concentration and the intensity of gamma ray from that nuclide. The calculation for the thermal neutron fission of ^{235}U at this cooling-time region does not show any discrepancy as shown in previous section. This means that the gamma-ray intensities contributing to the spectra at this cooling-time region are seemed to be reasonable. Therefore, the nuclide concentration or the fission yield data of the thermal neutron fission of ^{239}Pu may have some problems.

The calculated gamma-ray spectra at cooling times shorter than a few hundreds seconds show rather good agreement. The agreement, however, is somewhat worse than the case of the thermal neutron fission of ^{235}U at the same cooling time region. For example, measured gamma-ray spectrum at 2.7 seconds after a fission event shows a gamma-ray peak at 1.6 MeV, but the calculation can not reproduce this peak. For the gamma-ray spectra at cooling times longer than 5000 seconds, an apparent discrepancy between the calculations and the measurements is shown at energy of 2.8 MeV. The measurements show a gamma-ray peak at this energy, but the calculations do not show this peak. Dickens et al.[11] also cautioned this peak and suggested that this peak might be due to a contaminant viz. ^{24}Na. But they also commented that there was one problem with this explanation because of lacking a large peak corresponding to the companion 1.4 MeV gamma ray. The 2.8 MeV gamma-ray peak is not seen in the case of the fast neutron fission of ^{239}Pu (see later). The fission yield of the fast neutron fission of ^{239}Pu is not so different from that of the thermal neutron fission of ^{239}Pu.

Therefore, this 2.8 MeV peak may be due to a contamination.

4.2 Comparison with the measurement at the University of Tokyo

Akiyama et al.[13] measured gamma-ray spectra from aggregate fission product nuclides following fast neutron fissions of ^{233}U, ^{235}U, ^{239}Pu, ^{238}U, natural uranium and ^{232}Th. They also measured the spectra following thermal neutron fissions of ^{235}U to examine the discrepancy of the integral decay heat between the calculations by the JNDC library and the measurements at ORNL. These measurements were performed at YAYOI reactor of the University of Tokyo. Small samples were irradiated for 10 and 100 seconds and the gamma-rays from the sample were measured by using an NaI detector for cooling times between 11 and 22000 seconds after the irradiation. The spectrum data were grouped into 98 energy bins from 0.1 to 5 MeV. The measured spectra except for those of ^{233}U and natural uranium were used for the comparison.

For the fast neutron fission of ^{235}U, the gamma-ray component of decay heat is shown in **Fig. 87** and the gamma-ray spectra at each cooling time are shown in **Figs. 88** through **121**. The decay heat calculations agree within ±10% with the measurements for a whole range of cooling time. The gamma-ray spectra also show a good agreement between the calculations and the measurements. There is, however, one problem seen at cooling times between 4800 and 11000 seconds. The calculations in this cooling-time region do not reproduce gamma-ray peak of energy about 150 keV. This peak is also not observed in the measured spectra of the thermal neutron fission of ^{235}U at ORNL, which are shown in the previous section.

For the fast neutron fission of ^{239}Pu, the gamma-ray component of the decay heat is shown in **Fig. 122** and the gamma-ray spectra at each cooling time are shown in **Figs. 123** through **156**. As seen in **Fig. 122**, the decay heat calculations show the disagreement with the measured data at cooling times between 300 and 2000 seconds. The calculated gamma-ray spectra at this cooling time region show also disagreement with the measured ones for energy region between 1 and 2.5 MeV. The gamma-ray peaks measured for other energy region are well reproduced by the calculations. At cooling times shorter than 100 seconds, there is a little discrepancy between the calculations and the measurements at energy of about 150 keV. At this energy, the calculations exceed the measurements. The gamma-ray peak of 2.8 MeV observed for the thermal neutron fission of ORNL at cooling times longer than 5000 seconds is not identified in this case and the agreement becomes better than that of the thermal neutron fission of ^{239}Pu.

For the fast neutron fission of ^{238}U, the gamma-ray component of the decay heat is shown in **Fig. 157**. In the original YAYOI measurements, the decay heat from ^{239}U and ^{239}Np decays is included because of production of ^{239}U by neutron capture reaction of ^{238}U[14]. The contribution of the neutron capture effect was eliminated from the original measurement to derive the decay heat of the fission product nuclides. In **Fig. 157**, the original measurements and the corrected decay heat are shown by open circles and triangles, respectively. As seen in this figure, the effect is not so large. The calculated gamma-ray spectra are shown in **Figs. 158** through **191** with the measured data. In the measured spectra shown in these figures, the contribution from the neutron capture reaction is not eliminated and the gamma rays from the decays of ^{239}U and ^{239}Np are included. The gamma-ray peaks seen at energy of about 100 keV for a wide range of cooling times and the peaks at energy region from 200 to 300 keV for cooling times longer than 5000 seconds might be due to the gamma rays from ^{239}U and ^{239}Np decays. Apart from these discrepancies, the calculations of gamma-ray spectra reproduce the measured ones fairly well.

For the fast neutron fission of ^{232}Th, the gamma-ray component of the decay heat is shown in **Fig. 192**. In this case, there is remarkable contribution of neutron capture reaction of ^{232}Th[14]. The reaction produces ^{233}Th and its daughter nuclide ^{233}Pa. The contribution of the gamma rays from ^{233}Th and ^{233}Pa decays is large in this case. The original measurements including the contribution and the corrected decay heat are represented in the figure by open circles and triangles, respectively. The calculated decay heat agrees well with the corrected one. The gamma-ray spectra are shown in **Figs. 193** through **226** together with the measured data. In the measurements, the gamma rays from ^{233}Th and ^{233}Pa decays are included, but the calculations do not take the contribution into account because of lacking of the spectrum data of the actinides nuclides in the present gamma-ray spectrum library. Therefore, the calculated spectra at the cooling times when the contribution of the neutron capture reaction becomes large do not reproduce the measured ones. There are many gamma rays having energy below 1 MeV in the decays of ^{233}Th and ^{233}Pa. The gamma-ray peaks observed below 1 MeV in the measurements are due to this origin. For example, the measured gamma-ray spectrum at 2450 seconds after fission event shows many gamma-ray peaks below 1 MeV. They are from the decays of ^{233}Th and ^{233}Pa. Apart from the contribution of the neutron capture reaction, the agreement between the calculations and the measurements is seemed to be good.

The gamma-ray component of the decay heat of the thermal neutron fission of ^{235}U showed large discrepancy between the calculation and the measurement of ORNL at a few hundreds seconds cooling time. To settle down the discrepancy, Akiyama et al.[14] measured the decay heat and gave the gamma-ray spectrum data at cooling times from 450 to 11000 seconds when the discrepancy is prominent. The decay heat is shown in **Fig. 227** with the measured data at ORNL and at YAYOI together with the calculated results. The calculated results of the decay heat show better agreement with the measured ones at YAYOI than those at ORNL. The overestimation of the gamma-ray spectra observed in comparison with the ORNL measurements is also diminished in comparison with the YAYOI measurements as seen in **Figs. 228** through **244**.

Figure 245 shows an inter-comparison betwen the measurements of ORNL and YAYOI at the same cooling time, that is, the same t ($= t_{wait} + \frac{1}{2}(t_{irrad} + t_{count})$) after a fission event. In this figure, the open circles indicate the ORNL measurements and the triangles the YAYOI measurements. The calculations are also shown in the figure by solid, dashed and dotted lines. The solid line is the calculation with very fine energy group structure (about 1300 energy groups below 5 MeV) and with the same detector response as that of the ORNL measurement. The dashed and the dotted lines indicate the calculations with the same energy group structures and the same detector responses as those of respective measurements at ORNL and at YAYOI. As seen in this figure, calculation shows better agreement with the measurement of YAYOI than those of ORNL. The ORNL measurement is lower than the YAYOI measurement and the calculation.

5. Concluding Remarks

A gamma-ray spectrum data library was prepared from both the measured spectrum data of individual fission product nuclides and the calculated spectra to compensate the defect of the measured spectrum data and to apply them to the nuclides without experimental spectrum data. In the compensation, the calculated spectra were used to keep the consistency with energy release rate per decay adopted in the JNDC library 1.5. In this manner, the gamma-ray spectra from aggregate fission product nuclides can be calculated at any cooling time in a consistent way with the integrated decay heat calculation by using the JNDC library 1.5. In order to assess the gamma-ray spectrum data library, the calculated gamma-ray spectra were compared with the measured ones performed at ORNL and at the University of Tokyo. The calculations showed reasonable agreement with the measured data except for the spectra of the thermal neutron fission of ^{235}U performed at ORNL for cooling times of a few thousands seconds. However, for this case, there are discrepancies between the measurements at ORNL and those at the University of Tokyo. Our calculations showed agreement with the measured ones at the University of Tokyo for not only the decay heat, but also the gamma-ray spectra. This fact means that the measurements at the University of Tokyo seems to support our calculations.

Apart from this discrepancy, it was shown from the comparison with the measured data that the calculation of the gamma-ray spectrum from the aggregate fission product nuclides by using the present library have validity for a wide range of cooling time after a fission event of fissile nuclides from ^{232}Th to ^{239}Pu. Therefore, it is concluded that it becomes possible to evaluate both the gamma decay heat and the gamma-ray spectrum from aggregate fission product nuclides by the consistent way.

In this report, we presented the calculated results of the gamma-ray spectra from aggregate fission product nuclides. The computer code used in the calculations is under development for easy use and the code manual will be published in near future.

Acknowledgment

The authors are grateful to the members of Working Group on Evaluation of Decay Heat of Japanese Nuclear Data Committee for the continuous support and encouragement to the present work. They also acknowledge Miss S. Ishibashi for her aid to put the measured data listed in reports into a computer storage.

References

1) Yamamoto T., Akiyama M., Matumoto Z. and Nakasima R., "JNDC FP Decay Data File," JAERI–M 9357 (1981).
2) Yoshida T. and Nakasima R., J. Nucl. Sci. Technol., **18**, 393 (1981).
3) Yoshida T., "Theoretical Calculation of Decay Data of Short-Lived Nuclides for JNDC FP Decay Data File," JAERI–M 83-127 (1983).
4) Takahashi K., Yamada M. and Kondoh T., Atom. Data and Nucl. Data Tables **12**, 101 (1973) and references therein.
5) Tasaka K., Ihara H., Akiyama M., Yoshida T., Matumoto Z. and Nakasima R., "JNDC Nuclear Data Library of Fission Products," JAERI 1287 (1983).
6) Katakura J., Akiyama M., Yoshida T., Matsumoto Z. and Nakasima R., "An Attempt for Revision of JNDC FP Decay Data File," JAERI–M 84-117 (1984).
7) "Fission Product Decay Library of the Evaluated Nuclear Data, File, Version IV (ENDF/B–IV)".
8) Jurney E.T., Bendt P.J. and England T.R., LA-7620-Ms (1979).
9) England T.R. and Stamatelatos M.G., "Comparisons of Calculated and Experimental Delayed Fission-Product Beta and Gamma Spectra from ^{235}U Thermal Fission," LA-NUREG-6896-MS (1977).
10) Dickens J.K., Love T.A., McConnell J.W., Emery J.F., Northcutt K.J., Peelle R.W. and Weaver H., "Delayed Beta- and Gamma-Ray Production Due to Thermal-Neutron Fission of ^{235}U ; Spectral Distributions for Times After Fission Between 2 and 14000 sec : Tabular and Graphical Data," NUREG/CR-0162, ORNL/NUREG-39 (1978).
11) Dickens J.K., Love T.A., McConnell J.W., Emery J.F., Northcutt K.J., Peelle R.W. and Weaver H., "Delayed Beta- and Gamma-Ray Production Due to Thermal-Neutron Fission of ^{239}Pu : Tabular and Graphical Spectral Distributions for Times After Fission Between 2 and 14000 sec," NUREG/CR-1172, ORNL/NUREG-66 (1980).
12) Yoshida T. and Katakura J., Nucl. Sci. Eng., **93**, 193 (1986).
13) Akiyama M., Dr. Eng. Thesis, University of Tokyo [in Japanese] (1983).
14) Akiyama M., Oka Y., Kondo S. and An S., "Fission-Product Decay Heat for Fast-Neutron Fissions of ^{238}U and ^{232}Th," Proc. Conf. on Nuclear Data for Basic and Applied Science, Santa Fe, New Mexico, 743 (1985).
15) Brink D.M., PhD. Thesis, Oxford University (1955).
16) Axel P., Phys. Rev. **126**, 671 (1962).
17) Gilbert A. and Cameron A.G.W., Can. J. Phys., **43**, 1446 (1965).
18) Ihara H., Private Communication.

Table 1 Number of nuclides in JNDC library.

Total number of nuclides	1172
Number of stable nuclides	152
Number of nuclides with no-γ rays	37
Number of nuclides with estimated γ-decay energy	468 (87*)
Number of nuclides with experimental γ-decay energy	515

* Number of nuclides whose experimental decay energies are replaced by estimated ones.

Table 2 List of nuclides having experimental gamma-ray spectrum data

No.	Nuclide	Number of γ-rays	No.	Nuclide	Number of γ-rays	No.	Nuclide	Number of γ-rays
1	^{66}Cu	4	35	^{75}Ga	36	69	^{81}Rb	28
2	^{66}Ga	62	36	^{75m}Ge	7	70	^{82m}As*	13
3	^{66}Ge	90	37	^{75}Ge	20	71	^{82}As*	12
4	^{67}Ni	16	38	^{75}Se	22	72	^{82m}Br	13
5	^{67}Cu	6	39	^{75}Br	57	73	^{82}Br	37
6	^{67}Ga	10	40	^{76}Ga*	107	74	^{83}As*	22
7	^{67}Ge	58	41	^{76}As	51	75	^{83m}Se	24
8	^{68m}Cu*	19	42	^{77m}Ge	5	76	^{83}Se	59
9	^{68}Cu	24	43	^{77}Ge	153	77	^{83}Br	11
10	^{68}Ga	10	44	^{77}As	13	78	^{83m}Kr	2
11	^{69}Cu	17	45	^{77m}Se	1	79	^{83}Rb	13
12	^{69m}Zn	2	46	^{77m}Br	1	80	^{83}Sr	105
13	^{69}Zn	2	47	^{77}Br	52	81	^{84}As*	18
14	^{69}Ge	37	48	^{77}Kr	27	82	^{84}Se	1
15	^{69}As	7	49	^{78}Ge	2	83	^{84m}Br	6
16	^{70m}Cu*	13	50	^{78}As	55	84	^{84}Br	51
17	^{70}Cu*	2	51	^{78}Br	26	85	^{84m}Rb	3
18	^{70}Ga	3	52	^{79}Ge	5	86	^{84}Rb	4
19	^{71m}Zn	60	53	^{79}As	11	87	^{85}Se*	47
20	^{71}Zn	24	54	^{79m}Se	1	88	^{85}Br	43
21	^{71}As	83	55	^{79m}Br	1	89	^{85m}Kr	5
22	^{72}Zn	9	56	^{79m}Kr	1	90	^{85}Kr	1
23	^{72}Ga	71	57	^{79}Kr	45	91	^{85m}Sr	4
24	^{72}As	61	58	^{79}Rb	64	92	^{85}Sr	2
25	^{72}Se	1	59	^{80}As*	27	93	^{85m}Y	7
26	^{73}Zn	4	60	^{80m}Br	2	94	^{85}Y	144
27	^{73}Ga	16	61	^{80}Br	10	95	^{86}Se*	22
28	^{73m}Ge	1	62	^{81}Ge*	4	96	^{86}Br*	50
29	^{73m}Se	33	63	^{81}As	29	97	^{86m}Rb	37
30	^{73}Se	22	64	^{81m}Se	5	98	^{86}Rb	1
31	^{74}Zn	8	65	^{81}Se	9	99	^{87}Se*	11
32	^{74m}Ga	2	66	^{81m}Kr	1	100	^{87}Br*	108
33	^{74}Ga*	97	67	^{81}Kr	1	101	^{87}Kr	33
34	^{74}As	15	68	^{81m}Rb	2	102	^{87m}Sr	1

* Experimental decay energies not adopted in the JNDC library.

Table 2 (Continued)

No.	Nuclide	Number of γ-rays	No.	Nuclide	Number of γ-rays	No.	Nuclide	Number of γ-rays
103	^{87m}Y	2	149	^{93m}Mo	13	195	^{100}Zr	12
104	^{87}Y	2	150	^{93m}Tc	5	196	^{100m}Nb	18
105	^{87m}Zn	2	151	^{93}Tc	15	197	^{100}Nb	15
106	^{87}Zn	15	152	^{94}Sr	5	198	^{100}Tc	20
107	^{88}Se*	13	153	^{94}Y	54	199	^{101}Zr*	2
108	^{88}Br*	66	154	^{94m}Nb	4	200	^{101}Mo	185
109	^{88}Kr	86	155	^{94}Nb	2	201	^{101}Tc	34
110	^{88}Rb	27	156	^{95}Sr*	29	202	^{101m}Rh	18
111	^{88}Y	8	157	^{95}Y	44	203	^{101}Rh	17
112	^{88}Zr	1	158	^{95}Zr	2	204	^{101}Pd	51
113	^{89}Kr	299	159	^{95m}Nb	4	205	^{102}Mo	8
114	^{89}Rb	62	160	^{95}Nb	3	206	^{102m}Tc	30
115	^{89m}Y	1	161	^{95m}Tc	31	207	^{102}Tc	10
116	^{89m}Zn	3	162	^{95}Tc	23	208	^{102m}Rh	28
117	^{89}Zr	5	163	^{95}Ru	89	209	^{102}Rh	15
118	^{89m}Nb	5	164	^{96}Sr*	6	210	^{103}Tc	68
119	^{89}Nb	73	165	^{96m}Y	21	211	^{103}Ru	21
120	^{90}Br*	12	166	^{96}Nb	34	212	^{103m}Rh	1
121	^{90}Kr	103	167	^{97}Rb	12	213	^{103}Pd	11
122	^{90m}Rb	96	168	^{97}Sr*	17	214	^{103m}Ag	1
123	^{90}Rb*	105	169	^{97m}Y*	16	215	^{103}Ag	102
124	^{90m}Y	3	170	^{97}Y*	19	216	^{104}Tc*	121
125	^{90m}Zr	4	171	^{97}Zr	36	217	^{104m}Rh	15
126	^{90m}Nb	1	172	^{97m}Nb	1	218	^{104}Rh	10
127	^{90}Nb	37	173	^{97}Nb	13	219	^{105}Mo*	49
128	^{90}Mo	25	174	^{97m}Tc	1	220	^{105}Tc	83
129	^{91}Kr*	221	175	^{97}Ru	18	221	^{105}Ru	88
130	^{91}Rb*	125	176	^{98}Rb*	25	222	^{105m}Rh	1
131	^{91}Sr	49	177	^{98m}Y*	11	223	^{105}Rh	7
132	^{91m}Y	1	178	^{98m}Y*	11	224	^{105m}Ag	26
133	^{91}Y	1	179	^{98}Y*	26	225	^{105}Ag	45
134	^{91m}Nb	2	180	^{98m}Nb	259	226	^{105}Cd	277
135	^{91}Nb	1	181	^{98}Nb	10	227	^{106m}Rh	39
136	^{91m}Mo	11	182	^{98}Tc	2	228	^{106}Rh	78
137	^{91}Mo	22	183	^{99}Y*	16	229	^{106m}Ag	59
138	^{92}Kr*	96	184	^{99}Zr	13	230	^{106}Ag	11
139	^{92}Rb*	52	185	^{99m}Nb	52	231	^{107}Ru	7
140	^{92}Sr	9	186	^{99}Nb	2	232	^{107}Rh	39
141	^{92}Y	19	187	^{99}Mo	30	233	^{107m}Pd	1
142	^{92m}Nb	4	188	^{99m}Tc	4	234	^{107m}Ag	1
143	^{92}Nb	2	189	^{99}Tc	1	235	^{107}Cd	33
144	^{93}Kr*	217	190	^{99m}Rh	26	236	^{107}In	153
145	^{93}Rb*	243	191	^{99}Rh	33	237	^{108}Mo	3
146	^{93}Sr	160	192	^{99}Pd	126	238	^{108}Tc*	6
147	^{93m}Y	2	193	^{100m}Y	2	239	^{108}Ru	1
148	^{93}Y	23	194	^{100}Y	9	240	^{108m}Rh	14

* Experimental decay energies not adopted in the JNDC library.

Table 2 (Continued)

No.	Nuclide	Number of γ-rays	No.	Nuclide	Number of γ-rays	No.	Nuclide	Number of γ-rays
241	^{108}Rh	4	287	^{116n}In	1	333	^{122}In*	3
242	^{108m}Ag	8	288	^{116m}In	43	334	^{122m}Sb	3
243	^{108}Ag	14	289	^{116}In	5	335	^{122}Sb	8
244	^{109}Ru	2	290	^{117m}Ag	61	336	^{123m}In	11
245	^{109}Rh	37	291	^{117}Ag	83	337	^{123}In	16
246	^{109m}Pd	1	292	^{117m}Cd	70	338	^{123m}Sn	4
247	^{109}Pd	31	293	^{117}Cd	113	339	^{123}Sn	9
248	^{109m}Ag	1	294	^{117m}In	6	340	^{123m}Te	2
249	^{109n}In	4	295	^{117}In	4	341	^{123}Ir	48
250	^{109m}In	1	296	^{117m}Sn	2	342	^{124}Cd	4
251	^{109}In	68	297	^{117}Sn	14	343	^{124m}In*	4
252	^{110m}Rh*	23	298	^{117}Te	23	344	^{124}In*	3
253	^{110}Rh*	1	299	^{118m}Ag*	42	345	^{124n}Sb	1
254	^{110m}Ag	62	300	^{118}Ag*	12	346	^{124m}Sb	5
255	^{110}Ag	13	301	^{118n}In	1	347	^{124}Sb	84
256	^{111m}Pd	79	302	^{118m}In	18	348	^{125m}In*	2
257	^{111}Pd	80	303	^{118}In	8	349	^{125}In*	11
258	^{111m}Ag	6	304	^{118m}Sb	9	350	^{125m}Sn	19
259	^{111}Ag	10	305	^{118}Sb	14	351	^{125}Sn	48
260	^{111m}Cd	2	306	^{119}Ag	137	352	^{125}Sb	28
261	^{111m}In	1	307	^{119m}Cd	60	353	^{125m}Te	2
262	^{111}In	2	308	^{119}Cd	69	354	^{125}I	1
263	^{111}Sn	28	309	^{119m}In	12	355	^{125m}Xe	2
264	^{112}Pd	1	310	^{119}In	7	356	^{125}Xe	33
265	^{112}Ag	115	311	^{119m}Sn	2	357	^{126}Xe	11
266	^{112m}In	1	312	^{119}Sb	1	358	^{126m}In*	14
267	^{112}In	11	313	^{119m}Te	37	359	^{126}In*	6
268	^{113m}Ag	16	314	^{119}Te	13	360	^{126}Sn	8
269	^{113}Ag	38	315	^{120m}Ag	5	361	^{126m}Sb	9
270	^{113m}Cd	1	316	^{120}Ag	4	362	^{126}Sb	27
271	^{113m}In	1	317	^{120m}In	37	363	^{126}I	14
272	^{113m}Sn	1	318	^{120}In	11	364	^{127m}In*	3
273	^{113}Sn	4	319	^{120m}Sb	5	365	^{127}In*	18
274	^{113}Sb	10	320	^{120}Sb	4	366	^{127m}Sn	3
275	^{114}Ag	11	321	^{121}Ag	53	367	^{127}Sn	162
276	^{114m}In	3	322	^{121m}Cd	35	368	^{127}Sb	36
277	^{114}In	4	323	^{121}Cd	62	369	^{127m}Te	6
278	^{115m}Ag	13	324	^{121m}In*	11	370	^{127}Te	9
279	^{115}Ag	145	325	^{121}In	9	371	^{127m}Xe	2
280	^{115m}Cd	23	326	^{121m}Sn	2	372	^{127}Xe	6
281	^{115}Cd	16	327	^{121m}Te	13	373	^{127}Cs	53
282	^{115m}In	2	328	^{121}Te	5	374	^{128m}In*	5
283	^{115}Sb	19	329	^{121}I	62	375	^{128}In*	18
284	^{115}Te	34	330	^{122}Ag*	6	376	^{128}Sn	10
285	^{116m}Ag*	11	331	^{122}Cd	1	377	^{128m}Sb	16
286	^{116}Ag*	10	332	^{122m}In*	4	378	^{128}Sb	54

* Experimental decay energies not adopted in the JNDC library.

Table 2 (Continued)

No.	Nuclide	Number of γ-rays	No.	Nuclide	Number of γ-rays	No.	Nuclide	Number of γ-rays
379	^{128}I	8	425	^{133}La	129	471	^{141}La	29
380	^{129m}In*	4	426	^{134m}Sb*	4	472	^{141}Ce	1
381	^{129}In*	14	427	^{134}Te	27	473	^{141m}Nd	4
382	^{129m}Sn	1	428	^{134m}I	3	474	^{141}Nd	12
383	^{129}Sn	1	429	^{134}I	66	475	^{141}Pm	54
384	^{129}Sb	92	430	^{134m}Xe	3	476	^{142}Xe*	174
385	^{129m}Te	39	431	^{134m}Cs	2	477	^{142}Cs*	144
386	^{129}Te	50	432	^{134}Cs	12	478	^{142}Ba	55
387	^{129}I	1	433	^{135}Te*	3	479	^{142}La	155
388	^{129m}Xe	2	434	^{135}I	90	480	^{142}Pr	3
389	^{129}Cs	32	435	^{135m}Xe	5	481	^{143}Ba	69
390	^{130}In*	4	436	^{135}Xe	13	482	^{143}La	14
391	^{130m}Sn	20	437	^{135m}Cs	2	483	^{143}Ce	28
392	^{130}Sn	15	438	^{135m}Ba	1	484	^{143}Pr	1
393	^{130m}Sb	59	439	^{135}La	23	485	^{143}Pm	1
394	^{130}Sb	40	440	^{135m}Ce	4	486	^{143m}Sm	5
395	^{130m}I	35	441	^{135}Ce	133	487	^{143}Sm	26
396	^{130}I	52	442	^{136}Te	22	488	^{144}La*	13
397	^{131}In*	4	443	^{136m}I*	28	489	^{144}Ce	7
398	^{131m}Sn*	5	444	^{136}I*	117	490	^{144m}Pr	3
399	^{131}Sn	1	445	^{136}Ce	22	491	^{144}Pr	10
400	^{131}Sb	66	446	^{136m}Ba	3	492	^{144}Pm	12
401	^{131m}Te	185	447	^{137}I*	24	493	^{145}Ce	13
402	^{131}Te	80	448	^{137}Xe	94	494	^{145}Pr	61
403	^{131}I	19	449	^{137m}Ba	1	495	^{145}Pm	2
404	^{131m}Xe	1	450	^{137m}Ce	11	496	^{145}Sm	3
405	^{131m}Ba	1	451	^{137}Ce	21	497	^{146}La*	4
406	^{131}Ba	35	452	^{138}I	9	498	^{146}Ce	20
407	^{132}In*	5	453	^{138}Xe	100	499	^{146}Pr	43
408	^{132}Sn	10	454	^{138m}Cs*	11	500	^{146}Pm	6
409	^{132m}Sb	16	455	^{138}Cs*	86	501	^{147}Ce	11
410	^{132}Sb*	37	456	^{138}La	2	502	^{147}Pr	84
411	^{132}Te	4	457	^{139}Xe*	220	503	^{147}Nd	16
412	^{132m}I	8	458	^{139}Cs	179	504	^{147}Pm	1
413	^{132}I	121	459	^{139}Ba	28	505	^{147}Eu	27
414	^{132}Cs	14	460	^{139m}Ce	1	506	^{147}Gd	127
415	^{133}Sn*	1	461	^{139}Ce	1	507	^{148}La*	4
416	^{133}Sb	6	462	^{139}Pr	24	508	^{148}Ce	6
417	^{133m}Te	63	463	^{140}Xe	142	509	^{148}Pr	41
418	^{133}Te	29	464	^{140}Cs*	196	510	^{148m}Pm	16
419	^{133m}I	3	465	^{140}Ba	10	511	^{148}Pm	7
420	^{133}I	42	466	^{140}La	35	512	^{149}Ce	21
421	^{133m}Xe	1	467	^{140}Pr	19	513	^{149}Pr	40
422	^{133}Xe	6	468	^{141}Xe*	211	514	^{149}Nd	152
423	^{133m}Ba	3	469	^{141}Cs*	141	515	^{149}Pm	28
424	^{133}Ba	9	470	^{141}Ba	55	516	^{149}Eu	14

* Experimental decay energies not adopted in the JNDC library.

Table 2 (Continued)

No.	Nuclide	Number of γ-rays	No.	Nuclide	Number of γ-rays	No.	Nuclide	Number of γ-rays
517	^{149}Gd	38	546	^{156m}Tb	2	575	^{164m}Ho	3
518	^{150}Ce	12	547	^{156}Tb	118	576	^{164}Ho	4
519	^{150}Pr*	9	548	^{157}Sm	14	577	^{165m}Dy	12
520	^{150}Pm	140	549	^{157}Eu	32	578	^{165}Dy	52
521	^{151}Nd	190	550	^{157}Tb	1	579	^{165}Tm	105
522	^{151}Pm	127	551	^{157}Dy	25	580	^{166}Dy	5
523	^{151}Sm	1	552	^{158}Eu	132	581	^{166m}Ho	44
524	^{151}Gd	19	553	^{158m}Tb	1	582	^{166}Ho	10
525	^{151}Tb	92	554	^{158}Tb	13	583	^{166}Tm	154
526	^{152}Nd	7	555	^{159}Eu	60	584	^{166}Yb	1
527	^{152m}Pm	66	556	^{159}Gd	18	585	^{167}Dy	29
528	^{152}Pm*	74	557	^{159}Dy	6	586	^{167}Ho	26
529	^{152n}Eu	2	558	^{159m}Ho	2	587	^{167m}Er	1
530	^{152m}Eu	31	559	^{159}Ho	68	588	^{167}Tm	8
531	^{152}Eu	94	560	^{160}Eu	14	589	^{167}Yb	123
532	^{153}Pm	15	561	^{160}Tb	35	590	^{168}Ho	69
533	^{153}Sm	61	562	^{161}Gd	130	591	^{168}Tm	56
534	^{153}Gd	9	563	^{161}Tb	27	592	^{169}Ho	35
535	^{153}Tb	217	564	^{161m}Ho	1	593	^{169}Er	3
536	^{154m}Pm	41	565	^{161}Ho	16	594	^{169m}Yb	1
537	^{154}Pm	38	566	^{161}Er	151	595	^{169}Yb	36
538	^{154m}Eu	13	567	^{162}Gd	3	596	^{170m}Ho	21
539	^{154}Eu	172	568	^{162}Tb	47	597	^{170}Ho	31
540	^{155}Sm	53	569	^{162m}Ho	68	598	^{170}Tm	2
541	^{155}Eu	13	570	^{162}Ho	32	599	^{171}Er	63
542	^{155}Tb	140	571	^{163}Tb	81	600	^{171}Tm	1
543	^{155}Dy	129	572	^{163m}Ho	1	601	^{172}Er	43
544	^{156}Sm	12	573	^{163}Er	26	602	^{172}Tm	48
545	^{156}Eu	95	574	^{164}Tb	168			

* Experimental decay energies not adopted in the JNDC library.

Table 3 Examples of spectrum data list.

NO. 34 NUCLIDE ID. = 330740

NUMBER OF GAMMA RAYS = 15

NO.	ENERGY(MEV)	INTENSITY(1/DECAY) *
1	5.95900E-01	5.81000E-01
2	6.08390E-01	5.34520E-03
3	6.34780E-01	1.44088E-01
4	6.35000E-01	3.48600E-04
5	7.15300E-01	8.13400E-05
6	7.34200E-01	3.42790E-05
7	8.67000E-01	5.11280E-05
8	8.87000E-01	2.49830E-04
9	9.93460E-01	2.03350E-04
10	1.10110E+00	5.81000E-05
11	1.20434E+00	2.67260E-03
12	1.26960E+00	1.80110E-05
13	1.60210E+00	6.97200E-05
14	2.19810E+00	1.68490E-04
15	5.11006E-01	6.24320E-01

NO. 35 NUCLIDE ID. = 310750

NUMBER OF GAMMA RAYS = 36

NO.	ENERGY(MEV)	INTENSITY(1/DECAY)
1	1.24300E-01	2.77600E-03
2	1.77000E-01	3.71290E-02
3	2.03900E-01	1.83910E-02
4	2.52800E-01	3.47000E-01
5	2.79300E-01	1.00630E-02
6	3.10400E-01	2.29020E-02
7	3.16800E-01	1.14510E-02
8	3.21600E-01	6.94000E-03
9	4.28300E-01	3.81700E-03
10	4.42800E-01	3.12300E-03
11	4.44800E-01	5.55200E-03
12	4.57100E-01	1.56150E-02
13	5.68500E-01	8.32800E-03
14	5.74700E-01	1.09652E-01
15	5.84100E-01	5.20500E-03
16	6.32200E-01	1.90850E-02
17	6.47500E-01	6.24600E-03
18	7.61300E-01	4.16400E-03
19	7.83200E-01	7.28700E-03
20	8.85400E-01	3.85170E-02
21	9.27200E-01	2.29020E-02
22	9.87500E-01	4.85800E-03
23	1.04330E+00	9.02200E-03
24	1.17460E+00	5.20500E-03
25	1.18230E+00	4.85800E-03
26	1.22250E+00	4.51100E-03
27	1.23950E+00	1.04100E-03
28	1.24850E+00	1.90850E-02
29	1.35880E+00	1.38800E-03
30	1.42700E+00	3.12300E-03
31	1.50110E+00	1.56150E-02
32	1.54300E+00	3.81700E-03
33	1.74560E+00	3.47000E-04
34	1.79640E+00	2.08200E-03
35	2.08970E+00	6.93999E-04
36	2.10370E+00	6.93999E-04

NO. 36 NUCLIDE ID. = 320751

NUMBER OF GAMMA RAYS = 7

NO.	ENERGY(MEV)	INTENSITY(1/DECAY)
1	6.19200E-02	1.17000E-04
2	7.78600E-02	3.12000E-05
3	1.21150E-01	5.07000E-05
4	1.36010E-01	2.02800E-04
5	1.39680E-01	3.90000E-01
6	2.79480E-01	4.29000E-05
7	4.00200E-01	3.90000E-05

NO. 37 NUCLIDE ID. = 320750

NUMBER OF GAMMA RAYS = 20

NO.	ENERGY(MEV)	INTENSITY(1/DECAY)
1	4.52100E-02	2.22000E-06
2	6.60500E-02	1.55400E-03
3	1.49000E-01	7.77000E-06
4	1.98560E-01	1.14330E-02
5	1.98600E-01	1.55400E-06
6	2.04260E-01	2.88600E-06
7	2.17400E-01	5.55000E-07
8	2.64610E-01	1.11000E-01
9	2.70310E-01	3.66300E-05
10	2.79480E-01	7.88100E-05
11	3.38470E-01	8.32499E-05
12	3.53260E-01	2.99700E-04
13	4.00550E-01	1.11000E-05
14	4.19310E-01	2.66400E-03
15	4.60610E-01	2.66400E-06
16	4.68870E-01	2.55300E-03
17	5.72680E-01	4.99500E-06
18	5.95710E-01	2.10900E-05
19	6.17870E-01	9.32399E-04
20	8.60560E-01	6.54900E-06

NO. 38 NUCLIDE ID. = 340750

NUMBER OF GAMMA RAYS = 22

NO.	ENERGY(MEV)	INTENSITY(1/DECAY)
1	2.44500E-02	2.90000E-04
2	6.60400E-02	1.08460E-02
3	8.08700E-02	1.16000E-04
4	9.67100E-02	3.30600E-02
5	1.21090E-01	1.72840E-01
6	1.35960E-01	5.51000E-01
7	1.98560E-01	1.47320E-02
8	2.01990E-01	1.16000E-06
9	2.04260E-01	1.74000E-05
10	2.64610E-01	5.80000E-01
11	2.79480E-01	2.44760E-01
12	2.93180E-01	3.48000E-06
13	3.03880E-01	1.29340E-02
14	3.38470E-01	4.06000E-06
15	3.53260E-01	1.04400E-05
16	4.00550E-01	1.16000E-01
17	4.19310E-01	1.04400E-04
18	4.68870E-01	3.07400E-06
19	5.42370E-01	1.16000E-07
20	5.72660E-01	3.46840E-04
21	6.17870E-01	4.46600E-05
22	8.21850E-01	1.27600E-06

* Photons/decay

Table 3 (Continued)

NO. 39 NUCLIDE ID. = 350750

NUMBER OF GAMMA RAYS = 57

NO.	ENERGY(MEV)	INTENSITY(1/DECAY)
1	1.12100E-01	1.74990E-02
2	1.41190E-01	6.90750E-02
3	1.95500E-01	9.21000E-04
4	2.36100E-01	8.28900E-03
5	2.86500E-01	9.21000E-01
6	2.92850E-01	2.79063E-02
7	2.99400E-01	2.48670E-03
8	3.09400E-01	9.21000E-04
9	3.15610E-01	6.35490E-03
10	3.19700E-01	1.01310E-03
11	3.25400E-01	2.48670E-03
12	3.49200E-01	1.84200E-03
13	3.77390E-01	4.11687E-02
14	4.27790E-01	4.54974E-02
15	4.31750E-01	4.05240E-02
16	4.60900E-01	1.19730E-03
17	4.67300E-01	1.28940E-03
18	4.84400E-01	2.94720E-03
19	4.88100E-01	1.84200E-03
20	4.90700E-01	3.40770E-03
21	5.11000E-01	0.0
22	5.14000E-01	9.21000E-04
23	5.34800E-01	1.38150E-03
24	5.51650E-01	3.13140E-03
25	5.66430E-01	4.69710E-03
26	5.72930E-01	2.08146E-02
27	5.79800E-01	9.21000E-04
28	5.86100E-01	1.93410E-03
29	5.98200E-01	3.40770E-03
30	6.08900E-01	1.75911E-02
31	6.46100E-01	1.56570E-03
32	6.52200E-01	1.47360E-03
33	6.59100E-01	3.68400E-03
34	6.63800E-01	1.19730E-03
35	6.76600E-01	1.19730E-03
36	7.01600E-01	1.93410E-03
37	7.33940E-01	1.61175E-02
38	7.70800E-01	4.88130E-03
39	7.81000E-01	1.10520E-03
40	7.88700E-01	3.49980E-03
41	8.59300E-01	2.48670E-03
42	8.90700E-01	2.57880E-03
43	8.97600E-01	5.24970E-03
44	9.12050E-01	1.05915E-02
45	9.46200E-01	1.47360E-03
46	9.52100E-01	1.74069E-02
47	9.59000E-01	2.76300E-03
48	9.61400E-01	4.60500E-03
49	9.74900E-01	9.21000E-04
50	1.07420E+00	1.10520E-03
51	1.14450E+00	1.93410E-03
52	1.24550E+00	4.97340E-03
53	1.38050E+00	1.19730E-03
54	1.44890E+00	3.40770E-03
55	1.51580E+00	1.19730E-03
56	1.56100E+00	1.28940E-03
57	5.11006E-01	1.42763E+00

Table 3 (Continued)

NO. 40 NUCLIDE ID. = 310760

NUMBER OF GAMMA RAYS = 107

NO.	ENERGY(MEV)	INTENSITY(1/DECAY)	NO.	ENERGY(MEV)	INTENSITY(1/DECAY)
1	3.35900E-01	5.26400E-02	71	2.75995E+00	1.09886E-02
2	4.31000E-01	9.21200E-02	72	2.77910E+00	7.96180E-03
3	5.45510E-01	2.59252E-01	73	2.78270E+00	1.01332E-02
4	5.62930E-01	6.58000E-01	74	2.84350E+00	1.59236E-02
5	6.61400E-01	7.36960E-03	75	2.86810E+00	3.48740E-03
6	8.43800E-01	1.13834E-02	76	2.88290E+00	1.38180E-03
7	8.47150E-01	3.52030E-02	77	2.91460E+00	7.36960E-03
8	8.85830E-01	1.31600E-02	78	2.91985E+00	9.08040E-02
9	9.11400E-01	1.00016E-02	79	2.97090E+00	3.94800E-03
10	9.27050E-01	9.21199E-03	80	2.98120E+00	2.03980E-03
11	9.76500E-01	4.60600E-02	81	3.03460E+00	5.19820E-03
12	1.01420E+00	3.55320E-03	82	3.06990E+00	9.21199E-03
13	1.04360E+00	2.96100E-03	83	3.13070E+00	2.10560E-03
14	1.05170E+00	4.67180E-03	84	3.14140E+00	4.22436E-02
15	1.10841E+00	1.57920E-01	85	3.14530E+00	2.96100E-03
16	1.17570E+00	4.67180E-03	86	3.19060E+00	2.10560E-03
17	1.18210E+00	5.06660E-03	87	3.27590E+00	5.79040E-03
18	1.20802E+00	1.52656E-02	88	3.28360E+00	1.71080E-03
19	1.24910E+00	6.38260E-03	89	3.32520E+00	1.11860E-03
20	1.25990E+00	2.96100E-03	90	3.32870E+00	1.97400E-03
21	1.27305E+00	1.19756E-02	91	3.33460E+00	1.90820E-03
22	1.28290E+00	2.82940E-03	92	3.36650E+00	1.44760E-03
23	1.31060E+00	2.76360E-03	93	3.38875E+00	2.82282E-02
24	1.34813E+00	7.43540E-03	94	3.40240E+00	1.31600E-03
25	1.35890E+00	1.84240E-03	95	3.46550E+00	1.38180E-03
26	1.44390E+00	2.56620E-03	96	3.49670E+00	1.05280E-03
27	1.46120E+00	3.29000E-03	97	3.55950E+00	5.85620E-03
28	1.48250E+00	4.93500E-03	98	3.67560E+00	4.47440E-03
29	1.48960E+00	2.30300E-03	99	3.73690E+00	1.57920E-03
30	1.50230E+00	4.86920E-03	100	3.75210E+00	1.64500E-03
31	1.54600E+00	4.27700E-03	101	3.84230E+00	9.21199E-04
32	1.58390E+00	1.97400E-03	102	3.91330E+00	1.25020E-03
33	1.61270E+00	4.47440E-03	103	3.92520E+00	3.35580E-03
34	1.63400E+00	1.13834E-02	104	3.95170E+00	4.23094E-02
35	1.63930E+00	5.52720E-02	105	3.99430E+00	2.23720E-03
36	1.64280E+00	9.27780E-03	106	4.12180E+00	2.50040E-03
37	1.66030E+00	7.69860E-03	107	4.25330E+00	2.23720E-03
38	1.72190E+00	1.44760E-03			
39	1.73270E+00	7.23800E-03			
40	1.81110E+00	8.35660E-03			
41	1.87830E+00	3.61900E-03			
42	1.89270E+00	4.01380E-03			
43	1.90220E+00	4.21120E-03			
44	1.91270E+00	5.85620E-03			
45	1.92460E+00	1.97400E-03			
46	1.94030E+00	6.84320E-03			
47	1.98040E+00	2.17140E-03			
48	2.04070E+00	3.29000E-03			
49	2.07375E+00	4.23094E-02			
50	2.09190E+00	1.77660E-03			
51	2.12946E+00	2.19772E-02			
52	2.18520E+00	4.93500E-03			
53	2.20386E+00	1.36864E-02			
54	2.21436E+00	2.23062E-02			
55	2.27880E+00	4.40860E-03			
56	2.34740E+00	4.34280E-03			
57	2.35688E+00	2.46092E-02			
58	2.36980E+00	2.76360E-03			
59	2.43560E+00	3.68480E-03			
60	2.47660E+00	2.17140E-03			
61	2.48110E+00	1.97400E-03			
62	2.48960E+00	1.97400E-03			
63	2.52400E+00	7.96180E-03			
64	2.57855E+00	2.23720E-02			
65	2.59100E+00	2.69780E-03			
66	2.61920E+00	2.24378E-02			
67	2.66880E+00	1.57920E-03			
68	2.68090E+00	3.22420E-03			
69	2.69150E+00	1.51340E-03			
70	2.70050E+00	1.97400E-03			

Table 4 Estimated gamma-ray energy spectra of odd-even light mass nuclides.

ENERGY (MEV)	Q-VALUES 5 MEV	7 MEV	9 MEV	11 MEV
0.1	5.73080E-02	3.15460E-02	2.08350E-02	1.59510E-02
0.2	1.71920E-01	9.46380E-02	6.25050E-02	4.78540E-02
0.3	2.86540E-01	1.57730E-01	1.04170E-01	7.97570E-02
0.4	4.01160E-01	2.20820E-01	1.45840E-01	1.11660E-01
0.5	5.15770E-01	2.83910E-01	1.87510E-01	1.43560E-01
0.6	6.30390E-01	3.47010E-01	2.29180E-01	1.75460E-01
0.7	6.20790E-01	3.53400E-01	2.36890E-01	1.82500E-01
0.8	6.04200E-01	3.58000E-01	2.44700E-01	1.90140E-01
0.9	5.81510E-01	3.60520E-01	2.52310E-01	1.98160E-01
1.0	5.53840E-01	3.60820E-01	2.59480E-01	2.06370E-01
1.1	5.22370E-01	3.58940E-01	2.66010E-01	2.14590E-01
1.2	4.88310E-01	3.55040E-01	2.71770E-01	2.22670E-01
1.3	4.52770E-01	3.49380E-01	2.76690E-01	2.30460E-01
1.4	4.16770E-01	3.42280E-01	2.80740E-01	2.37880E-01
1.5	3.81200E-01	3.34110E-01	2.83950E-01	2.44860E-01
1.6	3.46790E-01	3.25240E-01	2.86390E-01	2.51340E-01
1.7	3.14140E-01	3.16020E-01	2.88140E-01	2.57290E-01
1.8	2.83710E-01	3.06790E-01	2.89310E-01	2.62720E-01
1.9	2.55790E-01	2.97820E-01	2.89990E-01	2.67600E-01
2.0	2.30600E-01	2.89340E-01	2.90290E-01	2.71950E-01
2.1	2.08200E-01	2.81550E-01	2.90290E-01	2.75790E-01
2.2	1.88600E-01	2.74540E-01	2.90080E-01	2.79100E-01
2.3	1.71690E-01	2.68390E-01	2.89710E-01	2.81900E-01
2.4	1.57340E-01	2.63090E-01	2.89200E-01	2.84190E-01
2.5	1.45330E-01	2.58630E-01	2.88590E-01	2.85970E-01
2.6	1.35440E-01	2.54910E-01	2.87860E-01	2.87220E-01
2.7	1.27420E-01	2.51850E-01	2.86990E-01	2.87930E-01
2.8	1.21020E-01	2.49310E-01	2.85950E-01	2.88100E-01
2.9	1.15970E-01	2.47180E-01	2.84710E-01	2.87710E-01
3.0	1.12050E-01	2.45320E-01	2.83230E-01	2.86750E-01
3.1	9.09440E-02	2.21790E-01	2.66060E-01	2.74650E-01
3.2	7.40340E-02	2.00820E-01	2.49890E-01	2.62730E-01
3.3	6.06440E-02	1.82200E-01	2.34700E-01	2.51010E-01
3.4	5.01670E-02	1.65730E-01	2.20480E-01	2.39540E-01
3.5	4.20690E-02	1.51190E-01	2.07180E-01	2.28350E-01
3.6	2.97570E-02	1.25270E-01	1.82920E-01	2.08730E-01
3.7	2.03870E-02	1.02500E-01	1.60380E-01	1.89930E-01
3.8	1.33900E-02	8.26440E-02	1.39550E-01	1.72010E-01
3.9	8.27680E-03	6.54550E-02	1.20420E-01	1.55030E-01
4.0	4.63070E-03	5.06900E-02	1.02960E-01	1.39020E-01
4.1	2.93730E-03	4.21890E-02	9.14920E-02	1.27690E-01
4.2	1.78310E-03	3.48770E-02	8.09590E-02	1.16920E-01
4.3	1.02600E-03	2.86300E-02	7.13350E-02	1.06730E-01
4.4	5.51920E-04	2.33300E-02	6.25900E-02	9.71300E-02
4.5	2.72060E-04	1.88660E-02	5.46830E-02	8.81240E-02
4.6	1.19070E-04	1.51330E-02	4.75720E-02	7.97130E-02
4.7	4.38430E-05	1.20350E-02	4.12100E-02	7.18870E-02
4.8	1.22180E-05	9.48470E-03	3.55450E-02	6.46350E-02
4.9	1.96440E-06	7.40270E-03	3.05260E-02	5.79400E-02
5.0	0.0	5.71780E-03	2.61020E-02	5.17820E-02
5.1	0.0	4.36700E-03	2.22220E-02	4.61390E-02
5.2	0.0	3.29500E-03	1.88340E-02	4.09850E-02
5.3	0.0	2.45320E-03	1.58910E-02	3.62960E-02
5.4	0.0	1.80000E-03	1.33460E-02	3.20450E-02
5.5	0.0	1.29950E-03	1.11570E-02	2.82030E-02
5.6	0.0	9.21470E-04	9.28170E-03	2.47440E-02
5.7	0.0	6.40320E-04	7.68420E-03	2.16420E-02
5.8	0.0	4.34850E-04	6.32950E-03	1.88680E-02
5.9	0.0	2.87650E-04	5.18650E-03	1.63960E-02
6.0	0.0	1.84550E-04	4.22700E-03	1.42030E-02

Table 4 (Continued)

ENERGY (MEV)	Q-VALUES 5 MEV	7 MEV	9 MEV	11 MEV
6.1	0.0	1.14220E-04	3.42560E-03	1.22630E-02
6.2	0.0	6.77010E-05	2.75980E-03	1.05530E-02
6.3	0.0	3.80610E-05	2.20960E-03	9.05140E-03
6.4	0.0	2.00190E-05	1.75770E-03	7.73760E-03
6.5	0.0	9.65510E-06	1.38850E-03	6.59220E-03
6.6	0.0	4.13720E-06	1.08890E-03	5.59730E-03
6.7	0.0	1.49230E-06	8.47220E-04	4.73630E-03
6.8	0.0	4.07650E-07	6.53710E-04	3.99400E-03
6.9	0.0	6.42900E-08	4.99860E-04	3.35620E-03
7.0	0.0	0.0	3.78520E-04	2.81040E-03
7.1	0.0	0.0	2.83620E-04	2.34490E-03
7.2	0.0	0.0	2.10070E-04	1.94940E-03
7.3	0.0	0.0	1.53640E-04	1.61460E-03
7.4	0.0	0.0	1.10810E-04	1.33220E-03
7.5	0.0	0.0	7.86850E-05	1.09500E-03
7.6	0.0	0.0	5.49130E-05	8.96430E-04
7.7	0.0	0.0	3.75790E-05	7.30830E-04
7.8	0.0	0.0	2.51490E-05	5.93270E-04
7.9	0.0	0.0	1.64040E-05	4.79450E-04
8.0	0.0	0.0	1.03850E-05	3.85670E-04
8.1	0.0	0.0	6.34580E-06	3.08700E-04
8.2	0.0	0.0	3.71610E-06	2.45820E-04
8.3	0.0	0.0	2.06540E-06	1.94680E-04
8.4	0.0	0.0	1.07460E-06	1.53280E-04
8.5	0.0	0.0	5.13040E-07	1.19940E-04
8.6	0.0	0.0	2.17750E-07	9.32230E-05
8.7	0.0	0.0	7.78470E-08	7.19420E-05
8.8	0.0	0.0	2.10900E-08	5.50910E-05
8.9	0.0	0.0	3.30100E-09	4.18360E-05
9.0	0.0	0.0	0.0	3.14810E-05
9.1	0.0	0.0	0.0	2.34540E-05
9.2	0.0	0.0	0.0	1.72840E-05
9.3	0.0	0.0	0.0	1.25840E-05
9.4	0.0	0.0	0.0	9.04050E-06
9.5	0.0	0.0	0.0	6.39820E-06
9.6	0.0	0.0	0.0	4.45260E-06
9.7	0.0	0.0	0.0	3.04010E-06
9.8	0.0	0.0	0.0	2.03100E-06
9.9	0.0	0.0	0.0	1.32310E-06
10.0	0.0	0.0	0.0	8.36900E-07
10.1	0.0	0.0	0.0	5.11230E-07
10.2	0.0	0.0	0.0	2.99420E-07
10.3	0.0	0.0	0.0	1.66510E-07
10.4	0.0	0.0	0.0	8.67250E-08
10.5	0.0	0.0	0.0	4.14620E-08
10.6	0.0	0.0	0.0	1.76300E-08
10.7	0.0	0.0	0.0	6.31710E-09
10.8	0.0	0.0	0.0	1.71600E-09
10.9	0.0	0.0	0.0	2.69410E-10
11.0	0.0	0.0	0.0	0.0
11.1	0.0	0.0	0.0	0.0
11.2	0.0	0.0	0.0	0.0
11.3	0.0	0.0	0.0	0.0
11.4	0.0	0.0	0.0	0.0
11.5	0.0	0.0	0.0	0.0
11.6	0.0	0.0	0.0	0.0
11.7	0.0	0.0	0.0	0.0
11.8	0.0	0.0	0.0	0.0
11.9	0.0	0.0	0.0	0.0
12.0	0.0	0.0	0.0	0.0

Table 5 Estimated gamma-ray energy spectra of odd-odd light mass nuclides.

ENERGY (MEV)	Q-VALUES 5 MEV	7 MEV	9 MEV	11 MEV
0.1	1.69900E-02	1.58170E-02	1.44590E-02	1.24910E-02
0.2	5.09710E-02	4.74520E-02	4.33770E-02	3.74730E-02
0.3	8.49520E-02	7.90870E-02	7.22940E-02	6.24550E-02
0.4	1.18930E-01	1.10720E-01	1.01210E-01	8.74370E-02
0.5	1.52910E-01	1.42360E-01	1.30130E-01	1.12420E-01
0.6	1.86890E-01	1.73990E-01	1.59050E-01	1.37400E-01
0.7	1.95460E-01	1.82300E-01	1.66790E-01	1.44190E-01
0.8	2.03970E-01	1.90930E-01	1.75070E-01	1.51690E-01
0.9	2.12100E-01	1.99550E-01	1.83610E-01	1.59720E-01
1.0	2.19750E-01	2.07980E-01	1.92240E-01	1.68140E-01
1.1	2.27020E-01	2.16190E-01	2.00860E-01	1.76840E-01
1.2	2.34240E-01	2.24280E-01	2.09500E-01	1.85780E-01
1.3	2.41790E-01	2.32480E-01	2.18250E-01	1.94970E-01
1.4	2.50170E-01	2.41050E-01	2.27240E-01	2.04410E-01
1.5	2.59850E-01	2.50290E-01	2.36640E-01	2.14160E-01
1.6	2.71240E-01	2.60490E-01	2.46630E-01	2.24250E-01
1.7	2.84680E-01	2.71890E-01	2.57340E-01	2.34710E-01
1.8	3.00380E-01	2.84660E-01	2.68880E-01	2.45560E-01
1.9	3.18420E-01	2.98900E-01	2.81310E-01	2.56780E-01
2.0	3.38710E-01	3.14600E-01	2.94610E-01	2.68310E-01
2.1	3.61060E-01	3.31660E-01	3.08710E-01	2.80090E-01
2.2	3.85120E-01	3.49890E-01	3.23480E-01	2.92000E-01
2.3	4.10450E-01	3.69030E-01	3.38730E-01	3.03900E-01
2.4	4.36550E-01	3.88750E-01	3.54240E-01	3.15630E-01
2.5	4.62850E-01	4.08660E-01	3.69730E-01	3.27020E-01
2.6	4.88800E-01	4.28390E-01	3.84930E-01	3.37880E-01
2.7	5.13870E-01	4.47530E-01	3.99560E-01	3.48050E-01
2.8	5.37560E-01	4.65730E-01	4.13350E-01	3.57350E-01
2.9	4.76860E-01	4.38700E-01	3.98240E-01	3.49380E-01
3.0	4.27920E-01	4.14480E-01	3.83820E-01	3.41180E-01
3.1	3.43720E-01	3.64520E-01	3.50730E-01	3.21090E-01
3.2	2.76440E-01	3.20060E-01	3.19850E-01	3.01600E-01
3.3	2.23310E-01	2.80700E-01	2.91160E-01	2.82780E-01
3.4	1.66430E-01	2.33510E-01	2.54480E-01	2.57950E-01
3.5	1.22510E-01	1.92260E-01	2.20850E-01	2.34350E-01
3.6	8.12620E-02	1.48450E-01	1.83070E-01	2.07110E-01
3.7	5.03970E-02	1.10710E-01	1.48940E-01	1.81590E-01
3.8	2.77520E-02	7.84540E-02	1.18300E-01	1.57800E-01
3.9	1.65960E-02	5.99300E-02	9.91860E-02	1.41600E-01
4.0	8.74800E-03	4.42510E-02	8.21190E-02	1.26470E-01
4.1	5.46740E-03	3.63770E-02	7.24640E-02	1.16500E-01
4.2	3.27120E-03	2.97220E-02	6.38150E-02	1.07090E-01
4.3	1.85550E-03	2.41310E-02	5.60950E-02	9.82630E-02
4.4	9.84290E-04	1.94630E-02	4.92300E-02	9.00020E-02
4.5	4.78570E-04	1.55900E-02	4.31480E-02	8.23030E-02
4.6	2.06650E-04	1.23980E-02	3.77760E-02	7.51560E-02
4.7	7.50840E-05	9.78660E-03	3.30480E-02	6.85460E-02
4.8	2.06510E-05	7.66530E-03	2.88970E-02	6.24520E-02
4.9	3.27770E-06	5.95570E-03	2.52650E-02	5.68530E-02
5.0	0.0	4.58930E-03	2.20950E-02	5.17250E-02
5.1	0.0	3.50670E-03	1.93340E-02	4.70420E-02
5.2	0.0	2.65700E-03	1.69360E-02	4.27770E-02
5.3	0.0	1.99680E-03	1.48560E-02	3.89030E-02
5.4	0.0	1.48930E-03	1.30560E-02	3.53900E-02
5.5	0.0	1.10370E-03	1.15000E-02	3.22110E-02
5.6	0.0	8.14340E-04	1.01560E-02	2.93380E-02
5.7	0.0	6.00040E-04	8.99610E-03	2.67450E-02
5.8	0.0	4.43570E-04	7.99480E-03	2.44060E-02
5.9	0.0	3.31020E-04	7.13020E-03	2.22970E-02
6.0	0.0	2.51290E-04	6.38280E-03	2.03950E-02

Table 5 (Continued)

ENERGY (MEV)	Q-VALUES 5 MEV	7 MEV	9 MEV	11 MEV
6.1	0.0	1.95660E-04	5.73560E-03	1.86790E-02
6.2	0.0	1.16370E-04	4.74440E-03	1.63640E-02
6.3	0.0	6.67040E-05	3.92800E-03	1.43440E-02
6.4	0.0	3.69410E-05	3.25780E-03	1.25830E-02
6.5	0.0	2.00500E-05	2.70910E-03	1.10490E-02
6.6	0.0	1.11010E-05	2.26110E-03	9.71380E-03
6.7	0.0	3.99570E-06	1.71580E-03	8.07500E-03
6.8	0.0	1.08940E-06	1.28140E-03	6.66800E-03
6.9	0.0	1.71510E-07	9.38360E-04	5.46510E-03
7.0	0.0	0.0	6.70010E-04	4.44110E-03
7.1	0.0	0.0	4.62310E-04	3.57360E-03
7.2	0.0	0.0	3.44980E-04	2.99550E-03
7.3	0.0	0.0	2.54210E-04	2.50170E-03
7.4	0.0	0.0	1.84730E-04	2.08130E-03
7.5	0.0	0.0	1.32190E-04	1.72490E-03
7.6	0.0	0.0	9.29620E-05	1.42370E-03
7.7	0.0	0.0	6.41130E-05	1.17030E-03
7.8	0.0	0.0	4.32430E-05	9.57870E-04
7.9	0.0	0.0	2.84290E-05	7.80480E-04
8.0	0.0	0.0	1.81400E-05	6.32980E-04
8.1	0.0	0.0	1.11730E-05	5.10830E-04
8.2	0.0	0.0	6.59520E-06	4.10120E-04
8.3	0.0	0.0	3.69500E-06	3.27460E-04
8.4	0.0	0.0	1.93810E-06	2.59940E-04
8.5	0.0	0.0	9.32760E-07	2.05060E-04
8.6	0.0	0.0	3.99110E-07	1.60690E-04
8.7	0.0	0.0	1.43850E-07	1.25020E-04
8.8	0.0	0.0	3.92920E-08	9.65220E-05
8.9	0.0	0.0	6.20070E-09	7.38940E-05
9.0	0.0	0.0	0.0	5.60570E-05
9.1	0.0	0.0	0.0	4.21030E-05
9.2	0.0	0.0	0.0	3.12780E-05
9.3	0.0	0.0	0.0	2.29560E-05
9.4	0.0	0.0	0.0	1.66240E-05
9.5	0.0	0.0	0.0	1.18590E-05
9.6	0.0	0.0	0.0	8.31860E-06
9.7	0.0	0.0	0.0	5.72470E-06
9.8	0.0	0.0	0.0	3.85450E-06
9.9	0.0	0.0	0.0	2.53070E-06
10.0	0.0	0.0	0.0	1.61320E-06
10.1	0.0	0.0	0.0	9.93070E-07
10.2	0.0	0.0	0.0	5.86090E-07
10.3	0.0	0.0	0.0	3.28410E-07
10.4	0.0	0.0	0.0	1.72350E-07
10.5	0.0	0.0	0.0	8.30160E-08
10.6	0.0	0.0	0.0	3.55630E-08
10.7	0.0	0.0	0.0	1.28370E-08
10.8	0.0	0.0	0.0	3.51290E-09
10.9	0.0	0.0	0.0	5.55590E-10
11.0	0.0	0.0	0.0	0.0
11.1	0.0	0.0	0.0	0.0
11.2	0.0	0.0	0.0	0.0
11.3	0.0	0.0	0.0	0.0
11.4	0.0	0.0	0.0	0.0
11.5	0.0	0.0	0.0	0.0
11.6	0.0	0.0	0.0	0.0
11.7	0.0	0.0	0.0	0.0
11.8	0.0	0.0	0.0	0.0
11.9	0.0	0.0	0.0	0.0
12.0	0.0	0.0	0.0	0.0

Table 6 Esitmated gamma-ray energy spectra of even-even light mass nuclides.

ENERGY (MEV)	Q-VALUES 5 MEV	7 MEV	9 MEV	11 MEV
0.1	5.83450E-02	3.86510E-02	2.78860E-02	2.17190E-02
0.2	1.75030E-01	1.15950E-01	8.36570E-02	6.51560E-02
0.3	2.91720E-01	1.93260E-01	1.39430E-01	1.08590E-01
0.4	4.08410E-01	2.70560E-01	1.95200E-01	1.52030E-01
0.5	5.25100E-01	3.47860E-01	2.50970E-01	1.95470E-01
0.6	6.41790E-01	4.25160E-01	3.06740E-01	2.38900E-01
0.7	6.43170E-01	4.35990E-01	3.16820E-01	2.47770E-01
0.8	6.37290E-01	4.45130E-01	3.26830E-01	2.57090E-01
0.9	6.24110E-01	4.51840E-01	3.36280E-01	2.66550E-01
1.0	6.04100E-01	4.55600E-01	3.44760E-01	2.75830E-01
1.1	5.78100E-01	4.56050E-01	3.51910E-01	2.84620E-01
1.2	5.47150E-01	4.53040E-01	3.57440E-01	2.92640E-01
1.3	5.12370E-01	4.46560E-01	3.61140E-01	2.99660E-01
1.4	4.74910E-01	4.36750E-01	3.62850E-01	3.05480E-01
1.5	4.35870E-01	4.23870E-01	3.62500E-01	3.09940E-01
1.6	3.96220E-01	4.08260E-01	3.60090E-01	3.12940E-01
1.7	3.56840E-01	3.90310E-01	3.55650E-01	3.14400E-01
1.8	3.18460E-01	3.70450E-01	3.49290E-01	3.14300E-01
1.9	2.81660E-01	3.49130E-01	3.41120E-01	3.12660E-01
2.0	2.46910E-01	3.26780E-01	3.31320E-01	3.09500E-01
2.1	2.14540E-01	3.03840E-01	3.20070E-01	3.04910E-01
2.2	1.84760E-01	2.80680E-01	3.07580E-01	2.98980E-01
2.3	1.57690E-01	2.57660E-01	2.94060E-01	2.91830E-01
2.4	1.33350E-01	2.35090E-01	2.79710E-01	2.83580E-01
2.5	1.11730E-01	2.13210E-01	2.64750E-01	2.74370E-01
2.6	9.27040E-02	1.92240E-01	2.49370E-01	2.64340E-01
2.7	7.61550E-02	1.72350E-01	2.33780E-01	2.53640E-01
2.8	6.19090E-02	1.53650E-01	2.18130E-01	2.42400E-01
2.9	4.97790E-02	1.36220E-01	2.02610E-01	2.30760E-01
3.0	3.95630E-02	1.20110E-01	1.87330E-01	2.18850E-01
3.1	3.10570E-02	1.05340E-01	1.72440E-01	2.06790E-01
3.2	2.40590E-02	9.18780E-02	1.58030E-01	1.94700E-01
3.3	1.83740E-02	7.97090E-02	1.44200E-01	1.82680E-01
3.4	1.38150E-02	6.87770E-02	1.31020E-01	1.70810E-01
3.5	1.02120E-02	5.90210E-02	1.18530E-01	1.59170E-01
3.6	7.40810E-03	5.03700E-02	1.06780E-01	1.47840E-01
3.7	5.26220E-03	4.27450E-02	9.57990E-02	1.36880E-01
3.8	3.65030E-03	3.60670E-02	8.55880E-02	1.26320E-01
3.9	2.46470E-03	3.02530E-02	7.61510E-02	1.16220E-01
4.0	1.61300E-03	2.52230E-02	6.74790E-02	1.06590E-01
4.1	1.01760E-03	2.08970E-02	5.95520E-02	9.74530E-02
4.2	6.14440E-04	1.72000E-02	5.23450E-02	8.88320E-02
4.3	3.51680E-04	1.40610E-02	4.58250E-02	8.07290E-02
4.4	1.88210E-04	1.14130E-02	3.99580E-02	7.31450E-02
4.5	9.23020E-05	9.19460E-03	3.47030E-02	6.60730E-02
4.6	4.01940E-05	7.34860E-03	3.00190E-02	5.95070E-02
4.7	1.47250E-05	5.82390E-03	2.58640E-02	5.34320E-02
4.8	4.08240E-06	4.57440E-03	2.21960E-02	4.78330E-02
4.9	6.53040E-07	3.55850E-03	1.89710E-02	4.26910E-02
5.0	0.0	2.73980E-03	1.61490E-02	3.79870E-02
5.1	0.0	2.08600E-03	1.36910E-02	3.36980E-02
5.2	0.0	1.56910E-03	1.15590E-02	2.98020E-02
5.3	0.0	1.16470E-03	9.71740E-03	2.62740E-02
5.4	0.0	8.52060E-04	8.13420E-03	2.30930E-02
5.5	0.0	6.13360E-04	6.77880E-03	2.02330E-02
5.6	0.0	4.33670E-04	5.62350E-03	1.76710E-02
5.7	0.0	3.00490E-04	4.64330E-03	1.53850E-02
5.8	0.0	2.03490E-04	3.81520E-03	1.33520E-02
5.9	0.0	1.34230E-04	3.11900E-03	1.15510E-02
6.0	0.0	8.58740E-05	2.53630E-03	9.96050E-03

Table 6 (Continued)

ENERGY (MEV)	Q-VALUES 5 MEV	7 MEV	9 MEV	11 MEV
6.1	0.0	5.29970E-05	2.05110E-03	8.56140E-03
6.2	0.0	3.13250E-05	1.64910E-03	7.33510E-03
6.3	0.0	1.75600E-05	1.31770E-03	6.26400E-03
6.4	0.0	9.20980E-06	1.04620E-03	5.33190E-03
6.5	0.0	4.42870E-06	8.24830E-04	4.52360E-03
6.6	0.0	1.89200E-06	6.45570E-04	3.82520E-03
6.7	0.0	6.80320E-07	5.01310E-04	3.22390E-03
6.8	0.0	1.85240E-07	3.86030E-04	2.70800E-03
6.9	0.0	2.91150E-08	2.94570E-04	2.26700E-03
7.0	0.0	0.0	2.22580E-04	1.89130E-03
7.1	0.0	0.0	1.66400E-04	1.57230E-03
7.2	0.0	0.0	1.22960E-04	1.30250E-03
7.3	0.0	0.0	8.97100E-05	1.07510E-03
7.4	0.0	0.0	6.45340E-05	8.84020E-04
7.5	0.0	0.0	4.57010E-05	7.24120E-04
7.6	0.0	0.0	3.18030E-05	5.90770E-04
7.7	0.0	0.0	2.16980E-05	4.79980E-04
7.8	0.0	0.0	1.44750E-05	3.88290E-04
7.9	0.0	0.0	9.40970E-06	3.12690E-04
8.0	0.0	0.0	5.93560E-06	2.50610E-04
8.1	0.0	0.0	3.61330E-06	1.99860E-04
8.2	0.0	0.0	2.10760E-06	1.58540E-04
8.3	0.0	0.0	1.16650E-06	1.25060E-04
8.4	0.0	0.0	6.04260E-07	9.80700E-05
8.5	0.0	0.0	2.87130E-07	7.64150E-05
8.6	0.0	0.0	1.21270E-07	5.91380E-05
8.7	0.0	0.0	4.31320E-08	4.54340E-05
8.8	0.0	0.0	1.16220E-08	3.46320E-05
8.9	0.0	0.0	1.80860E-09	2.61740E-05
9.0	0.0	0.0	0.0	1.95990E-05
9.1	0.0	0.0	0.0	1.45290E-05
9.2	0.0	0.0	0.0	1.06510E-05
9.3	0.0	0.0	0.0	7.71370E-06
9.4	0.0	0.0	0.0	5.51130E-06
9.5	0.0	0.0	0.0	3.87880E-06
9.6	0.0	0.0	0.0	2.68390E-06
9.7	0.0	0.0	0.0	1.82190E-06
9.8	0.0	0.0	0.0	1.20990E-06
9.9	0.0	0.0	0.0	7.83440E-07
10.0	0.0	0.0	0.0	4.92520E-07
10.1	0.0	0.0	0.0	2.98980E-07
10.2	0.0	0.0	0.0	1.74000E-07
10.3	0.0	0.0	0.0	9.61380E-08
10.4	0.0	0.0	0.0	4.97440E-08
10.5	0.0	0.0	0.0	2.36230E-08
10.6	0.0	0.0	0.0	9.97620E-09
10.7	0.0	0.0	0.0	3.54980E-09
10.8	0.0	0.0	0.0	9.57410E-10
10.9	0.0	0.0	0.0	1.49220E-10
11.0	0.0	0.0	0.0	0.0
11.1	0.0	0.0	0.0	0.0
11.2	0.0	0.0	0.0	0.0
11.3	0.0	0.0	0.0	0.0
11.4	0.0	0.0	0.0	0.0
11.5	0.0	0.0	0.0	0.0
11.6	0.0	0.0	0.0	0.0
11.7	0.0	0.0	0.0	0.0
11.8	0.0	0.0	0.0	0.0
11.9	0.0	0.0	0.0	0.0
12.0	0.0	0.0	0.0	0.0

Table 7 Estimated gamma-ray energy spectra of even-odd light mass nuclides.

ENERGY (MEV)	Q-VALUES 5 MEV	7 MEV	9 MEV	11 MEV
0.1	5.05770E-02	2.88610E-02	2.00390E-02	1.57170E-02
0.2	1.51730E-01	8.65830E-02	6.01180E-02	4.71510E-02
0.3	2.52880E-01	1.44310E-01	1.00200E-01	7.85850E-02
0.4	3.54040E-01	2.02030E-01	1.40280E-01	1.10020E-01
0.5	4.55190E-01	2.59750E-01	1.80350E-01	1.41450E-01
0.6	5.56350E-01	3.17470E-01	2.20430E-01	1.72890E-01
0.7	5.50090E-01	3.24160E-01	2.28210E-01	1.79980E-01
0.8	5.38040E-01	3.29250E-01	2.36060E-01	1.87610E-01
0.9	5.20870E-01	3.32480E-01	2.43690E-01	1.95560E-01
1.0	4.99490E-01	3.33790E-01	2.50910E-01	2.03690E-01
1.1	4.74920E-01	3.33310E-01	2.57600E-01	2.11860E-01
1.2	4.48240E-01	3.31320E-01	2.63730E-01	2.19990E-01
1.3	4.20490E-01	3.28170E-01	2.69320E-01	2.28020E-01
1.4	3.92630E-01	3.24280E-01	2.74450E-01	2.35920E-01
1.5	3.65520E-01	3.20080E-01	2.79210E-01	2.43680E-01
1.6	3.39840E-01	3.15960E-01	2.83730E-01	2.51290E-01
1.7	3.16160E-01	3.12270E-01	2.88110E-01	2.58740E-01
1.8	2.94880E-01	3.09280E-01	2.92450E-01	2.66030E-01
1.9	2.76240E-01	3.07200E-01	2.96820E-01	2.73140E-01
2.0	2.60360E-01	3.06140E-01	3.01270E-01	2.80040E-01
2.1	2.47220E-01	3.06140E-01	3.05800E-01	2.86700E-01
2.2	2.36700E-01	3.07160E-01	3.10400E-01	2.93040E-01
2.3	2.28630E-01	3.09100E-01	3.15000E-01	2.99010E-01
2.4	2.22720E-01	3.11820E-01	3.19550E-01	3.04540E-01
2.5	2.18700E-01	3.15130E-01	3.23950E-01	3.09560E-01
2.6	2.16250E-01	3.18820E-01	3.28090E-01	3.13980E-01
2.7	2.15060E-01	3.22700E-01	3.31880E-01	3.17730E-01
2.8	1.80840E-01	2.96210E-01	3.15490E-01	3.07750E-01
2.9	1.52600E-01	2.72280E-01	2.99820E-01	2.97640E-01
3.0	1.29550E-01	2.50750E-01	2.84880E-01	2.87440E-01
3.1	1.10940E-01	2.31440E-01	2.70680E-01	2.77230E-01
3.2	9.60640E-02	2.14170E-01	2.57220E-01	2.67030E-01
3.3	7.12920E-02	1.80260E-01	2.29460E-01	2.46290E-01
3.4	5.15250E-02	1.49900E-01	2.03240E-01	2.26080E-01
3.5	3.59780E-02	1.22910E-01	1.78620E-01	2.06490E-01
3.6	2.39430E-02	9.90840E-02	1.55680E-01	1.87650E-01
3.7	1.47900E-02	7.82180E-02	1.34420E-01	1.69630E-01
3.8	1.03220E-02	6.63640E-02	1.20770E-01	1.57210E-01
3.9	7.00960E-03	5.59630E-02	1.08050E-01	1.45220E-01
4.0	4.61320E-03	4.68960E-02	9.62600E-02	1.33710E-01
4.1	2.92620E-03	3.90450E-02	8.53970E-02	1.22720E-01
4.2	1.77630E-03	3.22910E-02	7.54430E-02	1.12280E-01
4.3	1.02190E-03	2.65200E-02	6.63740E-02	1.02410E-01
4.4	5.49640E-04	2.16220E-02	5.81520E-02	9.31080E-02
4.5	2.70870E-04	1.74950E-02	5.07390E-02	8.43940E-02
4.6	1.18510E-04	1.40410E-02	4.40870E-02	7.62600E-02
4.7	4.36150E-05	1.11740E-02	3.81490E-02	6.86980E-02
4.8	1.21470E-05	8.81160E-03	3.28740E-02	6.16960E-02
4.9	1.95160E-06	6.88150E-03	2.82110E-02	5.52370E-02
5.0	0.0	5.31840E-03	2.41070E-02	4.93030E-02
5.1	0.0	4.06440E-03	2.05130E-02	4.38700E-02
5.2	0.0	3.06830E-03	1.73810E-02	3.89150E-02
5.3	0.0	2.28570E-03	1.46620E-02	3.44120E-02
5.4	0.0	1.67790E-03	1.23140E-02	3.03350E-02
5.5	0.0	1.21200E-03	1.02950E-02	2.66570E-02
5.6	0.0	8.59760E-04	8.56700E-03	2.33520E-02
5.7	0.0	5.97660E-04	7.09500E-03	2.03910E-02
5.8	0.0	4.06030E-04	5.84690E-03	1.77500E-02
5.9	0.0	2.68660E-04	4.79370E-03	1.54020E-02
6.0	0.0	1.72410E-04	3.90930E-03	1.33210E-02

Table 7 (Continued)

ENERGY (MEV)	Q-VALUES 5 MEV	7 MEV	9 MEV	11 MEV
6.1	0.0	1.06720E-04	3.17030E-03	1.14850E-02
6.2	0.0	6.32680E-05	2.55610E-03	9.87070E-03
6.3	0.0	3.55710E-05	2.04810E-03	8.45580E-03
6.4	0.0	1.87100E-05	1.63050E-03	7.22040E-03
6.5	0.0	9.02260E-06	1.28920E-03	6.14560E-03
6.6	0.0	3.86540E-06	1.01180E-03	5.21380E-03
6.7	0.0	1.39390E-06	7.87950E-04	4.40890E-03
6.8	0.0	3.80590E-07	6.08490E-04	3.71600E-03
6.9	0.0	5.99910E-08	4.65680E-04	3.12160E-03
7.0	0.0	0.0	3.52930E-04	2.61340E-03
7.1	0.0	0.0	2.64660E-04	2.18060E-03
7.2	0.0	0.0	1.96180E-04	1.81310E-03
7.3	0.0	0.0	1.43590E-04	1.50220E-03
7.4	0.0	0.0	1.03640E-04	1.24010E-03
7.5	0.0	0.0	7.36450E-05	1.01980E-03
7.6	0.0	0.0	5.14300E-05	8.35480E-04
7.7	0.0	0.0	3.52180E-05	6.81690E-04
7.8	0.0	0.0	2.35840E-05	5.53890E-04
7.9	0.0	0.0	1.53920E-05	4.48070E-04
8.0	0.0	0.0	9.74870E-06	3.60800E-04
8.1	0.0	0.0	5.95980E-06	2.89120E-04
8.2	0.0	0.0	3.49150E-06	2.30490E-04
8.3	0.0	0.0	1.94120E-06	1.82750E-04
8.4	0.0	0.0	1.01030E-06	1.44060E-04
8.5	0.0	0.0	4.82410E-07	1.12850E-04
8.6	0.0	0.0	2.04770E-07	8.78200E-05
8.7	0.0	0.0	7.32050E-08	6.78520E-05
8.8	0.0	0.0	1.98300E-08	5.20200E-05
8.9	0.0	0.0	3.10300E-09	3.95480E-05
9.0	0.0	0.0	0.0	2.97930E-05
9.1	0.0	0.0	0.0	2.22210E-05
9.2	0.0	0.0	0.0	1.63920E-05
9.3	0.0	0.0	0.0	1.19470E-05
9.4	0.0	0.0	0.0	8.59100E-06
9.5	0.0	0.0	0.0	6.08570E-06
9.6	0.0	0.0	0.0	4.23890E-06
9.7	0.0	0.0	0.0	2.89660E-06
9.8	0.0	0.0	0.0	1.93660E-06
9.9	0.0	0.0	0.0	1.26250E-06
10.0	0.0	0.0	0.0	7.99160E-07
10.1	0.0	0.0	0.0	4.88480E-07
10.2	0.0	0.0	0.0	2.86250E-07
10.3	0.0	0.0	0.0	1.59260E-07
10.4	0.0	0.0	0.0	8.29840E-08
10.5	0.0	0.0	0.0	3.96860E-08
10.6	0.0	0.0	0.0	1.68780E-08
10.7	0.0	0.0	0.0	6.04820E-09
10.8	0.0	0.0	0.0	1.64290E-09
10.9	0.0	0.0	0.0	2.57880E-10
11.0	0.0	0.0	0.0	0.0
11.1	0.0	0.0	0.0	0.0
11.2	0.0	0.0	0.0	0.0
11.3	0.0	0.0	0.0	0.0
11.4	0.0	0.0	0.0	0.0
11.5	0.0	0.0	0.0	0.0
11.6	0.0	0.0	0.0	0.0
11.7	0.0	0.0	0.0	0.0
11.8	0.0	0.0	0.0	0.0
11.9	0.0	0.0	0.0	0.0
12.0	0.0	0.0	0.0	0.0

Table 8 Estimated gamma-ray energy spectra of odd-even heavy mass nuclides.

ENERGY (MEV)	Q-VALUES 5 MEV	7 MEV	9 MEV	11 MEV
0.1	4.37430E-02	2.57620E-02	1.93550E-02	1.59270E-02
0.2	1.31230E-01	7.72860E-02	5.80640E-02	4.77820E-02
0.3	2.18710E-01	1.28810E-01	9.67730E-02	7.96370E-02
0.4	3.06200E-01	1.80330E-01	1.35480E-01	1.11490E-01
0.5	3.93690E-01	2.31860E-01	1.74190E-01	1.43350E-01
0.6	4.81170E-01	2.83380E-01	2.12900E-01	1.75200E-01
0.7	4.83310E-01	2.93060E-01	2.22860E-01	1.84530E-01
0.8	4.80810E-01	3.02060E-01	2.33280E-01	1.94760E-01
0.9	4.73860E-01	3.10060E-01	2.43830E-01	2.05610E-01
1.0	4.62930E-01	3.16860E-01	2.54250E-01	2.16870E-01
1.1	4.48770E-01	3.22420E-01	2.64370E-01	2.28320E-01
1.2	4.32240E-01	3.26840E-01	2.74060E-01	2.39780E-01
1.3	4.14270E-01	3.30300E-01	2.83260E-01	2.51090E-01
1.4	3.95740E-01	3.33020E-01	2.91980E-01	2.62130E-01
1.5	3.77470E-01	3.35250E-01	3.00210E-01	2.72800E-01
1.6	3.60140E-01	3.37250E-01	3.08000E-01	2.83020E-01
1.7	3.44290E-01	3.39200E-01	3.15350E-01	2.92690E-01
1.8	3.30280E-01	3.41260E-01	3.22280E-01	3.01760E-01
1.9	3.18310E-01	3.43520E-01	3.28790E-01	3.10130E-01
2.0	3.08460E-01	3.45990E-01	3.34830E-01	3.17740E-01
2.1	3.00630E-01	3.48650E-01	3.40350E-01	3.24500E-01
2.2	2.94670E-01	3.51390E-01	3.45270E-01	3.30340E-01
2.3	2.90300E-01	3.54080E-01	3.49510E-01	3.35170E-01
2.4	2.87240E-01	3.56570E-01	3.52980E-01	3.38940E-01
2.5	2.85160E-01	3.58700E-01	3.55570E-01	3.41590E-01
2.6	2.45810E-01	3.32780E-01	3.38960E-01	3.30600E-01
2.7	2.12720E-01	3.08910E-01	3.22690E-01	3.19180E-01
2.8	1.85150E-01	2.87000E-01	3.06820E-01	3.07430E-01
2.9	1.62370E-01	2.66950E-01	2.91400E-01	2.95430E-01
3.0	1.43660E-01	2.48620E-01	2.76480E-01	2.83290E-01
3.1	1.09940E-01	2.12780E-01	2.47560E-01	2.60440E-01
3.2	8.23230E-02	1.80330E-01	2.20250E-01	2.38230E-01
3.3	6.00020E-02	1.51170E-01	1.94630E-01	2.16810E-01
3.4	4.22210E-02	1.25180E-01	1.70780E-01	1.96300E-01
3.5	2.82790E-02	1.02180E-01	1.48720E-01	1.76800E-01
3.6	2.06400E-02	8.76700E-02	1.33720E-01	1.62670E-01
3.7	1.47450E-02	7.47610E-02	1.19740E-01	1.49140E-01
3.8	1.02830E-02	6.33590E-02	1.06790E-01	1.36270E-01
3.9	6.97770E-03	5.33560E-02	9.48590E-02	1.24100E-01
4.0	4.58790E-03	4.46400E-02	8.39330E-02	1.12650E-01
4.1	2.90730E-03	3.70990E-02	7.39740E-02	1.01930E-01
4.2	1.76290E-03	3.06190E-02	6.49440E-02	9.19380E-02
4.3	1.01310E-03	2.50890E-02	5.67940E-02	8.26740E-02
4.4	5.44360E-04	2.04050E-02	4.94740E-02	7.41210E-02
4.5	2.68010E-04	1.64650E-02	4.29290E-02	6.62550E-02
4.6	1.17170E-04	1.31760E-02	3.71040E-02	5.90510E-02
4.7	4.30930E-05	1.04530E-02	3.19430E-02	5.24790E-02
4.8	1.19950E-05	8.21640E-03	2.73910E-02	4.65070E-02
4.9	1.92590E-06	6.39500E-03	2.33930E-02	4.11000E-02
5.0	0.0	4.92500E-03	1.98980E-02	3.62220E-02
5.1	0.0	3.75010E-03	1.68560E-02	3.18370E-02
5.2	0.0	2.82060E-03	1.42190E-02	2.79080E-02
5.3	0.0	2.09320E-03	1.19440E-02	2.44000E-02
5.4	0.0	1.53080E-03	9.98930E-03	2.12770E-02
5.5	0.0	1.10140E-03	8.31730E-03	1.85060E-02
5.6	0.0	7.78360E-04	6.89340E-03	1.60540E-02
5.7	0.0	5.39020E-04	5.68640E-03	1.38920E-02
5.8	0.0	3.64820E-04	4.66790E-03	1.19900E-02
5.9	0.0	2.40510E-04	3.81250E-03	1.03220E-02
6.0	0.0	1.53800E-04	3.09750E-03	8.86370E-03

Table 8 (Continued)

ENERGY (MEV)	Q-VALUES 5 MEV	7 MEV	9 MEV	11 MEV
6.1	0.0	9.48810E-05	2.50280E-03	7.59190E-03
6.2	0.0	5.60680E-05	2.01070E-03	6.48590E-03
6.3	0.0	3.14300E-05	1.60560E-03	5.52670E-03
6.4	0.0	1.64870E-05	1.27400E-03	4.69710E-03
6.5	0.0	7.93250E-06	1.00410E-03	3.98150E-03
6.6	0.0	3.39180E-06	7.85760E-04	3.36590E-03
6.7	0.0	1.22130E-06	6.10220E-04	2.83770E-03
6.8	0.0	3.33080E-07	4.70030E-04	2.38580E-03
6.9	0.0	5.24440E-08	3.58880E-04	2.00010E-03
7.0	0.0	0.0	2.71420E-04	1.67190E-03
7.1	0.0	0.0	2.03170E-04	1.39340E-03
7.2	0.0	0.0	1.50370E-04	1.15770E-03
7.3	0.0	0.0	1.09930E-04	9.5877uE-04
7.4	0.0	0.0	7.92690E-05	7.91410E-04
7.5	0.0	0.0	5.62970E-05	6.51020E-04
7.6	0.0	0.0	3.93060E-05	5.33610E-04
7.7	0.0	0.0	2.69190E-05	4.35730E-04
7.8	0.0	0.0	1.80350E-05	3.54400E-04
7.9	0.0	0.0	1.17800E-05	2.87060E-04
8.0	0.0	0.0	7.47060E-06	2.31500E-04
8.1	0.0	0.0	4.57450E-06	1.85830E-04
8.2	0.0	0.0	2.68540E-06	1.48440E-04
8.3	0.0	0.0	1.49670E-06	1.17950E-04
8.4	0.0	0.0	7.81260E-07	9.32010E-05
8.5	0.0	0.0	3.74310E-07	7.32070E-05
8.6	0.0	0.0	1.59500E-07	5.71330E-05
8.7	0.0	0.0	5.72740E-08	4.42810E-05
8.8	0.0	0.0	1.55900E-08	3.40640E-05
8.9	0.0	0.0	2.45140E-09	2.59910E-05
9.0	0.0	0.0	0.0	1.96570E-05
9.1	0.0	0.0	0.0	1.47220E-05
9.2	0.0	0.0	0.0	1.09090E-05
9.3	0.0	0.0	0.0	7.98840E-06
9.4	0.0	0.0	0.0	5.77340E-06
9.5	0.0	0.0	0.0	4.11160E-06
9.6	0.0	0.0	0.0	2.88010E-06
9.7	0.0	0.0	0.0	1.97980E-06
9.8	0.0	0.0	0.0	1.33200E-06
9.9	0.0	0.0	0.0	8.74090E-07
10.0	0.0	0.0	0.0	5.57120E-07
10.1	0.0	0.0	0.0	3.43010E-07
10.2	0.0	0.0	0.0	2.02540E-07
10.3	0.0	0.0	0.0	1.13580E-07
10.4	0.0	0.0	0.0	5.96750E-08
10.5	0.0	0.0	0.0	2.87870E-08
10.6	0.0	0.0	0.0	1.23550E-08
10.7	0.0	0.0	0.0	4.46930E-09
10.8	0.0	0.0	0.0	1.22590E-09
10.9	0.0	0.0	0.0	1.94300E-10
11.0	0.0	0.0	0.0	0.0
11.1	0.0	0.0	0.0	0.0
11.2	0.0	0.0	0.0	0.0
11.3	0.0	0.0	0.0	0.0
11.4	0.0	0.0	0.0	0.0
11.5	0.0	0.0	0.0	0.0
11.6	0.0	0.0	0.0	0.0
11.7	0.0	0.0	0.0	0.0
11.8	0.0	0.0	0.0	0.0
11.9	0.0	0.0	0.0	0.0
12.0	0.0	0.0	0.0	0.0

Table 9 Estimated gamma-ray energy spectra of odd-odd heavy mass nuclides.

ENERGY (MEV)	Q-VALUES 5 MEV	7 MEV	9 MEV	11 MEV
0.1	2.03950E-02	1.83300E-02	1.55450E-02	1.30980E-02
0.2	6.11840E-02	5.49890E-02	4.66340E-02	3.92930E-02
0.3	1.01970E-01	9.16490E-02	7.77230E-02	6.54880E-02
0.4	1.42760E-01	1.28310E-01	1.08810E-01	9.16840E-02
0.5	1.83550E-01	1.64970E-01	1.39900E-01	1.17880E-01
0.6	2.24340E-01	2.01630E-01	1.70990E-01	1.44070E-01
0.7	2.35090E-01	2.12280E-01	1.80620E-01	1.52590E-01
0.8	2.45270E-01	2.23040E-01	1.90870E-01	1.62020E-01
0.9	2.54890E-01	2.33740E-01	2.01580E-01	1.72250E-01
1.0	2.64390E-01	2.44500E-01	2.12740E-01	1.83230E-01
1.1	2.74490E-01	2.55650E-01	2.24470E-01	1.94960E-01
1.2	2.86040E-01	2.67600E-01	2.36900E-01	2.07440E-01
1.3	2.99890E-01	2.80830E-01	2.50230E-01	2.20680E-01
1.4	3.16770E-01	2.95750E-01	2.64600E-01	2.34680E-01
1.5	3.37170E-01	3.12670E-01	2.80100E-01	2.49370E-01
1.6	3.61300E-01	3.31720E-01	2.96720E-01	2.64640E-01
1.7	3.89110E-01	3.52900E-01	3.14370E-01	2.80350E-01
1.8	4.20210E-01	3.75990E-01	3.32850E-01	2.96270E-01
1.9	4.53990E-01	4.00640E-01	3.51890E-01	3.12150E-01
2.0	4.89630E-01	4.26340E-01	3.71130E-01	3.27720E-01
2.1	5.26210E-01	4.52510E-01	3.90180E-01	3.42680E-01
2.2	5.62730E-01	4.78530E-01	4.08620E-01	3.56710E-01
2.3	5.98250E-01	5.03760E-01	4.26040E-01	3.69570E-01
2.4	5.45660E-01	4.81340E-01	4.15870E-01	3.65820E-01
2.5	5.01550E-01	4.60590E-01	4.05400E-01	3.61070E-01
2.6	4.23360E-01	4.16180E-01	3.79600E-01	3.46360E-01
2.7	3.57880E-01	3.75570E-01	3.54600E-01	3.31240E-01
2.8	3.03550E-01	3.38630E-01	3.30510E-01	3.15820E-01
2.9	2.39100E-01	2.90670E-01	2.98140E-01	2.94520E-01
3.0	1.86370E-01	2.47610E-01	2.67630E-01	2.73600E-01
3.1	1.32700E-01	1.99710E-01	2.32620E-01	2.49120E-01
3.2	8.97870E-02	1.57420E-01	2.00240E-01	2.25640E-01
3.3	5.59690E-02	1.20380E-01	1.70500E-01	2.03280E-01
3.4	3.81360E-02	9.83120E-02	1.51170E-01	1.87470E-01
3.5	2.44130E-02	7.90860E-02	1.33380E-01	1.72320E-01
3.6	1.74330E-02	6.76430E-02	1.21420E-01	1.60970E-01
3.7	1.21830E-02	5.76380E-02	1.10320E-01	1.50010E-01
3.8	8.30900E-03	4.89380E-02	1.00050E-01	1.39490E-01
3.9	5.51260E-03	4.14160E-02	9.05890E-02	1.29440E-01
4.0	3.54280E-03	3.49490E-02	8.19210E-02	1.19890E-01
4.1	2.19360E-03	2.94190E-02	7.40070E-02	1.10870E-01
4.2	1.29930E-03	2.47170E-02	6.68100E-02	1.02380E-01
4.3	7.29120E-04	2.07390E-02	6.02870E-02	9.44320E-02
4.4	3.82430E-04	1.73930E-02	5.43930E-02	8.70110E-02
4.5	1.83770E-04	1.45920E-02	4.90830E-02	8.01060E-02
4.6	7.83990E-05	1.22580E-02	4.43090E-02	7.37010E-02
4.7	2.81360E-05	1.03230E-02	4.00270E-02	6.77750E-02
4.8	7.64220E-06	8.72520E-03	3.61890E-02	6.23020E-02
4.9	1.19740E-06	7.40990E-03	3.27540E-02	5.72580E-02
5.0	0.0	6.33010E-03	2.96800E-02	5.26140E-02
5.1	0.0	5.44520E-03	2.69290E-02	4.83430E-02
5.2	0.0	4.72020E-03	2.44650E-02	4.44170E-02
5.3	0.0	3.60620E-03	2.10270E-02	3.94760E-02
5.4	0.0	2.75740E-03	1.80890E-02	3.50840E-02
5.5	0.0	2.11630E-03	1.55810E-02	3.11850E-02
5.6	0.0	1.63630E-03	1.34440E-02	2.77250E-02
5.7	0.0	1.27980E-03	1.16230E-02	2.46580E-02
5.8	0.0	8.51150E-04	9.35800E-03	2.10120E-02
5.9	0.0	5.47040E-04	7.46850E-03	1.78330E-02
6.0	0.0	3.36290E-04	5.90110E-03	1.50680E-02

Table 9 (Continued)

ENERGY (MEV)	Q-VALUES 5 MEV	7 MEV	9 MEV	11 MEV
6.1	0.0	1.94230E-04	4.60850E-03	1.26710E-02
6.2	0.0	1.01620E-04	3.54930E-03	1.06020E-02
6.3	0.0	5.73900E-05	2.85820E-03	9.11000E-03
6.4	0.0	3.03300E-05	2.28710E-03	7.80820E-03
6.5	0.0	1.47030E-05	1.81790E-03	6.67500E-03
6.6	0.0	6.33470E-06	1.43470E-03	5.69120E-03
6.7	0.0	2.29860E-06	1.12360E-03	4.83920E-03
6.8	0.0	6.31890E-07	8.72890E-04	4.10350E-03
6.9	0.0	1.00300E-07	6.72150E-04	3.46970E-03
7.0	0.0	0.0	5.12680E-04	2.92530E-03
7.1	0.0	0.0	3.87020E-04	2.45900E-03
7.2	0.0	0.0	2.88870E-04	2.06060E-03
7.3	0.0	0.0	2.12960E-04	1.72120E-03
7.4	0.0	0.0	1.54850E-04	1.43290E-03
7.5	0.0	0.0	1.10890E-04	1.18870E-03
7.6	0.0	0.0	7.80640E-05	9.82630E-04
7.7	0.0	0.0	5.39020E-05	8.09170E-04
7.8	0.0	0.0	3.64060E-05	6.63680E-04
7.9	0.0	0.0	2.39720E-05	5.42070E-04
8.0	0.0	0.0	1.53230E-05	4.40790E-04
8.1	0.0	0.0	9.45730E-06	3.56750E-04
8.2	0.0	0.0	5.59530E-06	2.87300E-04
8.3	0.0	0.0	3.14280E-06	2.30150E-04
8.4	0.0	0.0	1.65310E-06	1.83330E-04
8.5	0.0	0.0	7.98110E-07	1.45150E-04
8.6	0.0	0.0	3.42690E-07	1.14180E-04
8.7	0.0	0.0	1.23990E-07	8.91850E-05
8.8	0.0	0.0	3.40090E-08	6.91390E-05
8.9	0.0	0.0	5.38880E-09	5.31590E-05
9.0	0.0	0.0	0.0	4.05080E-05
9.1	0.0	0.0	0.0	3.05660E-05
9.2	0.0	0.0	0.0	2.28170E-05
9.3	0.0	0.0	0.0	1.68300E-05
9.4	0.0	0.0	0.0	1.22510E-05
9.5	0.0	0.0	0.0	8.78680E-06
9.6	0.0	0.0	0.0	6.19790E-06
9.7	0.0	0.0	0.0	4.28990E-06
9.8	0.0	0.0	0.0	2.90570E-06
9.9	0.0	0.0	0.0	1.91950E-06
10.0	0.0	0.0	0.0	1.23140E-06
10.1	0.0	0.0	0.0	7.63020E-07
10.2	0.0	0.0	0.0	4.53390E-07
10.3	0.0	0.0	0.0	2.55850E-07
10.4	0.0	0.0	0.0	1.35250E-07
10.5	0.0	0.0	0.0	6.56390E-08
10.6	0.0	0.0	0.0	2.83390E-08
10.7	0.0	0.0	0.0	1.03130E-08
10.8	0.0	0.0	0.0	2.84570E-09
10.9	0.0	0.0	0.0	4.53730E-10
11.0	0.0	0.0	0.0	0.0
11.1	0.0	0.0	0.0	0.0
11.2	0.0	0.0	0.0	0.0
11.3	0.0	0.0	0.0	0.0
11.4	0.0	0.0	0.0	0.0
11.5	0.0	0.0	0.0	0.0
11.6	0.0	0.0	0.0	0.0
11.7	0.0	0.0	0.0	0.0
11.8	0.0	0.0	0.0	0.0
11.9	0.0	0.0	0.0	0.0
12.0	0.0	0.0	0.0	0.0

Table 10 Estimated gamma-ray energy spectra of even-even heavy mass nuclides.

ENERGY (MEV)	Q-VALUES 5 MEV	7 MEV	9 MEV	11 MEV
0.1	5.50240E-02	3.79600E-02	2.86450E-02	2.28350E-02
0.2	1.65070E-01	1.13880E-01	8.59340E-02	6.85050E-02
0.3	2.75120E-01	1.89800E-01	1.43220E-01	1.14170E-01
0.4	3.85170E-01	2.65720E-01	2.00510E-01	1.59840E-01
0.5	4.95210E-01	3.41640E-01	2.57800E-01	2.05510E-01
0.6	6.05260E-01	4.17560E-01	3.15090E-01	2.51180E-01
0.7	6.11740E-01	4.29980E-01	3.27470E-01	2.62560E-01
0.8	6.11850E-01	4.40490E-01	3.39620E-01	2.74450E-01
0.9	6.05180E-01	4.48390E-01	3.50950E-01	2.86410E-01
1.0	5.91810E-01	4.53140E-01	3.60940E-01	2.97990E-01
1.1	5.72180E-01	4.54440E-01	3.69150E-01	3.08770E-01
1.2	5.47050E-01	4.52140E-01	3.75230E-01	3.18380E-01
1.3	5.17330E-01	4.46250E-01	3.78950E-01	3.26480E-01
1.4	4.84030E-01	4.36960E-01	3.80160E-01	3.32840E-01
1.5	4.48200E-01	4.24530E-01	3.78820E-01	3.37260E-01
1.6	4.10830E-01	4.09300E-01	3.74980E-01	3.39650E-01
1.7	3.72880E-01	3.91700E-01	3.68740E-01	3.39950E-01
1.8	3.35150E-01	3.72150E-01	3.60290E-01	3.38180E-01
1.9	2.98370E-01	3.51100E-01	3.49830E-01	3.34420E-01
2.0	2.63130E-01	3.28990E-01	3.37610E-01	3.28770E-01
2.1	2.29860E-01	3.06240E-01	3.23910E-01	3.21400E-01
2.2	1.98910E-01	2.83230E-01	3.08990E-01	3.12470E-01
2.3	1.70500E-01	2.60310E-01	2.93140E-01	3.02180E-01
2.4	1.44740E-01	2.37790E-01	2.76630E-01	2.90740E-01
2.5	1.21670E-01	2.15910E-01	2.59700E-01	2.78350E-01
2.6	1.01250E-01	1.94900E-01	2.42590E-01	2.65220E-01
2.7	8.33890E-02	1.74910E-01	2.25510E-01	2.51550E-01
2.8	6.79390E-02	1.56080E-01	2.08650E-01	2.37540E-01
2.9	5.47300E-02	1.38490E-01	1.92170E-01	2.23340E-01
3.0	4.35670E-02	1.22200E-01	1.76200E-01	2.09120E-01
3.1	3.42470E-02	1.07210E-01	1.60850E-01	1.95030E-01
3.2	2.65610E-02	9.35450E-02	1.46220E-01	1.81190E-01
3.3	2.03030E-02	8.11600E-02	1.32370E-01	1.67690E-01
3.4	1.52780E-02	7.00180E-02	1.19340E-01	1.54640E-01
3.5	1.13020E-02	6.00620E-02	1.07160E-01	1.42090E-01
3.6	8.20320E-03	5.12240E-02	9.58480E-02	1.30120E-01
3.7	5.83010E-03	4.34300E-02	8.53930E-02	1.18750E-01
3.8	4.04650E-03	3.66010E-02	7.57850E-02	1.08030E-01
3.9	2.73360E-03	3.06570E-02	6.70010E-02	9.79550E-02
4.0	1.79000E-03	2.55160E-02	5.90100E-02	8.85440E-02
4.1	1.13000E-03	2.10990E-02	5.17750E-02	7.97910E-02
4.2	6.82890E-04	1.73290E-02	4.52560E-02	7.16880E-02
4.3	3.91230E-04	1.41330E-02	3.94090E-02	6.42170E-02
4.4	2.09620E-04	1.14420E-02	3.41870E-02	5.73570E-02
4.5	1.02950E-04	9.19250E-03	2.95450E-02	5.10830E-02
4.6	4.49040E-05	7.32550E-03	2.54350E-02	4.53670E-02
4.7	1.64830E-05	5.78800E-03	2.18130E-02	4.01780E-02
4.8	4.58020E-06	4.53170E-03	1.86340E-02	3.54830E-02
4.9	7.34200E-07	3.51390E-03	1.58550E-02	3.12510E-02
5.0	0.0	2.69650E-03	1.34370E-02	2.74490E-02
5.1	0.0	2.04620E-03	1.13410E-02	2.40440E-02
5.2	0.0	1.53390E-03	9.53210E-03	2.10040E-02
5.3	0.0	1.13480E-03	7.97760E-03	1.83000E-02
5.4	0.0	8.27400E-04	6.64750E-03	1.59000E-02
5.5	0.0	5.93660E-04	5.51420E-03	1.37790E-02
5.6	0.0	4.18410E-04	4.55300E-03	1.19080E-02
5.7	0.0	2.89020E-04	3.74140E-03	1.02630E-02
5.8	0.0	1.95150E-04	3.05920E-03	8.82120E-03
5.9	0.0	1.28370E-04	2.48860E-03	7.56140E-03
6.0	0.0	8.19200E-05	2.01350E-03	6.46380E-03

Table 10 (Continued)

ENERGY (MEV)	Q-VALUES 5 MEV	7 MEV	9 MEV	11 MEV
6.1	0.0	5.04400E-05	1.62010E-03	5.51040E-03
6.2	0.0	2.97520E-05	1.29590E-03	4.68460E-03
6.3	0.0	1.66500E-05	1.03020E-03	3.97150E-03
6.4	0.0	8.72010E-06	8.13720E-04	3.35750E-03
6.5	0.0	4.18910E-06	6.38320E-04	2.83030E-03
6.6	0.0	1.78850E-06	4.97090E-04	2.37910E-03
6.7	0.0	6.43050E-07	3.84110E-04	1.99390E-03
6.8	0.0	1.75130E-07	2.94360E-04	1.66610E-03
6.9	0.0	2.75330E-08	2.23580E-04	1.38800E-03
7.0	0.0	0.0	1.68190E-04	1.15270E-03
7.1	0.0	0.0	1.25200E-04	9.54220E-04
7.2	0.0	0.0	9.21520E-05	7.87350E-04
7.3	0.0	0.0	6.69850E-05	6.47480E-04
7.4	0.0	0.0	4.80250E-05	5.30610E-04
7.5	0.0	0.0	3.39090E-05	4.33270E-04
7.6	0.0	0.0	2.35360E-05	3.52470E-04
7.7	0.0	0.0	1.60240E-05	2.85620E-04
7.8	0.0	0.0	1.06720E-05	2.30510E-04
7.9	0.0	0.0	6.93020E-06	1.85250E-04
8.0	0.0	0.0	4.36920E-06	1.48210E-04
8.1	0.0	0.0	2.65990E-06	1.18010E-04
8.2	0.0	0.0	1.55260E-06	9.35060E-05
8.3	0.0	0.0	8.60470E-07	7.36970E-05
8.4	0.0	0.0	4.46680E-07	5.77590E-05
8.5	0.0	0.0	2.12860E-07	4.49960E-05
8.6	0.0	0.0	9.02300E-08	3.48290E-05
8.7	0.0	0.0	3.22340E-08	2.67730E-05
8.8	0.0	0.0	8.73030E-09	2.04270E-05
8.9	0.0	0.0	1.36600E-09	1.54590E-05
9.0	0.0	0.0	0.0	1.15970E-05
9.1	0.0	0.0	0.0	8.61590E-06
9.2	0.0	0.0	0.0	6.33350E-06
9.3	0.0	0.0	0.0	4.60150E-06
9.4	0.0	0.0	0.0	3.29980E-06
9.5	0.0	0.0	0.0	2.33210E-06
9.6	0.0	0.0	0.0	1.62140E-06
9.7	0.0	0.0	0.0	1.10640E-06
9.8	0.0	0.0	0.0	7.39080E-07
9.9	0.0	0.0	0.0	4.81650E-07
10.0	0.0	0.0	0.0	3.04930E-07
10.1	0.0	0.0	0.0	1.86520E-07
10.2	0.0	0.0	0.0	1.09450E-07
10.3	0.0	0.0	0.0	6.10160E-08
10.4	0.0	0.0	0.0	3.18760E-08
10.5	0.0	0.0	0.0	1.52950E-08
10.6	0.0	0.0	0.0	6.53080E-09
10.7	0.0	0.0	0.0	2.35130E-09
10.8	0.0	0.0	0.0	6.42060E-10
10.9	0.0	0.0	0.0	1.01340E-10
11.0	0.0	0.0	0.0	0.0
11.1	0.0	0.0	0.0	0.0
11.2	0.0	0.0	0.0	0.0
11.3	0.0	0.0	0.0	0.0
11.4	0.0	0.0	0.0	0.0
11.5	0.0	0.0	0.0	0.0
11.6	0.0	0.0	0.0	0.0
11.7	0.0	0.0	0.0	0.0
11.8	0.0	0.0	0.0	0.0
11.9	0.0	0.0	0.0	0.0
12.0	0.0	0.0	0.0	0.0

Table 11 Estimated gamma-ray energy spectra of even-odd heavy mass nuclides.

ENERGY (MEV)	Q-VALUES 5 MEV	7 MEV	9 MEV	11 MEV
0.1	3.93640E-02	2.46460E-02	1.90960E-02	1.59220E-02
0.2	1.18090E-01	7.39390E-02	5.72890E-02	4.77650E-02
0.3	1.96820E-01	1.23230E-01	9.54820E-02	7.96080E-02
0.4	2.75550E-01	1.72520E-01	1.33680E-01	1.11450E-01
0.5	3.54280E-01	2.21820E-01	1.71870E-01	1.43290E-01
0.6	4.33010E-01	2.71110E-01	2.10060E-01	1.75140E-01
0.7	4.36730E-01	2.80860E-01	2.19980E-01	1.84440E-01
0.8	4.36520E-01	2.89970E-01	2.30260E-01	1.94550E-01
0.9	4.32610E-01	2.98210E-01	2.40690E-01	2.05270E-01
1.0	4.25590E-01	3.05550E-01	2.51100E-01	2.16440E-01
1.1	4.16320E-01	3.12130E-01	2.61450E-01	2.27950E-01
1.2	4.05750E-01	3.18200E-01	2.71740E-01	2.39700E-01
1.3	3.94870E-01	3.24070E-01	2.82040E-01	2.51620E-01
1.4	3.84550E-01	3.30050E-01	2.92390E-01	2.63640E-01
1.5	3.75560E-01	3.36410E-01	3.02840E-01	2.75690E-01
1.6	3.68420E-01	3.43340E-01	3.13410E-01	2.87670E-01
1.7	3.63500E-01	3.50950E-01	3.24070E-01	2.99480E-01
1.8	3.60910E-01	3.59260E-01	3.34740E-01	3.10980E-01
1.9	3.60600E-01	3.68170E-01	3.45310E-01	3.22030E-01
2.0	3.62350E-01	3.77510E-01	3.55620E-01	3.32460E-01
2.1	3.65840E-01	3.87060E-01	3.65480E-01	3.42110E-01
2.2	3.70640E-01	3.96550E-01	3.74700E-01	3.50820E-01
2.3	3.76330E-01	4.05680E-01	3.83080E-01	3.58440E-01
2.4	3.30910E-01	3.80830E-01	3.68990E-01	3.50400E-01
2.5	2.92130E-01	3.57670E-01	3.54900E-01	3.41640E-01
2.6	2.59340E-01	3.36170E-01	3.40860E-01	3.32230E-01
2.7	2.31810E-01	3.16270E-01	3.26960E-01	3.22280E-01
2.8	2.08870E-01	2.97880E-01	3.13230E-01	3.11860E-01
2.9	1.63620E-01	2.57590E-01	2.82730E-01	2.88840E-01
3.0	1.25630E-01	2.20560E-01	2.53490E-01	2.66070E-01
3.1	9.41310E-02	1.86810E-01	2.25690E-01	2.43790E-01
3.2	6.83440E-02	1.56300E-01	1.99470E-01	2.22170E-01
3.3	4.75270E-02	1.28950E-01	1.74940E-01	2.01350E-01
3.4	3.60000E-02	1.11910E-01	1.58540E-01	1.86540E-01
3.5	2.67980E-02	9.65520E-02	1.43080E-01	1.72180E-01
3.6	1.95690E-02	8.28040E-02	1.28590E-01	1.58360E-01
3.7	1.39890E-02	7.05830E-02	1.15100E-01	1.45140E-01
3.8	9.76290E-03	5.97950E-02	1.02610E-01	1.32560E-01
3.9	6.63060E-03	5.03370E-02	9.11160E-02	1.20680E-01
4.0	4.36410E-03	4.21010E-02	8.05900E-02	1.09500E-01
4.1	2.76860E-03	3.49780E-02	7.10010E-02	9.90430E-02
4.2	1.68100E-03	2.88600E-02	6.23110E-02	8.93060E-02
4.3	9.67410E-04	2.36430E-02	5.44710E-02	8.02800E-02
4.4	5.20590E-04	1.92240E-02	4.74330E-02	7.19500E-02
4.5	2.56740E-04	1.55100E-02	4.11440E-02	6.42940E-02
4.6	1.12440E-04	1.24110E-02	3.55490E-02	5.72840E-02
4.7	4.14390E-05	9.84490E-03	3.05940E-02	5.08920E-02
4.8	1.15590E-05	7.73810E-03	2.62240E-02	4.50850E-02
4.9	1.86000E-06	6.02280E-03	2.23890E-02	3.98280E-02
5.0	0.0	4.63880E-03	1.90360E-02	3.50860E-02
5.1	0.0	3.53270E-03	1.61190E-02	3.08240E-02
5.2	0.0	2.65760E-03	1.35910E-02	2.70070E-02
5.3	0.0	1.97280E-03	1.14110E-02	2.35990E-02
5.4	0.0	1.44320E-03	9.53890E-03	2.05670E-02
5.5	0.0	1.03890E-03	7.93820E-03	1.78770E-02
5.6	0.0	7.34550E-04	6.57570E-03	1.54980E-02
5.7	0.0	5.09000E-04	5.42120E-03	1.34010E-02
5.8	0.0	3.44740E-04	4.44760E-03	1.15580E-02
5.9	0.0	2.27460E-04	3.63030E-03	9.94230E-03
6.0	0.0	1.45590E-04	2.94760E-03	8.53030E-03

Table 11 (Continued)

ENERGY (MEV)	Q-VALUES 5 MEV	7 MEV	9 MEV	11 MEV
6.1	0.0	8.99080E-05	2.38010E-03	7.29990E-03
6.2	0.0	5.31900E-05	1.91080E-03	6.23060E-03
6.3	0.0	2.98550E-05	1.52480E-03	5.30400E-03
6.4	0.0	1.56830E-05	1.20900E-03	4.50320E-03
6.5	0.0	7.55700E-06	9.52210E-04	3.81310E-03
6.6	0.0	3.23670E-06	7.44590E-04	3.22000E-03
6.7	0.0	1.16750E-06	5.77820E-04	2.71160E-03
6.8	0.0	3.19020E-07	4.44750E-04	2.27710E-03
6.9	0.0	5.03310E-08	3.39340E-04	1.90670E-03
7.0	0.0	0.0	2.56470E-04	1.59180E-03
7.1	0.0	0.0	1.91850E-04	1.32500E-03
7.2	0.0	0.0	1.41910E-04	1.09940E-03
7.3	0.0	0.0	1.03680E-04	9.09330E-04
7.4	0.0	0.0	7.47240E-05	7.49600E-04
7.5	0.0	0.0	5.30460E-05	6.15790E-04
7.6	0.0	0.0	3.70230E-05	5.04040E-04
7.7	0.0	0.0	2.53490E-05	4.11020E-04
7.8	0.0	0.0	1.69800E-05	3.33850E-04
7.9	0.0	0.0	1.10910E-05	2.70040E-04
8.0	0.0	0.0	7.03390E-06	2.17470E-04
8.1	0.0	0.0	4.30810E-06	1.74330E-04
8.2	0.0	0.0	2.53000E-06	1.39060E-04
8.3	0.0	0.0	1.41090E-06	1.10350E-04
8.4	0.0	0.0	7.36980E-07	8.70830E-05
8.5	0.0	0.0	3.53420E-07	6.83120E-05
8.6	0.0	0.0	1.50770E-07	5.32450E-05
8.7	0.0	0.0	5.42100E-08	4.12170E-05
8.8	0.0	0.0	1.47780E-08	3.16680E-05
8.9	0.0	0.0	2.32760E-09	2.41360E-05
9.0	0.0	0.0	0.0	1.82340E-05
9.1	0.0	0.0	0.0	1.36420E-05
9.2	0.0	0.0	0.0	1.00990E-05
9.3	0.0	0.0	0.0	7.38910E-06
9.4	0.0	0.0	0.0	5.33610E-06
9.5	0.0	0.0	0.0	3.79760E-06
9.6	0.0	0.0	0.0	2.65860E-06
9.7	0.0	0.0	0.0	1.82680E-06
9.8	0.0	0.0	0.0	1.22870E-06
9.9	0.0	0.0	0.0	8.06190E-07
10.0	0.0	0.0	0.0	5.13850E-07
10.1	0.0	0.0	0.0	3.16430E-07
10.2	0.0	0.0	0.0	1.86920E-07
10.3	0.0	0.0	0.0	1.04890E-07
10.4	0.0	0.0	0.0	5.51520E-08
10.5	0.0	0.0	0.0	2.66340E-08
10.6	0.0	0.0	0.0	1.14450E-08
10.7	0.0	0.0	0.0	4.14680E-09
10.8	0.0	0.0	0.0	1.13950E-09
10.9	0.0	0.0	0.0	1.80980E-10
11.0	0.0	0.0	0.0	0.0
11.1	0.0	0.0	0.0	0.0
11.2	0.0	0.0	0.0	0.0
11.3	0.0	0.0	0.0	0.0
11.4	0.0	0.0	0.0	0.0
11.5	0.0	0.0	0.0	0.0
11.6	0.0	0.0	0.0	0.0
11.7	0.0	0.0	0.0	0.0
11.8	0.0	0.0	0.0	0.0
11.9	0.0	0.0	0.0	0.0
12.0	0.0	0.0	0.0	0.0

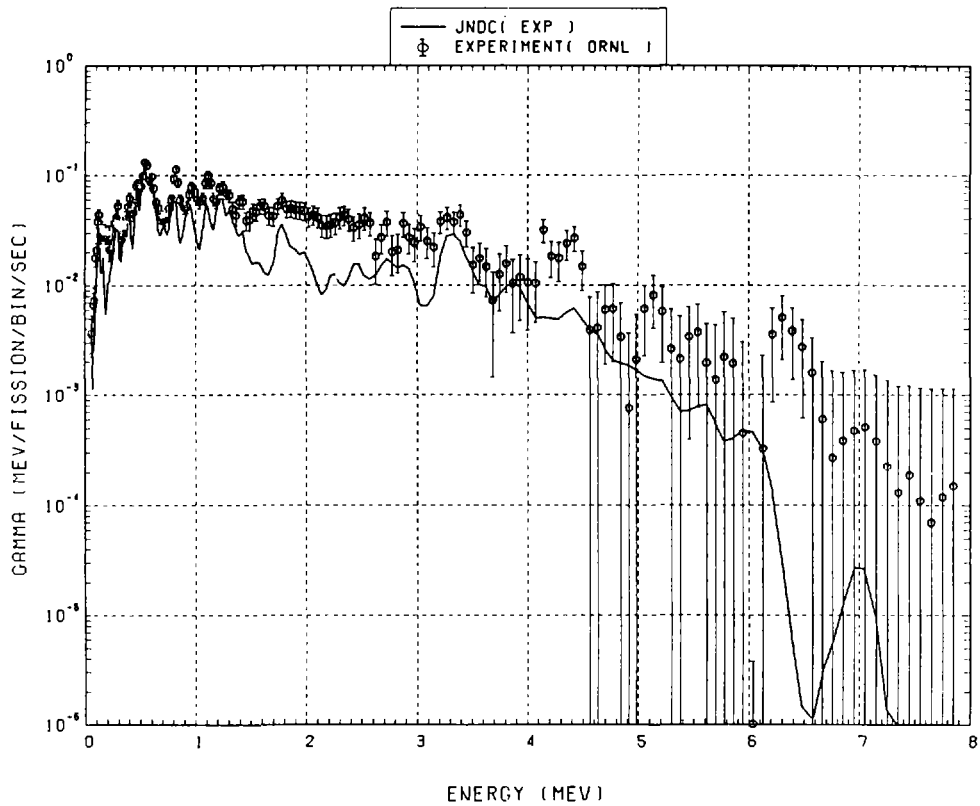

Fig. 1 Gamma-ray energy spectrum at 2.7 seconds after instantaneous fissions of ^{235}U by thermal neutron. Solid line is the calculation where only experimental spectra of individual nuclides are taken into consideration. Open circles are the measurements at Oak Ridge National Laboratory.

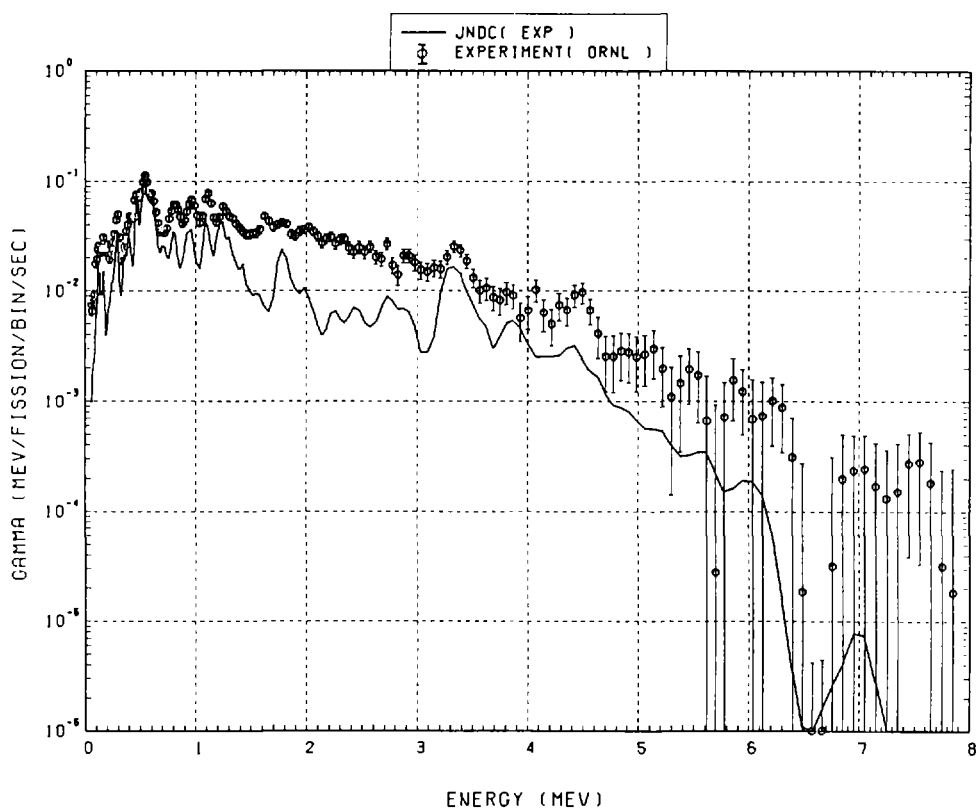

Fig. 2 Gamma-ray energy spectrum at 2.7 seconds after instantaneous fissions of ^{239}Pu by thermal neutron. Solid line is the calculation where only experimental spectra of individual nuclides are taken into consideration. Open circles are the measurements at Oak Ridge National Laboratory.

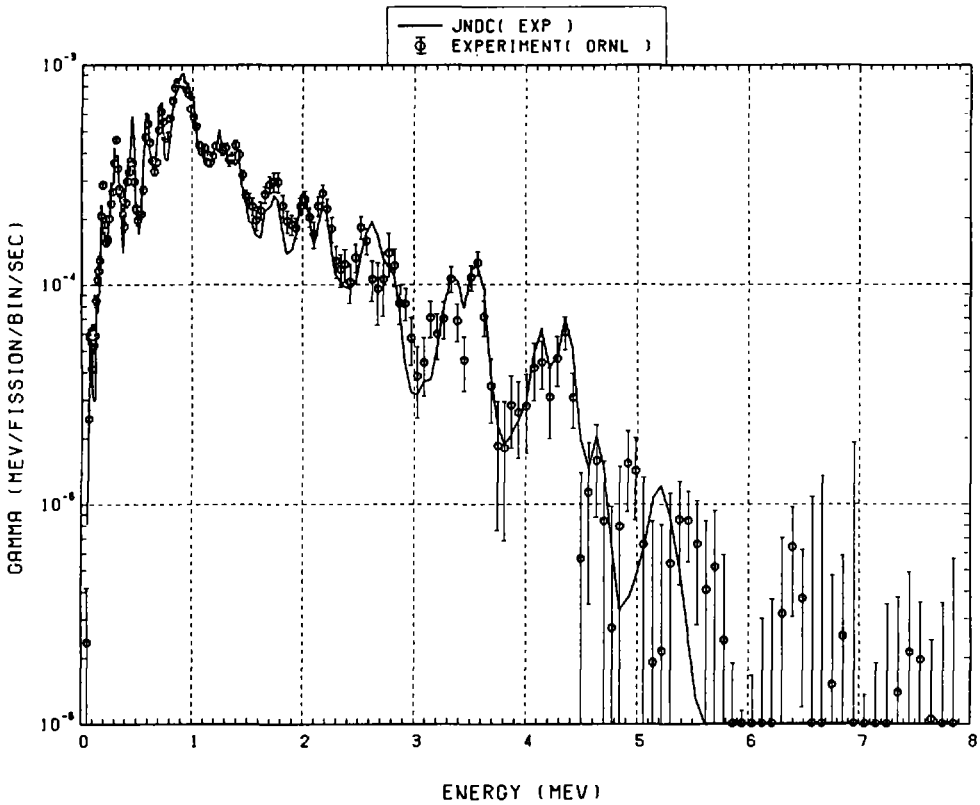

Fig. 3 Gamma-ray energy spectrum at 500.0 seconds after instantaneous fissions of ^{235}U by thermal neutron. Solid line is the calculation where only experimental spectra of individual nuclides are taken into consideration. Open circles are the measurements at Oak Ridge National Laboratory.

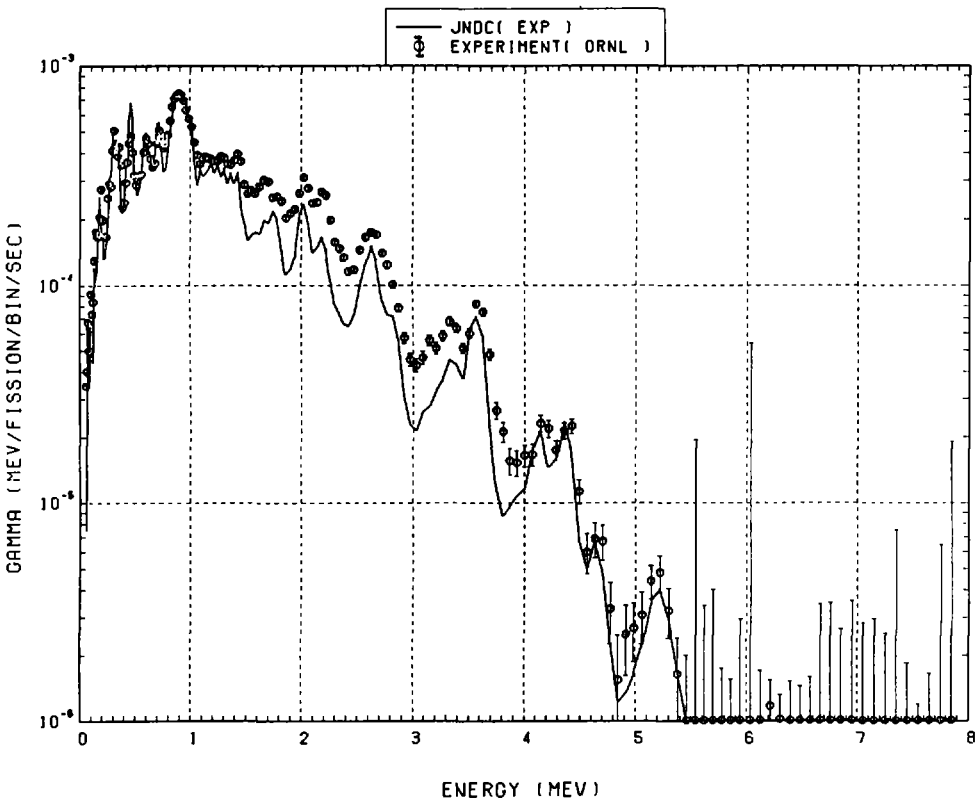

Fig. 4 Gamma-ray energy spectrum at 500.0 seconds after instantaneous fissions of ^{239}Pu by thermal neutron. Solid line is the calculation where only experimental spectra of individual nuclides are taken into consideration. Open circles are the measurements at Oak Ridge National Laboratory.

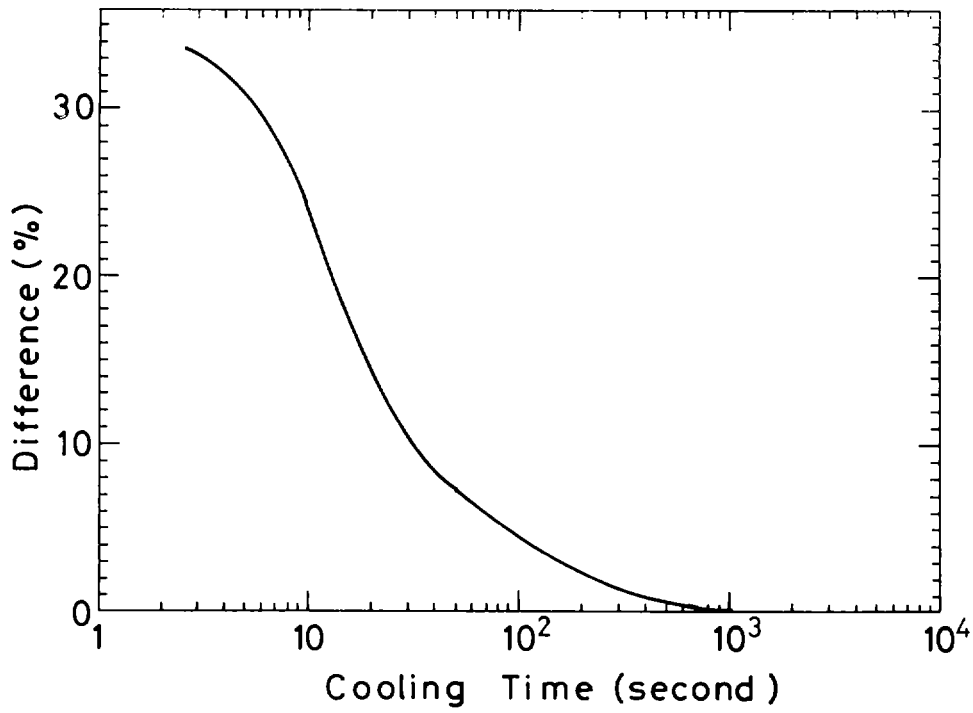

Fig. 5 Contribution of nuclides without experimental spectral data. The contribution is represented by percent difference between the decay heat from all fission product nuclides and the decay heat taking only the nuclides with spectral data into account.

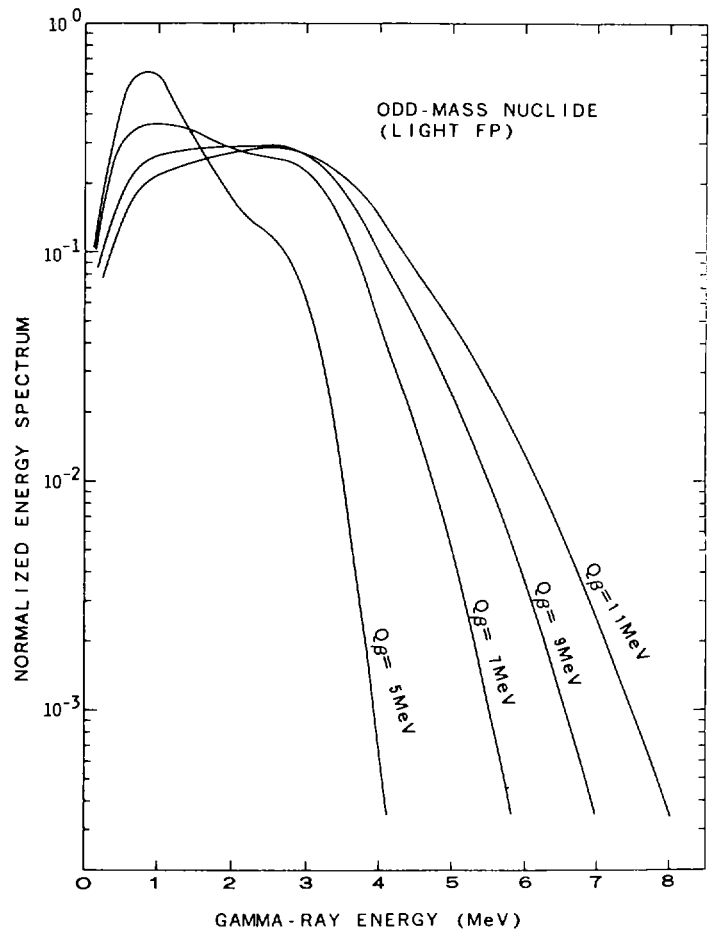

Fig. 6 Estimated gamma-ray energy spectra of odd-mass nuclides near the light mass peak of the mass yield curve.

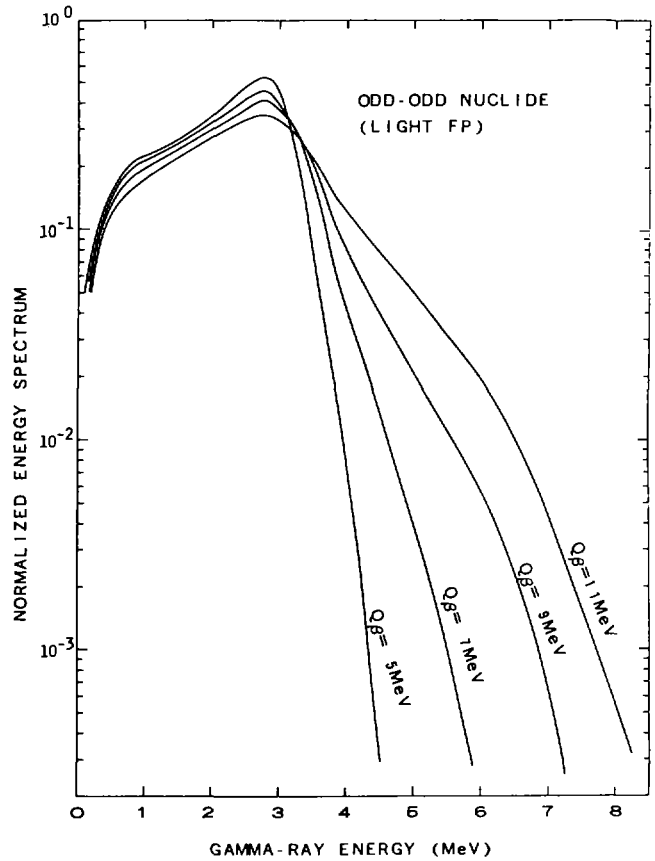

Fig. 7 Estimated gamma-ray energy spectra of odd-odd nuclides near the light mass peak of the mass yield curve.

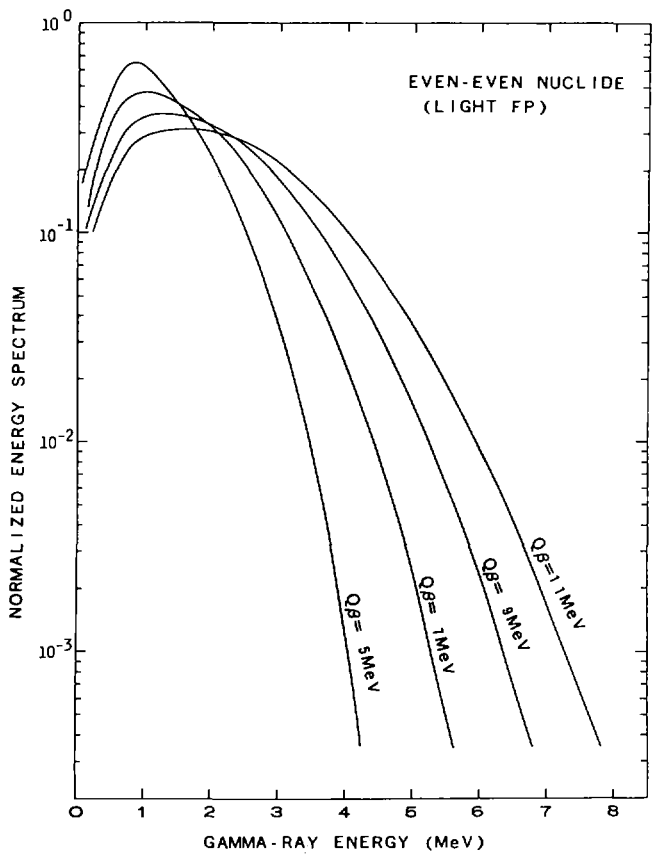

Fig. 8 Estimated gamma-ray energy spectra of even-even nuclides near the light mass peak of the mass yield curve.

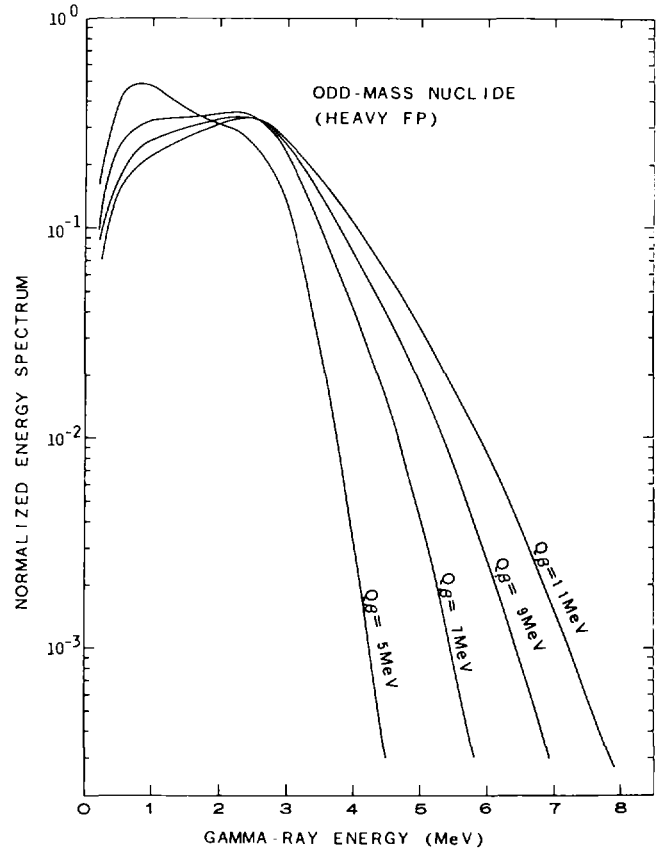

Fig. 9 Estimated gamma-ray energy spectra of odd-mass nuclides near the heavy mass peak of the mass yield curve.

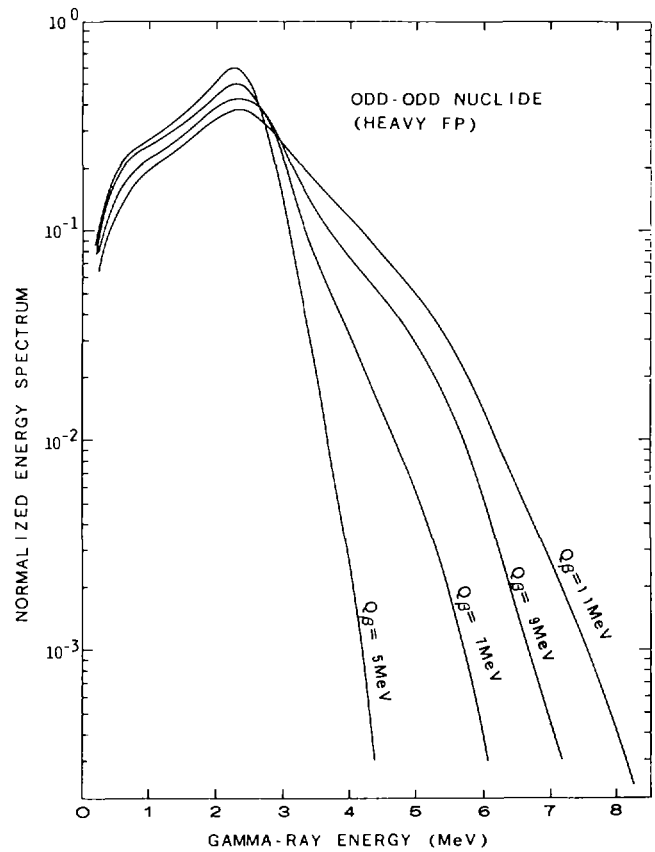

Fig. 10 Estimated gamma-ray energy spectra of odd-odd nuclides near the heavy mass peak of the mass yield curve.

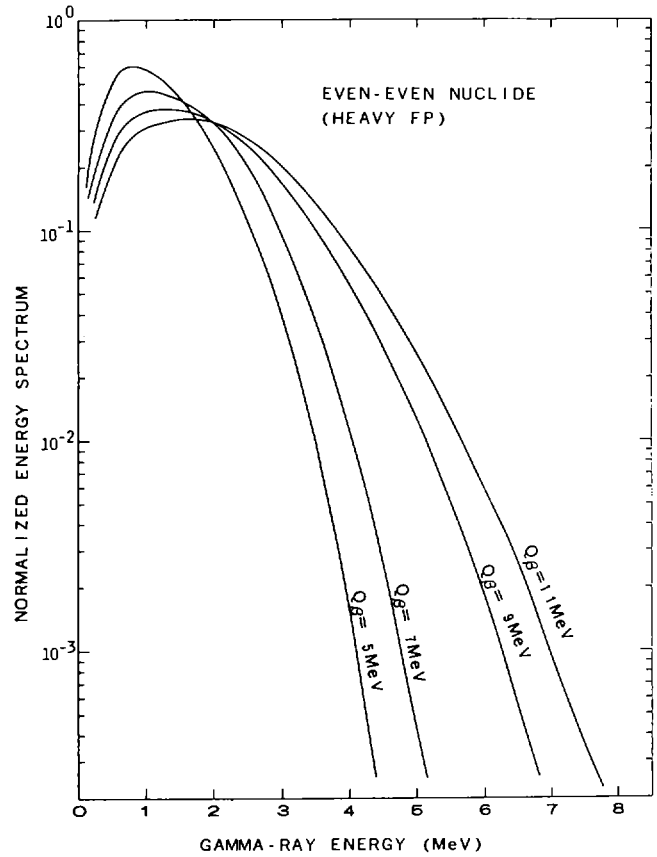

Fig. 11 Estimated gamma-ray energy spectra of even-even nuclides near the heavy mass peak of the mass yield curve.

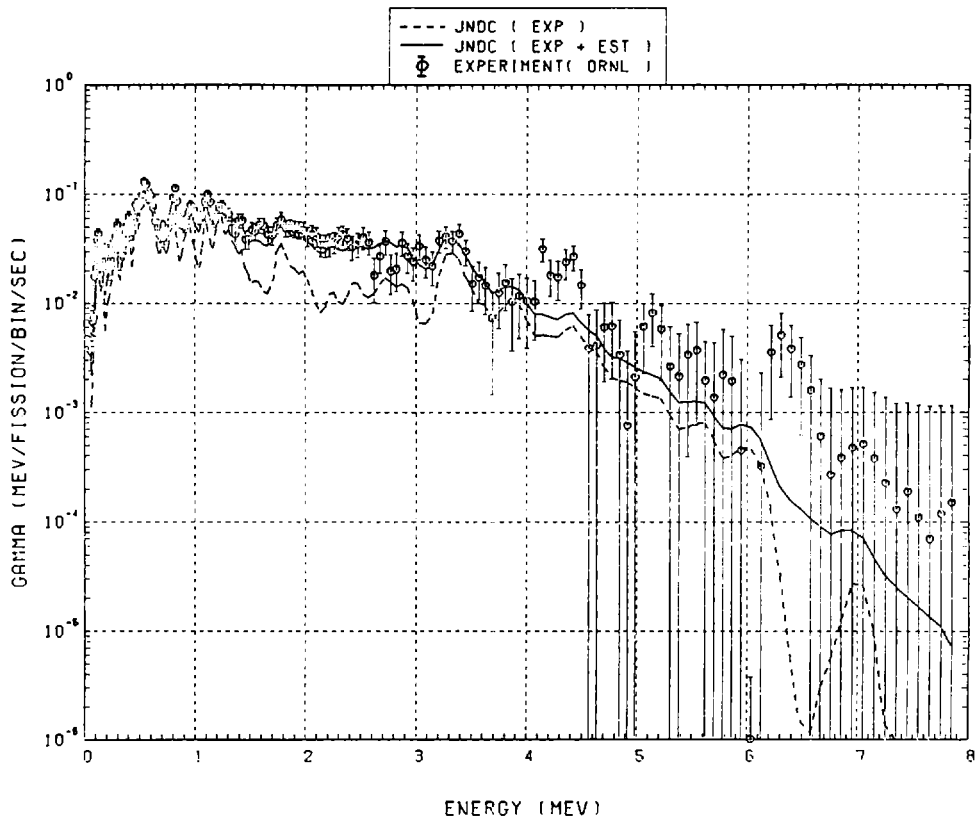

Fig. 12 Gamma-ray energy spectrum at 2.7 seconds after instantaneous fission of ^{235}U by thermal neutron. Dotted line is the calculation where only experimental spectra of individual nuclides are included. Solid line indicates the calculation compensated by the estimated spectra of nuclides without experimental spectral data. Open circles are the measurements at Oak Ridge National Laboratory.

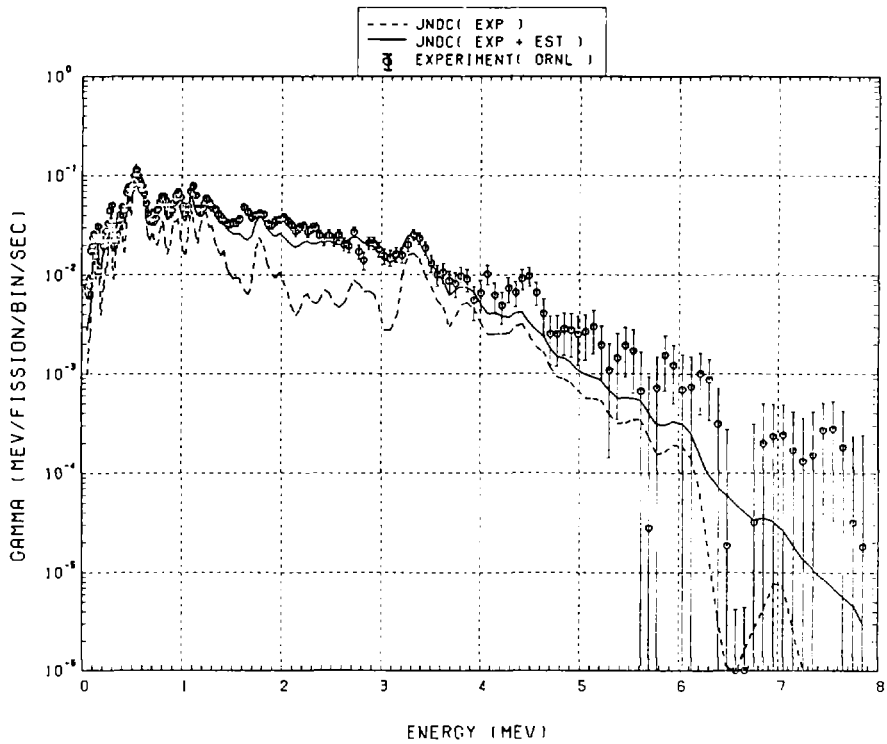

Fig. 13 Gamma-ray energy spectrum at 2.7 seconds after instantaneous fission of ^{239}Pu by thermal neutron. Dotted line is the calculation where only experimental spectra of individual nuclides are included. Solid line indicates the calculation compensated by the estimated spectra of nuclides without experimental spectral data. Open circles are the measurements at Oak Ridge National Laboratory.

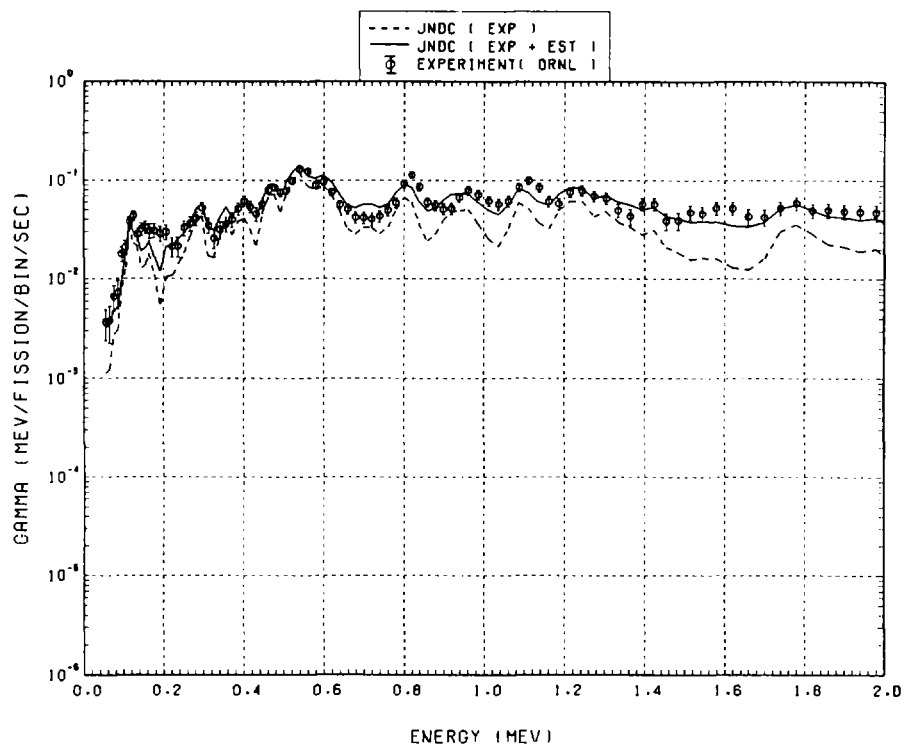

Fig. 14 Low-energy part of gamma-ray energy spectrum at 2.7 seconds after instantaneous fission of ^{235}U by thermal neutron. Dotted line is the calculation where only experimental spectra of individual nuclides are included. Solid line indicates the calculation compensated by the estimated spectra of nuclides without experimental spectral data. Open circles are the measurements at Oak Ridge National Laboratory.

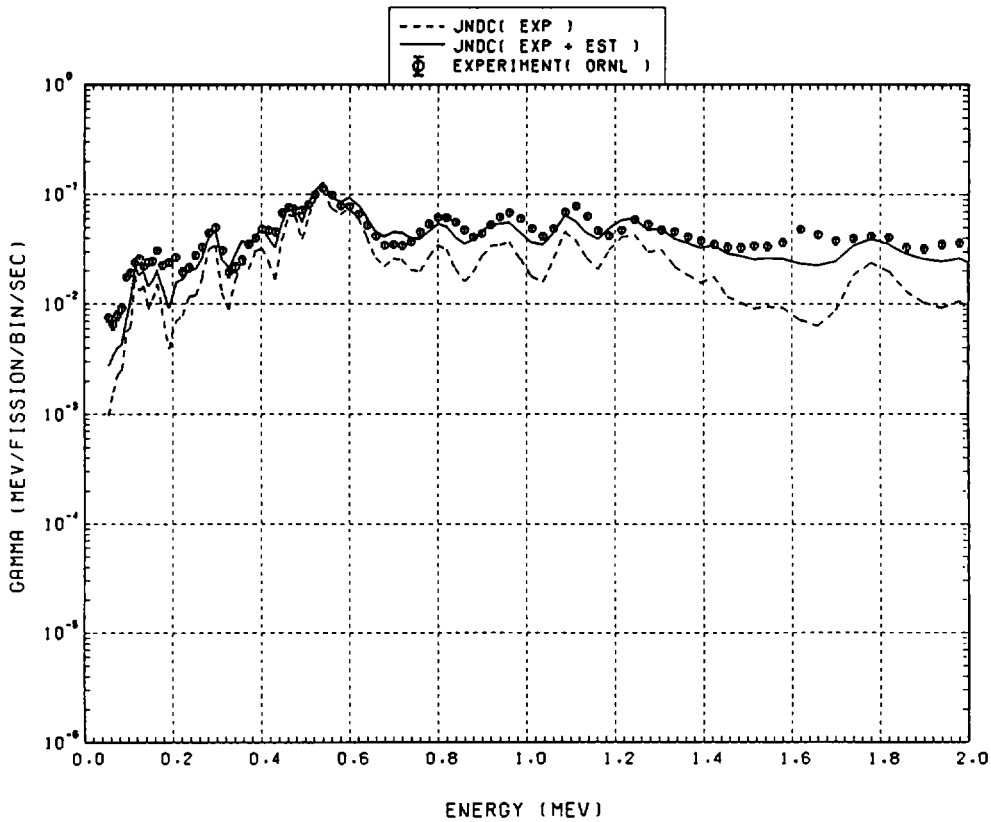

Fig. 15 Low-energy part of gamma-ray energy spectrum at 2.7 seconds after instantaneous fission of ^{239}Pu by thermal neutron. Dotted line is the calculation where only experimental spectra of individual nuclides are included. Solid line indicates the calculation compensated by the estimated spectra of nuclides without experimental spectral data. Open circles are the measurements at Oak Ridge National Laboratory.

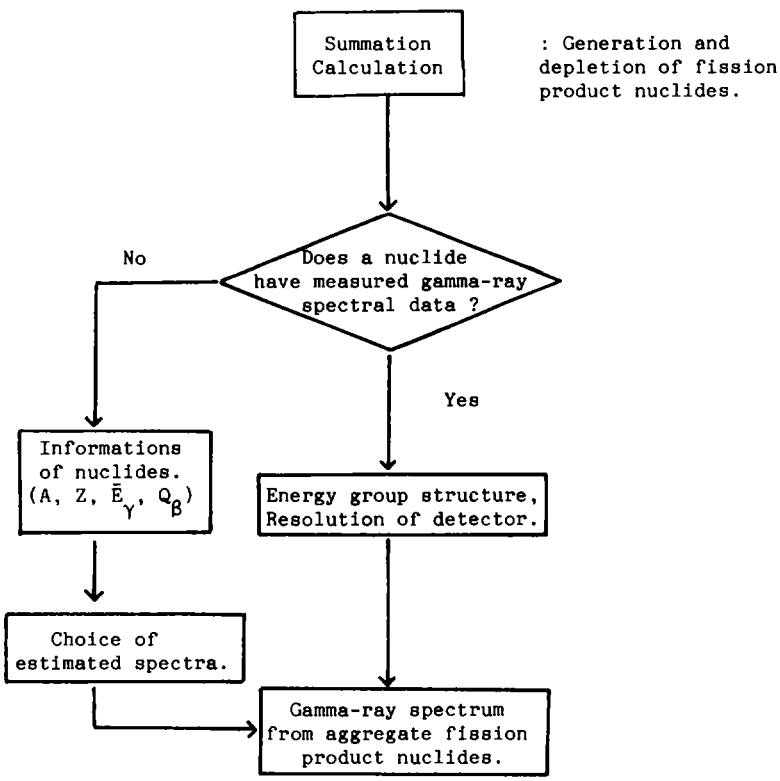

Fig. 16 Calculation flow of gamma-ray spectrum from aggregate fission product nuclides.

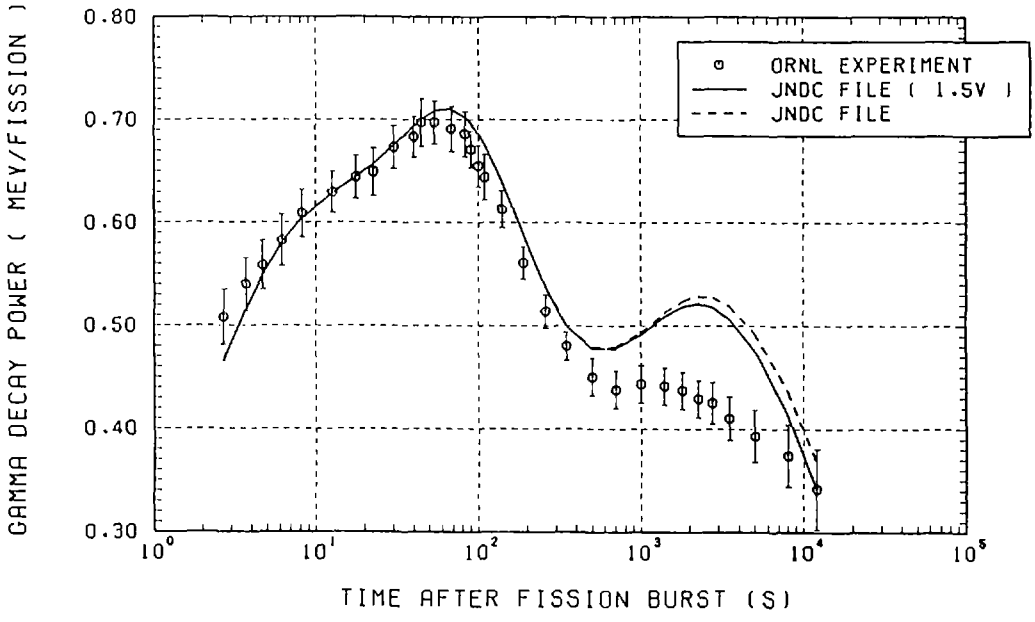

Fig. 17 Comparison of calculated gamma-decay heat with measured results at ORNL for thermal neutron fission of ^{235}U.

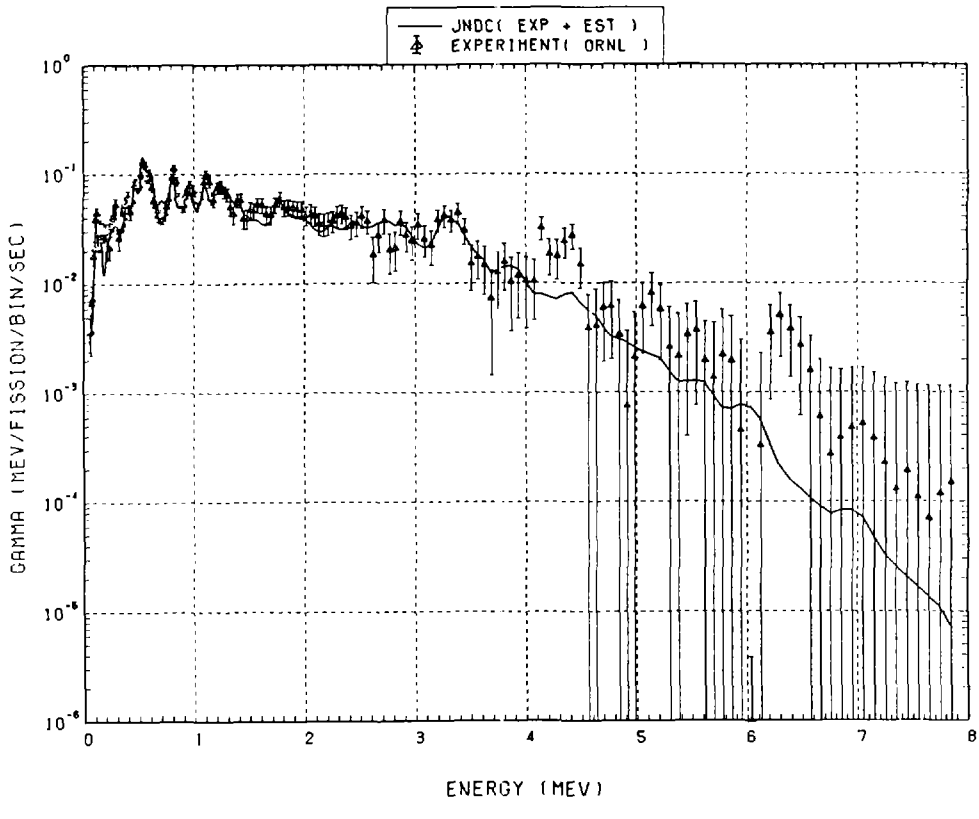

Fig. 18 Comparison of calculated gamma-ray energy spectrum with measured results at 2.7 seconds after thermal neutron fission of ^{235}U. (t_{irrad} = 1.0 s, t_{wait} = 1.7 s, t_{count} = 1.0 s)

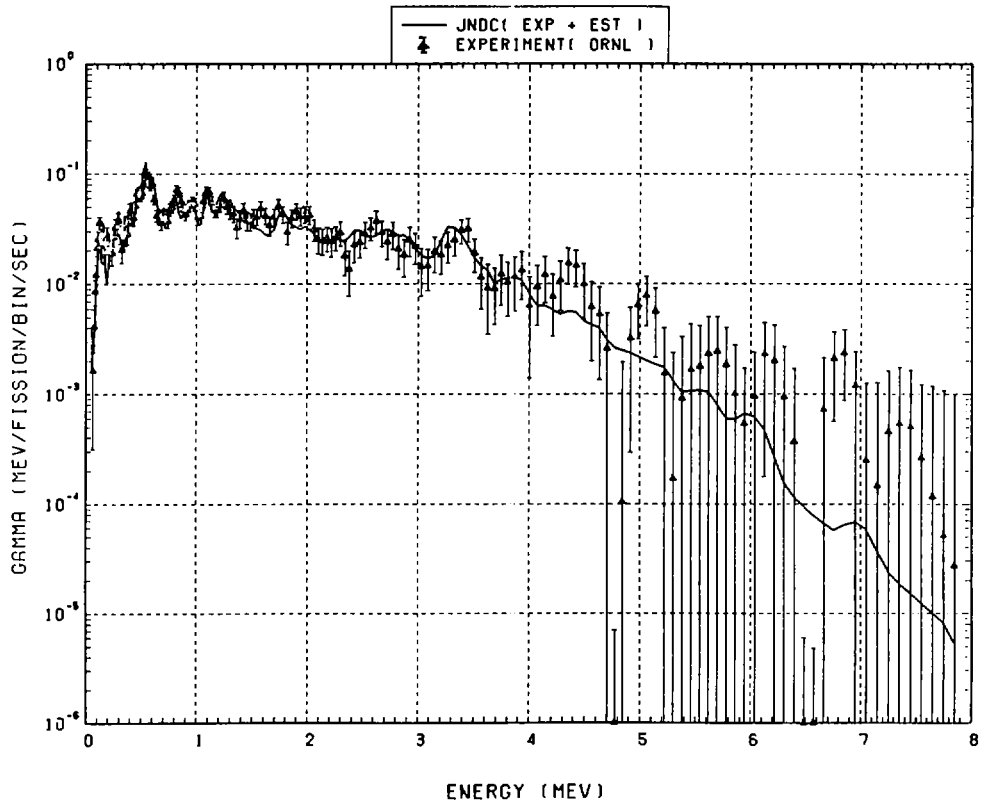

Fig. 19 Comparison of calculated gamma-ray energy spectrum with measured results at 3.7 seconds after thermal neutron fission of ^{235}U. (t_{irrad} = 1.0 s, t_{wait} = 2.7 s, t_{count} = 1.0 s)

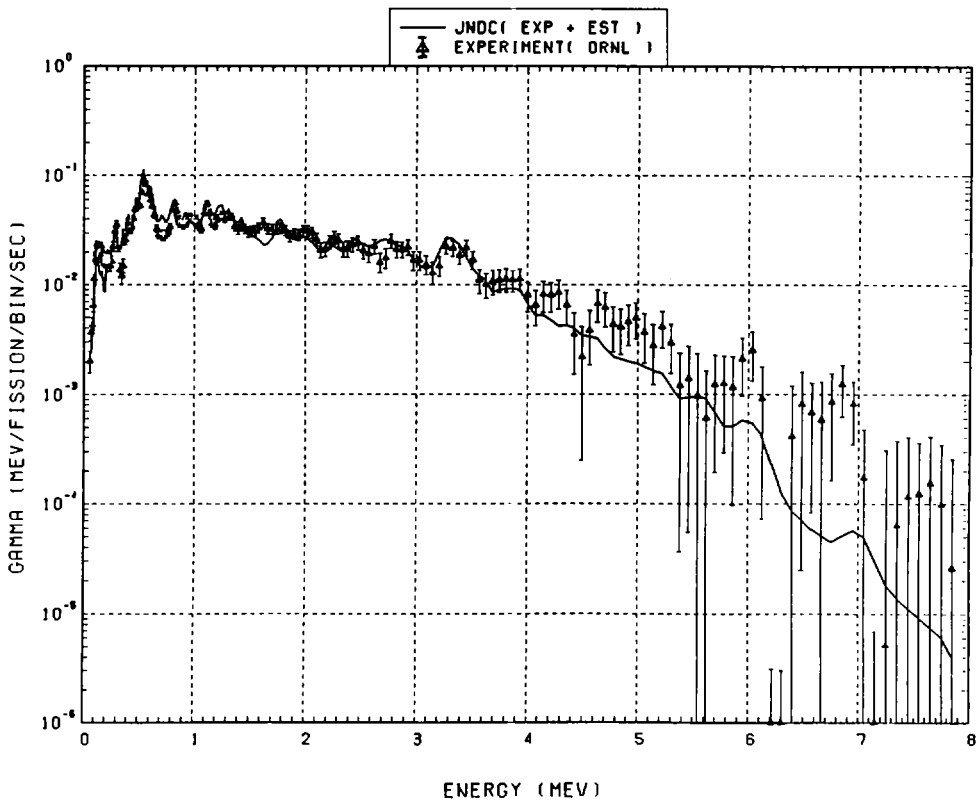

Fig. 20 Comparison of calculated gamma-ray energy spectrum with measured results at 4.7 seconds after thermal neutron fission of ^{235}U. (t_{irrad} = 1.0 s, t_{wait} = 3.7 s, t_{count} = 1.0 s)

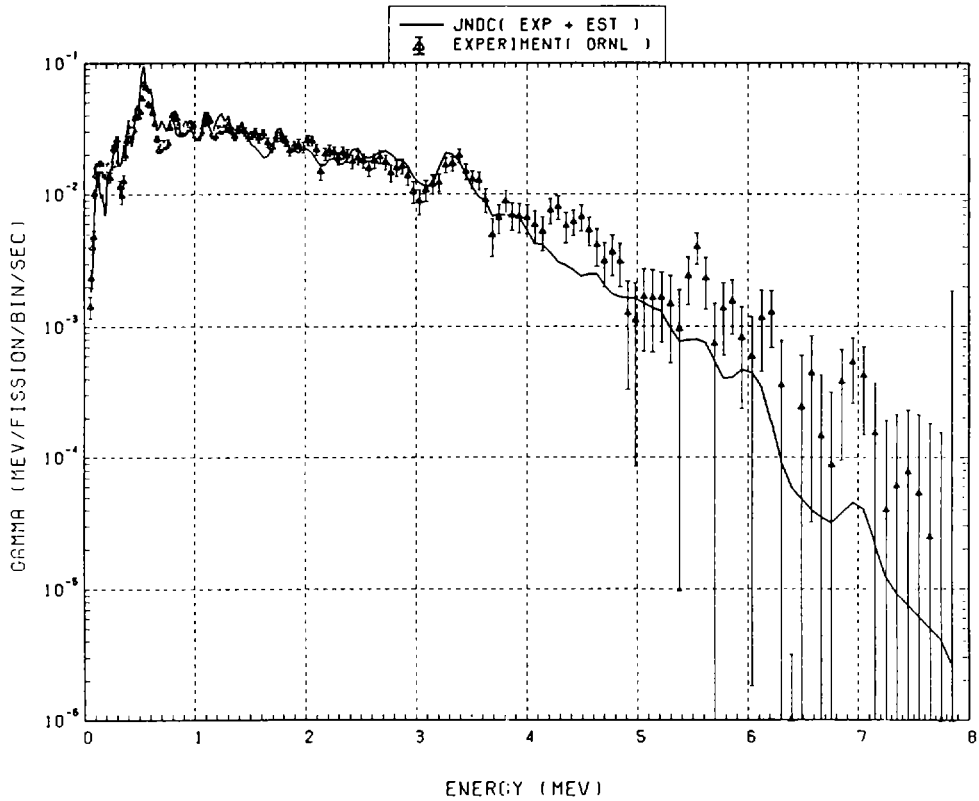

Fig. 21 Comparison of calculated gamma-ray energy spectrum with measured results at 6.2 seconds after thermal neutron fission of ^{235}U. (t_{irrad} = 1.0 s, t_{wait} = 4.7 s, t_{count} = 2.0 s)

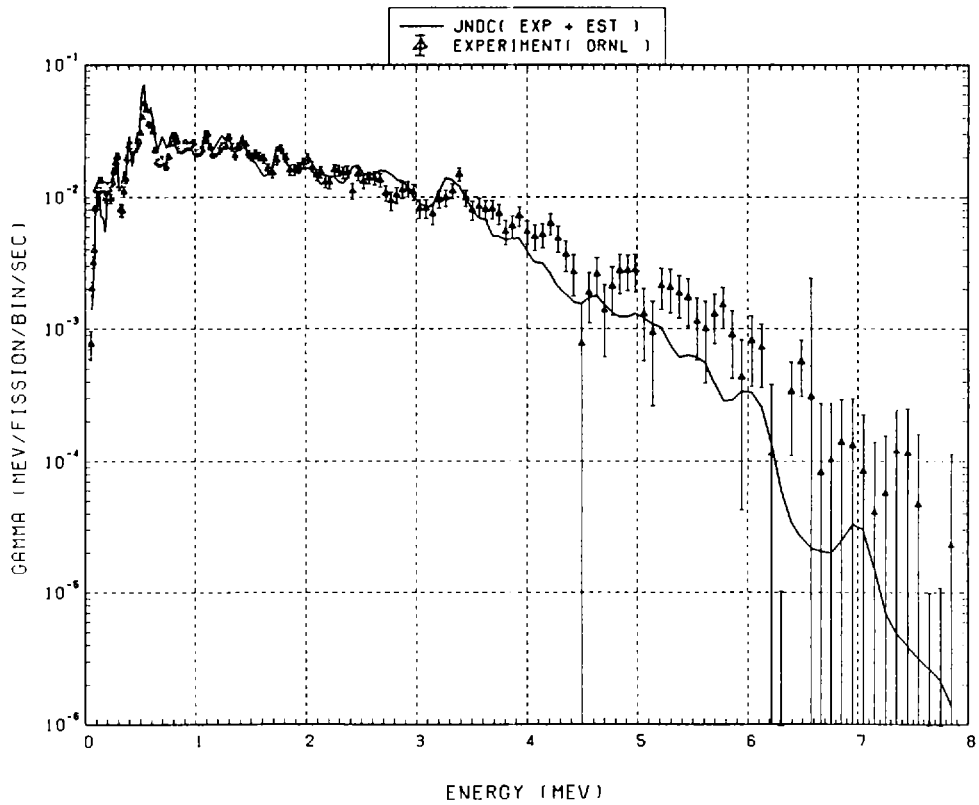

Fig. 22 Comparison of calculated gamma-ray energy spectrum with measured results at 8.7 seconds after thermal neutron fission of ^{235}U. (t_{irrad} = 1.0 s, t_{wait} = 6.7 s, t_{count} = 3.0 s)

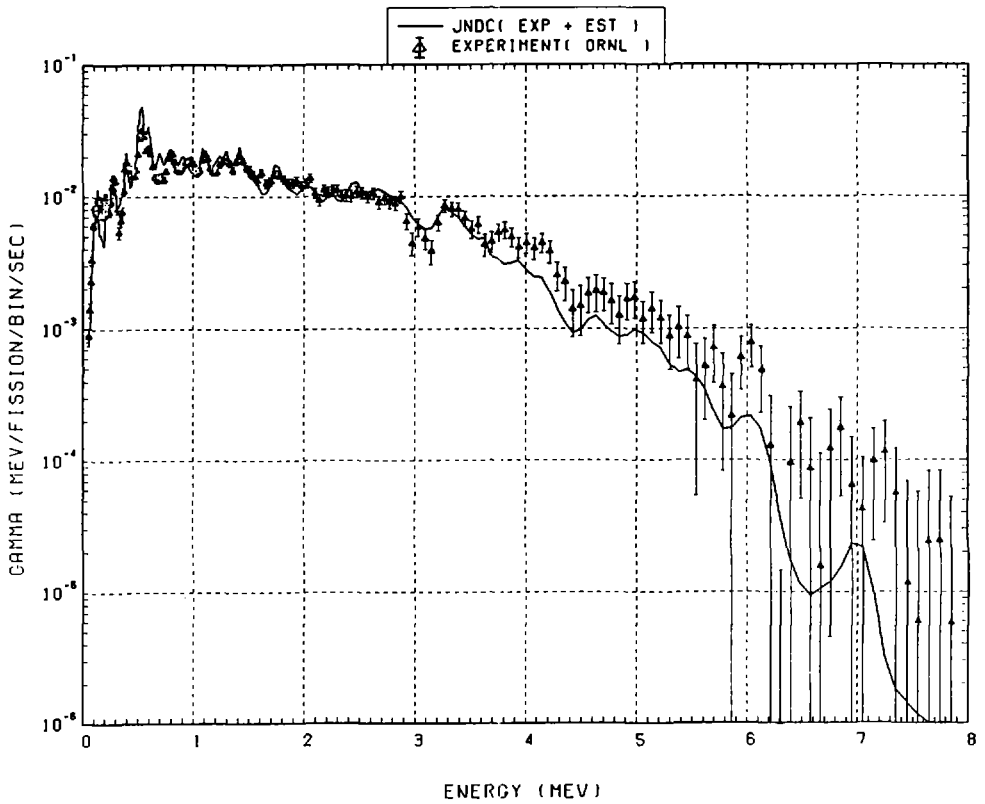

Fig. 23 Comparison of calculated gamma-ray energy spectrum with measured results at 12.7 seconds after thermal neutron fission of ^{235}U. (t_{irrad} = 1.0 s, t_{wait} = 9.7 s, t_{count} = 5.0 s)

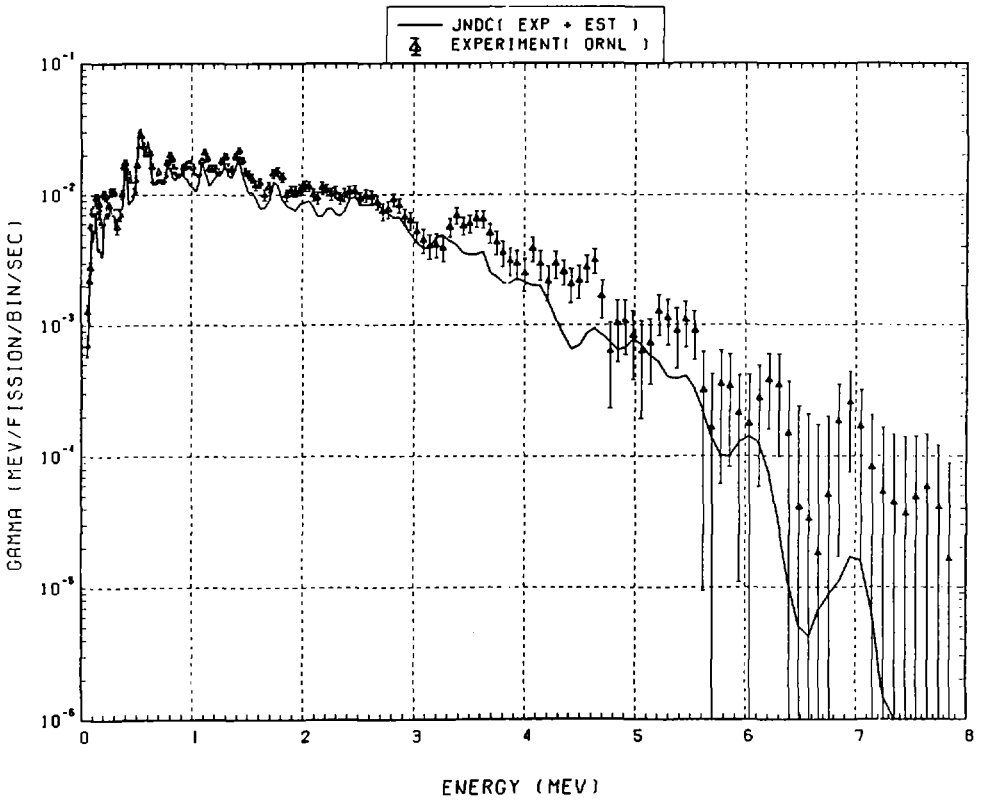

Fig. 24 Comparison of calculated gamma-ray energy spectrum with measured results at 17.2 seconds after thermal neutron fission of ^{235}U. (t_{irrad} = 1.0 s, t_{wait} = 14.7 s, t_{count} = 4.0 s)

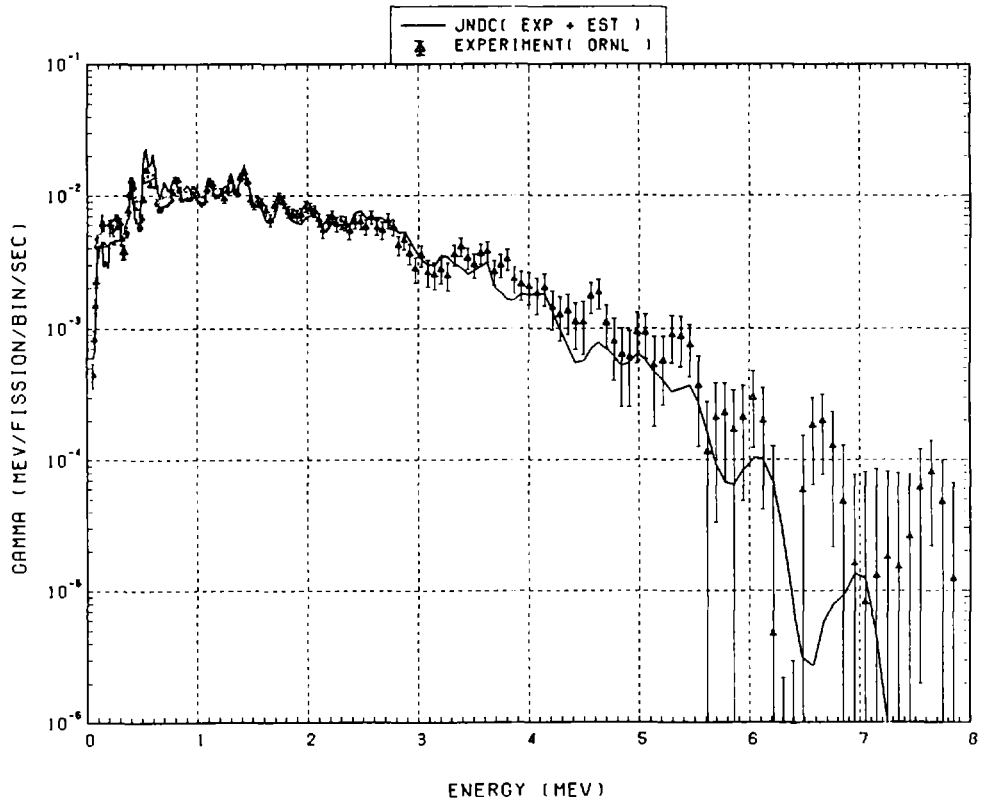

Fig. 25 Comparison of calculated gamma-ray energy spectrum with measured results at 18.2 seconds after thermal neutron fission of ^{235}U. (t_{irrad} = 10.0 s, t_{wait} = 10.7 s, t_{count} = 5.0 s)

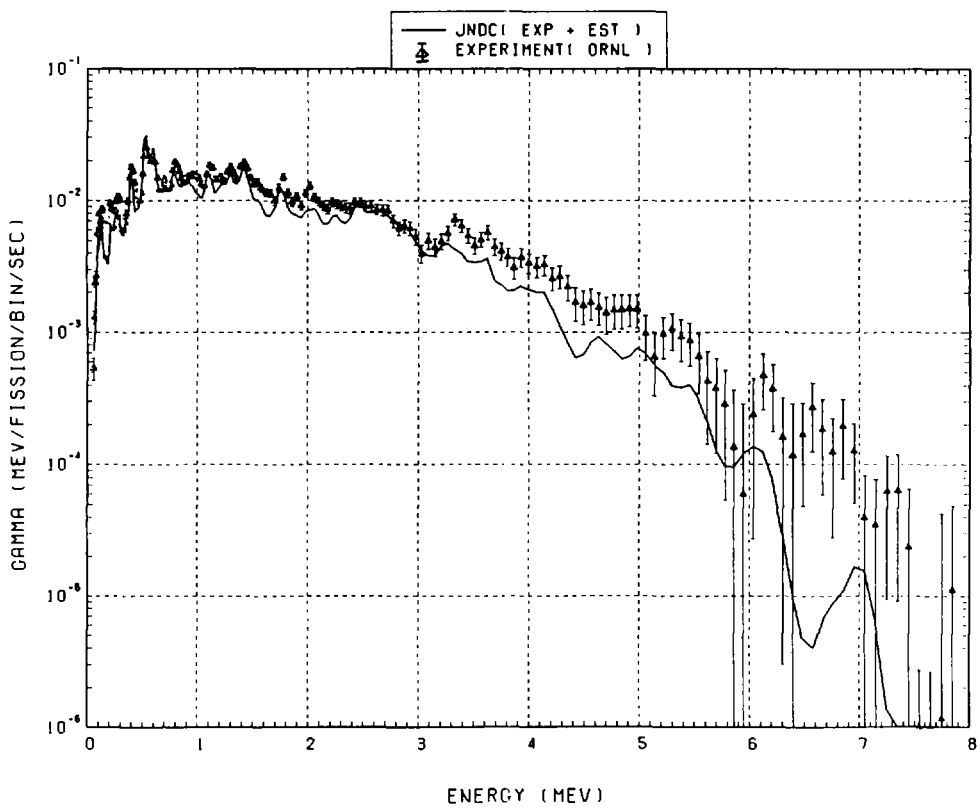

Fig. 26 Comparison of calculated gamma-ray energy spectrum with measured results at 22.7 seconds after thermal neutron fission of ^{235}U. (t_{irrad} = 1.0 s, t_{wait} = 19.7 s, t_{count} = 5.0 s)

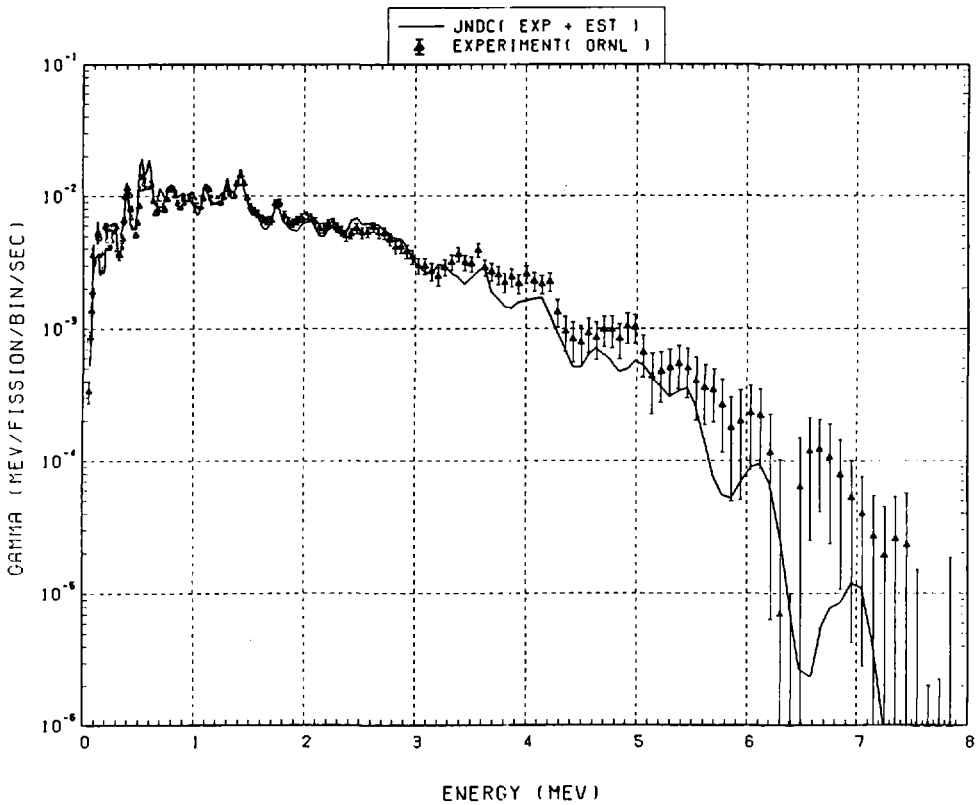

Fig. 27 Comparison of caluclated gamma-ray energy spectrum with measured results at 25.7 seconds after thermal neutron fission of ^{235}U. (t_{irrad} = 10.0 s, t_{wait} = 16.7 s, t_{count} = 8.0 s)

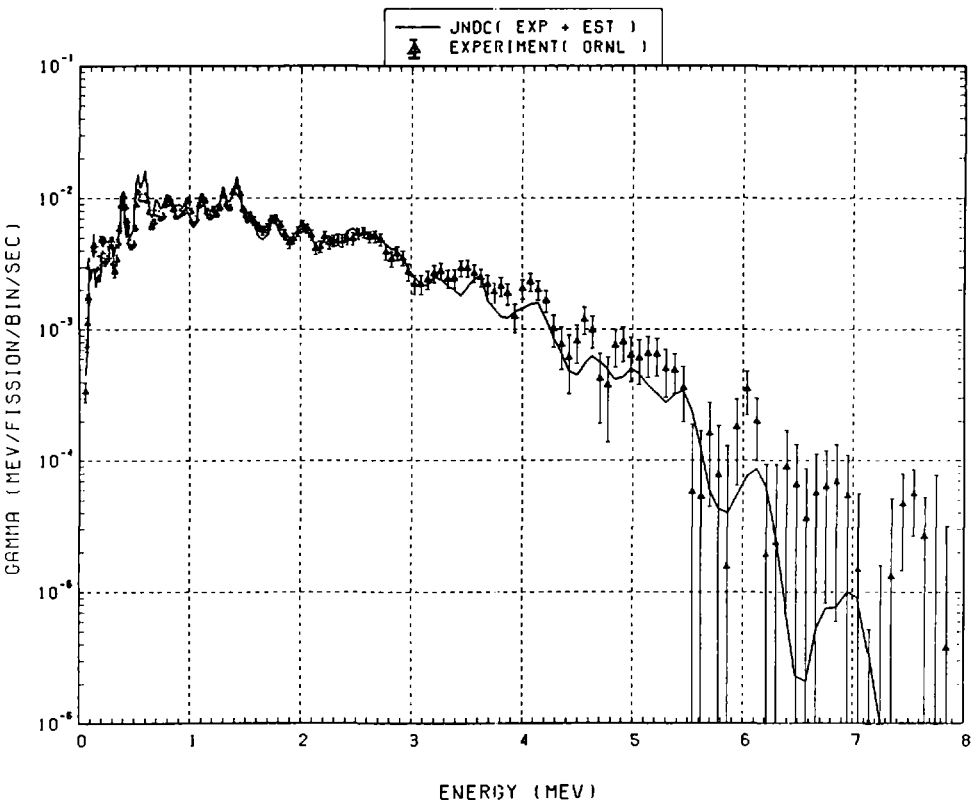

Fig. 28 Comparison of calculated gamma-ray energy spectrum with measured results at 30.2 seconds after thermal neutron fission of ^{235}U. (t_{irrad} = 1.0 s, t_{wait} = 24.7 s, t_{count} = 10.0 s)

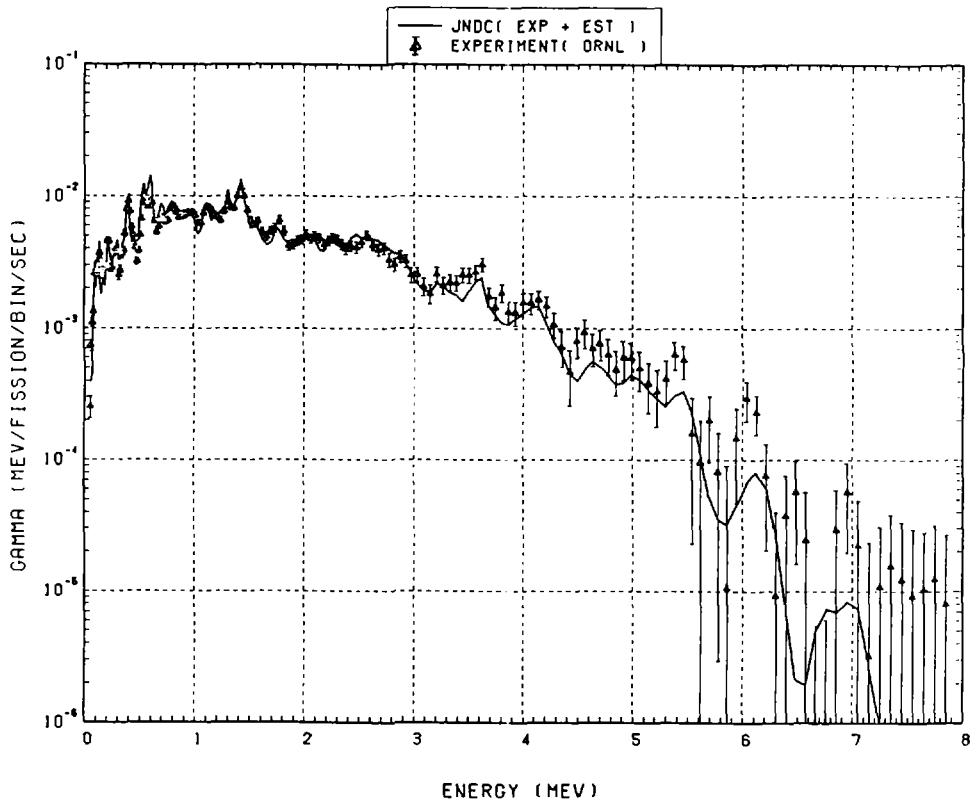

Fig. 29 Comparison of calculated gamma-ray energy spectrum with measured results at 34.7 seconds after thermal neutron fission of ^{235}U. (t_{irrad} = 10.0 s, t_{wait} = 24.7 s, t_{count} = 10.0 s)

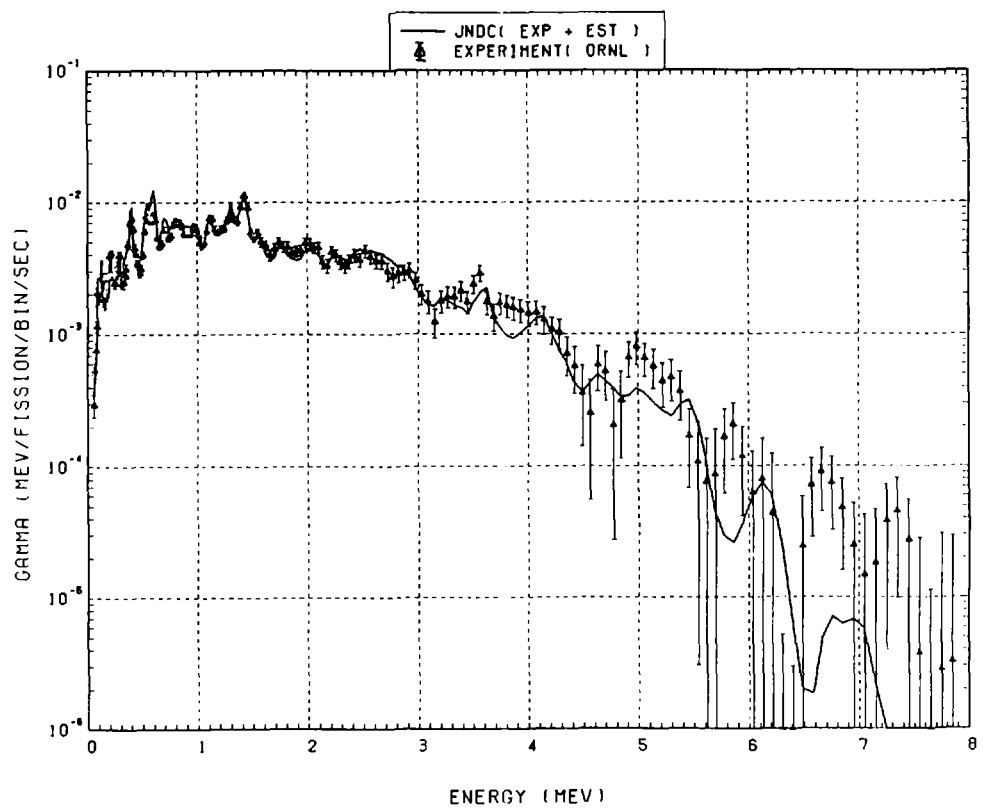

Fig. 30 Comparison of calculated gamma-ray energy spectrum with measured results at 40.2 seconds after thermal neutron fission of ^{235}U. (t_{irrad} = 1.0 s, t_{wait} = 34.7 s, t_{count} = 10.0 s)

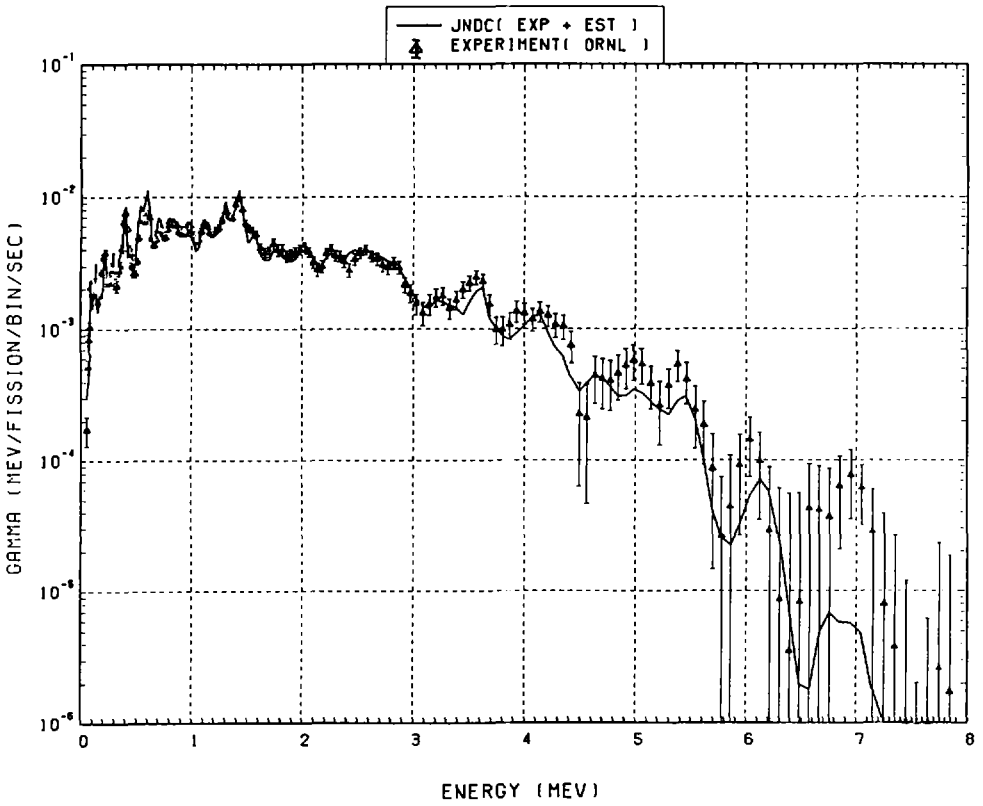

Fig. 31 Comparison of calculated gamma-ray energy spectrum with measured results at 44.7 seconds after thermal neutron fission of ^{235}U. (t_{irrad} = 10.0 s, t_{wait} = 34.7 s, t_{count} = 10.0 s)

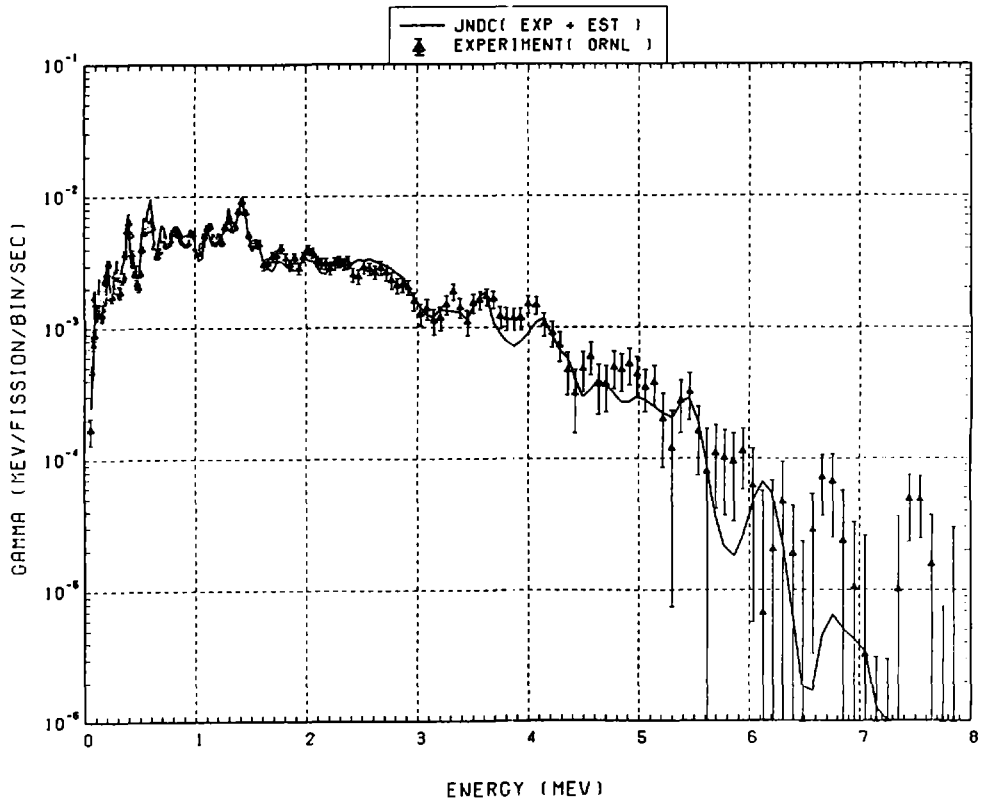

Fig. 32 Comparison of calculated gamma-ray energy spectrum with measured results at 52.7 seconds after thermal neutron fission of ^{235}U. (t_{irrad} = 1.0 s, t_{wait} = 44.7 s, t_{count} = 15.0 s)

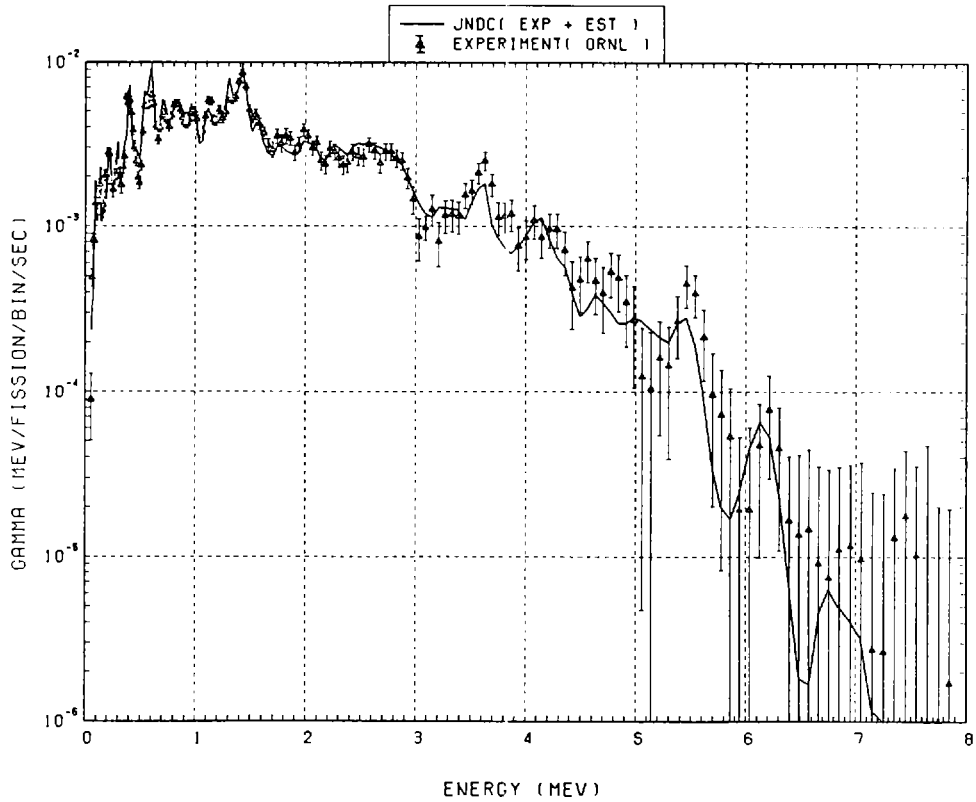

Fig. 33 Comparison of calculated gamma-ray energy spectrum with measured results at 54.7 seconds after thermal neutron fission of ^{235}U. (t_{irrad} = 10.0 s, t_{wait} = 44.7 s, t_{count} = 10.0 s)

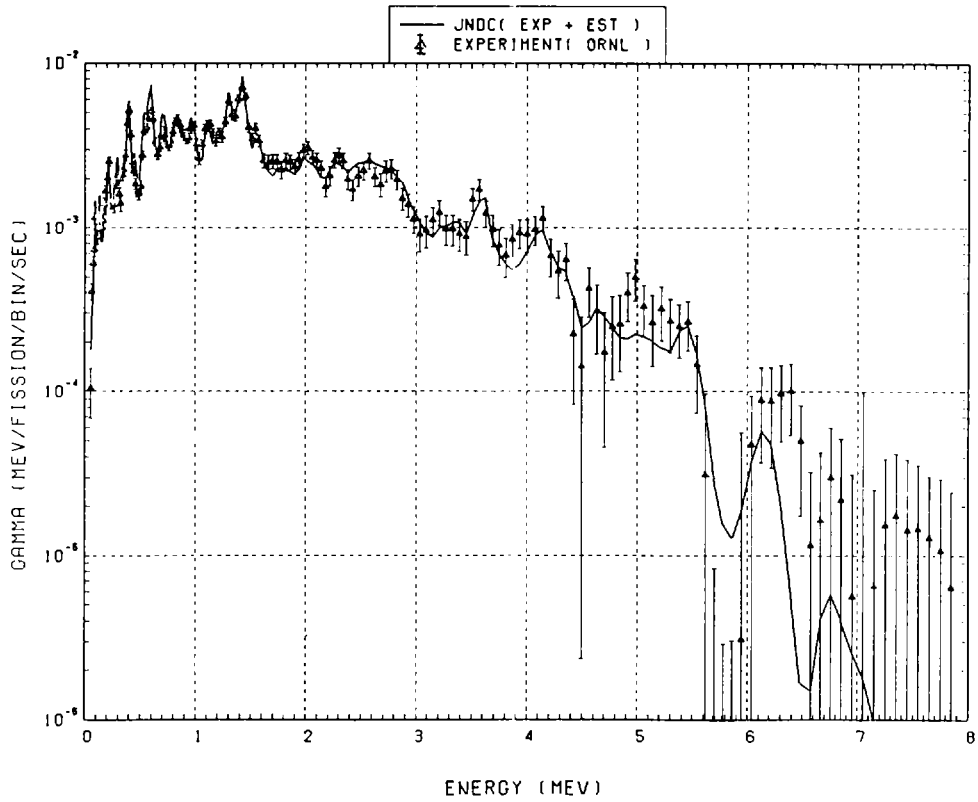

Fig. 34 Comparison of calculated gamma-ray energy spectrum with measured results at 67.7 seconds after thermal neutron fission of ^{235}U. (t_{irrad} = 1.0 s, t_{wait} = 59.7 s, t_{count} = 15.0 s)

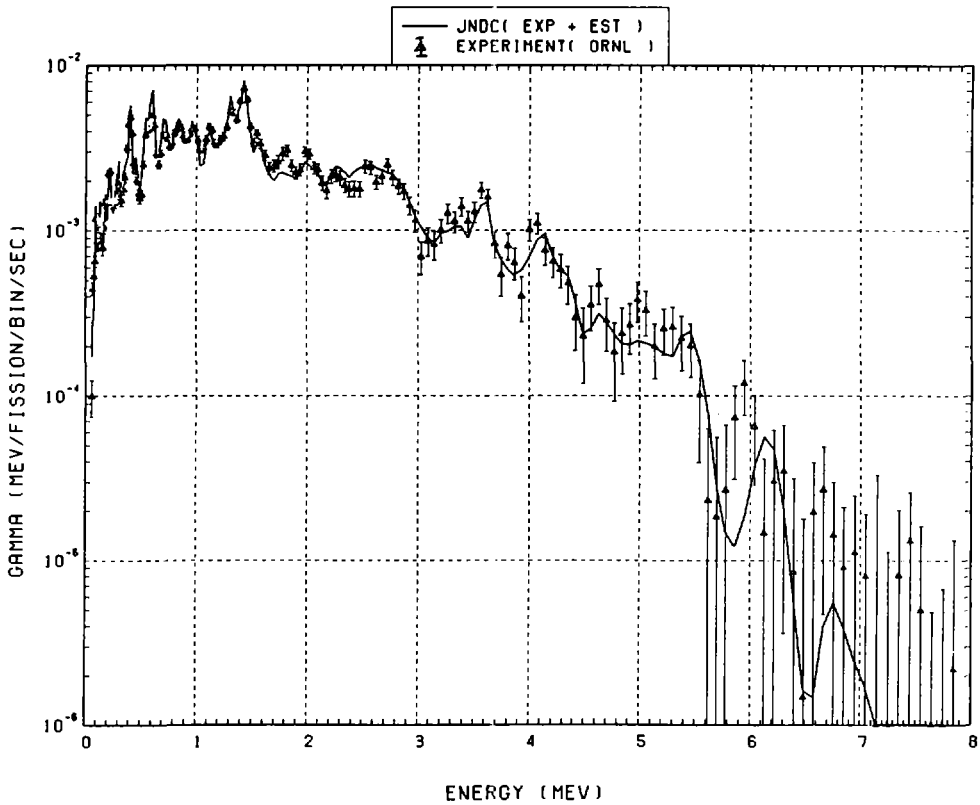

Fig. 35 Comparison of calculated gamma-ray energy spectrum with measured results at 69.7 seconds after thermal neutron fission of ^{235}U. (t_{irrad} = 10.0 s, t_{wait} = 54.7 s, t_{count} = 20.0 s)

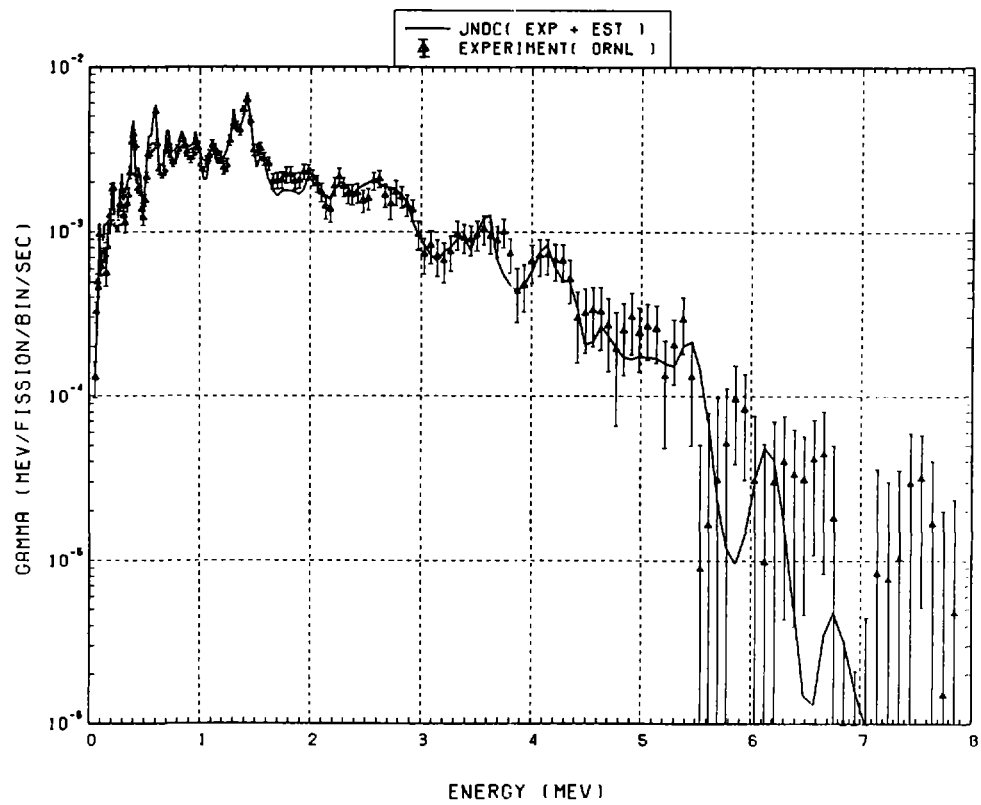

Fig. 36 Comparison of calculated gamma-ray energy spectrum with measured results at 83.0 seconds after thermal neutron fission of ^{235}U. (t_{irrad} = 1.0 s, t_{wait} = 75.0 s, t_{count} = 15.0 s)

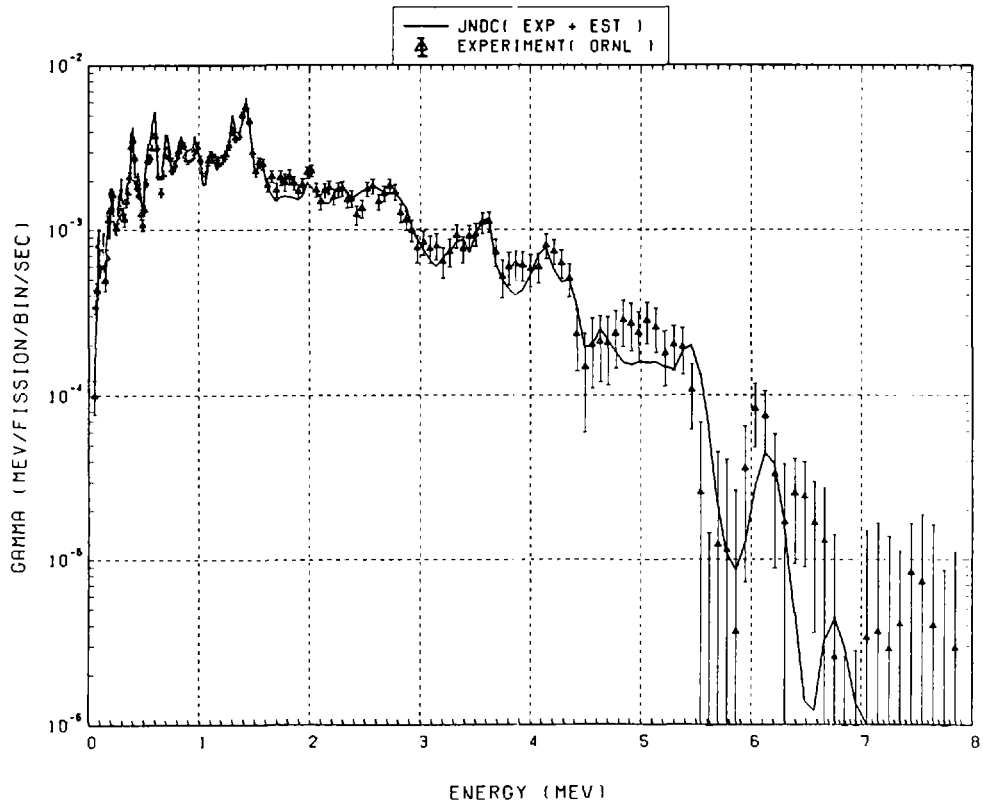

Fig. 37 Comparison of calculated gamma-ray energy spectrum with measured results at 90.0 seconds after thermal neutron fission of ^{235}U. (t_{irrad} = 10.0 s, t_{wait} = 75.0 s, t_{count} = 20.0 s)

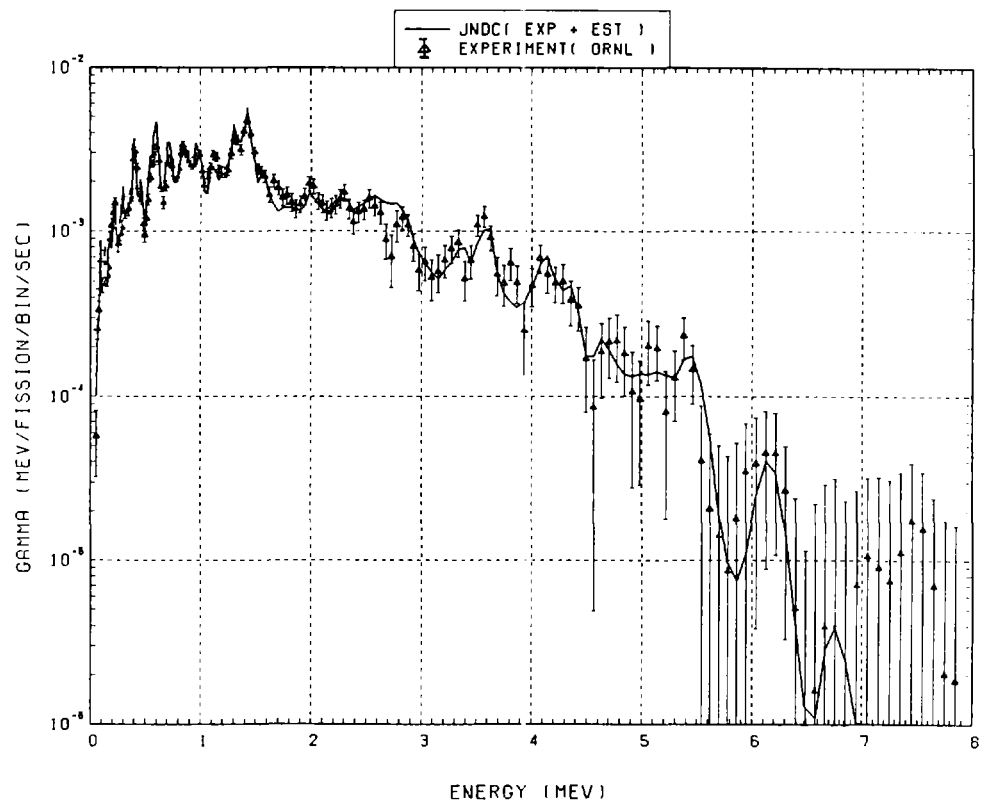

Fig. 38 Comparison of calculated gamma-ray energy spectrum with measured results at 100.5 seconds after thermal neutron fission of ^{235}U. (t_{irrad} = 1.0 s, t_{wait} = 90.0 s, t_{count} = 20.0 s)

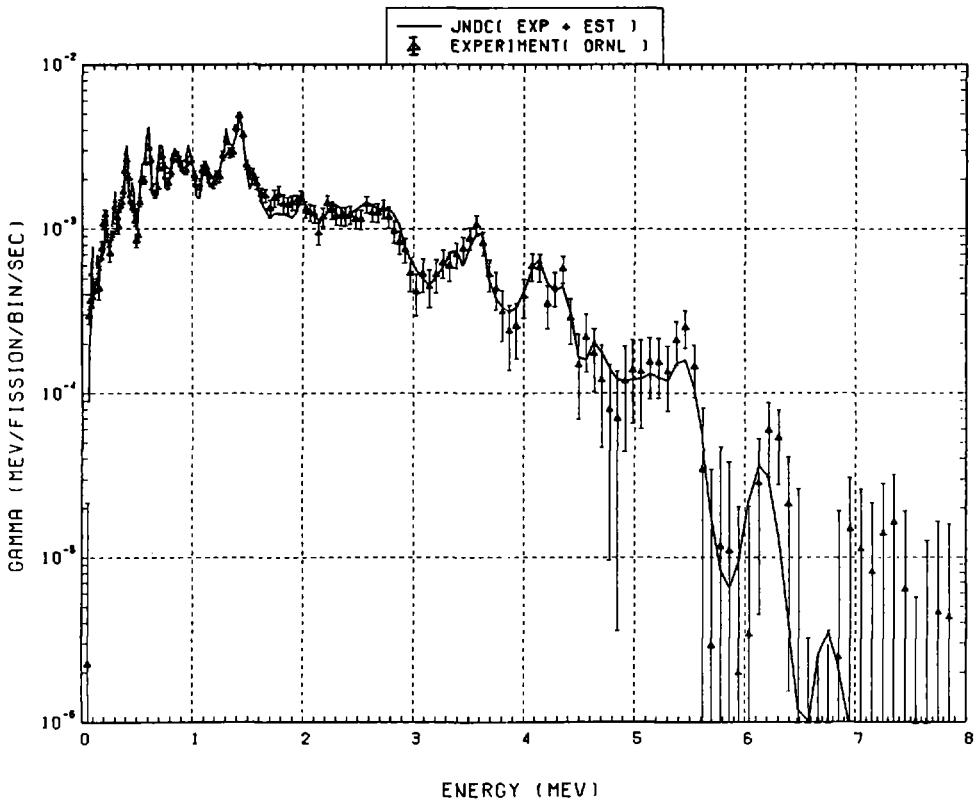

Fig. 39 Comparison of calculated gamma-ray energy spectrum with measured results at 110 seconds after thermal neutron fission of ^{235}U. (t_{irrad} = 10 s, t_{wait} = 95 s, t_{count} = 20 s)

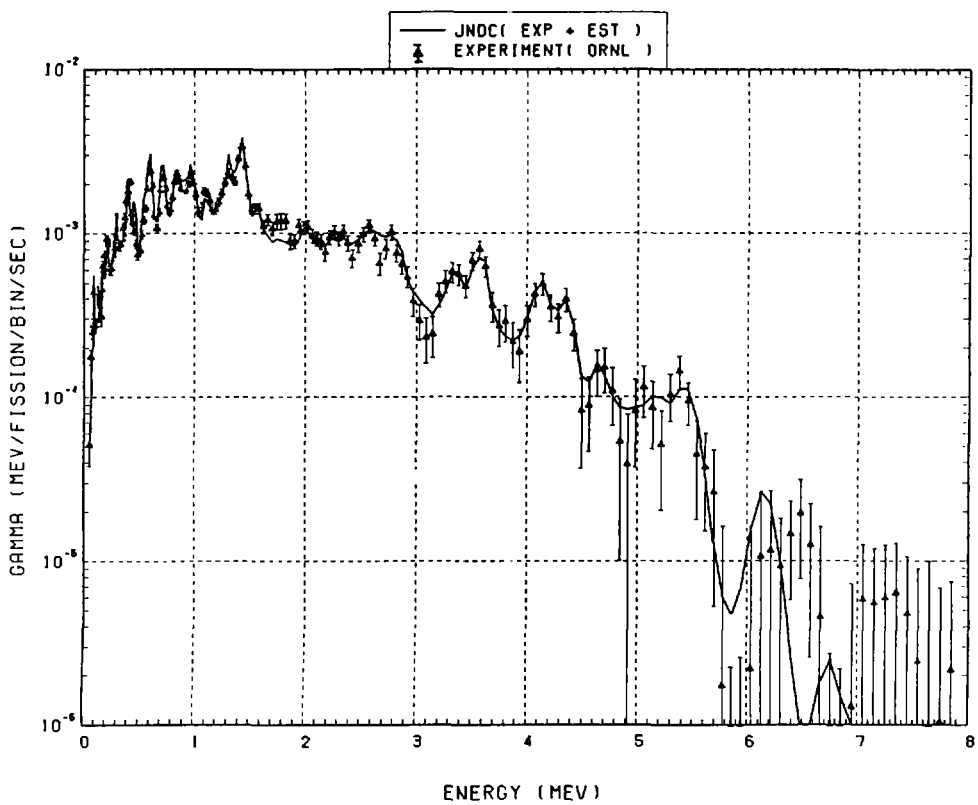

Fig. 40 Comparison of calculated gamma-ray energy spectrum with measured results at 140 seconds after thermal neutron fission of ^{235}U. (t_{irrad} = 10 s, t_{wait} = 115 s, t_{count} = 40 s)

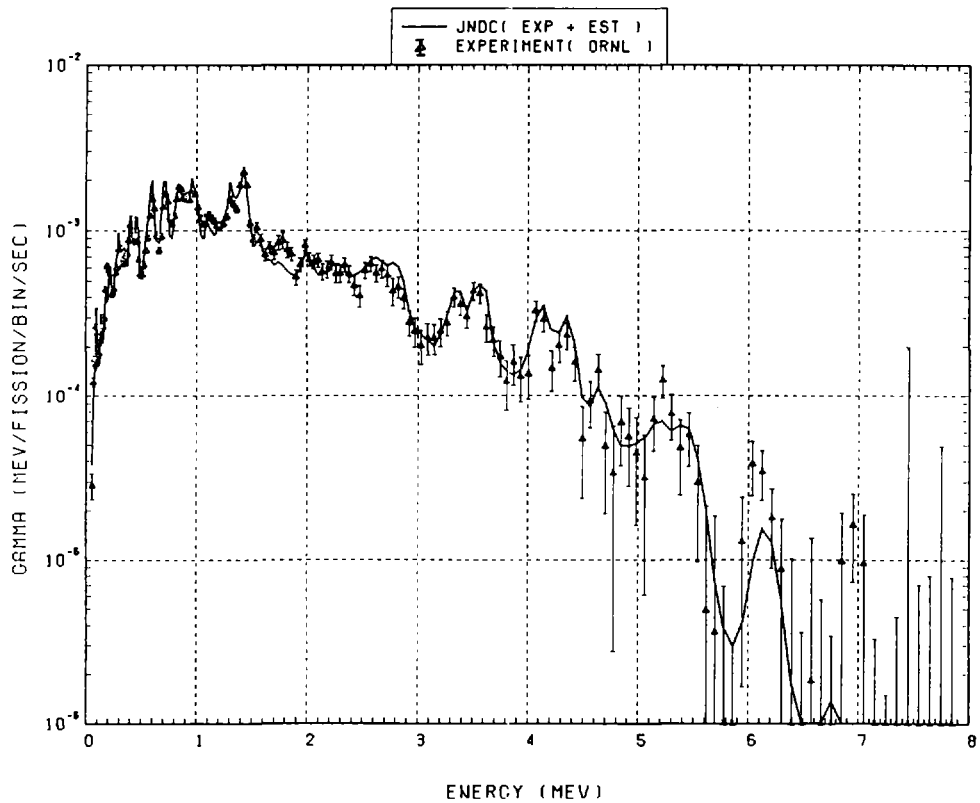

Fig. 41 Comparison of calculated gamma-ray energy spectrum with measured results at 190 seconds after thermal neutron fission of ^{235}U. (t_{irrad} = 10 s, t_{wait} = 155 s, t_{count} = 60 s)

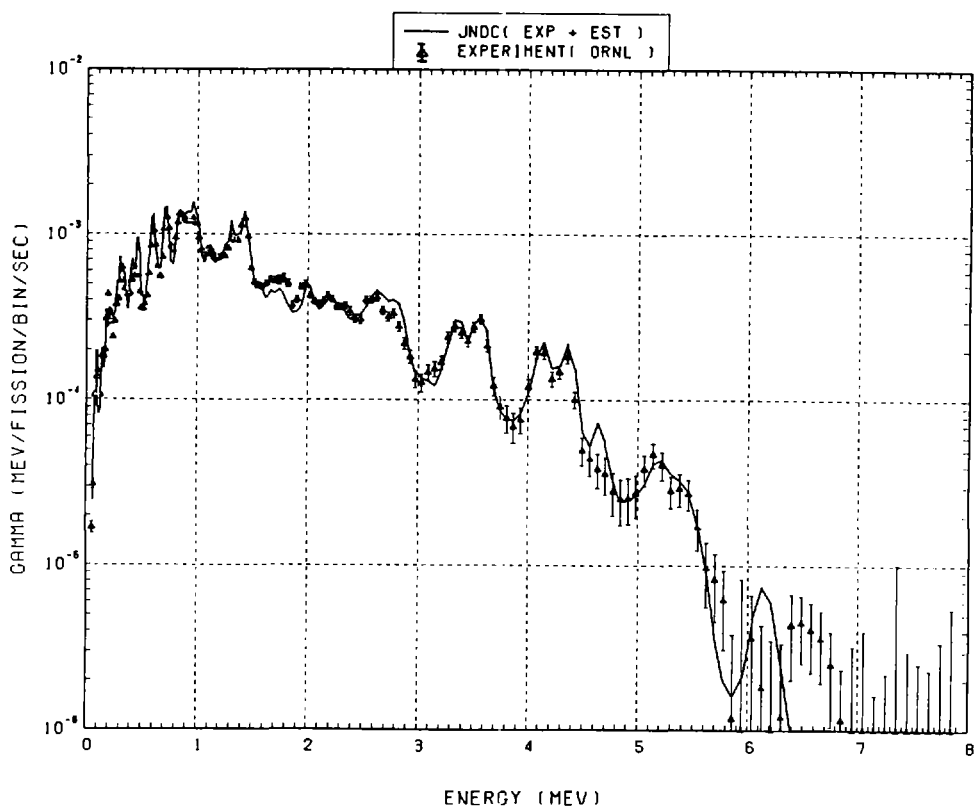

Fig. 42 Comparison of calculated gamma-ray energy spectrum with measured results at 260 seconds after thermal neutron fission of ^{235}U. (t_{irrad} = 100 s, t_{wait} = 170 s, t_{count} = 80 s)

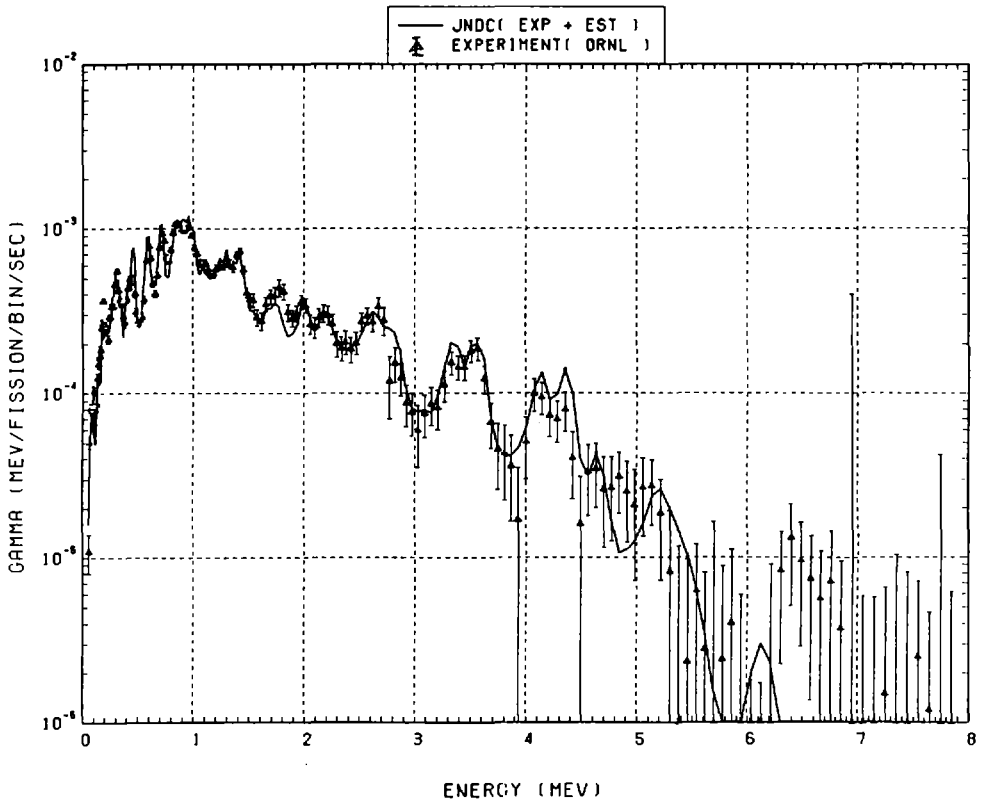

Fig. 43 Comparison of calculated gamma-ray energy spectrum with measured results at 350 seconds after thermal neutron fission of ^{235}U. (t_{irrad} = 10 s, t_{wait} = 295 s, t_{count} = 100 s)

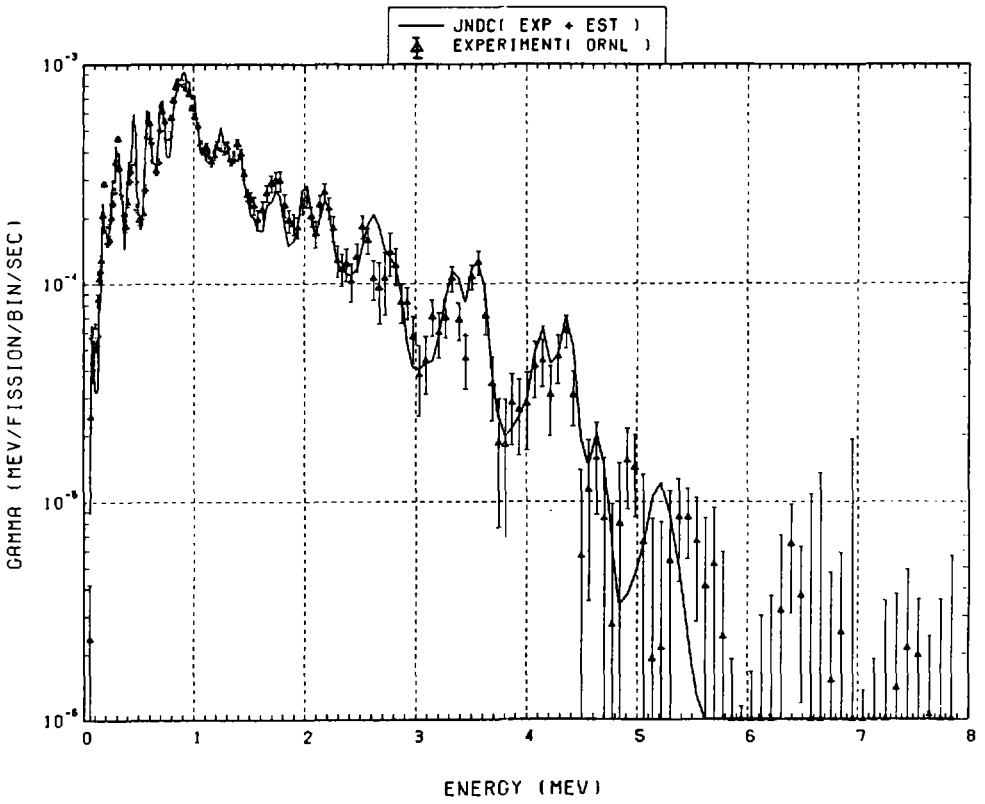

Fig. 44 Comparison of calculated gamma-ray energy spectrum with measured results at 500 seconds after thermal neutron fission of ^{235}U. (t_{irrad} = 10 s, t_{wait} = 395 s, t_{count} = 200 s)

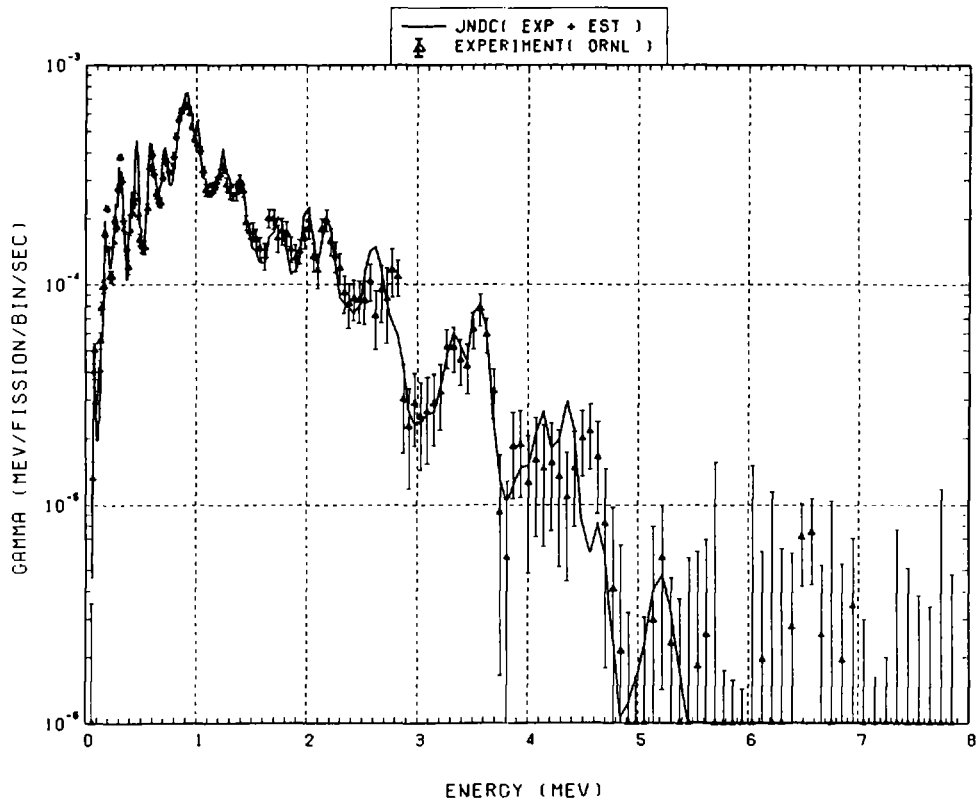

Fig. 45 Comparison of calculated gamma-ray energy spectrum with measured results at 700 seconds after thermal neutron fission of ^{235}U. (t_{irrad} = 10 s, t_{wait} = 595 s, t_{count} = 200 s)

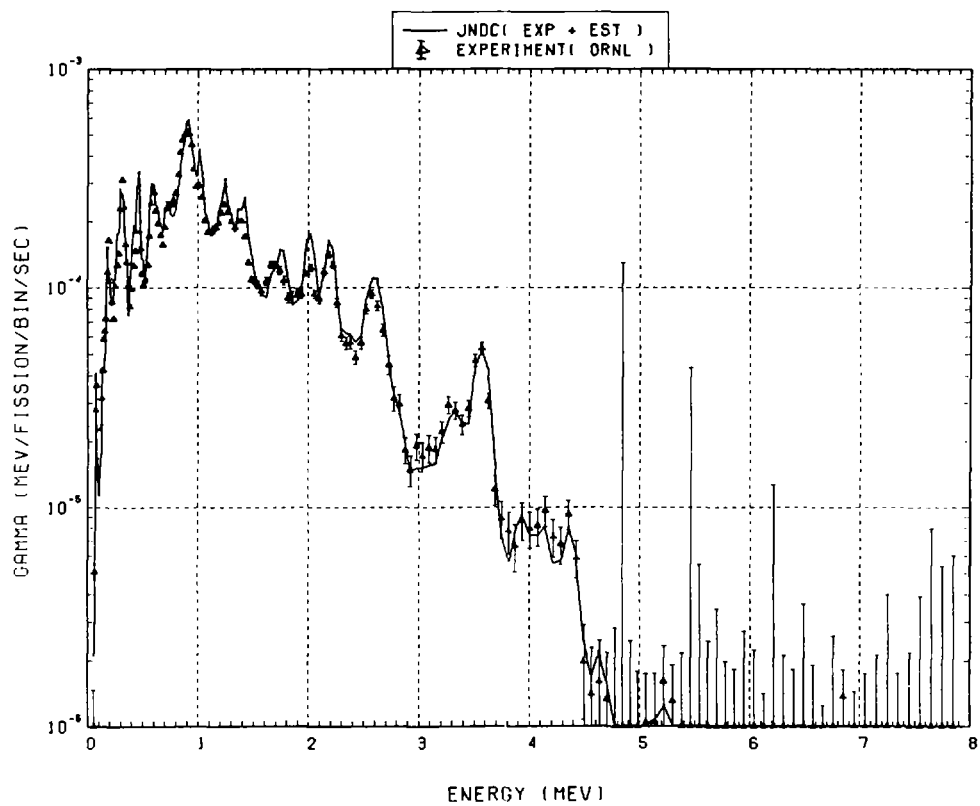

Fig. 46 Comparison of calculated gamma-ray energy spectrum with measured results at 1000 seconds after thermal neutron fission of ^{235}U. (t_{irrad} = 100 s, t_{wait} = 750 s, t_{count} = 400 s)

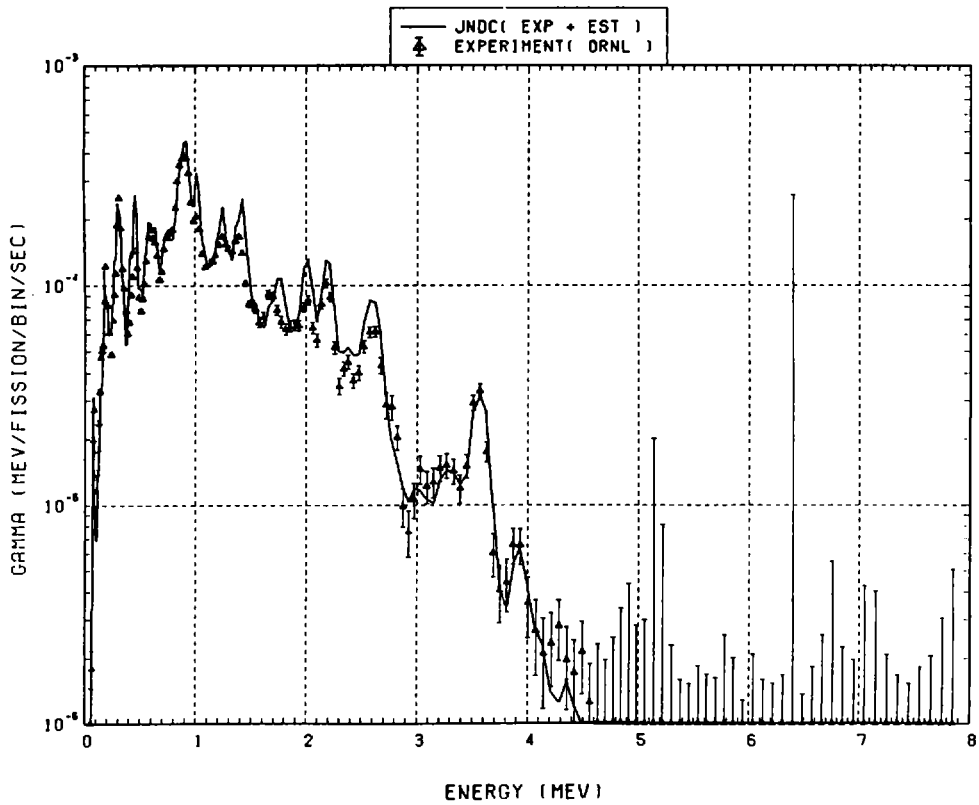

Fig. 47 Comparison of calculated gamma-ray energy spectrum with measured results at 1400 seconds after thermal neutron fission of ^{235}U. (t_{irrad} = 100 s, t_{wait} = 1150 s, t_{count} = 400 s)

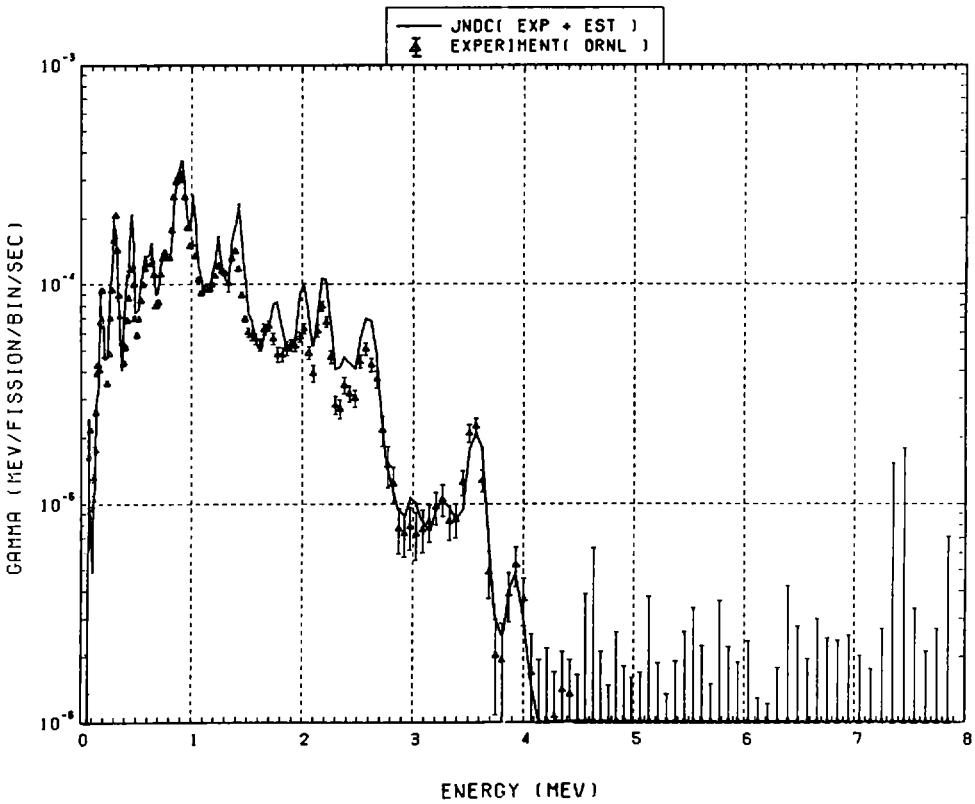

Fig. 48 Comparison of calculated gamma-ray energy spectrum with measured results at 1800 seconds after thermal neutron fission of ^{235}U. (t_{irrad} = 100 s, t_{wait} = 1550 s, t_{count} = 400 s)

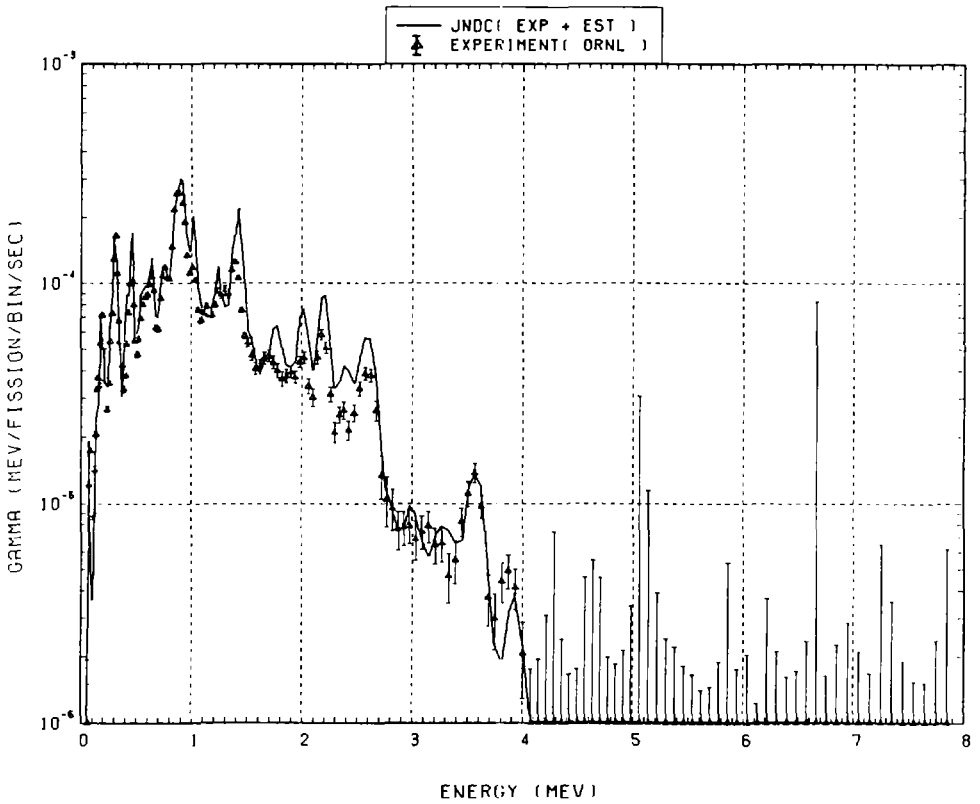

Fig. 49 Comparison of calculated gamma-ray energy spectrum with measured results at 2250 seconds after thermal neutron fission of ^{235}U. (t_{irrad} = 100 s, t_{wait} = 1950 s, t_{count} = 500 s)

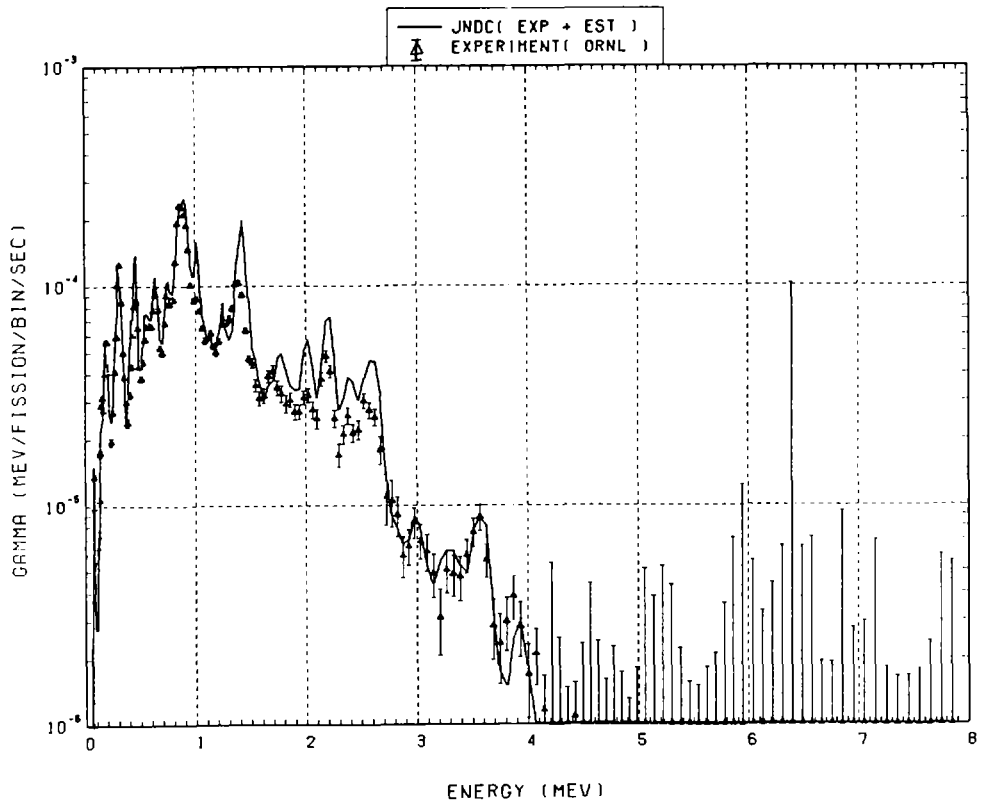

Fig. 50 Comparison of calculated gamma-ray energy spectrum with measured results at 2750 seconds after thermal neutron fission of ^{235}U. (t_{irrad} = 100 s, t_{wait} = 2450 s, t_{count} = 500 s)

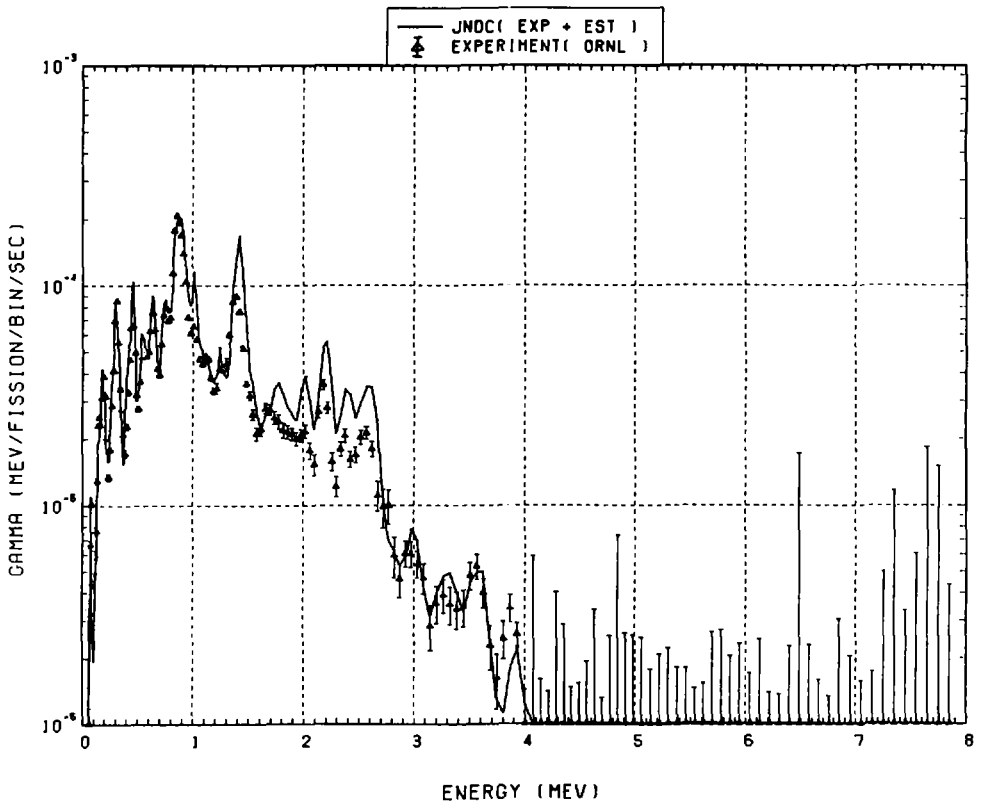

Fig. 51 Comparison of calculated gamma-ray energy spectrum with measured results at 3500 seconds after thermal neutron fission of ^{235}U. (t_{irrad} = 100 s, t_{wait} = 2950 s, t_{count} = 1000 s)

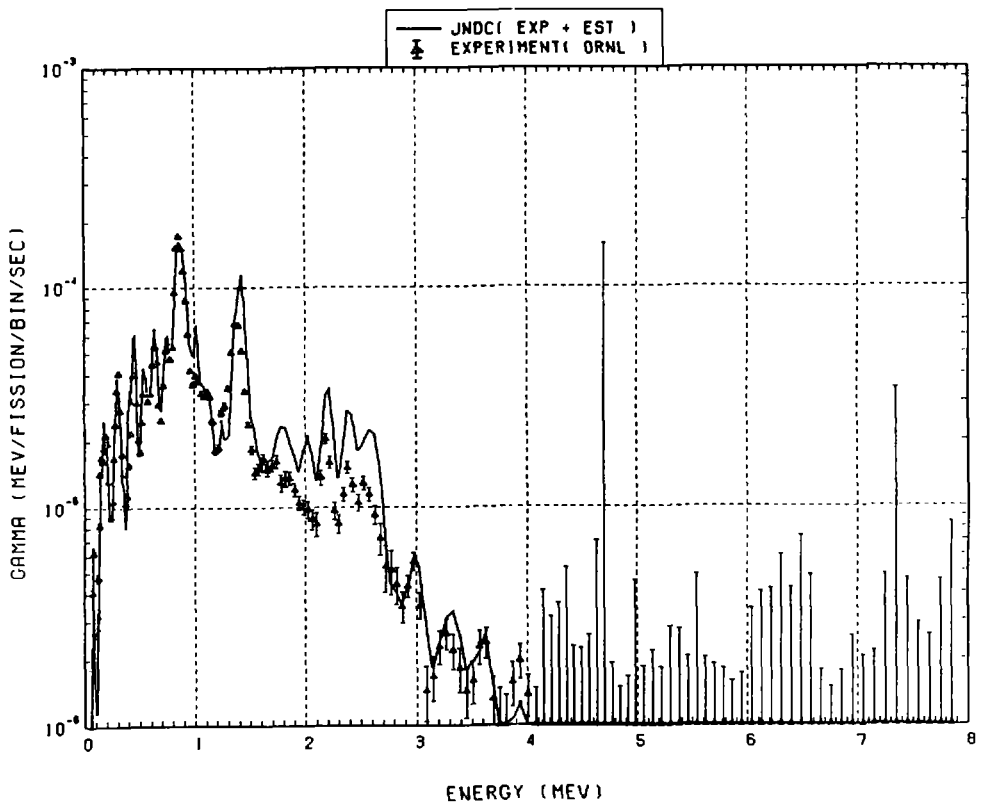

Fig. 52 Comparison of calculated gamma-ray energy spectrum with measured results at 5000 seconds after thermal neutron fission of ^{235}U. (t_{irrad} = 100 s, t_{wait} = 3950 s, t_{count} = 2000 s)

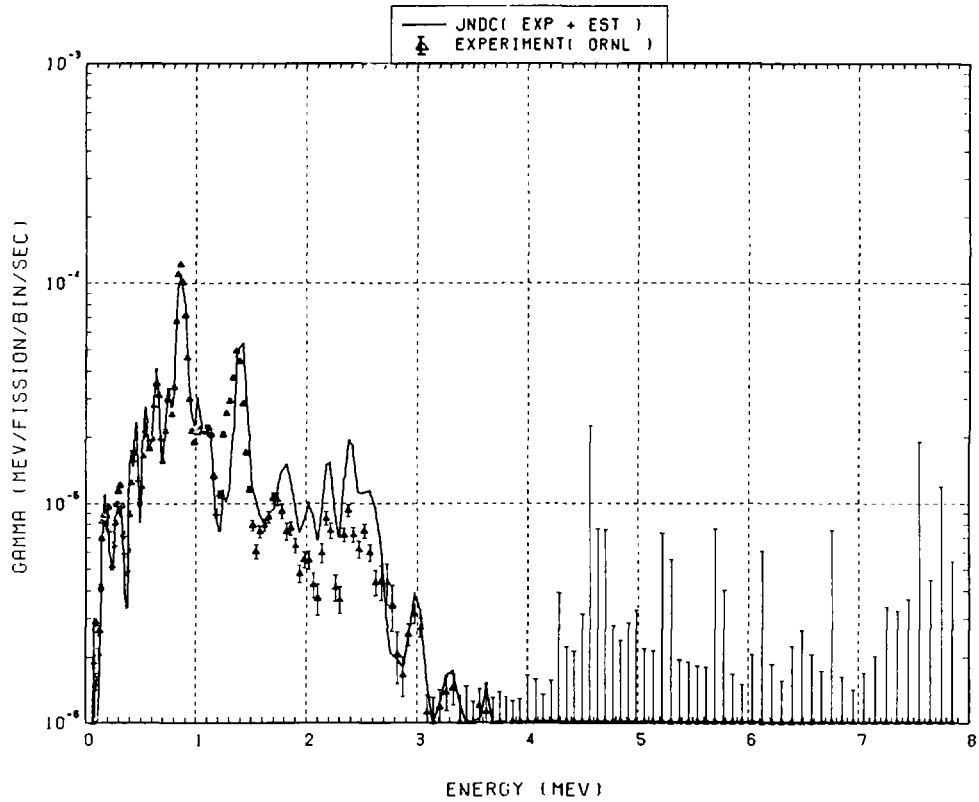

Fig. 53 Comparison of calculated gamma-ray energy spectrum with measured results at 8000 seconds after thermal neutron fission of ^{235}U. (t_{irrad} = 100 s, t_{wait} = 5950 s, t_{count} = 4000 s)

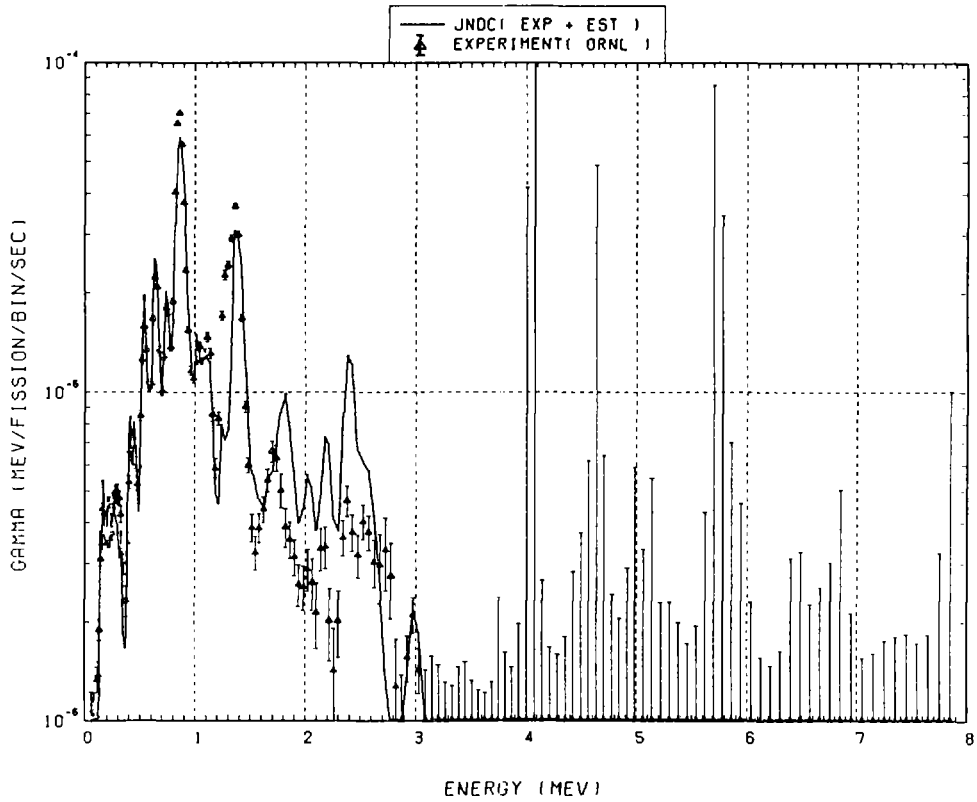

Fig. 54 Comparison of calculated gamma-ray energy spectrum with measured results at 12000 seconds after thermal neutron fission of ^{235}U. (t_{irrad} = 100 s, t_{wait} = 9950 s, t_{count} = 4000 s)

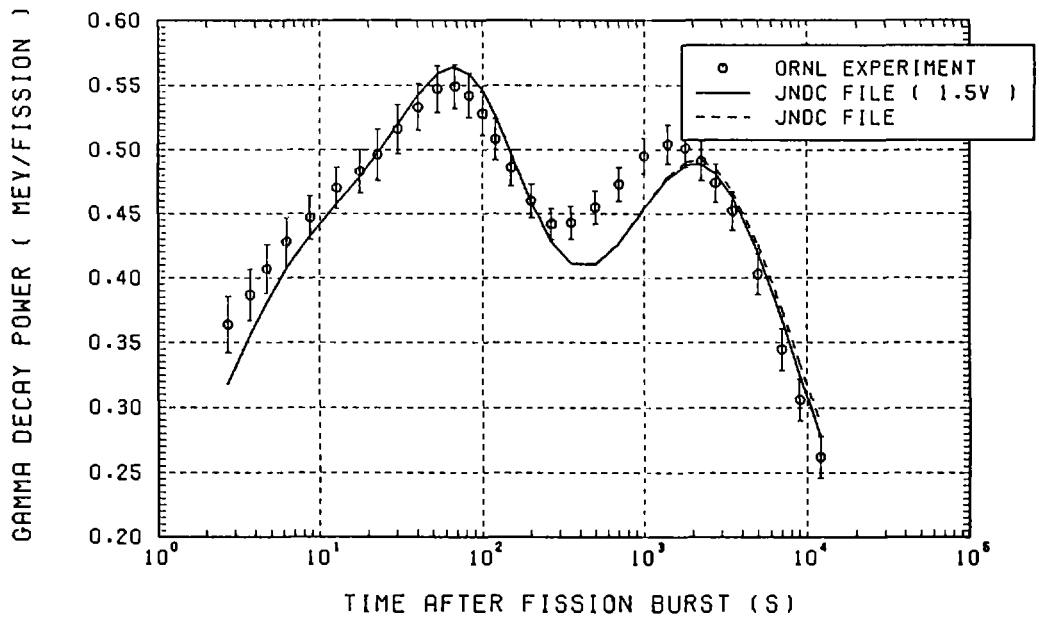

Fig. 55 Comparison of calculated gamma-decay heat with measured results at ORNL for thermal neutron fission of ^{239}Pu.

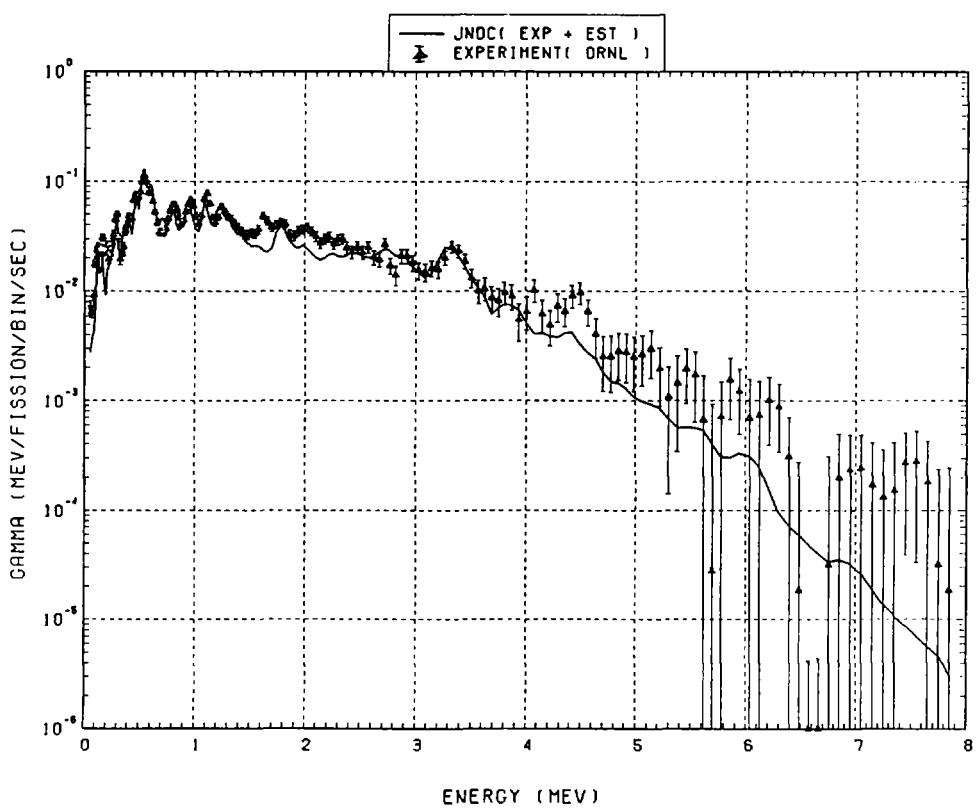

Fig. 56 Comparison of calculated gamma-ray energy spectrum with measured results at 2.7 seconds after thermal neutron fission of ^{239}Pu. (t_{irrad} = 1.0 s, t_{wait} = 1.7 s, t_{count} = 1.0 s)

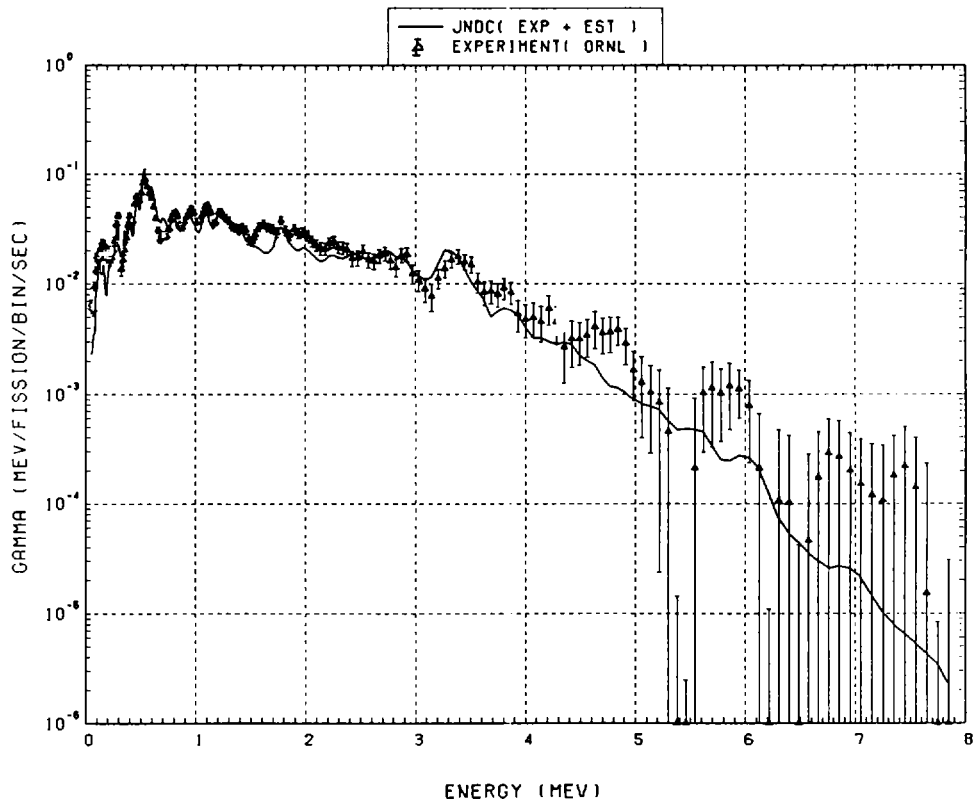

Fig. 57 Comparison of calculated gamma-ray energy spectrum with measured results at 3.7 seconds after thermal neutron fission of ^{239}Pu. (t_{irrad} = 1.0 s, t_{wait} = 2.7 s, t_{count} = 1.0 s)

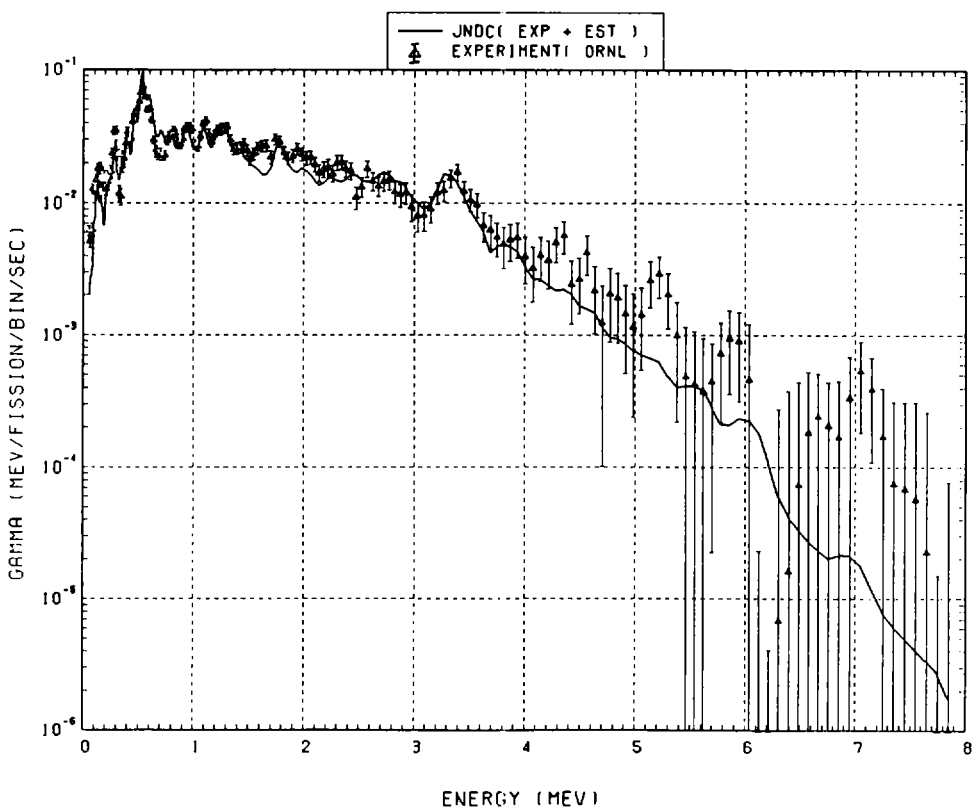

Fig. 58 Comparison of calculated gamma-ray energy spectrum with measured results at 4.7 seconds after thermal neutron fission of ^{239}Pu. (t_{irrad} = 1.0 s, t_{wait} = 3.7 s, t_{count} = 1.0 s)

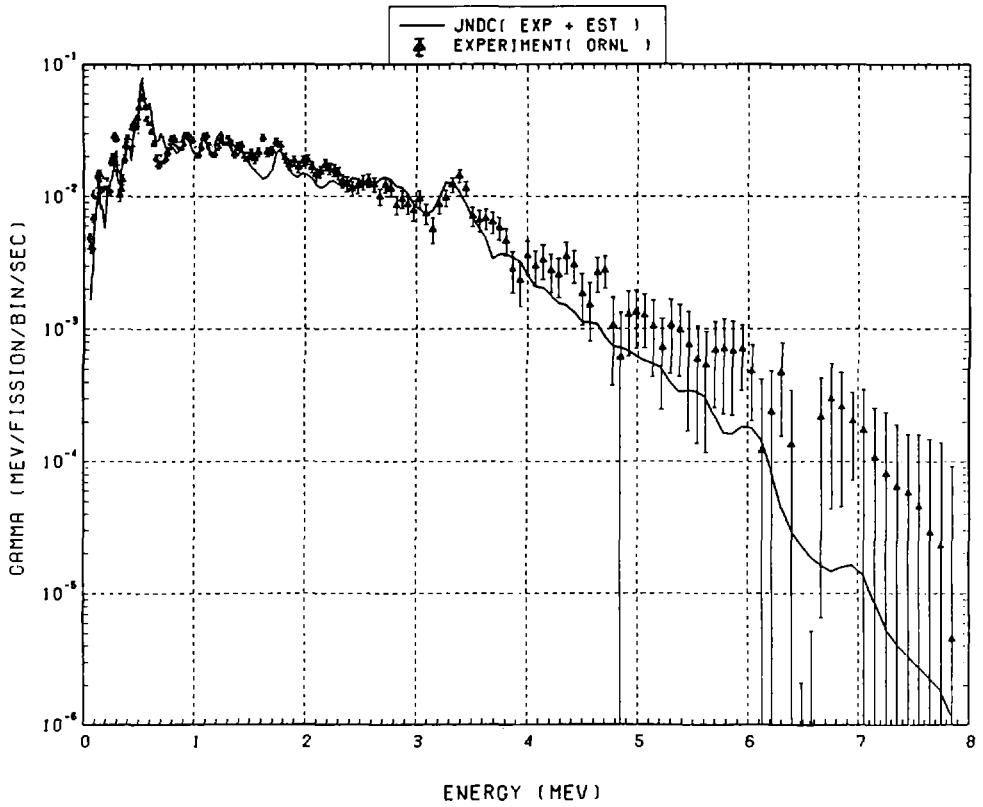

Fig. 59 Comparison of calculated gamma-ray energy spectrum with measured results at 6.2 seconds after thermal neutron fission of ^{239}Pu. (t_{irrad} = 1.0 s, t_{wait} = 4.7 s, t_{count} = 2.0 s)

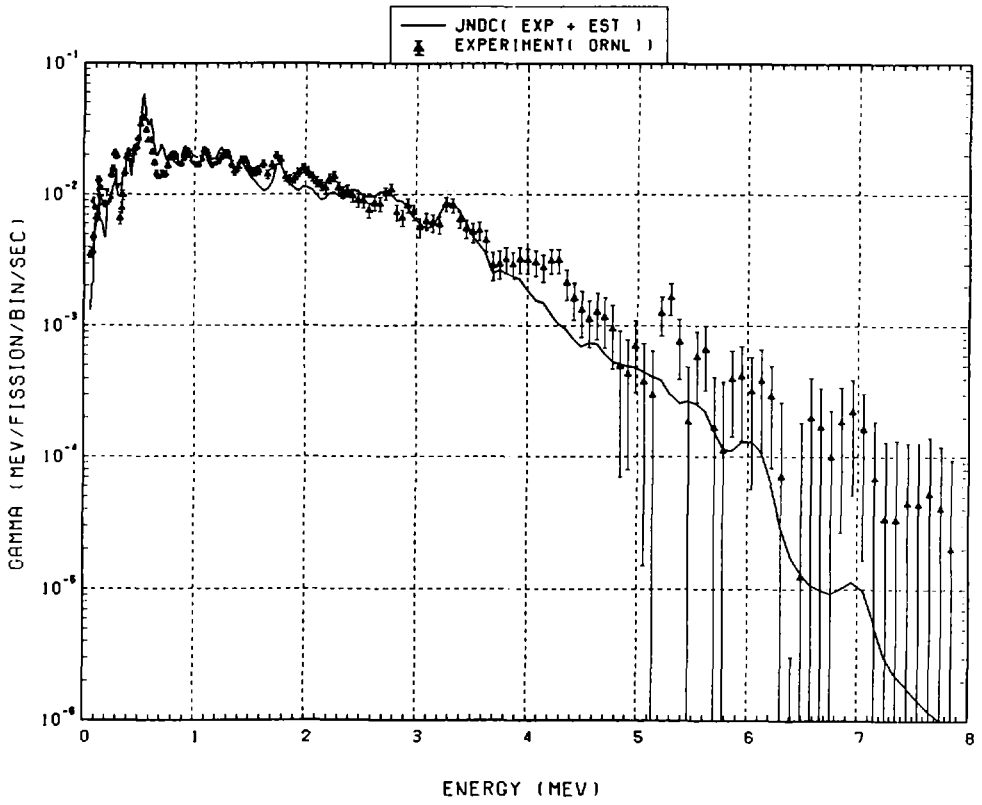

Fig. 60 Comparison of calculated gamma-ray energy spectrum with measured results at 8.7 seconds after thermal neutron fission of ^{239}Pu. (t_{irrad} = 1.0 s, t_{wait} = 6.7 s, t_{count} = 3.0 s)

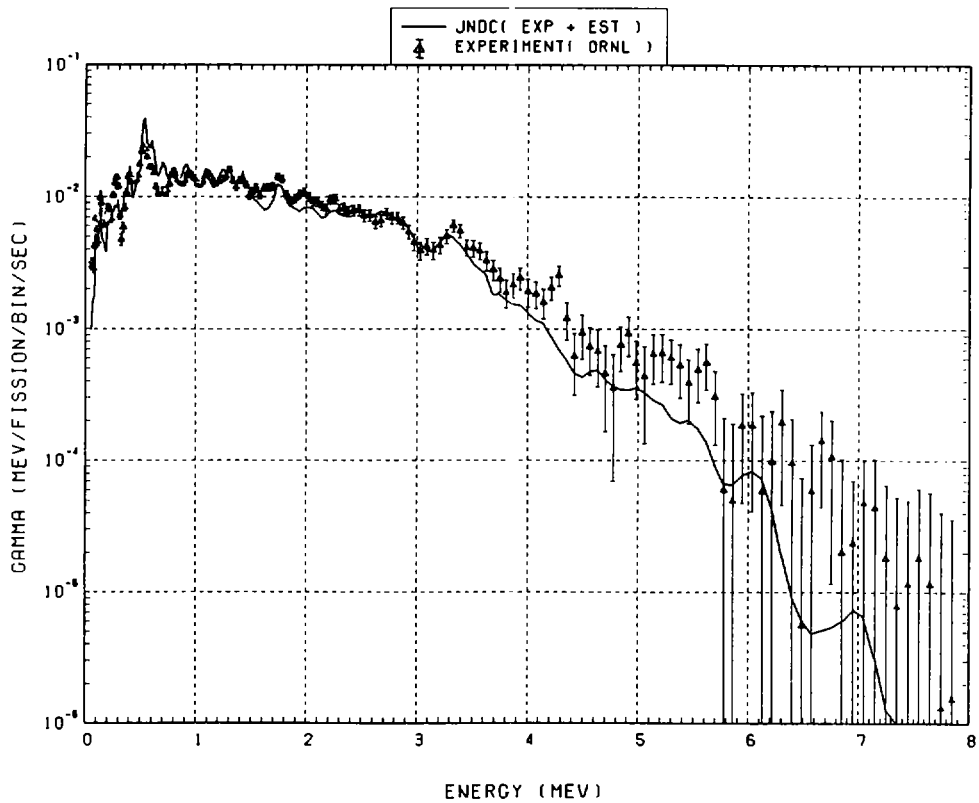

Fig. 61 Comparison of calculated gamma-ray energy spectrum with measured results at 12.7 seconds after thermal neutron fission of ^{239}Pu. (t_{irrad} = 1.0 s, t_{wait} = 9.7 s, t_{count} = 5.0 s)

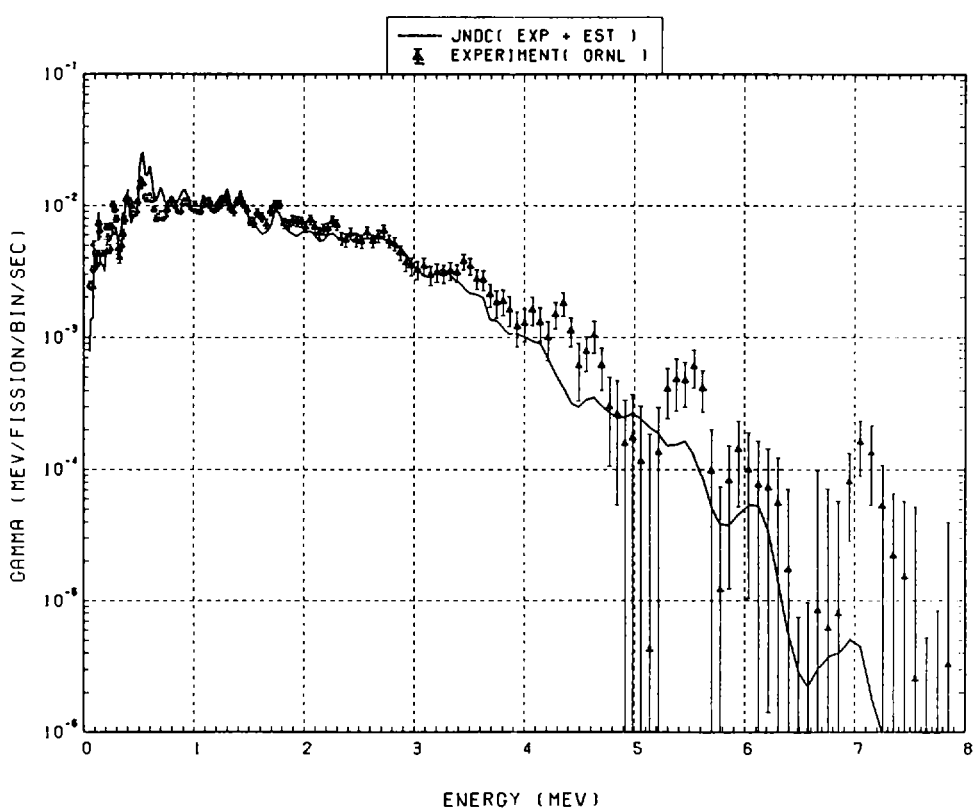

Fig. 62 Comparison of calculated gamma-ray energy spectrum with measured results at 17.7 seconds after thermal neutron fission of ^{239}Pu. (t_{irrad} = 1.0 s, t_{wait} = 14.7 s, t_{count} = 5.0 s)

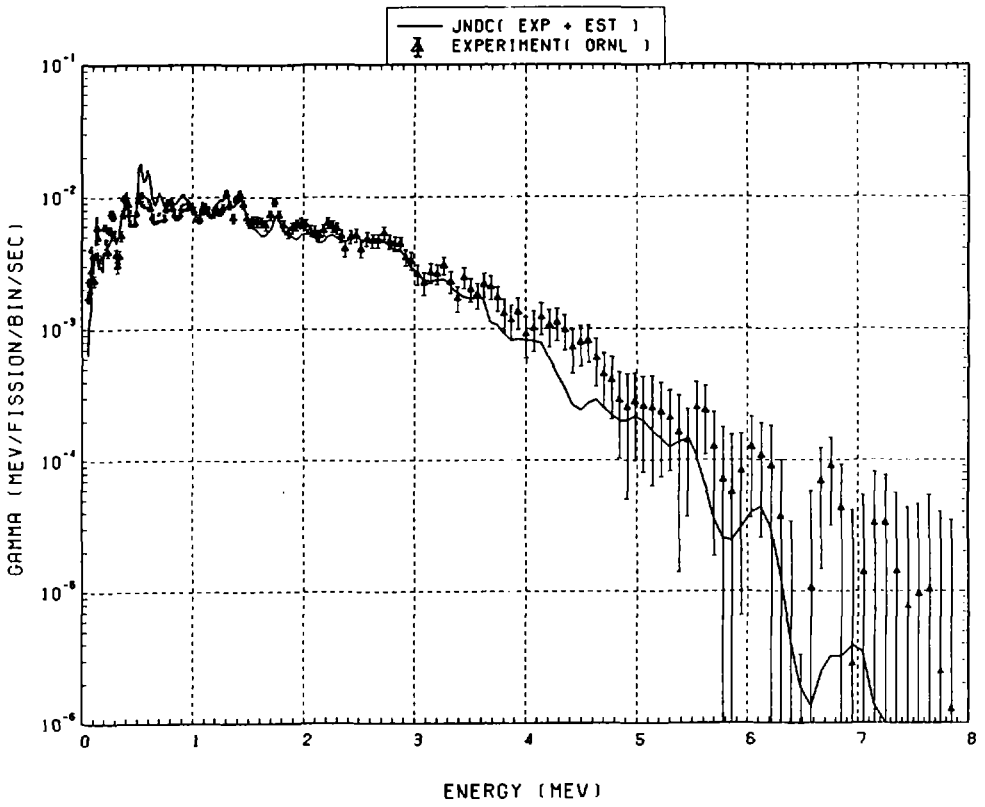

Fig. 63 Comparison of calculated gamma-ray energy spectrum with measured results at 22.7 seconds after thermal neutron fission of ^{239}Pu. (t_{irrad} = 1.0 s, t_{wait} = 19.7 s, t_{count} = 5.0 s)

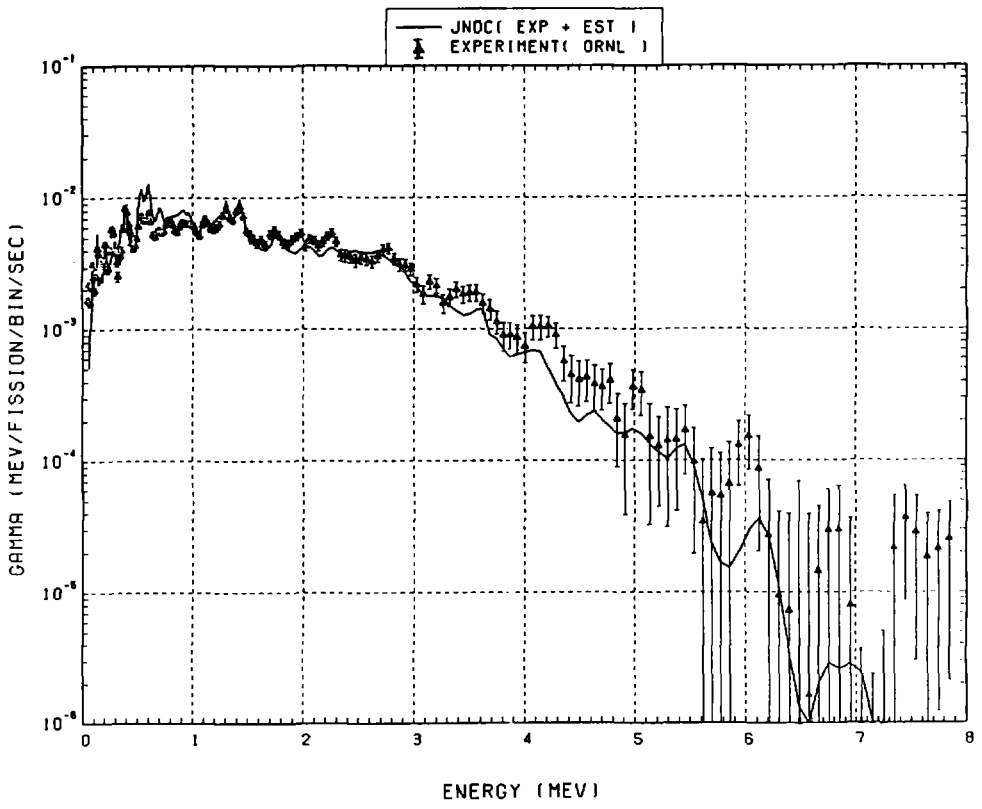

Fig. 64 Comparison of calculated gamma-ray energy spectrum with measured results at 30.2 seconds after thermal neutron fission of ^{239}Pu. (t_{irrad} = 1.0 s, t_{wait} = 24.7 s, t_{count} = 10.0 s)

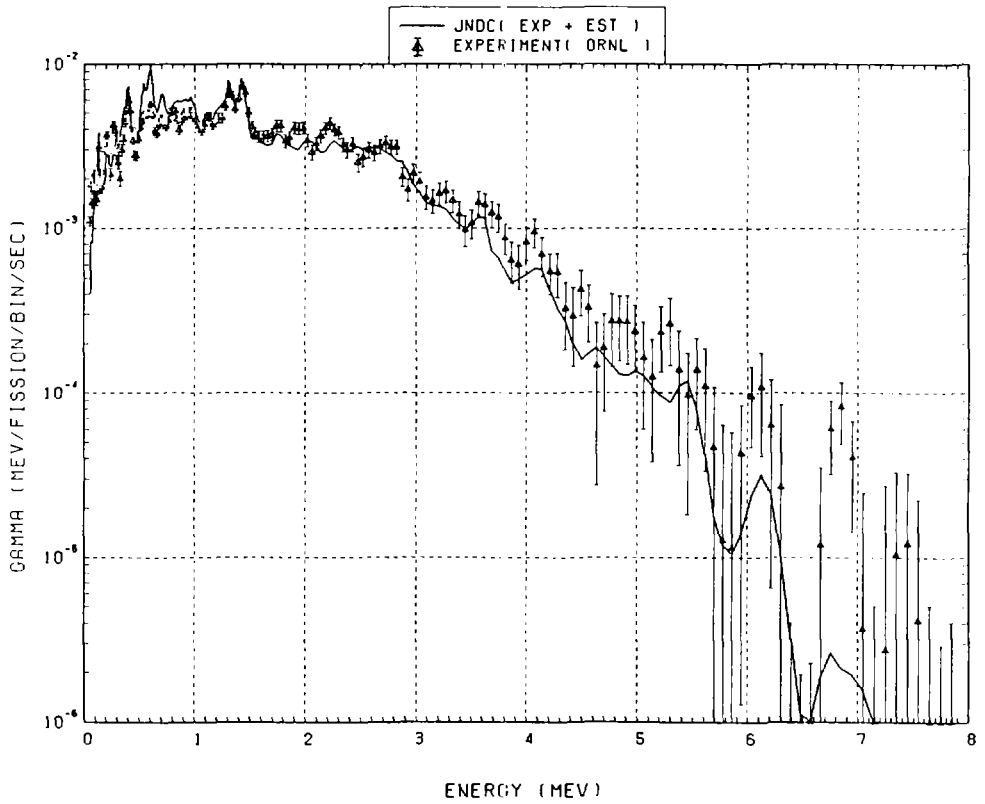

Fig. 65 Comparison of calculated gamma-ray energy spectrum with measured results at 40.2 seconds after thermal neutron fission of ^{239}Pu. (t_{irrad} = 1.0 s, t_{wait} = 34.7 s, t_{count} = 10.0 s)

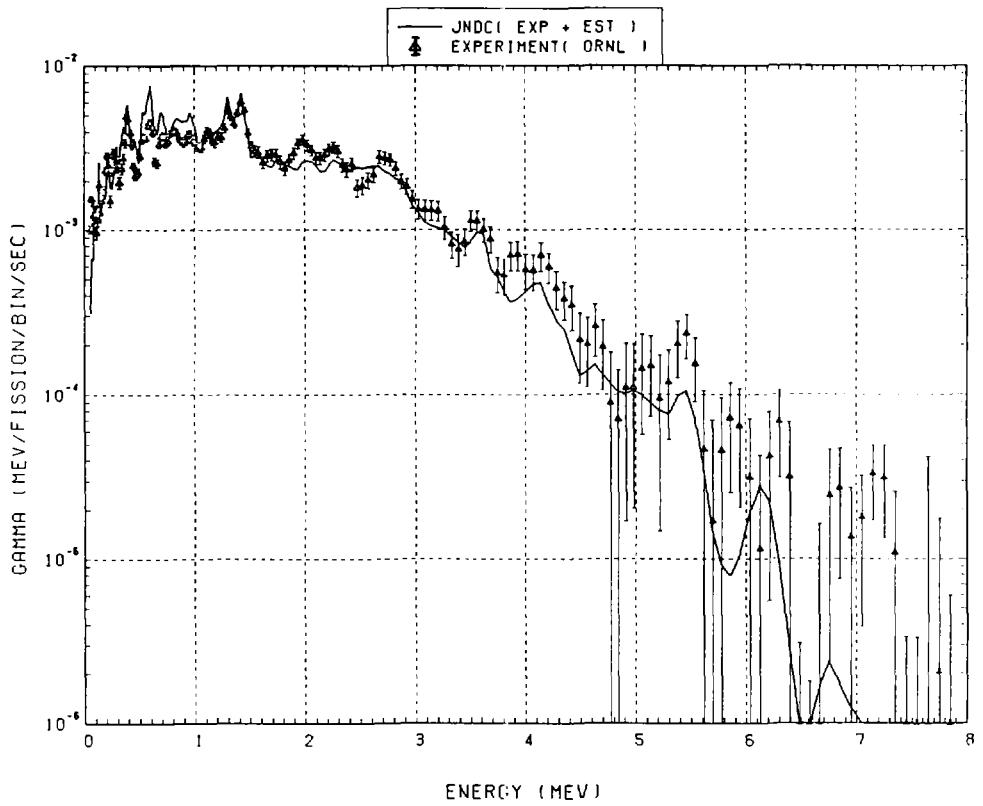

Fig. 66 Comparison of calculated gamma-ray energy spectrum with measured results at 52.7 seconds after thermal neutron fission of ^{239}Pu. (t_{irrad} = 1.0 s, t_{wait} = 44.7 s, t_{count} = 15.0 s)

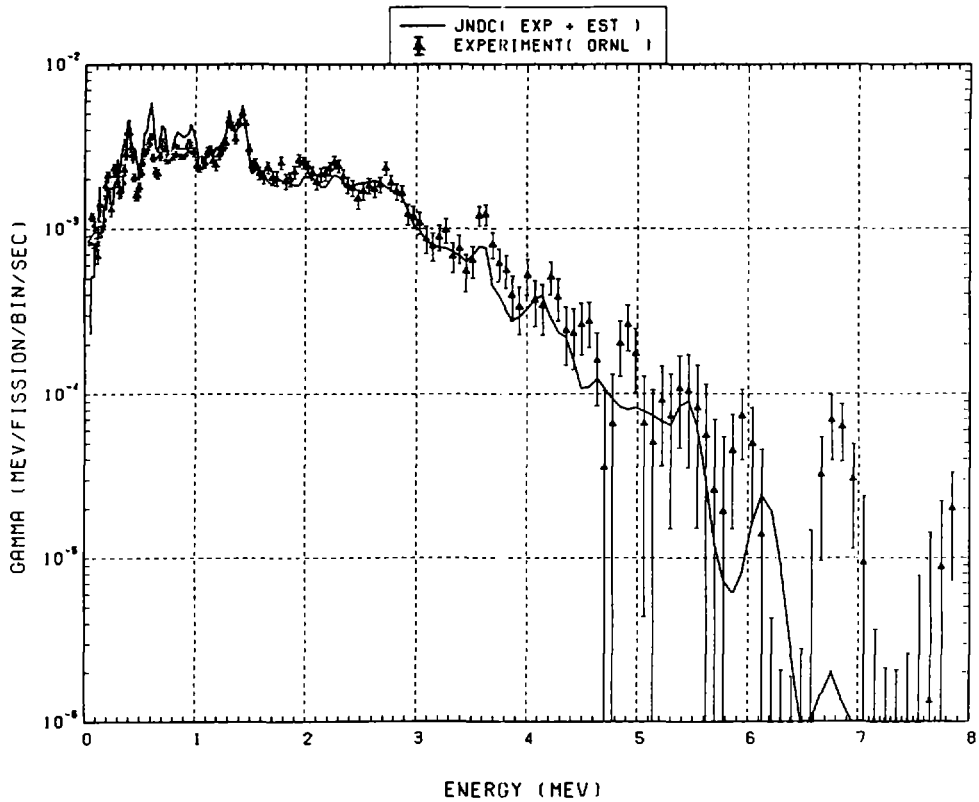

Fig. 67 Comparison of calculated gamma-ray energy spectrum with measured results at 67.7 seconds after thermal neutron fission of ^{239}Pu. (t_{irrad} = 1.0 s, t_{wait} = 59.7 s, t_{count} = 15.0 s)

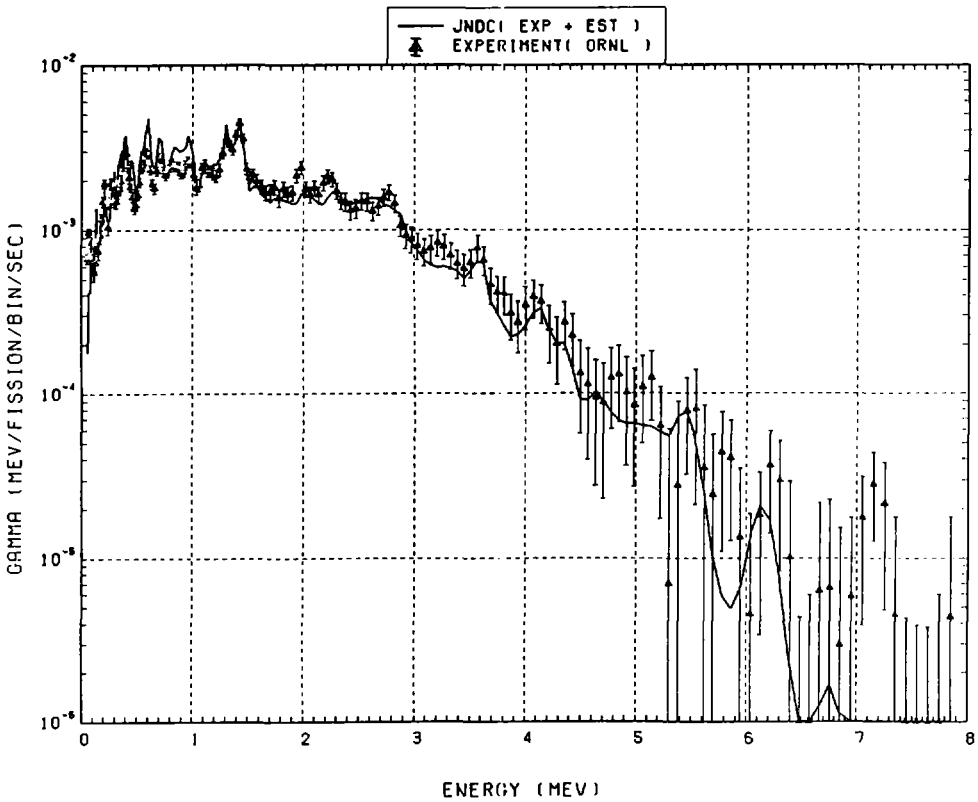

Fig. 68 Comparison of calculated gamma-ray energy spectrum with measured results at 82.7 seconds after thermal neutron fission of ^{239}Pu. (t_{irrad} = 1.0 s, t_{wait} = 74.7 s, t_{count} = 15.0 s)

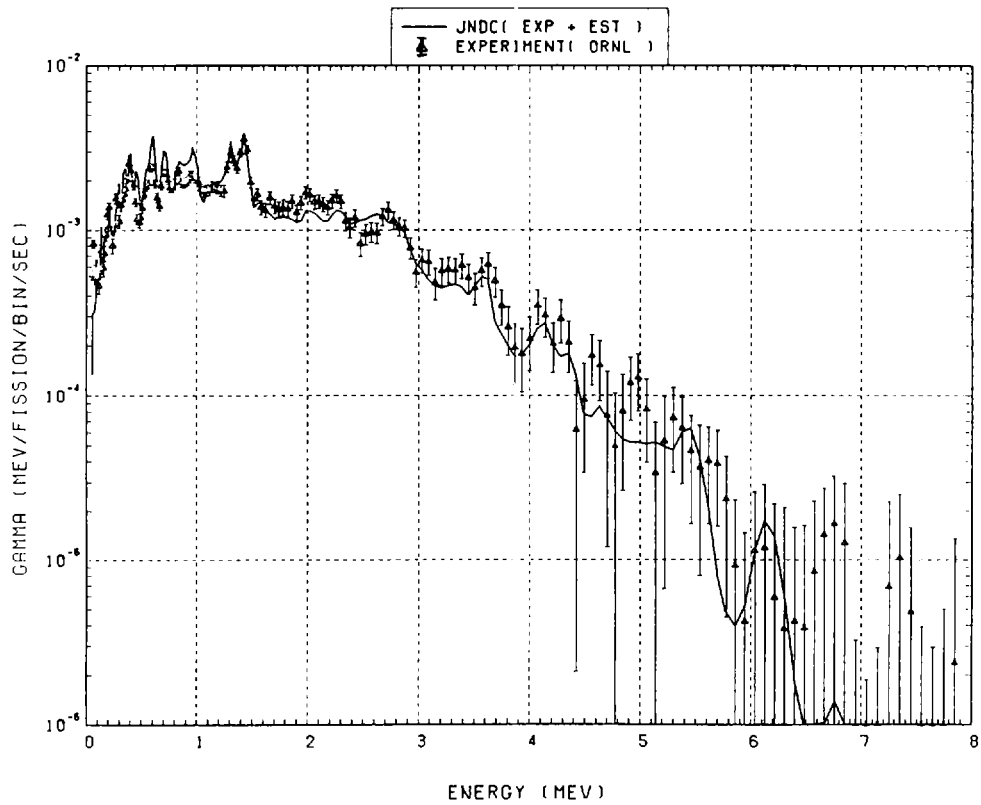

Fig. 69 Comparison of calculated gamma-ray energy spectrum with measured results at 100.2 seconds after thermal neutron fission of ^{239}Pu. (t_{irrad} = 1.0 s, t_{wait} = 89.7 s, t_{count} = 20.0 s)

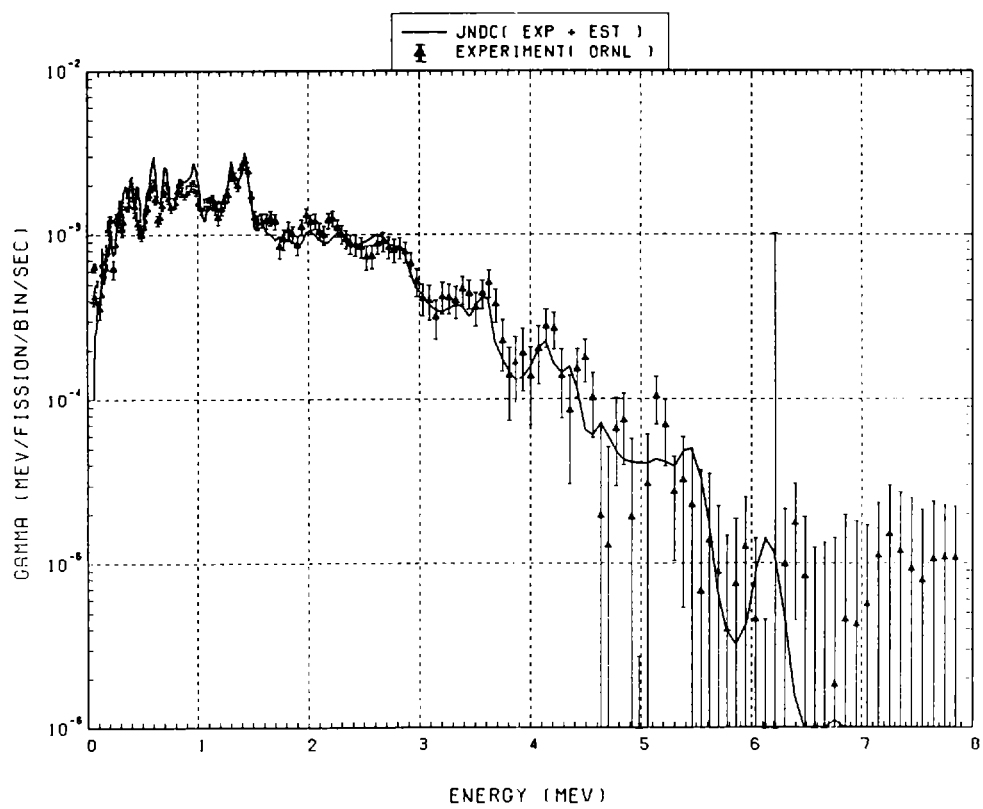

Fig. 70 Comparison of calculated gamma-ray energy spectrum with measured results at 120.5 seconds after thermal neutron fission of ^{239}Pu. (t_{irrad} = 1 s, t_{wait} = 110 s, t_{count} = 20 s)

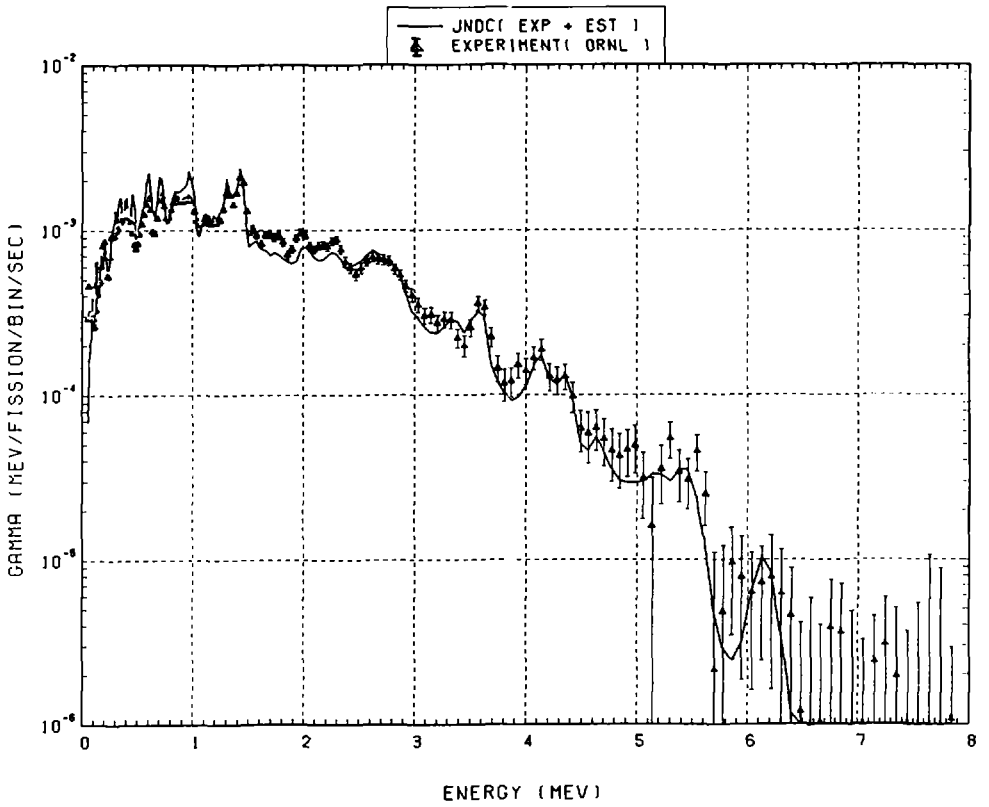

Fig. 71 Comparison of calculated gamma-ray energy spectrum with measured results at 150.5 seconds after thermal neutron fission of ^{239}Pu. (t_{irrad} = 5 s, t_{wait} = 128 s, t_{count} = 40 s)

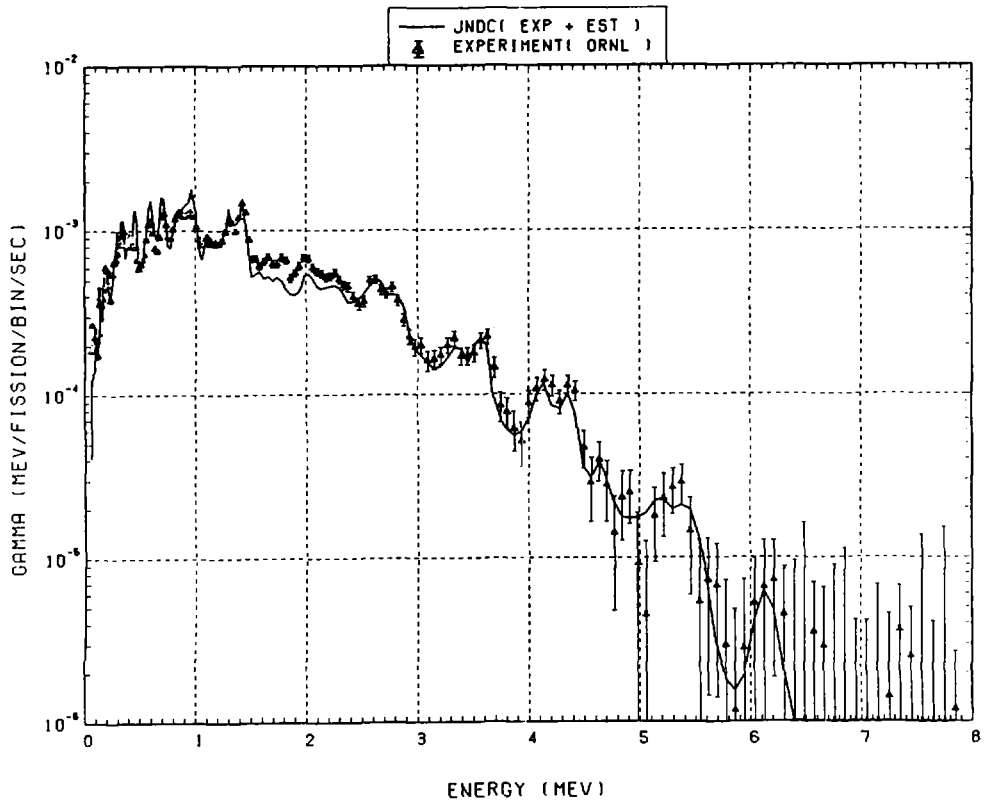

Fig. 72 Comparison of calculated gamma-ray energy spectrum with measured results at 200.5 seconds after thermal neutron fission of ^{239}Pu. (t_{irrad} = 5 s, t_{wait} = 168 s, t_{count} = 60 s)

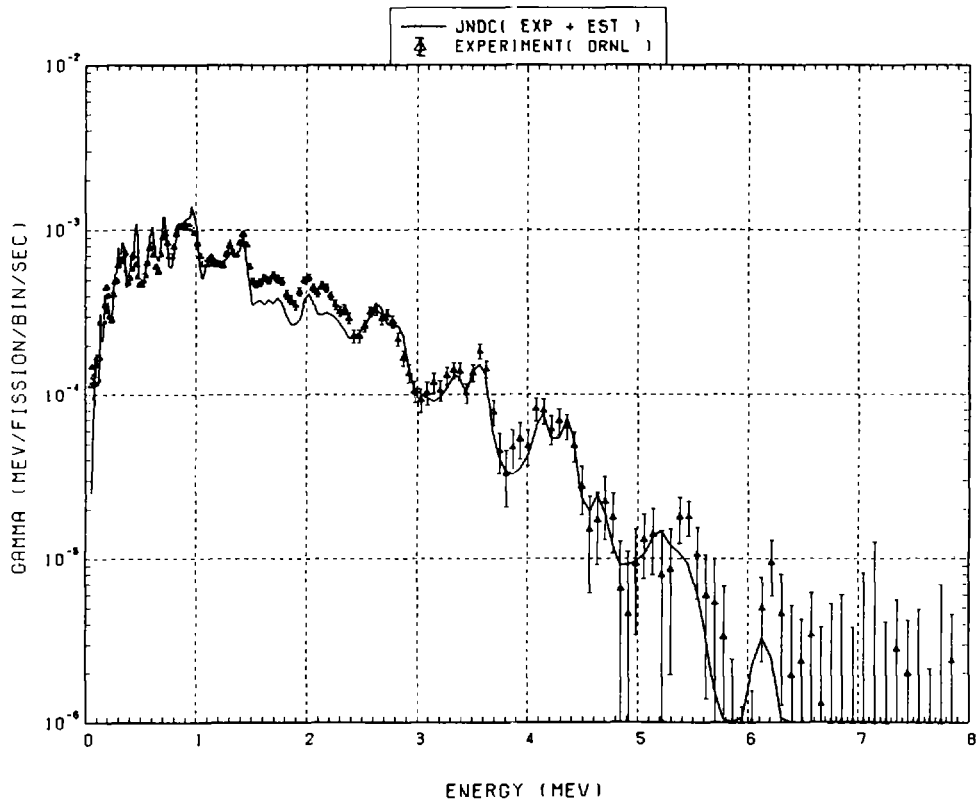

Fig. 73 Comparison of calculated gamma-ray energy spectrum with measured results at 265.5 seconds after thermal neutron fission of ^{239}Pu. (t_{irrad} = 5 s, t_{wait} = 228 s, t_{count} = 70 s)

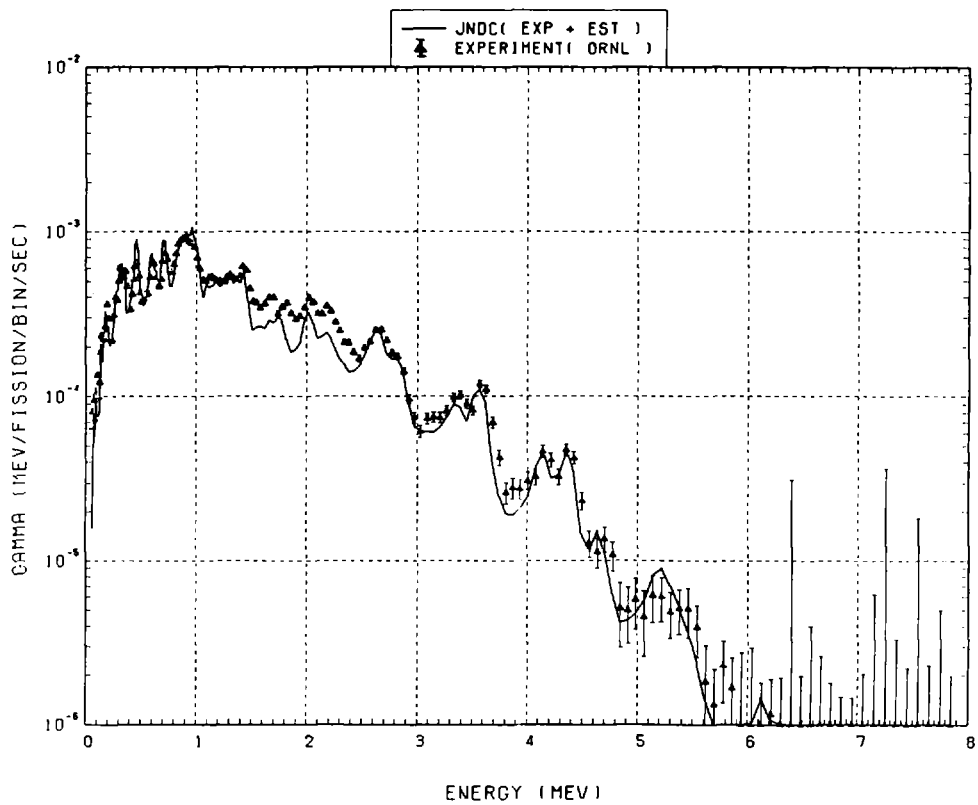

Fig. 74 Comparison of calculated gamma-ray energy spectrum with measured results at 350 seconds after thermal neutron fission of ^{239}Pu. (t_{irrad} = 100 s, t_{wait} = 250 s, t_{count} = 100 s)

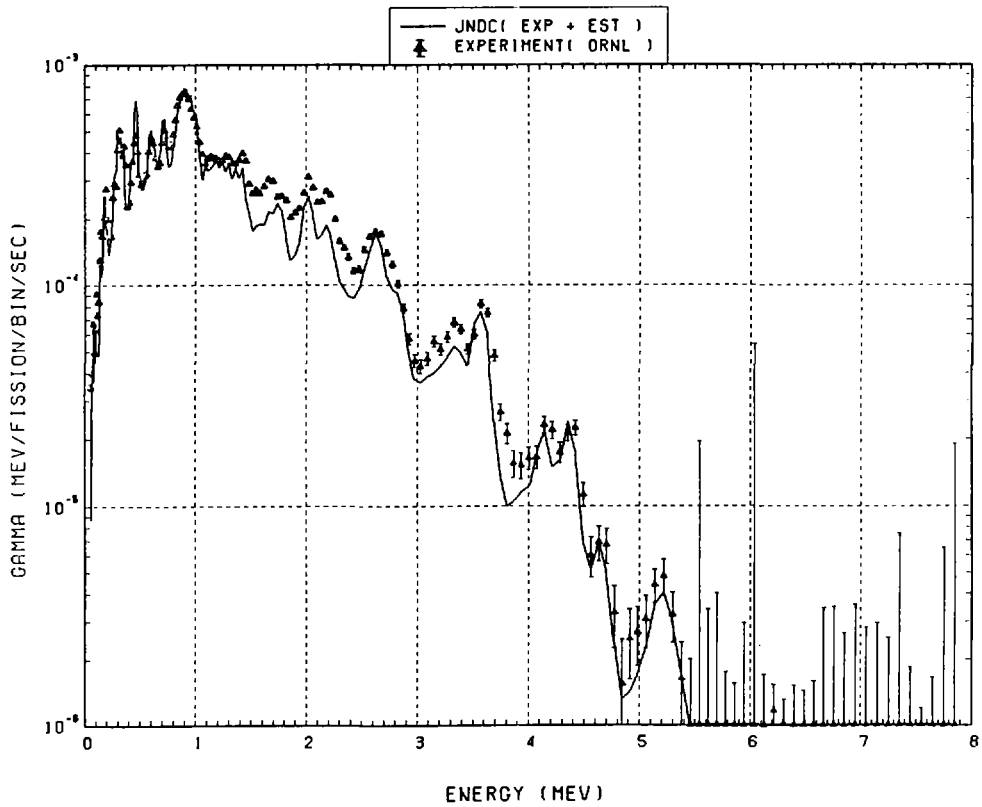

Fig. 75 Comparison of calculated gamma-ray energy spectrum with measured results at 500 seconds after thermal neutron fission of ^{239}Pu. (t_{irrad} = 100 s, t_{wait} = 350 s, t_{count} = 200 s)

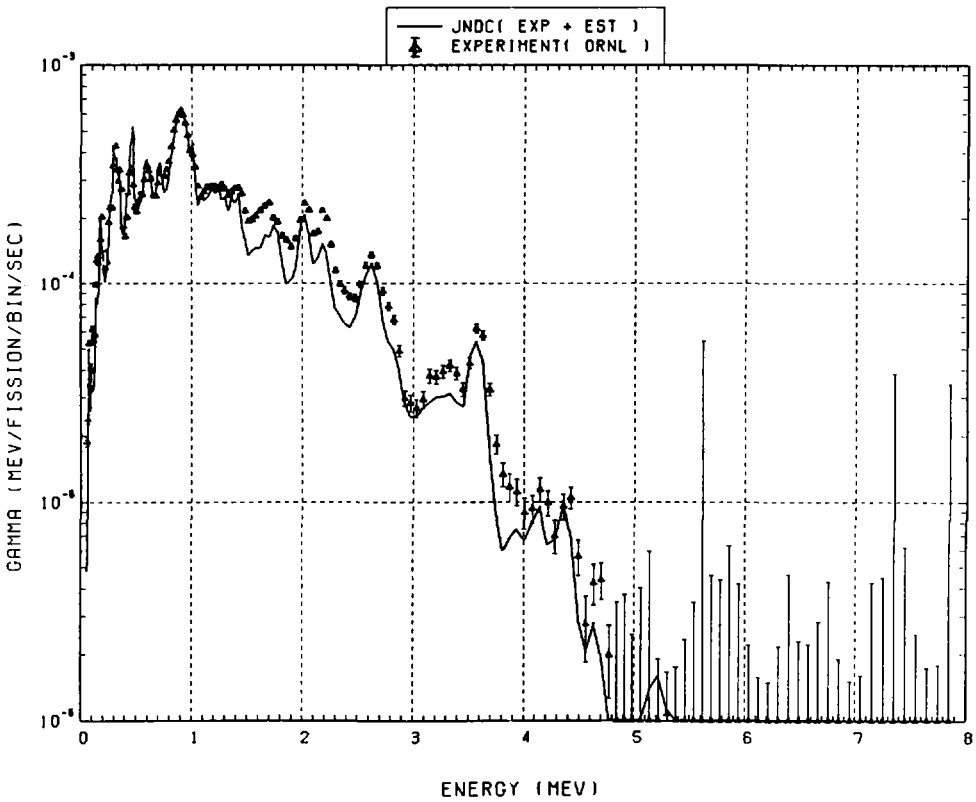

Fig. 76 Comparison of calculated gamma-ray energy spectrum with measured results at 700 seconds after thermal neutron fission of ^{239}Pu. (t_{irrad} = 100 s, t_{wait} = 550 s, t_{count} = 200 s)

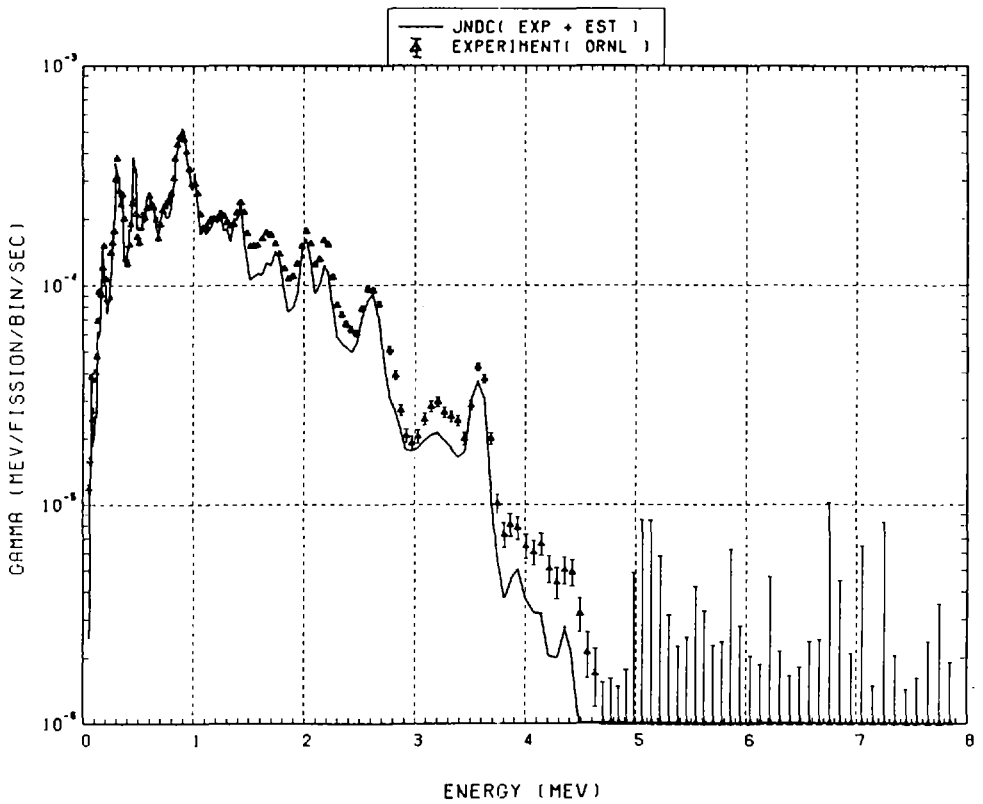

Fig. 77 Comparison of calculated gamma-ray energy spectrum with measured results at 1000 seconds after thermal neutron fission of ^{239}Pu. (t_{irrad} = 100 s, t_{wait} = 750 s, t_{count} = 400 s)

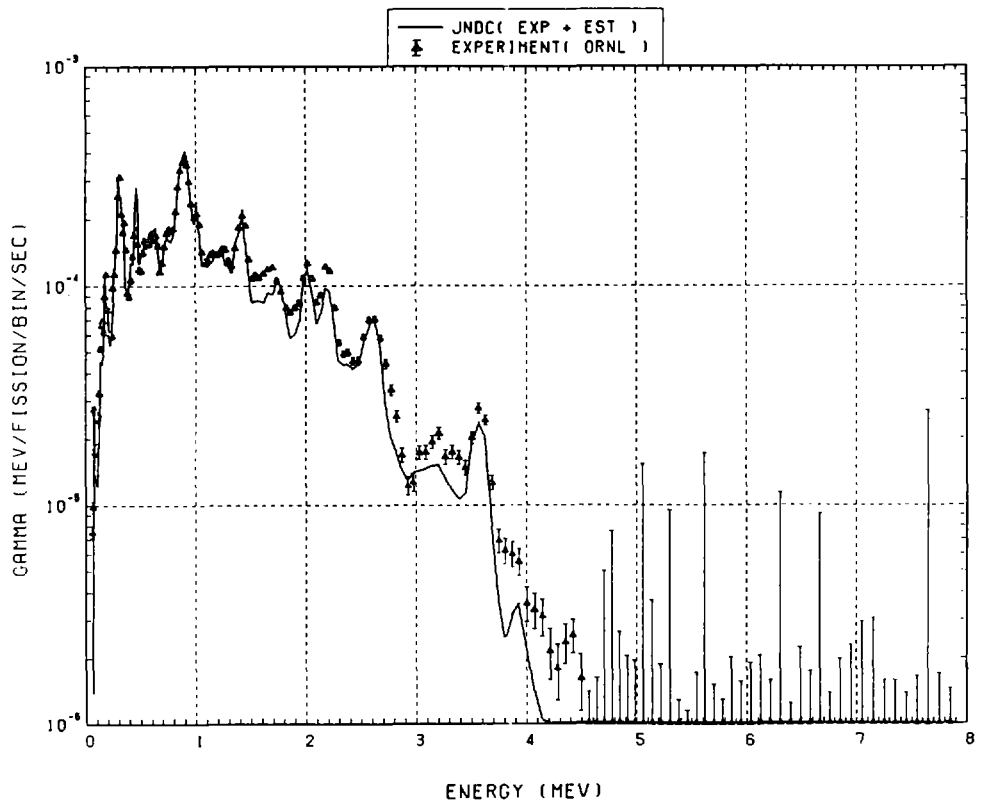

Fig. 78 Comparison of calculated gamma-ray energy spectrum with measured results at 1400 seconds after thermal neutron fission of ^{239}Pu. (t_{irrad} = 100 s, t_{wait} = 1150 s, t_{count} = 400 s)

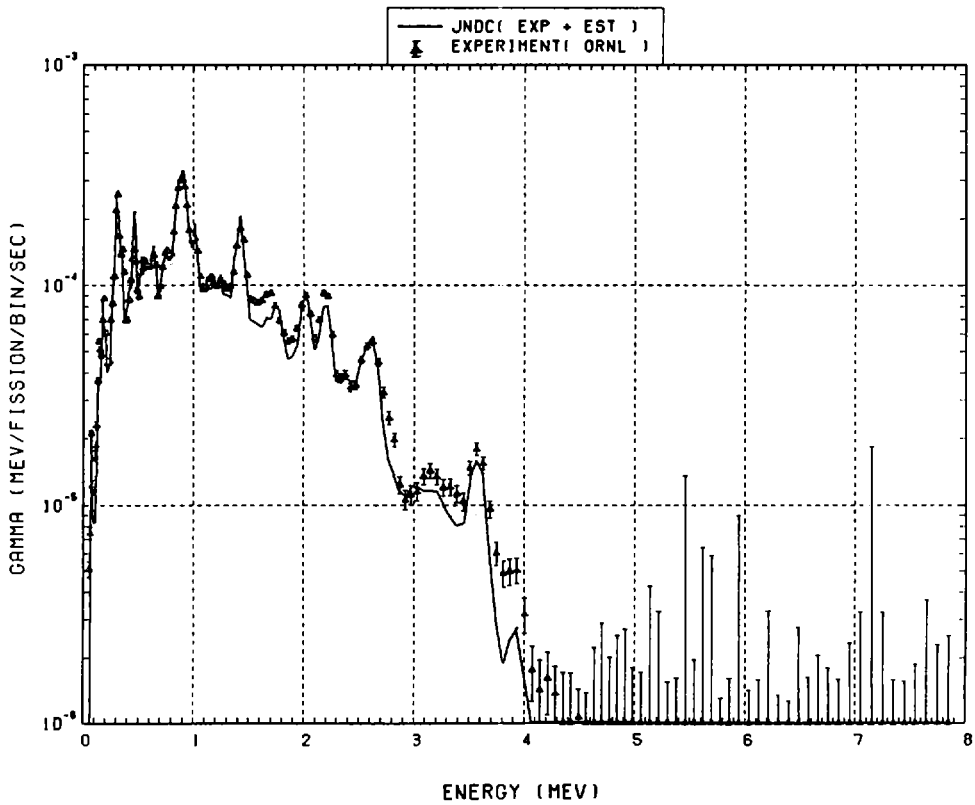

Fig. 79 Comparison of calculated gamma-ray energy spectrum with measured results at 1800 seconds after thermal neutron fission of ^{239}Pu. (t_{irrad} = 100 s, t_{wait} = 1550 s, t_{count} = 400 s)

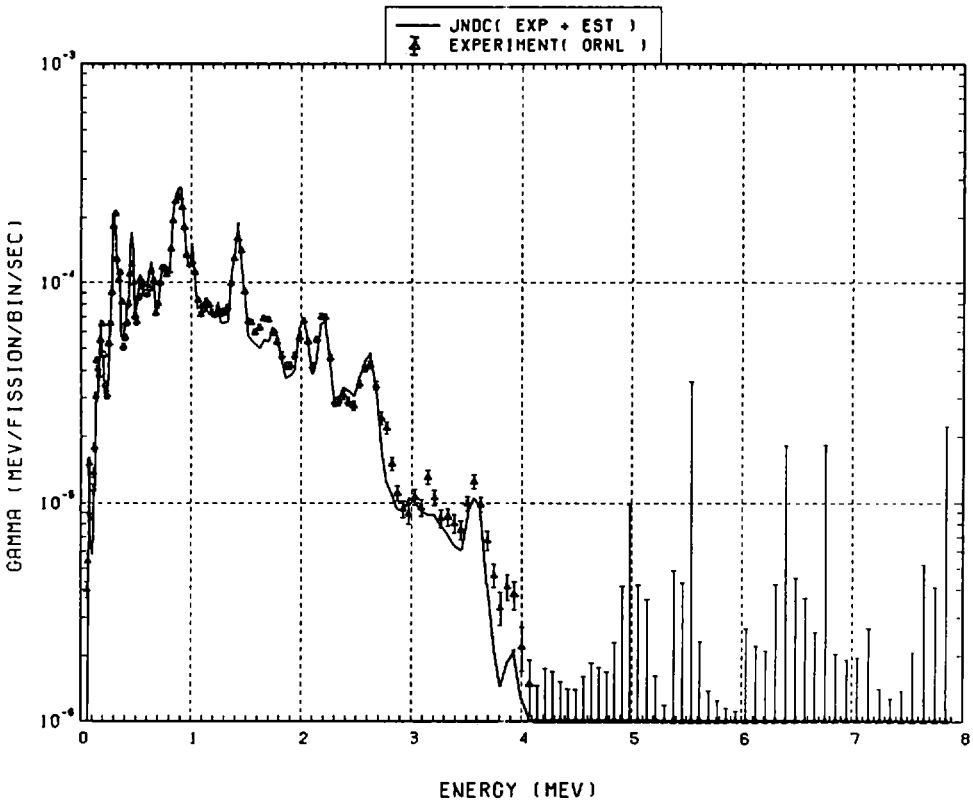

Fig. 80 Comparison of calculated gamma-ray energy spectrum with measured results at 2250 seconds after thermal neutron fission of ^{239}Pu. (t_{irrad} = 100 s, t_{wait} = 1950 s, t_{count} = 500 s)

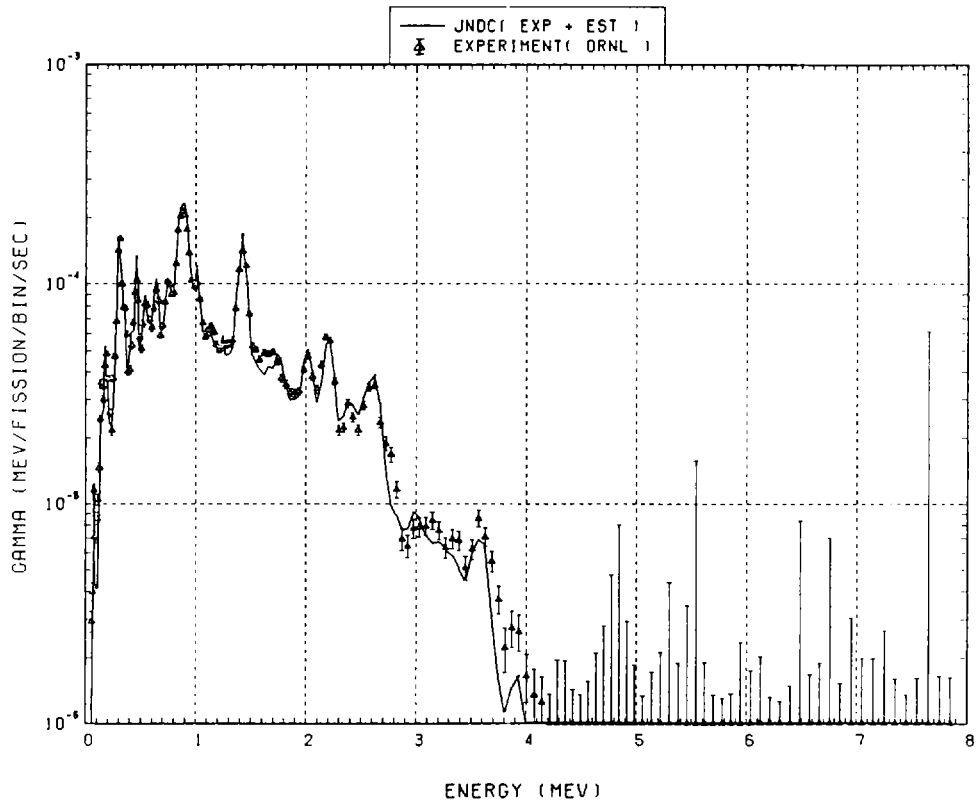

Fig. 81 Comparison of calculated gamma-ray energy spectrum with measured results at 2750 seconds after thermal neutron fission of ^{239}Pu. (t_{irrad} = 100 s, t_{wait} = 2450 s, t_{count} = 500 s)

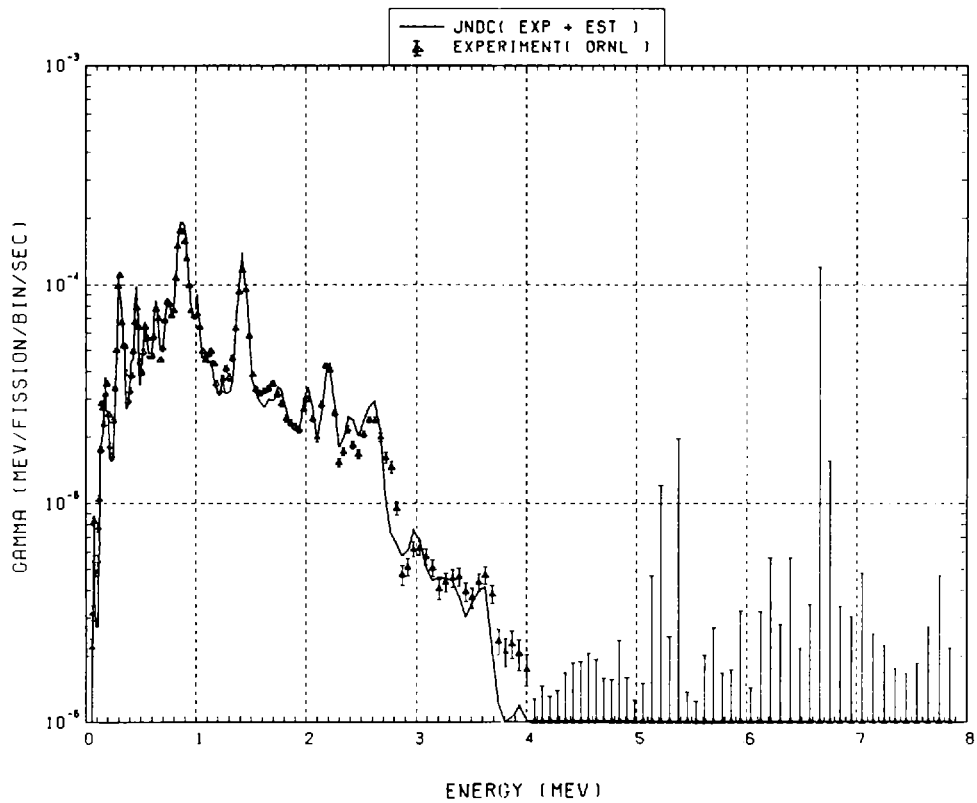

Fig. 82 Comparison of calculated gamma-ray energy spectrum with measured results at 3500 seconds after thermal neutron fission of ^{239}Pu. (t_{irrad} = 100 s, t_{wait} = 2950 s, t_{count} = 1000 s)

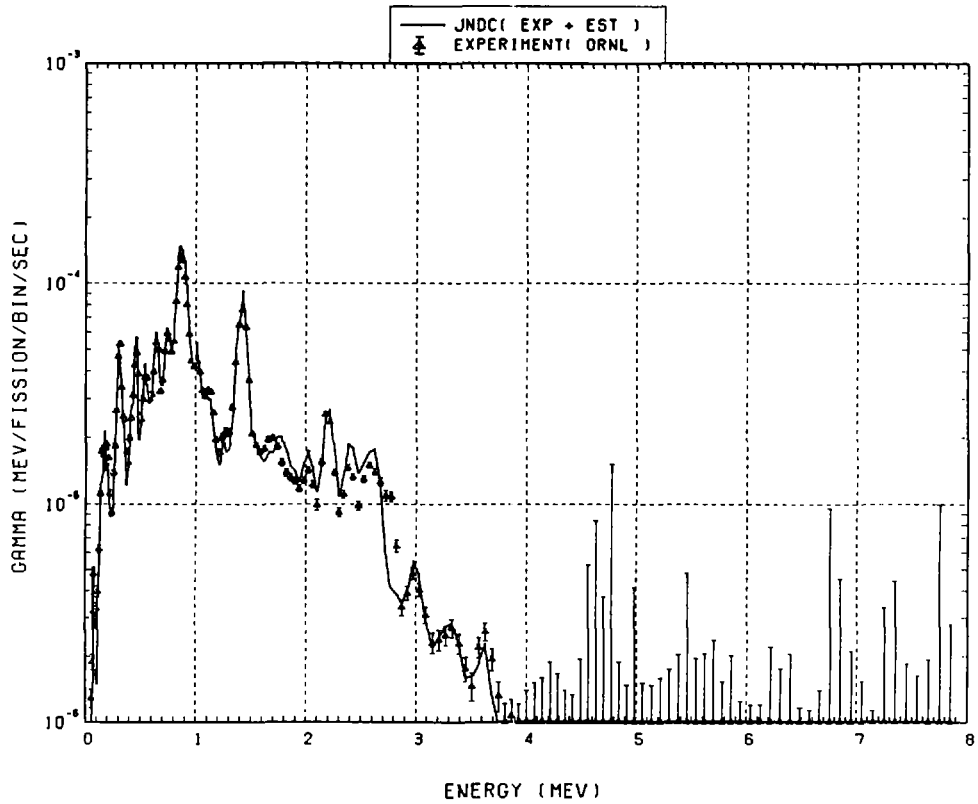

Fig. 83 Comparison of calculated gamma-ray energy spectrum with measured results at 5000 seconds after thermal neutron fission of ^{239}Pu. (t_{irrad} = 100 s, t_{wait} = 3950 s, t_{count} = 2000 s)

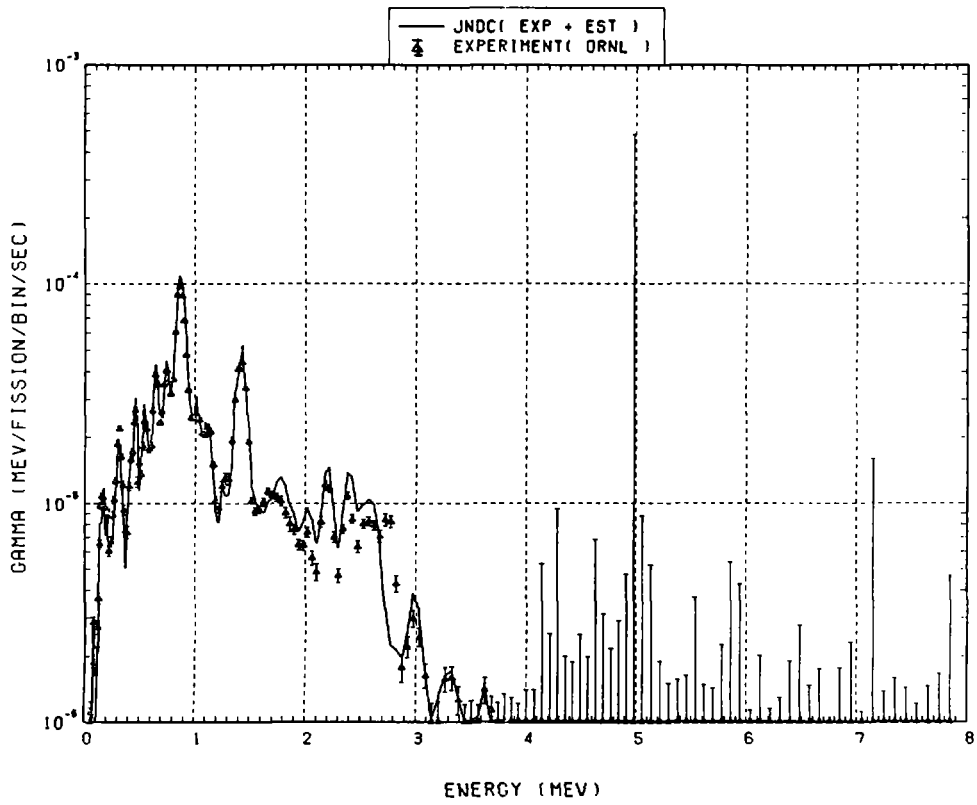

Fig. 84 Comparison of calculated gamma-ray energy spectrum with measured results at 7000 seconds after thermal neutron fission of ^{239}Pu. (t_{irrad} = 100 s, t_{wait} = 5950 s, t_{count} = 2000 s)

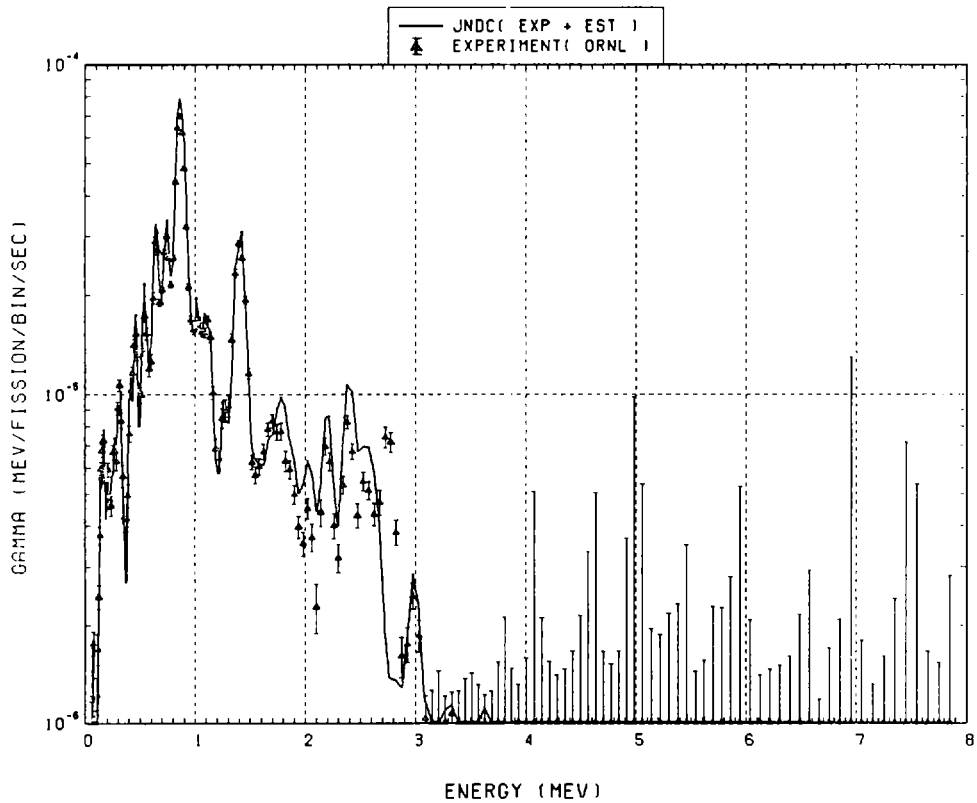

Fig. 85 Comparison of calculated gamma-ray energy spectrum with measured results at 9000 seconds after thermal neutron fission of ^{239}Pu. (t_{irrad} = 100 s, t_{wait} = 7950 s, t_{count} = 2000 s)

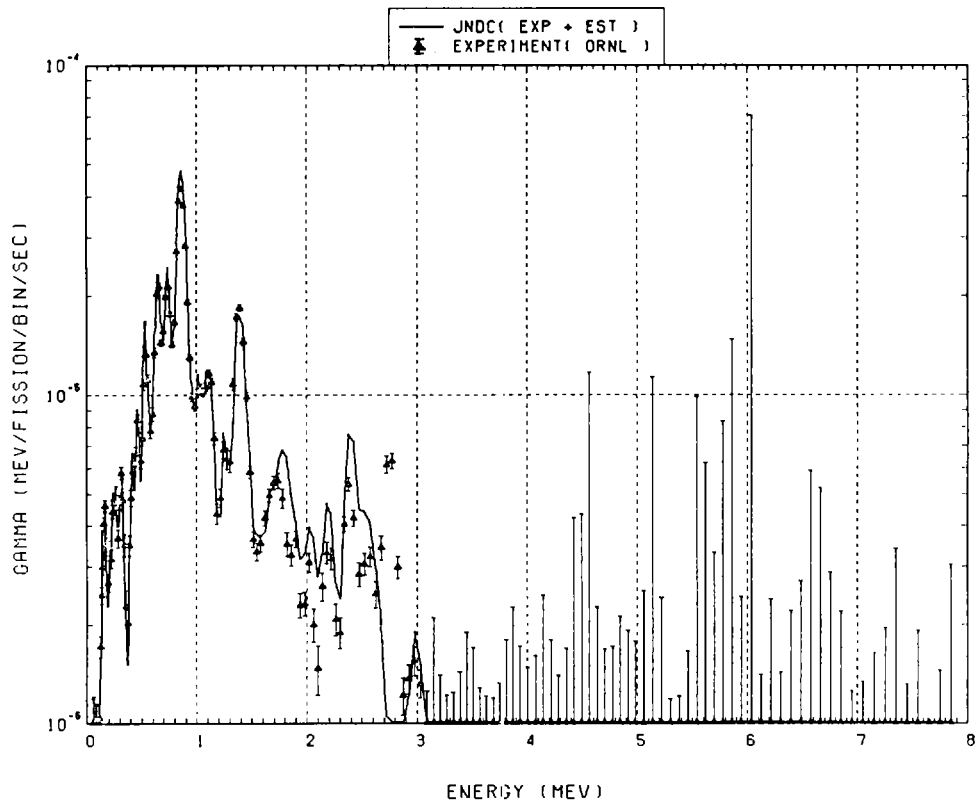

Fig. 86 Comparison of calculated gamma-ray energy spectrum with measured results at 12000 seconds after thermal neutron fission of ^{239}Pu. (t_{irrad} = 100 s, t_{wait} = 9950 s, t_{count} = 4000 s)

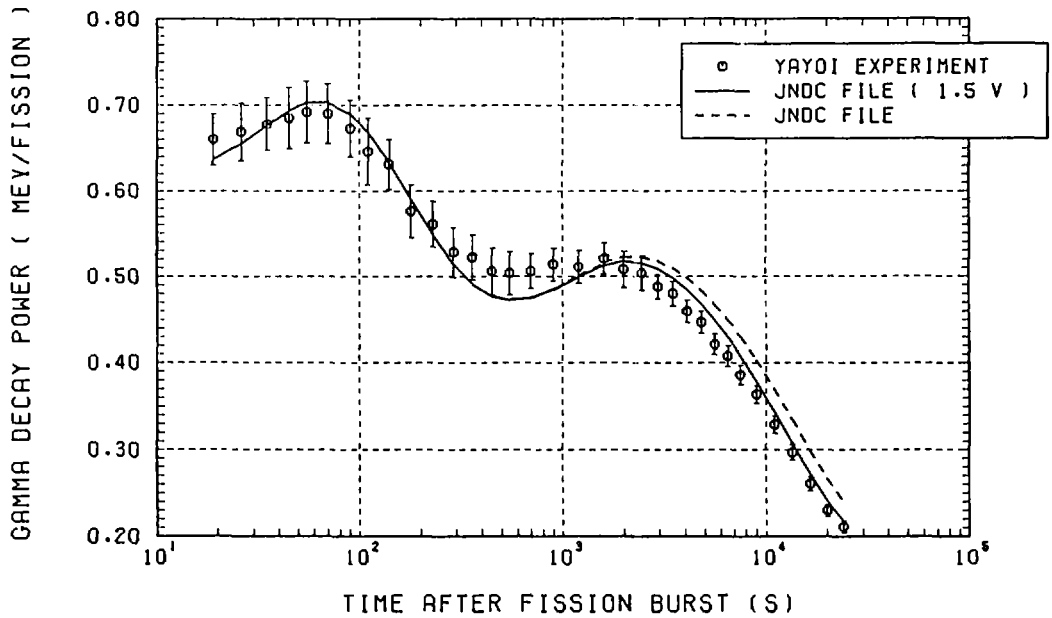

Fig. 87 Comparison of calculated gamma-decay heat with measured results at YAYOI for fast neutron fission of ^{235}U.

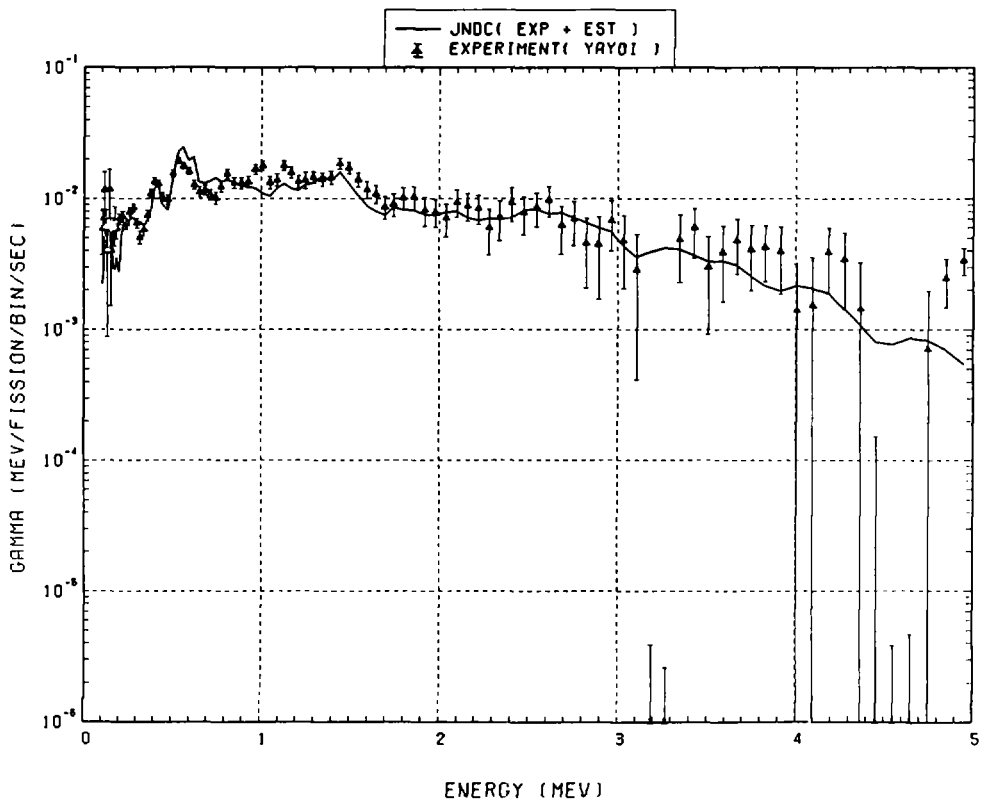

Fig. 88 Comparison of calculated gamma-ray energy spectrum with measured results at 19 seconds after fast neutron fission of ^{235}U. (t_{irrad} = 10 s, t_{wait} = 11 s, t_{count} = 6 s)

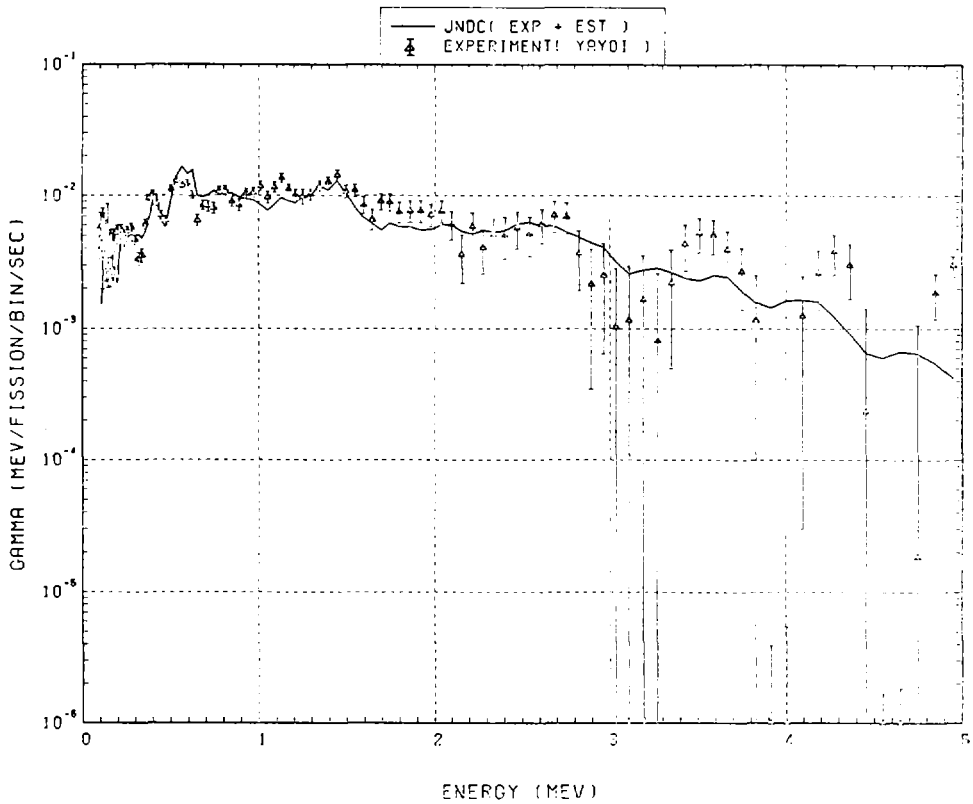

Fig. 89 Comparison of calculated gamma-ray energy spectrum with measured results at 26 seconds after fast neutron fission of ^{235}U. (t_{irrad} = 10 s, t_{wait} = 17 s, t_{count} = 8 s)

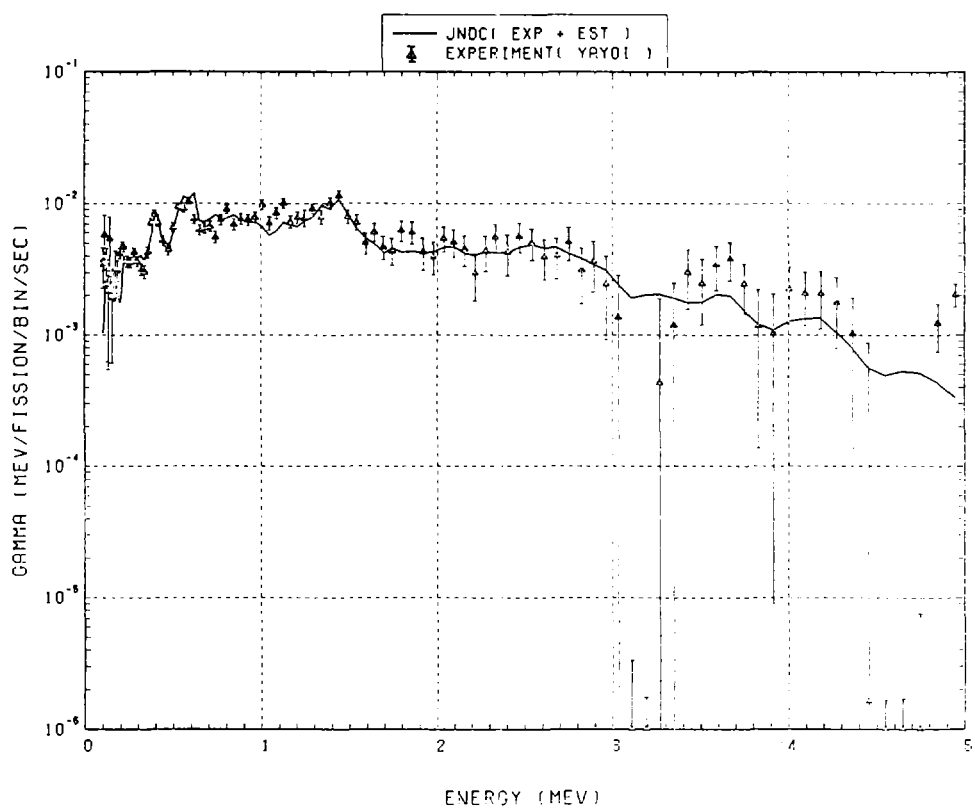

Fig. 90 Comparison of calculated gamma-ray energy spectrum with measured results at 35 seconds after fast neutron fission of ^{235}U. (t_{irrad} = 10 s, t_{wait} = 25 s, t_{count} = 10 s)

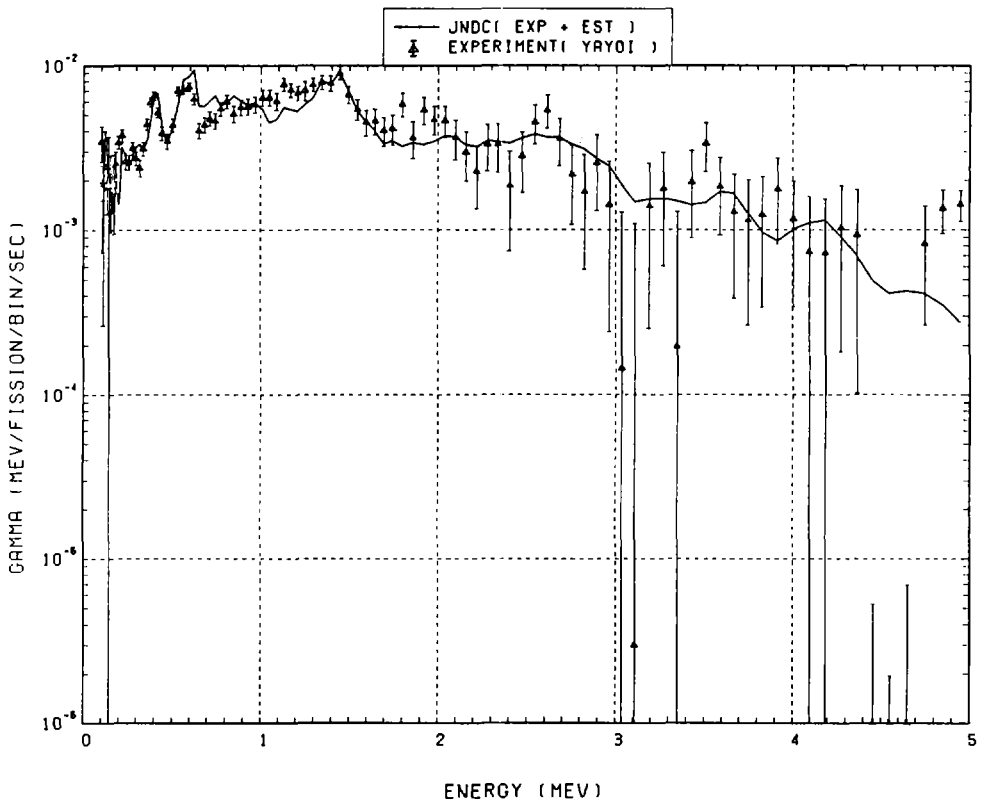

Fig. 91 Comparison of calculated gamma-ray energy spectrum with measured results at 45 seconds after fast neutron fission of ^{235}U. (t_{irrad} = 10 s, t_{wait} = 35 s, t_{count} = 10 s)

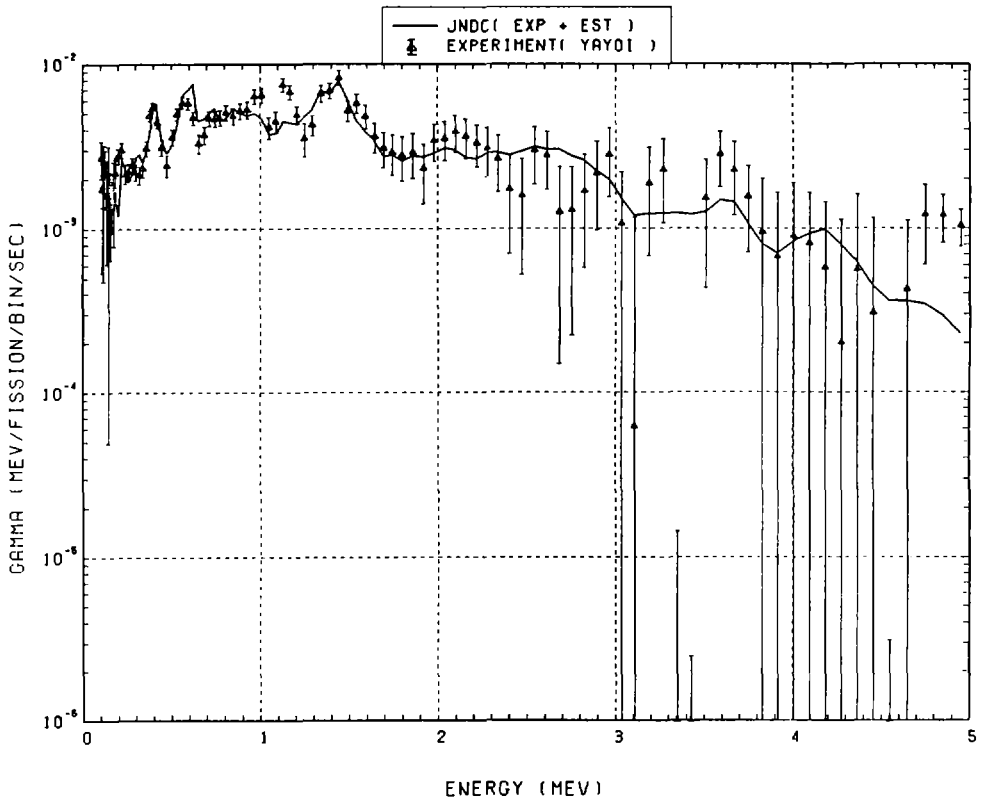

Fig. 92 Comparison of calculated gamma-ray energy spectrum with measured results at 55 seconds after fast neutron fission of ^{235}U. (t_{irrad} = 10 s, t_{wait} = 45 s, t_{count} = 10 s)

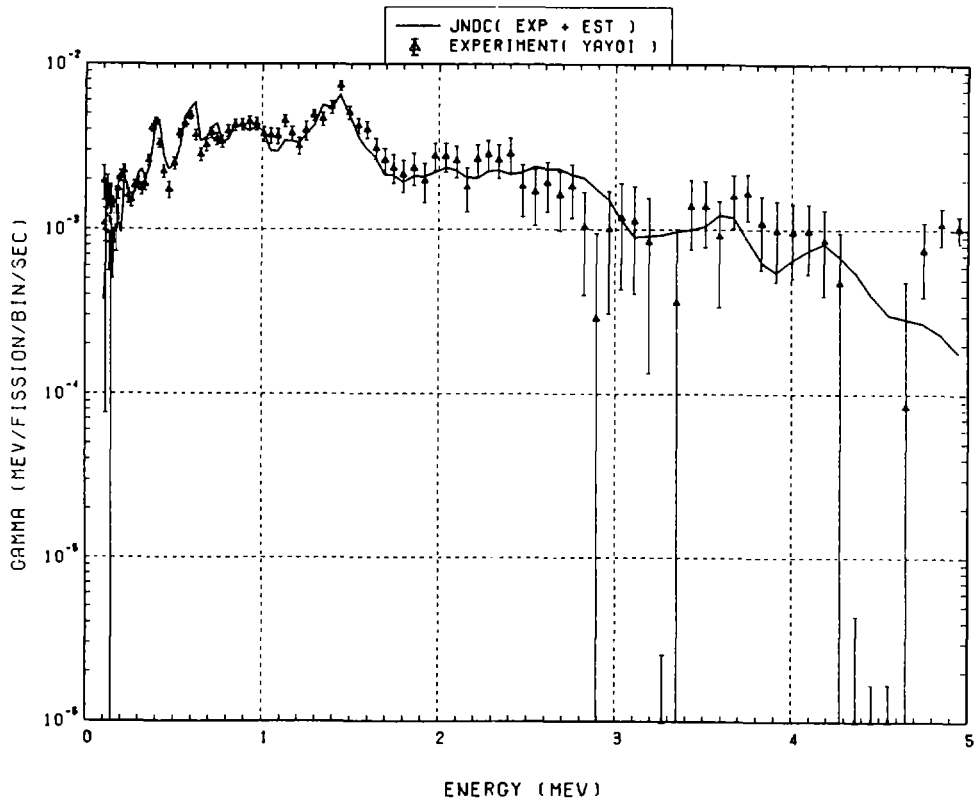

Fig. 93 Comparison of calculated gamma-ray energy spectrum with measured results at 70 seconds after fast neutron fission of ^{235}U. (t_{irrad} = 10 s, t_{wait} = 55 s, t_{count} = 20 s)

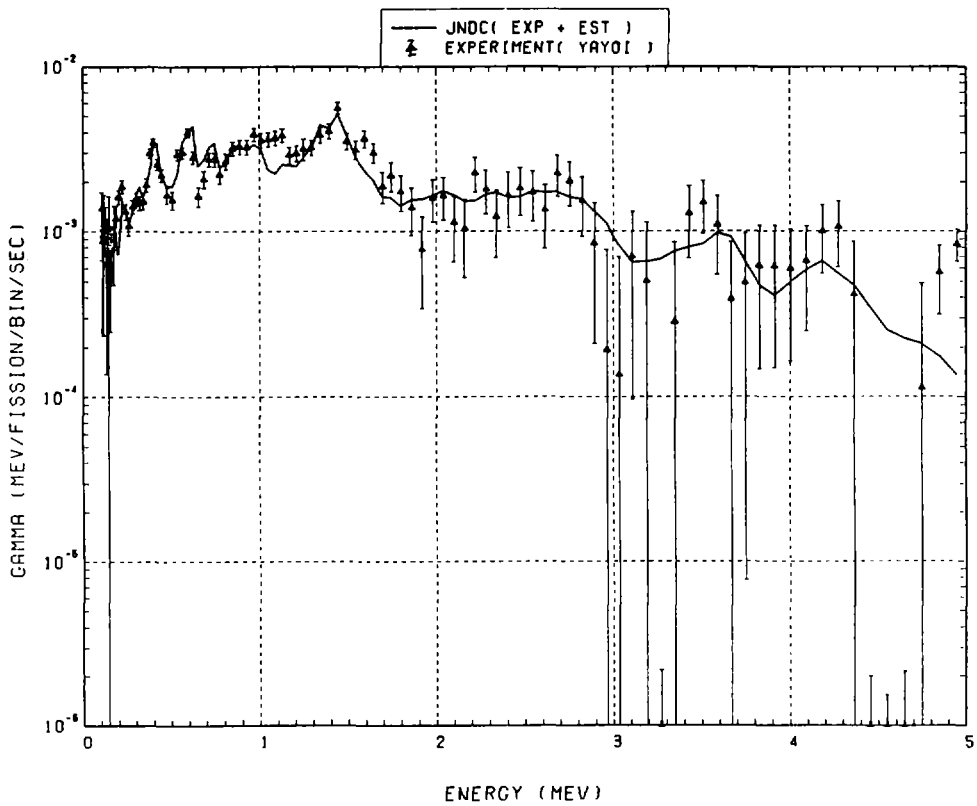

Fig. 94 Comparison of calculated gamma-ray energy spectrum with measured results at 90 seconds after fast neutron fission of ^{235}U. (t_{irrad} = 10 s, t_{wait} = 75 s, t_{count} = 20 s)

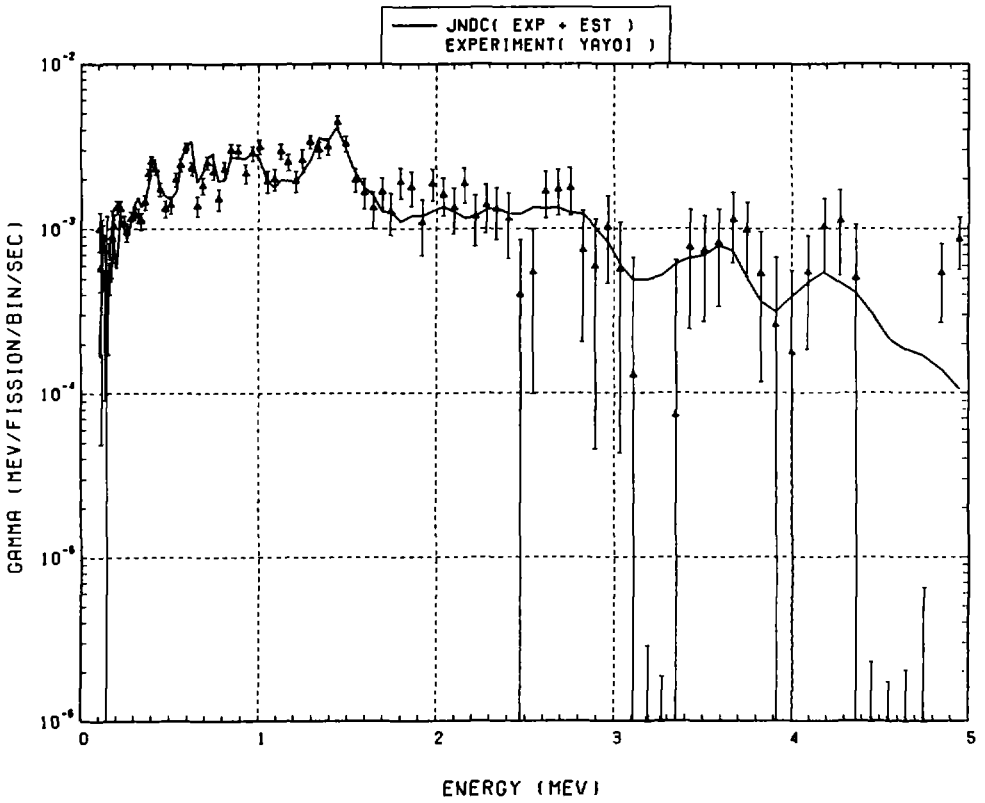

Fig. 95 Comparison of calculated gamma-ray energy spectrum with measured results at 110 seconds after fast neutron fission of ^{235}U. (t_{irrad} = 10 s, t_{wait} = 95 s, t_{count} = 20 s)

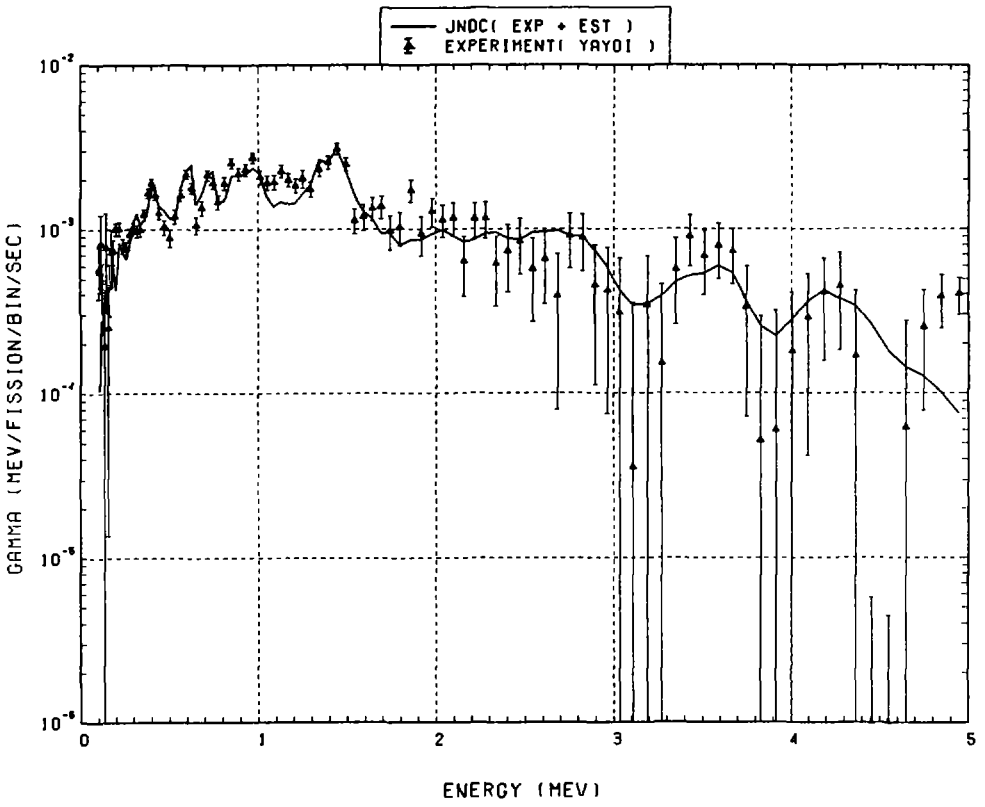

Fig. 96 Comparison of calculated gamma-ray energy spectrum with measured results at 140 seconds after fast neutron fission of ^{235}U. (t_{irrad} = 10 s, t_{wait} = 115 s, t_{count} = 40 s)

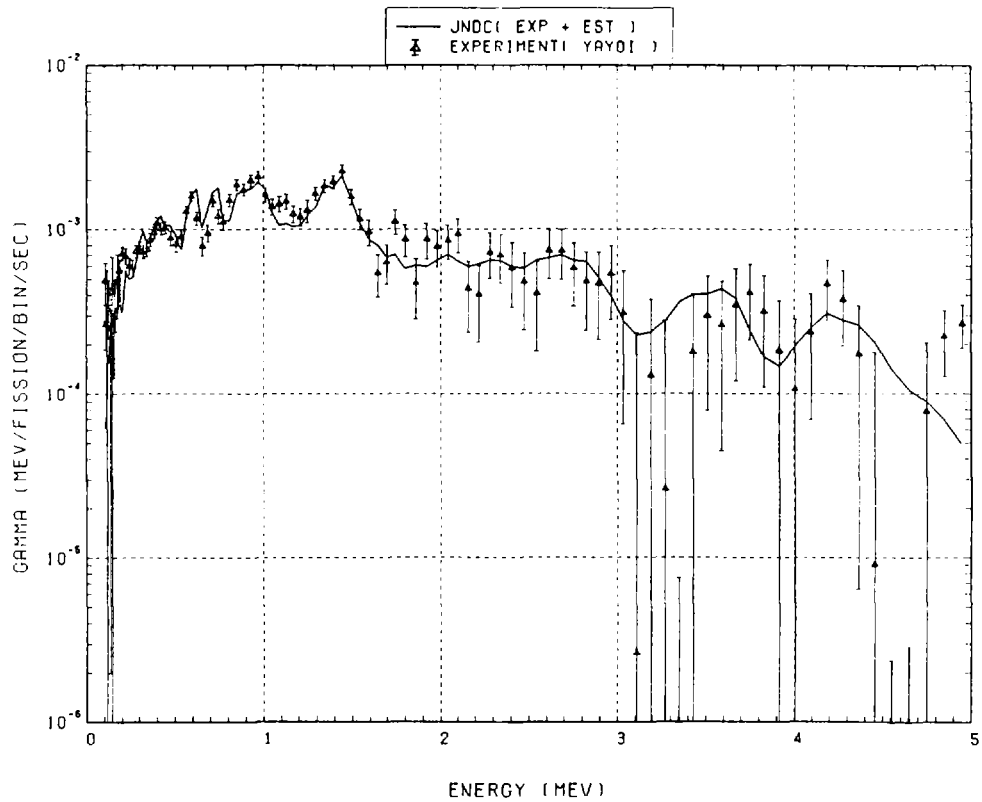

Fig. 97 Comparison of calculated gamma-ray energy spectrum with measured results at 180 seconds after fast neutron fission of ^{235}U. (t_{irrad} = 10 s, t_{wait} = 150 s, t_{count} = 40 s)

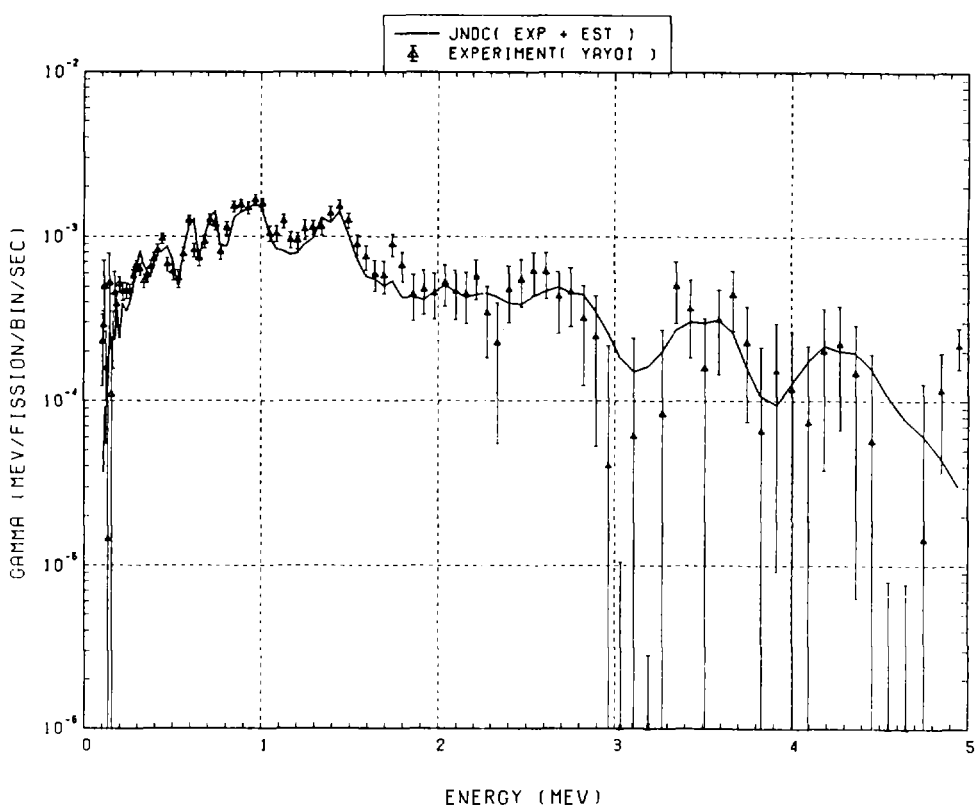

Fig. 98 Comparison of calculated gamma-ray energy spectrum with measured results at 230 seconds after fast neutron fission of ^{235}U. (t_{irrad} = 10 s, t_{wait} = 195 s, t_{count} = 60 s)

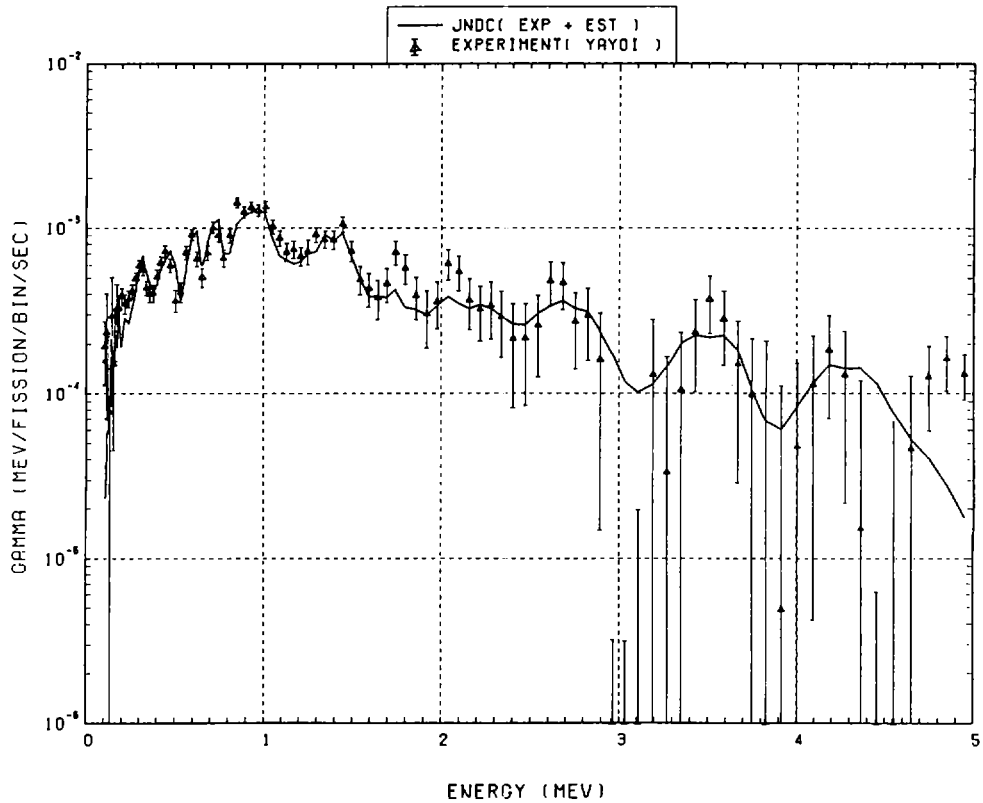

Fig. 99 Comparison of calculated gamma-ray energy spectrum with measured results at 290 seconds after fast neutron fission of ^{235}U. (t_{irrad} = 10 s, t_{wait} = 225 s, t_{count} = 60 s)

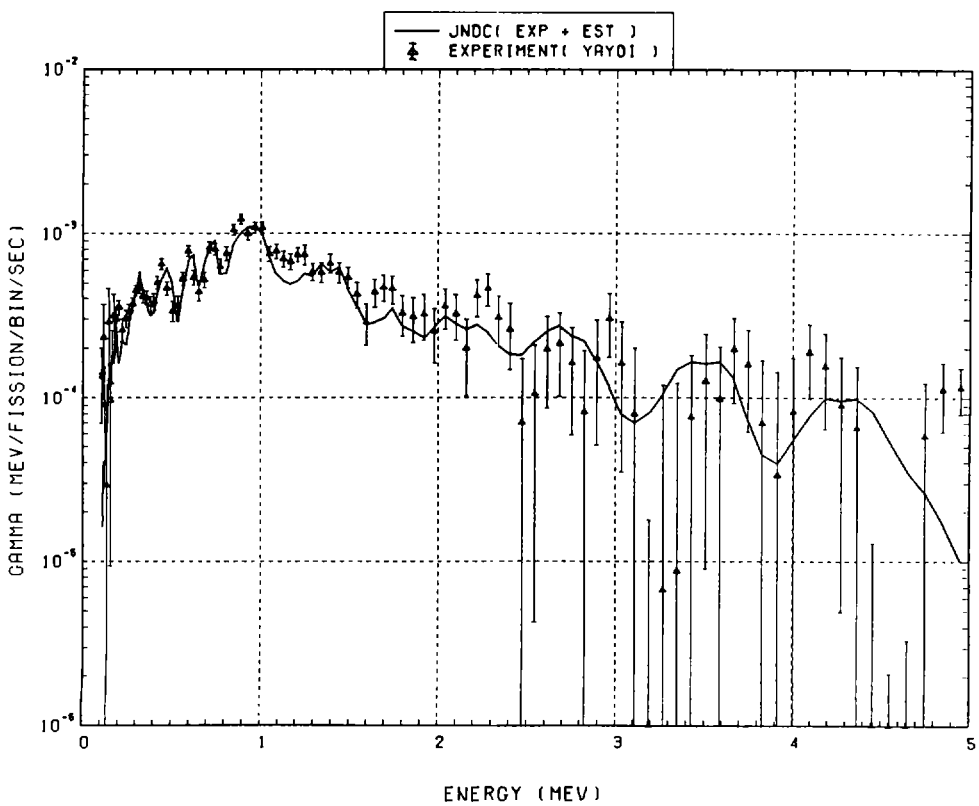

Fig. 100 Comparison of calculated gamma-ray energy spectrum with measured results at 360 seconds after fast neutron fission of ^{235}U. (t_{irrad} = 10 s, t_{wait} = 315 s, t_{count} = 80 s)

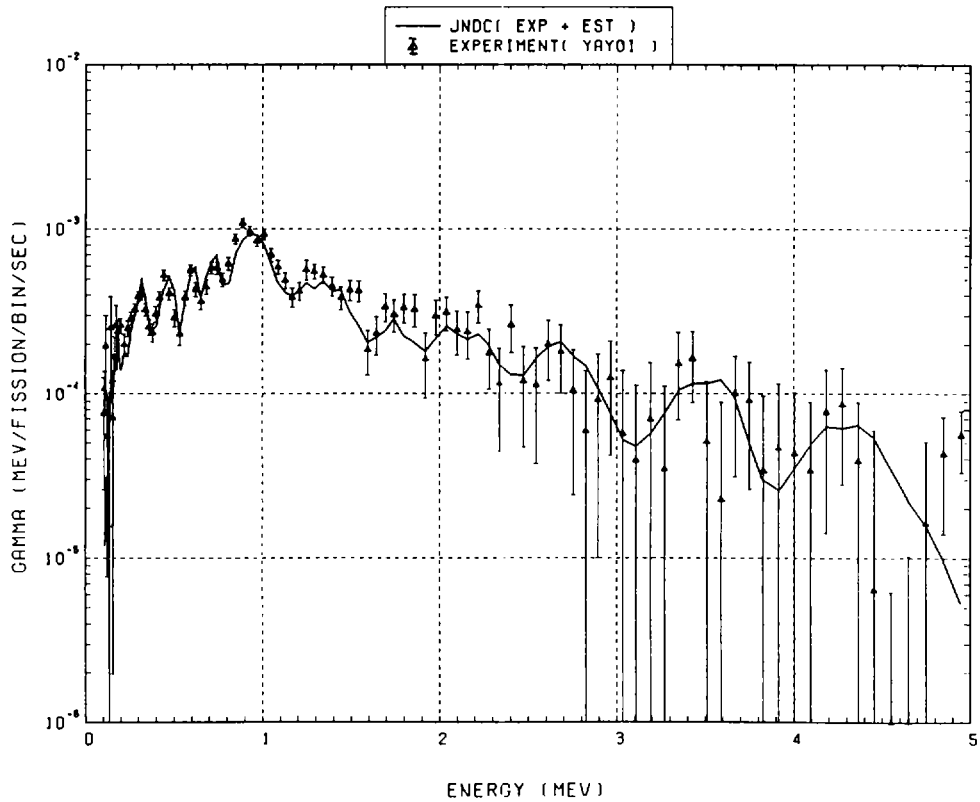

Fig. 101 Comparison of calculated gamma-ray energy spectrum with measured results at 450 seconds after fast neutron fission of ^{235}U. (t_{irrad} = 10 s, t_{wait} = 395 s, t_{count} = 100 s)

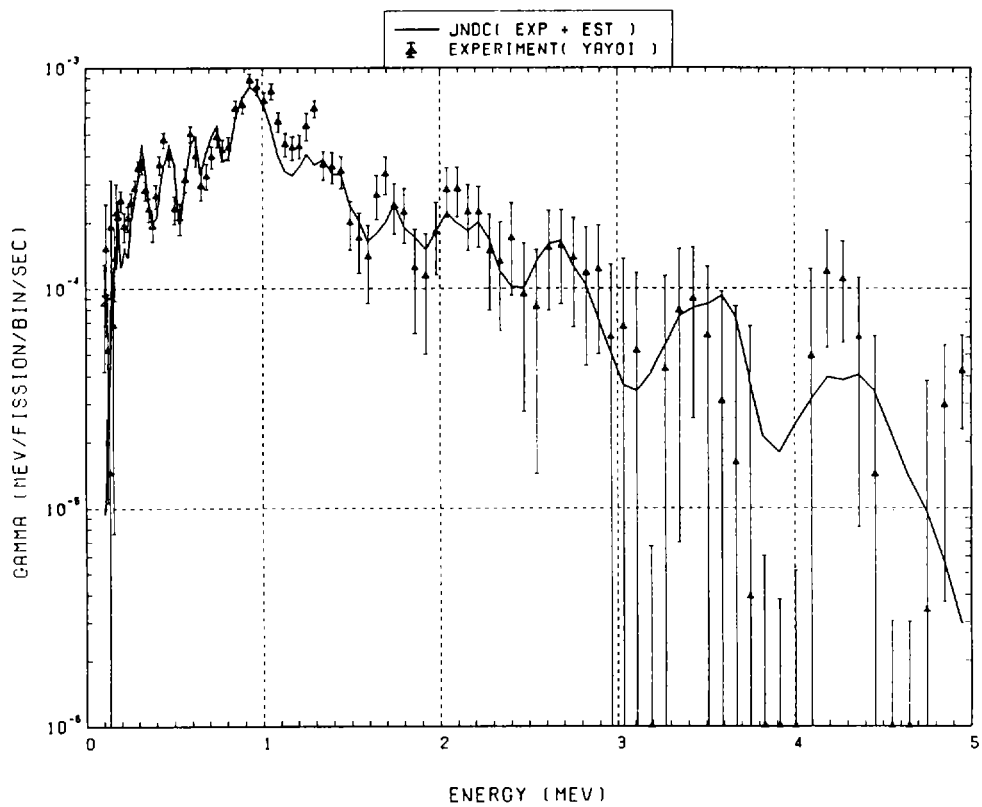

Fig. 102 Comparison of calculated gamma-ray energy spectrum with measured results at 550 seconds after fast neutron fission of ^{235}U. (t_{irrad} = 10 s, t_{wait} = 495 s, t_{count} = 100 s)

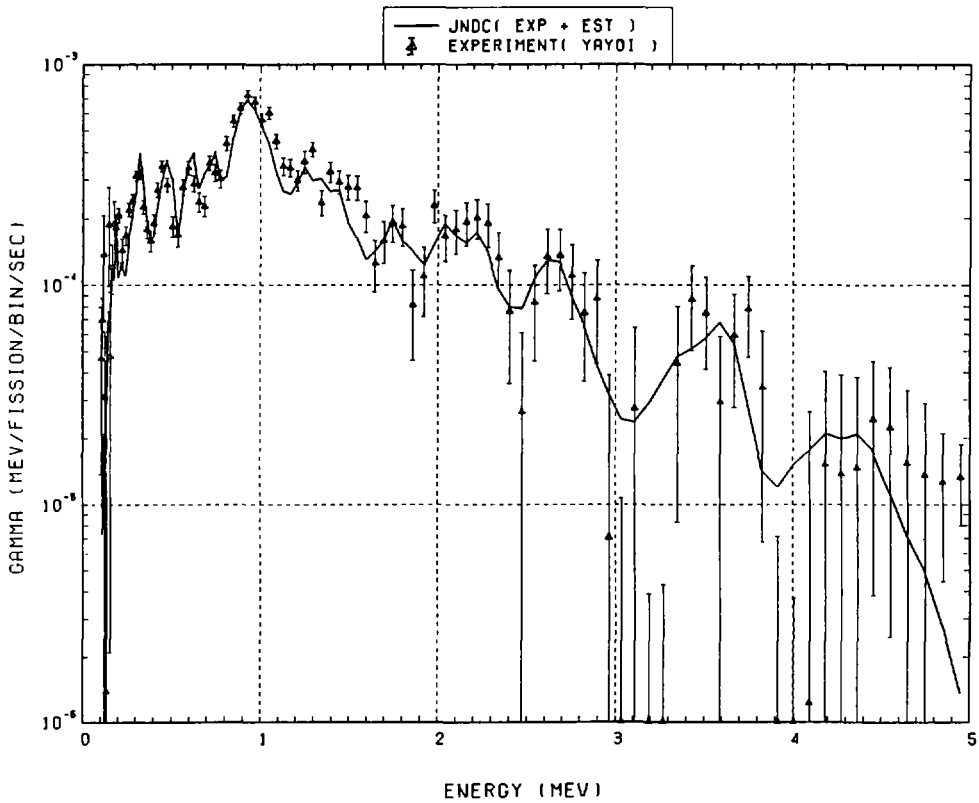

Fig. 103 Comparison of calculated gamma-ray energy spectrum with measured results at 700 seconds after fast neutron fission of ^{235}U. (t_{irrad} = 10 s, t_{wait} = 595 s, t_{count} = 200 s)

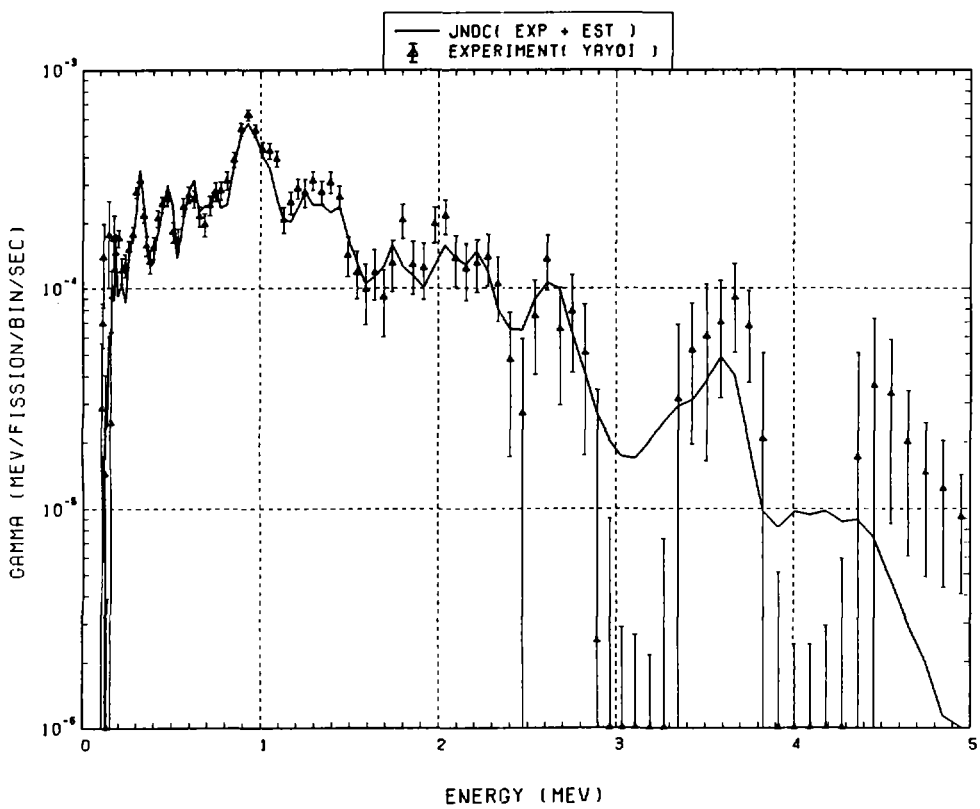

Fig. 104 Comparison of calculated gamma-ray energy spectrum with measured results at 900 seconds after fast neutron fission of ^{235}U. (t_{irrad} = 10 s, t_{wait} = 795 s, t_{count} = 200 s)

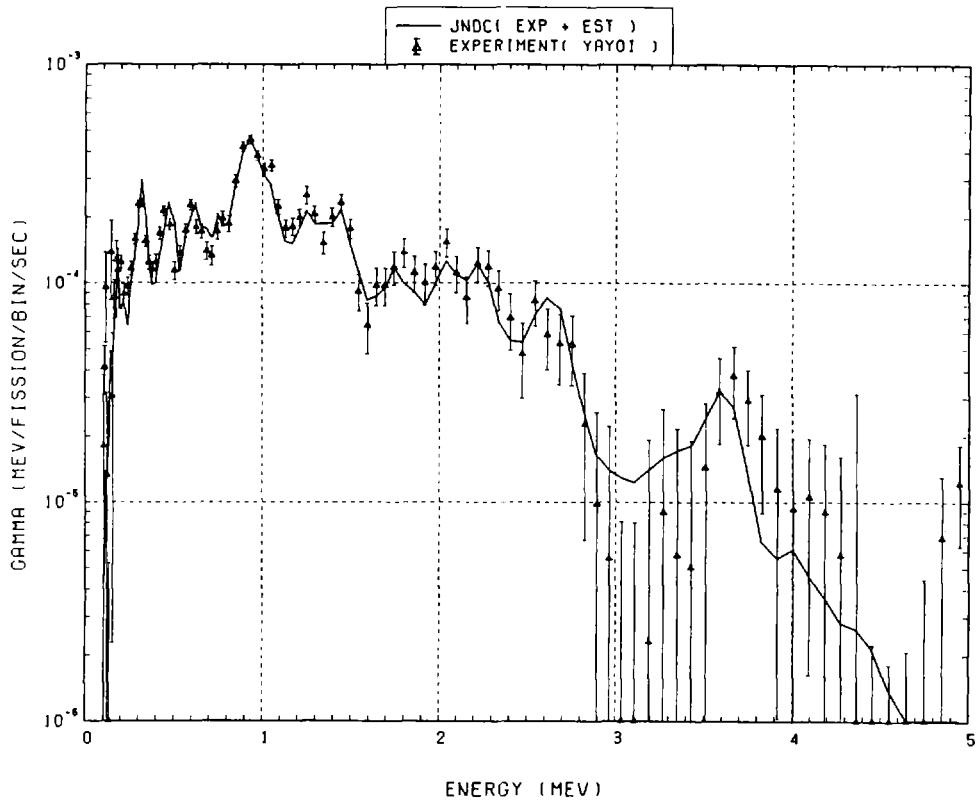

Fig. 105 Comparison of calculated gamma-ray energy spectrum with measured results at 1200 seconds after fast neutron fission of ^{235}U. (t_{irrad} = 10 s, t_{wait} = 995 s, t_{count} = 400 s)

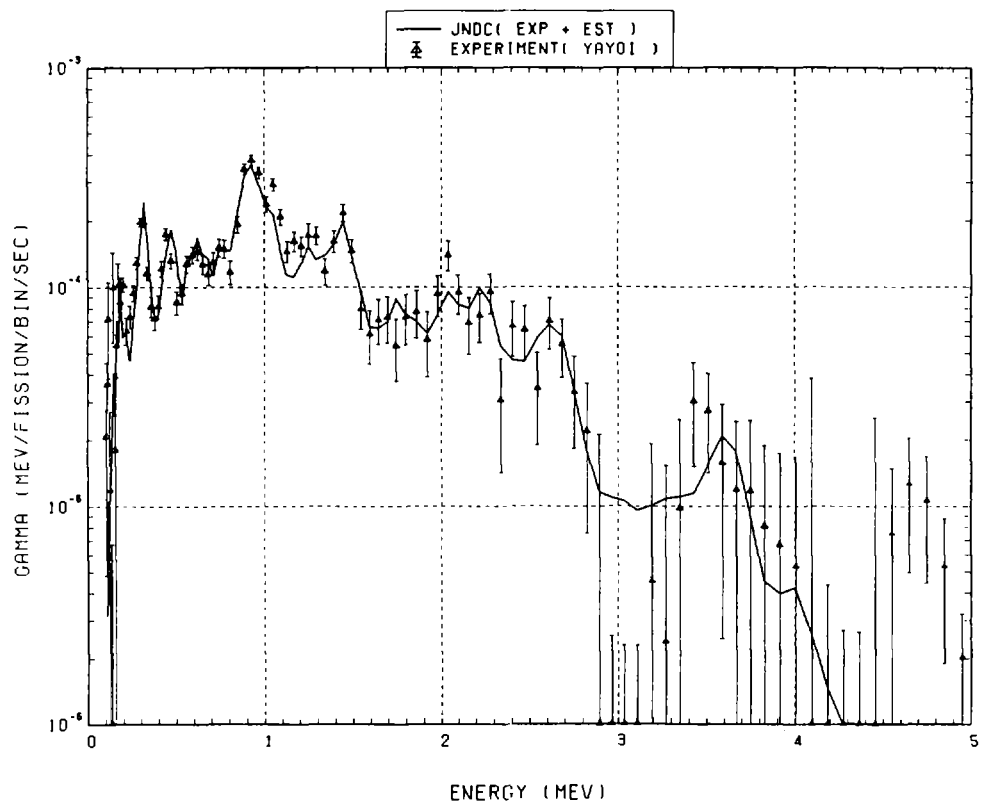

Fig. 106 Comparison of calculated gamma-ray energy spectrum with measured results at 1600 seconds after fast neutron fission of ^{235}U. (t_{irrad} = 10 s, t_{wait} = 1395 s, t_{count} = 400 s)

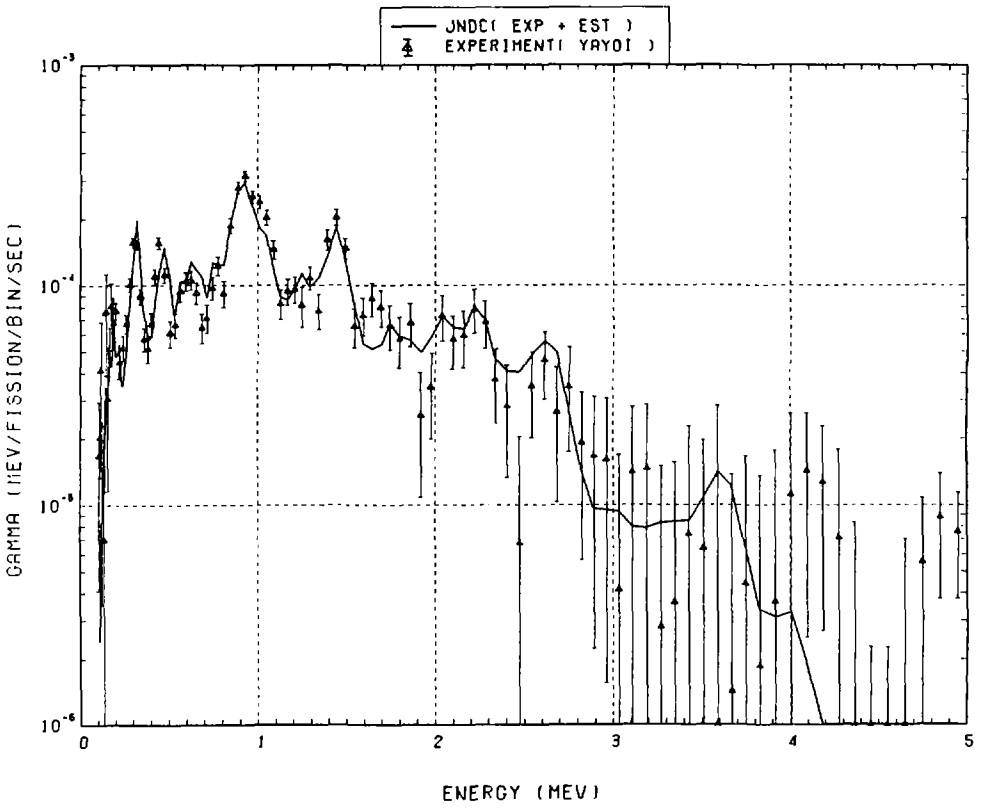

Fig. 107 Comparison of calculated gamma-ray energy spectrum with measured results at 2000 seconds after fast neutron fission of ^{235}U. (t_{irrad} = 10 s, t_{wait} = 1795 s, t_{count} = 400 s)

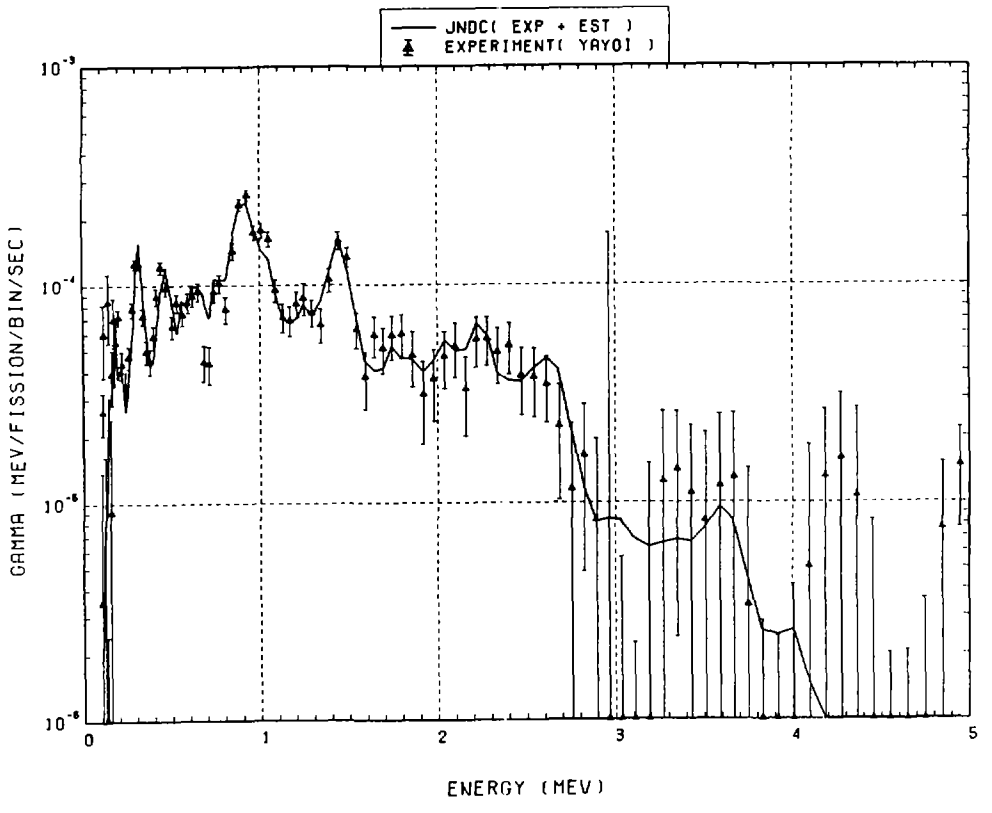

Fig. 108 Comparison of calculated gamma-ray energy spectrum with measured results at 2450 seconds after fast neutron fission of ^{235}U. (t_{irrad} = 10 s, t_{wait} = 2195 s, t_{count} = 500 s)

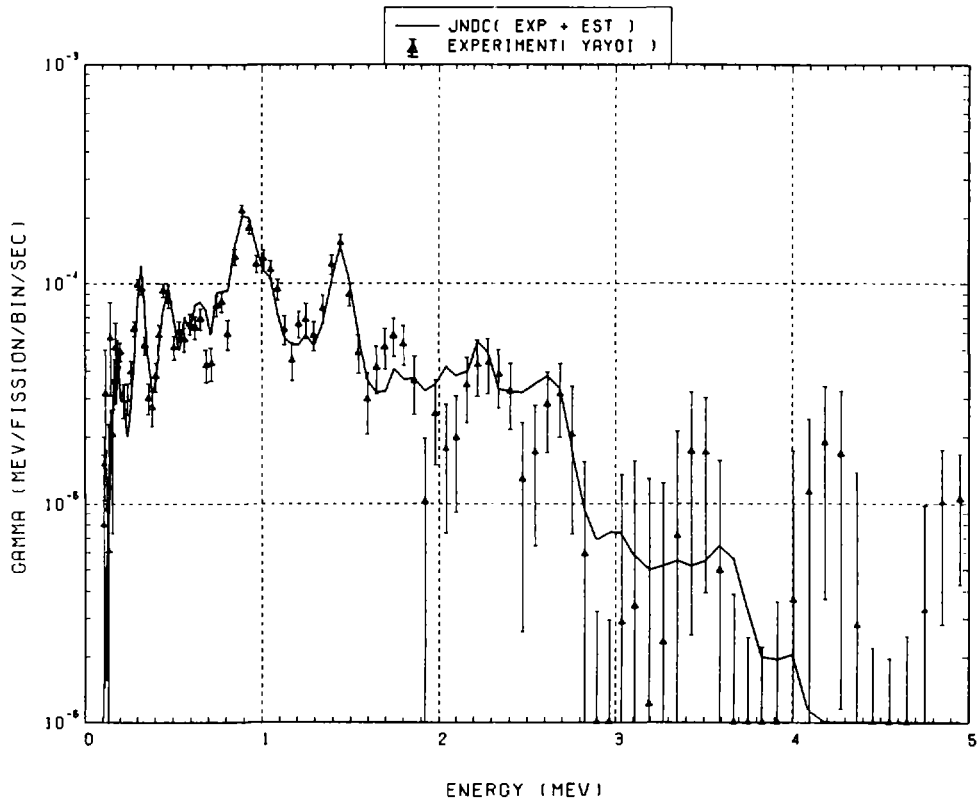

Fig. 109 Comparison of calculated gamma-ray energy spectrum with measured results at 2950 seconds after fast neutron fission of ^{235}U. (t_{irrad} = 10 s, t_{wait} = 2695 s, t_{count} = 500 s)

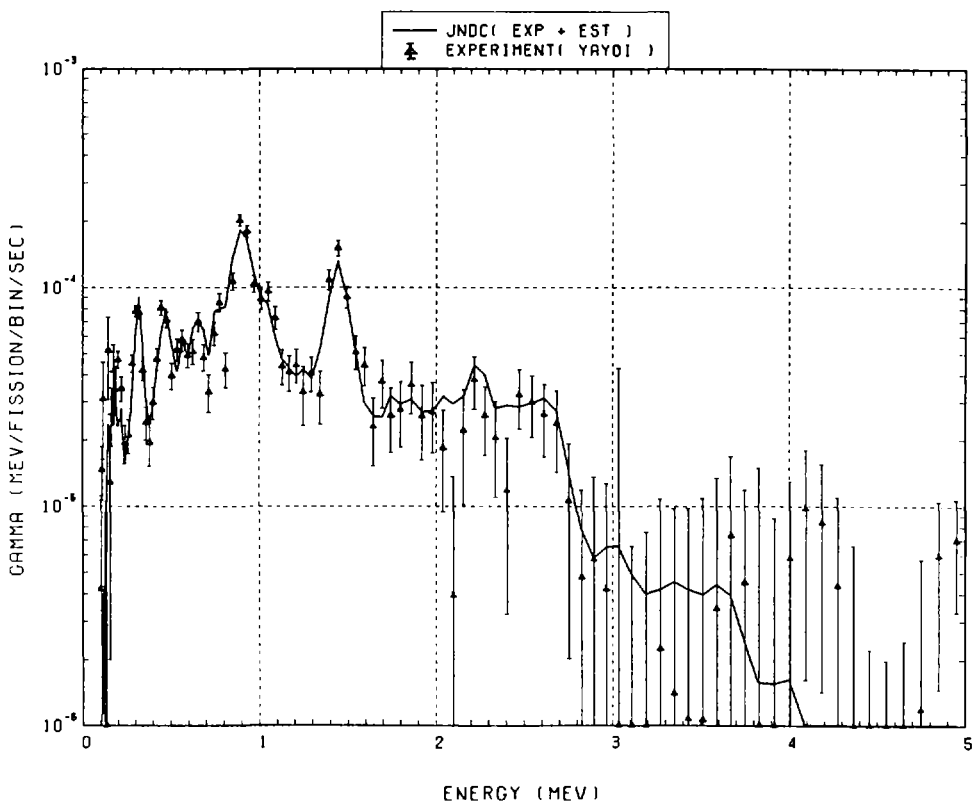

Fig. 110 Comparison of calculated gamma-ray energy spectrum with measured results at 3500 seconds after fast neutron fission of ^{235}U. (t_{irrad} = 10 s, t_{wait} = 3195 s, t_{count} = 600 s)

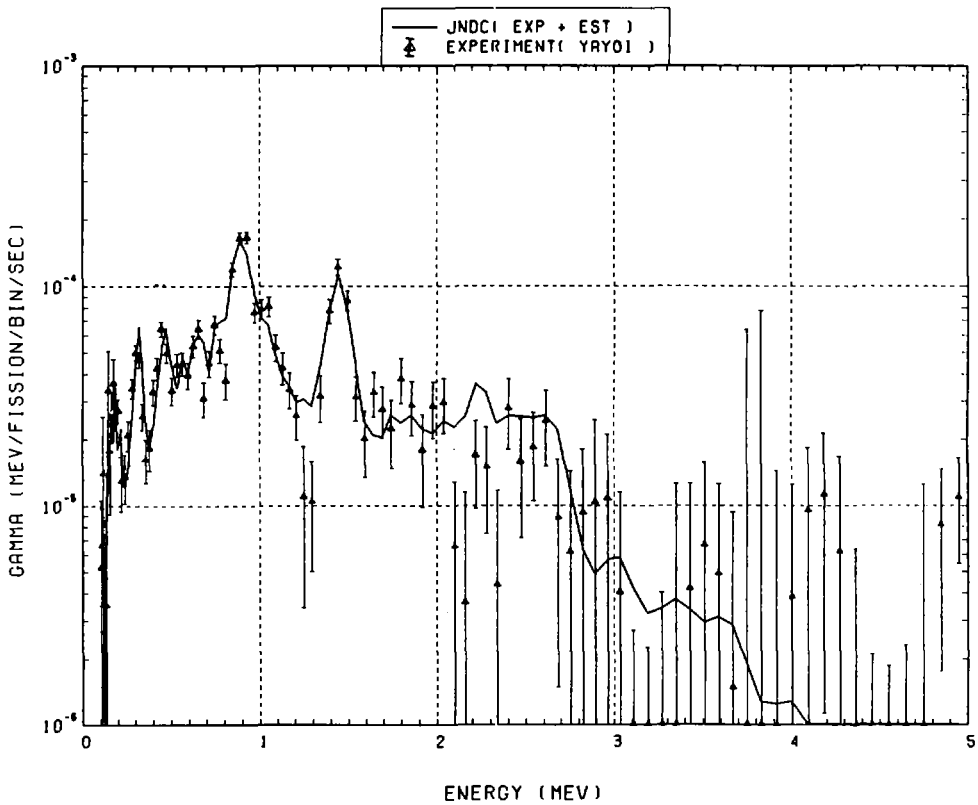

Fig. 111 Comparison of calculated gamma-ray energy spectrum with measured results at 4100 seconds after fast neutron fission of ^{235}U. (t_{irrad} = 10 s, t_{wait} = 3795 s, t_{count} = 600 s)

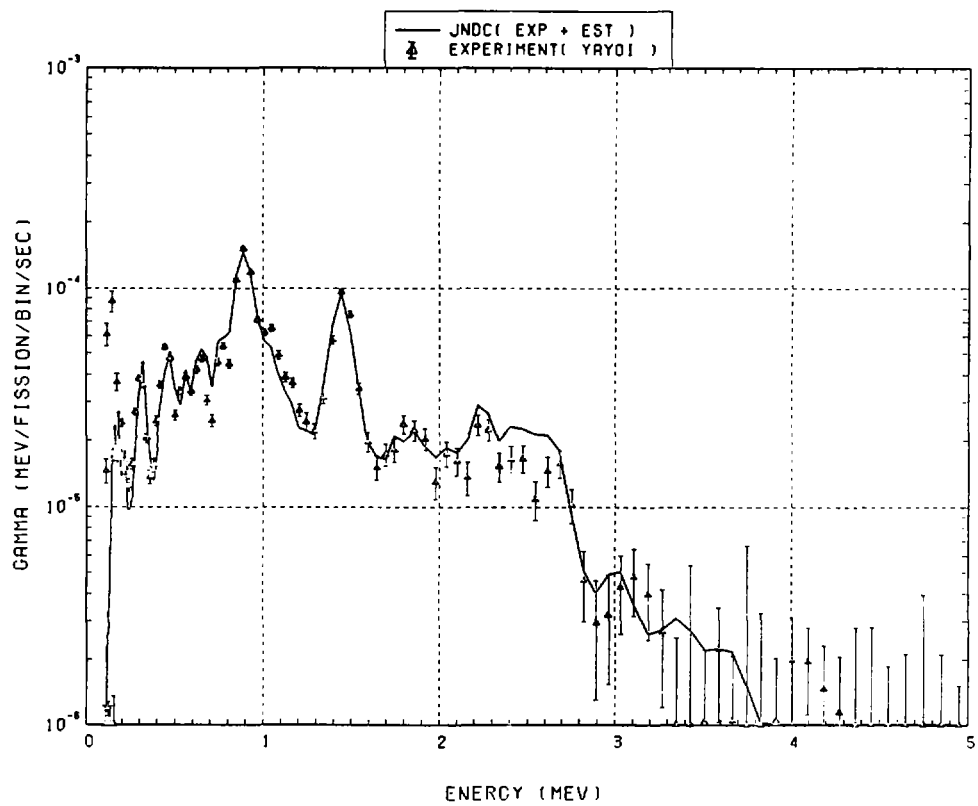

Fig. 112 Comparison of calculated gamma-ray energy spectrum with measured results at 4800 seconds after fast neutron fission of ^{235}U. (t_{irrad} = 100 s, t_{wait} = 4350 s, t_{count} = 800 s)

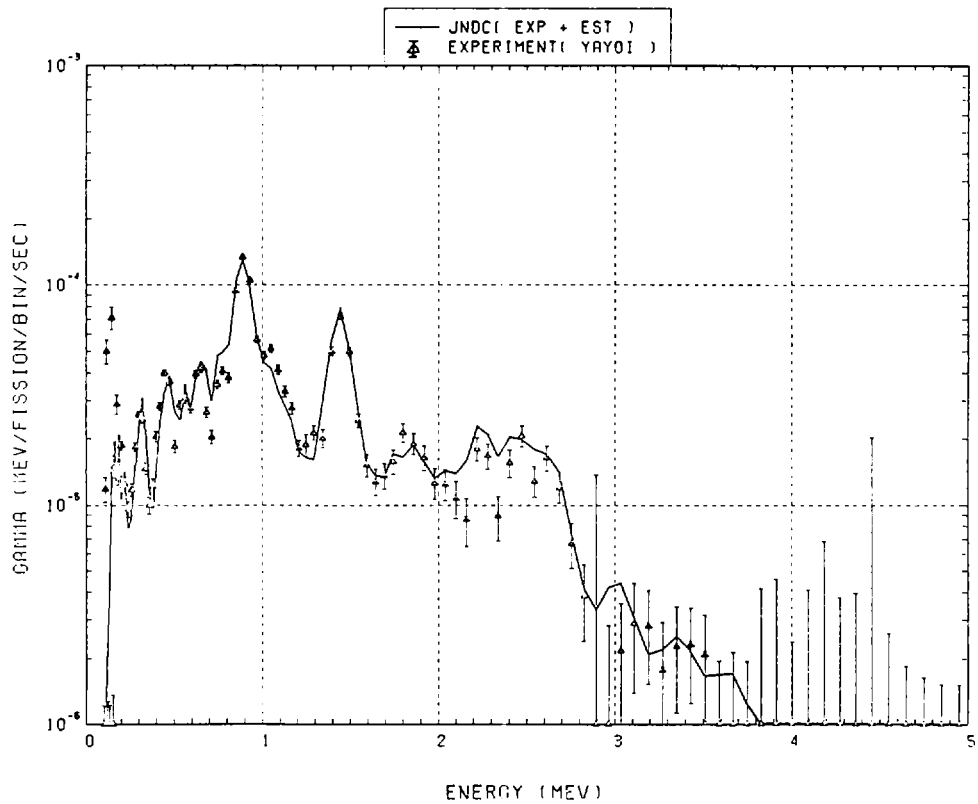

Fig. 113 Comparison of calculated gamma-ray energy spectrum with measured results at 5600 seconds after fast neutron fission of ^{235}U. (t_{irrad} = 100 s, t_{wait} = 5150 s, t_{count} = 800 s)

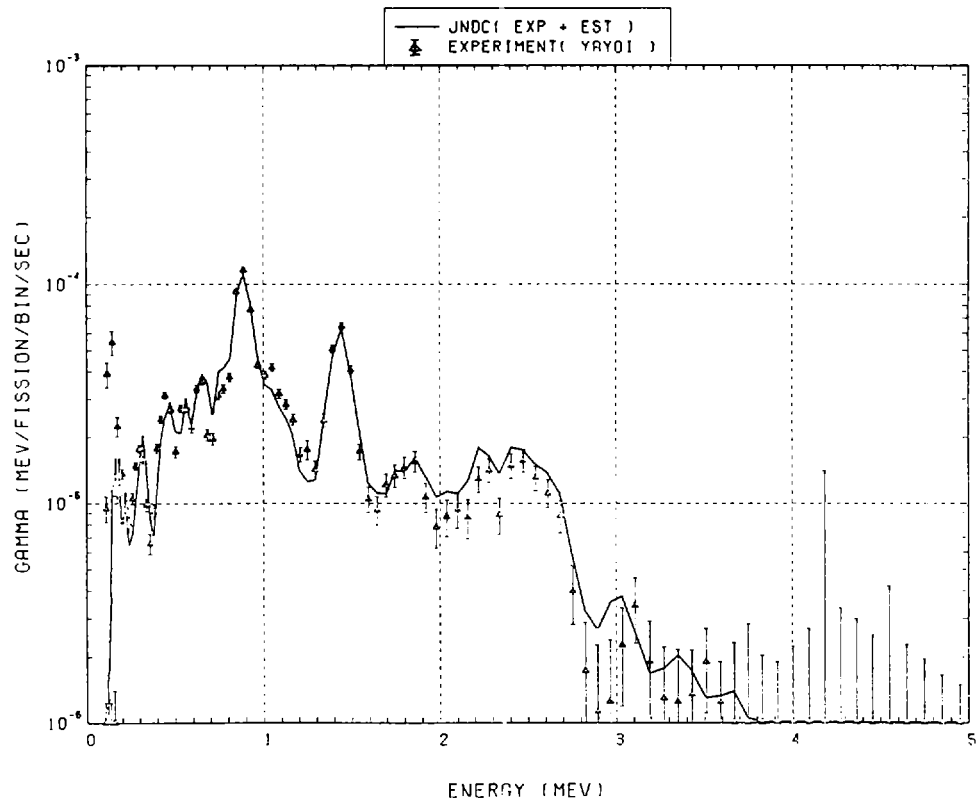

Fig. 114 Comparison of calculated gamma-ray energy spectrum with measured results at 6500 seconds after fast neutron fission of ^{235}U. (t_{irrad} = 100 s, t_{wait} = 5950 s, t_{count} = 1000 s)

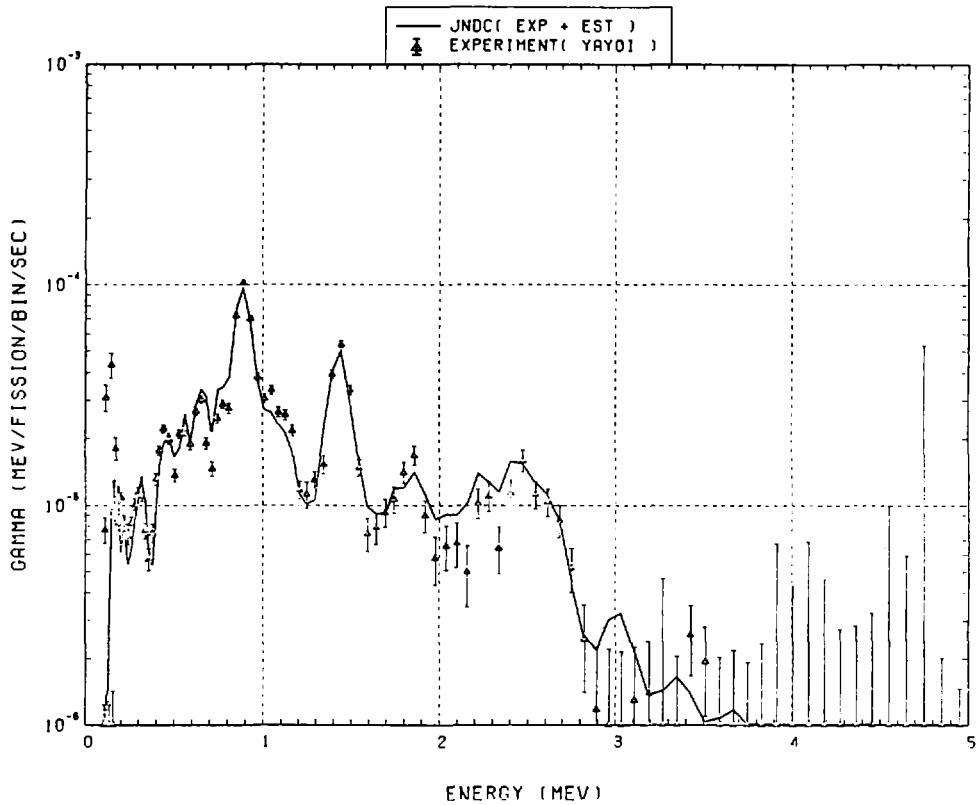

Fig. 115 Comparison of calculated gamma-ray energy spectrum with measured results at 7500 seconds after fast neutron fission of ^{235}U. (t_{irrad} = 100 s, t_{wait} = 6950 s, t_{count} = 1000 s)

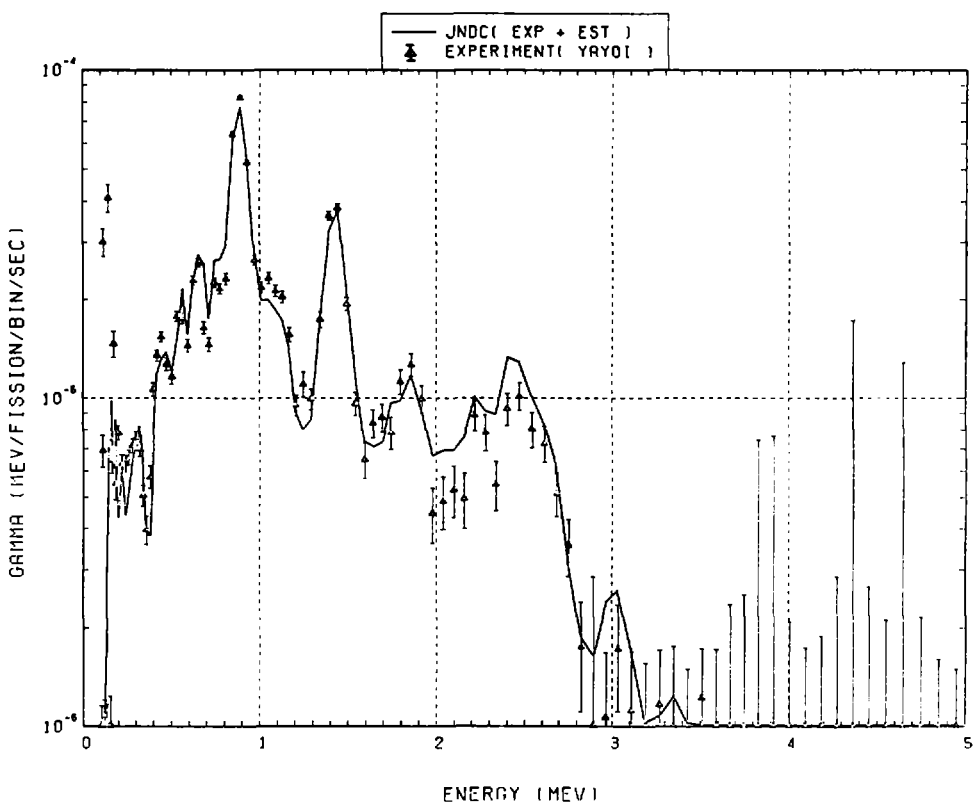

Fig. 116 Comparison of calculated gamma-ray energy spectrum with measured results at 9000 seconds after fast neutron fission of ^{235}U. (t_{irrad} = 100 s, t_{wait} = 7950 s, t_{count} = 2000 s)

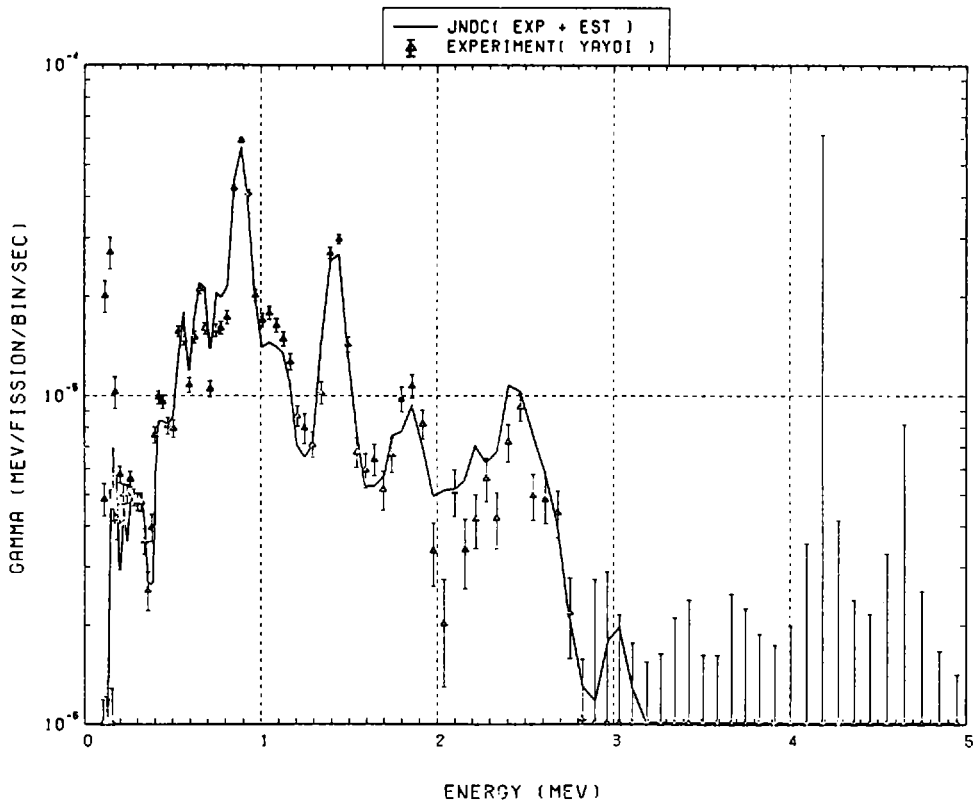

Fig. 117 Comparison of calculated gamma-ray energy spectrum with measured results at 11000 seconds after fast neutron fission of ^{235}U. (t_{irrad} = 100 s, t_{wait} = 9950 s, t_{count} = 2000 s)

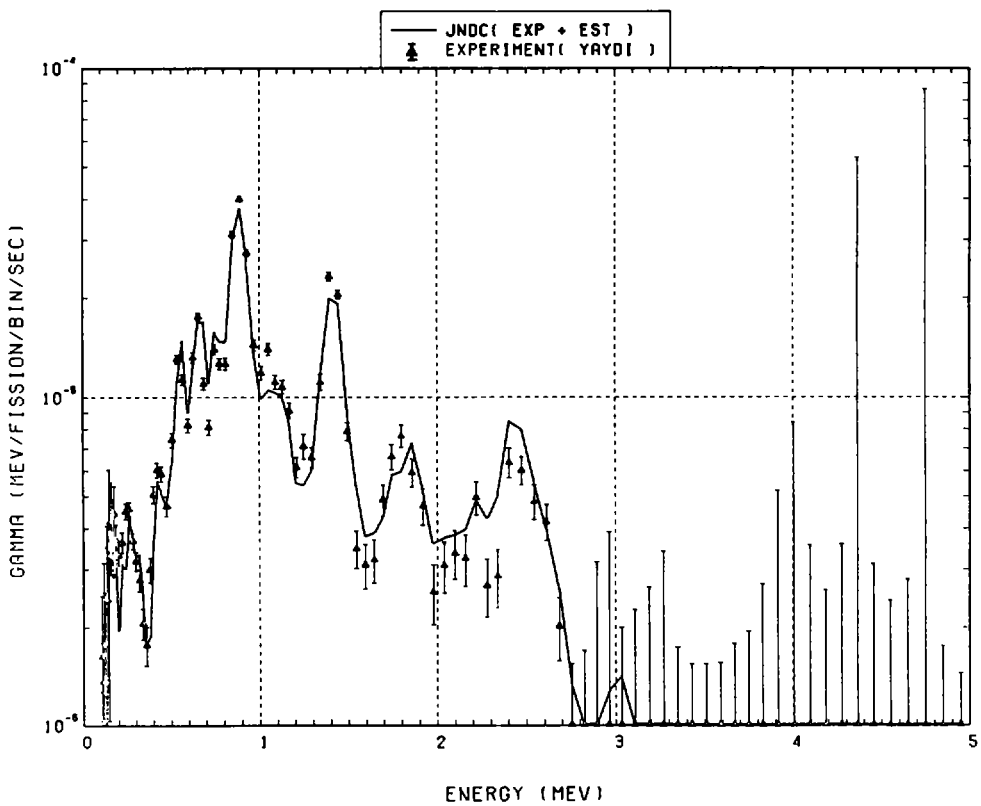

Fig. 118 Comparison of calculated gamma-ray energy spectrum with measured results at 13500 seconds after fast neutron fission of ^{235}U. (t_{irrad} = 100 s, t_{wait} = 11950 s, t_{count} = 300 s)

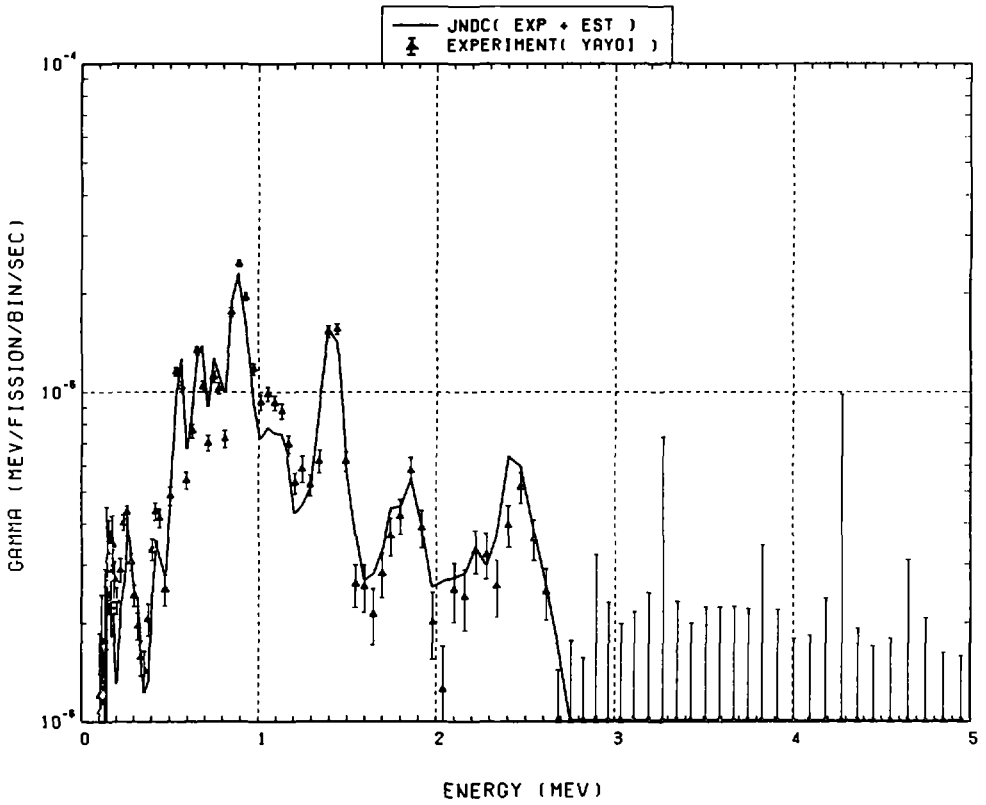

Fig. 119 Comparison of calculated gamma-ray energy spectrum with measured results at 16500 seconds after fast neutron fission of ^{235}U. (t_{irrad} = 100 s, t_{wait} = 14950 s, t_{count} = 3000 s)

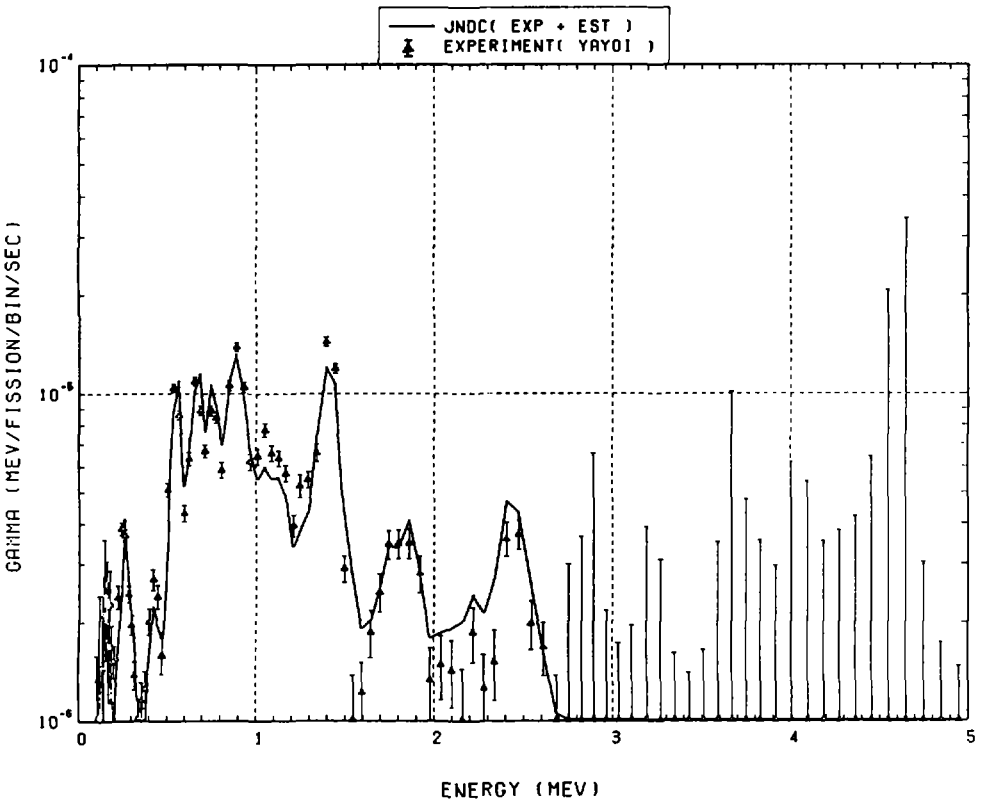

Fig. 120 Comparison of calculated gamma-ray energy spectrum with measured results at 20000 seconds after fast neutron fission of ^{235}U. (t_{irrad} = 100 s, t_{wait} = 17950 s, t_{count} = 4000 s)

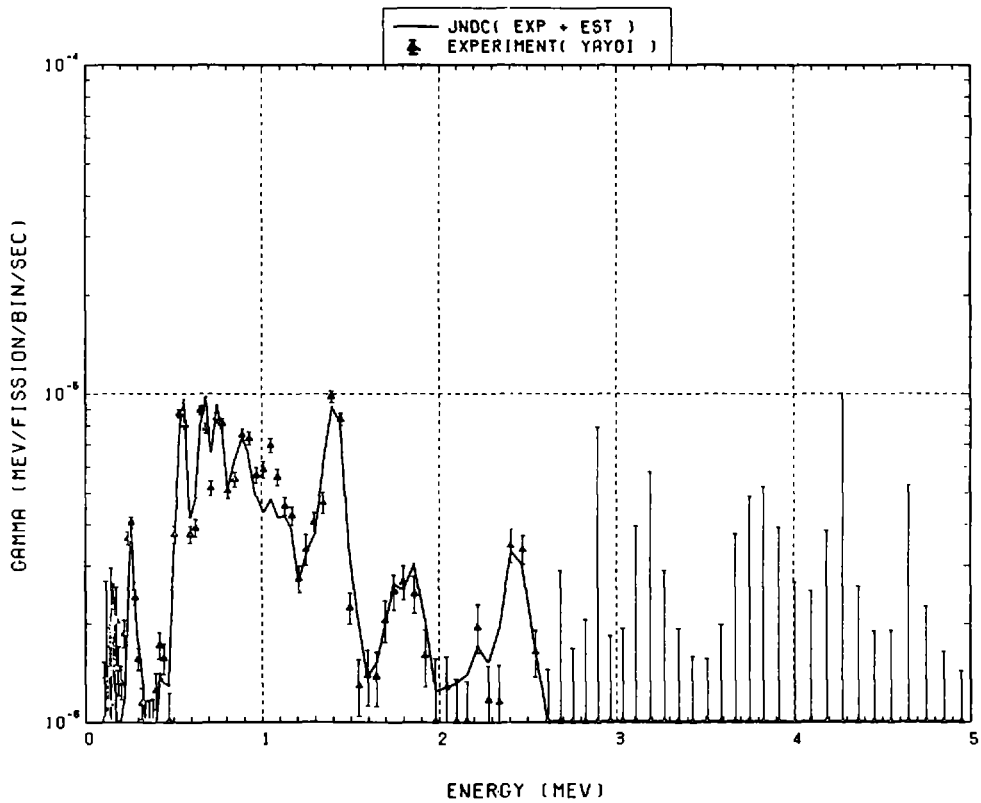

Fig. 121 Comparison of calculated gamma-ray energy spectrum with measured results at 24000 seconds after fast neutron fission of ^{235}U. (t_{irrad} = 100 s, t_{wait} = 21950 s, t_{count} = 4000 s)

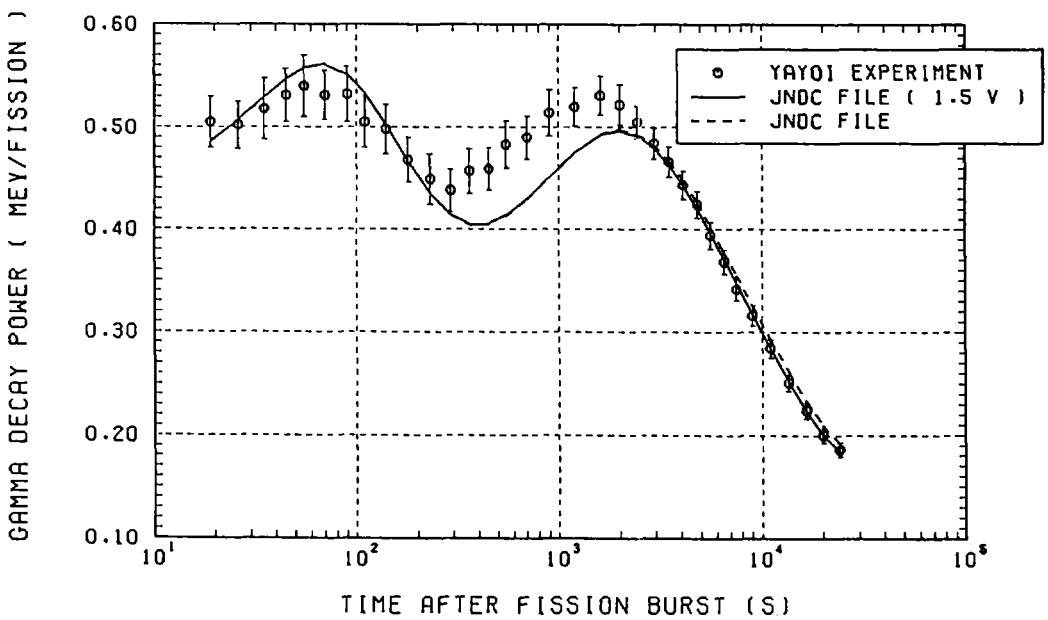

Fig. 122 Comparison of calculated gamma-decay heat with measured results at YAYOI for fast neutron fission of ^{239}Pu.

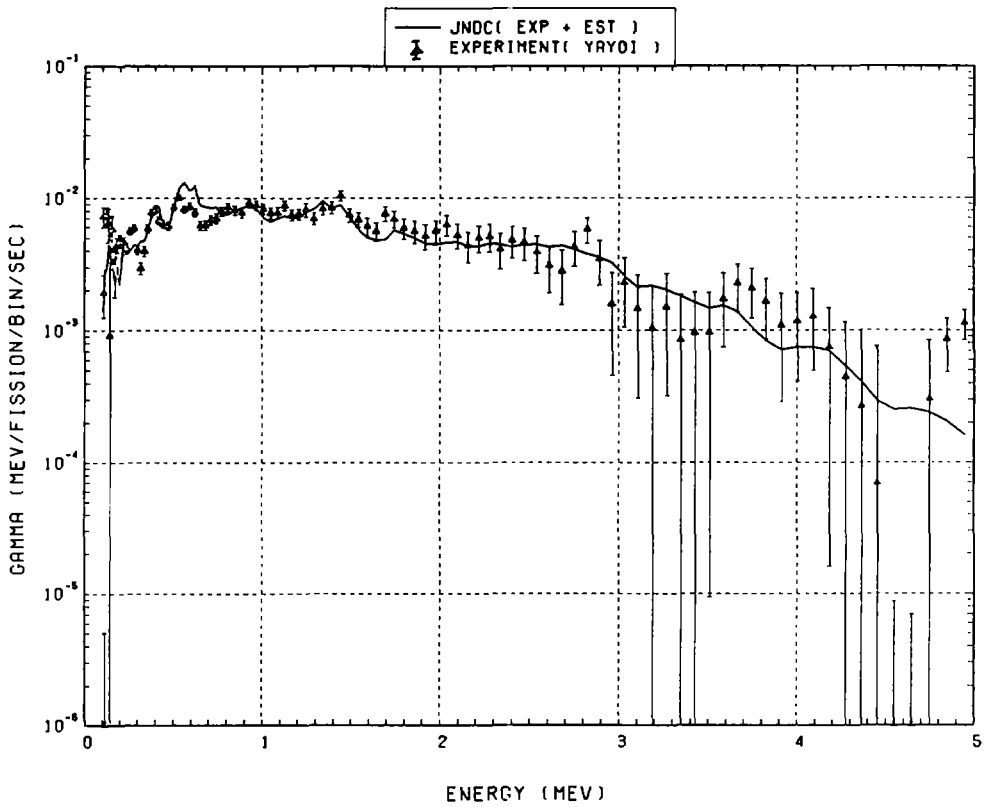

Fig. 123 Comparison of calculated gamma-ray energy spectrum with measured results at 19 seconds after fast neutron fission of ^{239}Pu. (t_{irrad} = 10 s, t_{wait} = 11 s, t_{count} = 6 s)

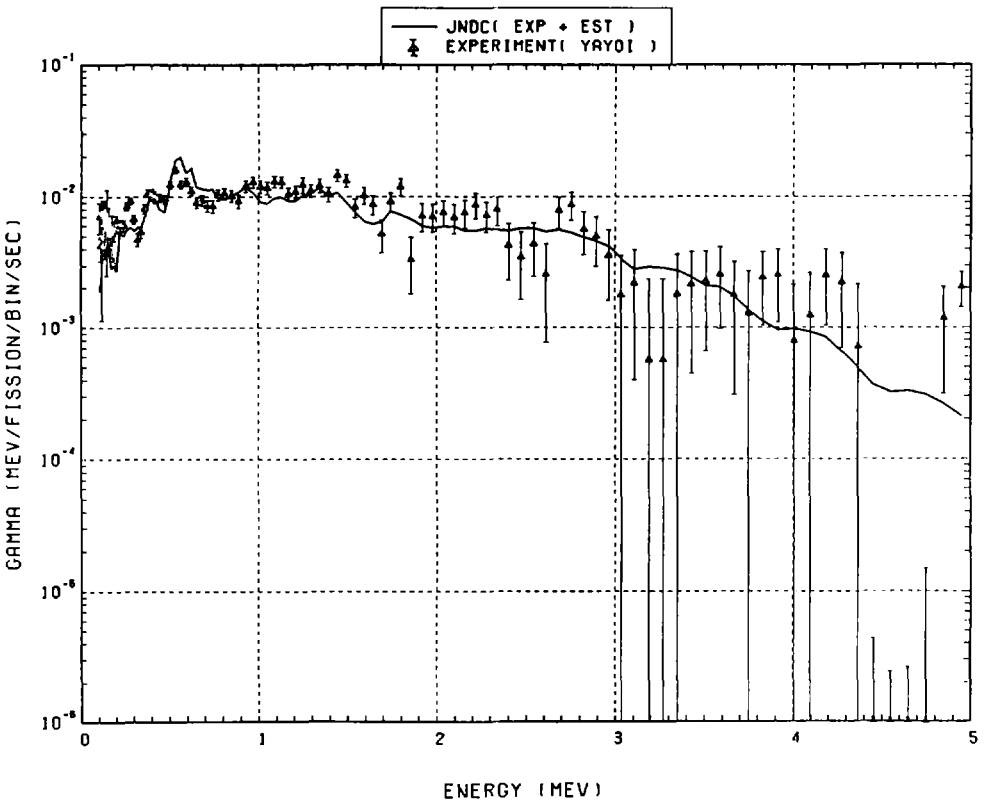

Fig. 124 Comparison of calculated gamma-ray energy spectrum with measured results at 26 seconds after fast neutron fission of ^{239}Pu. (t_{irrad} = 10 s, t_{wait} = 17 s, t_{count} = 8 s)

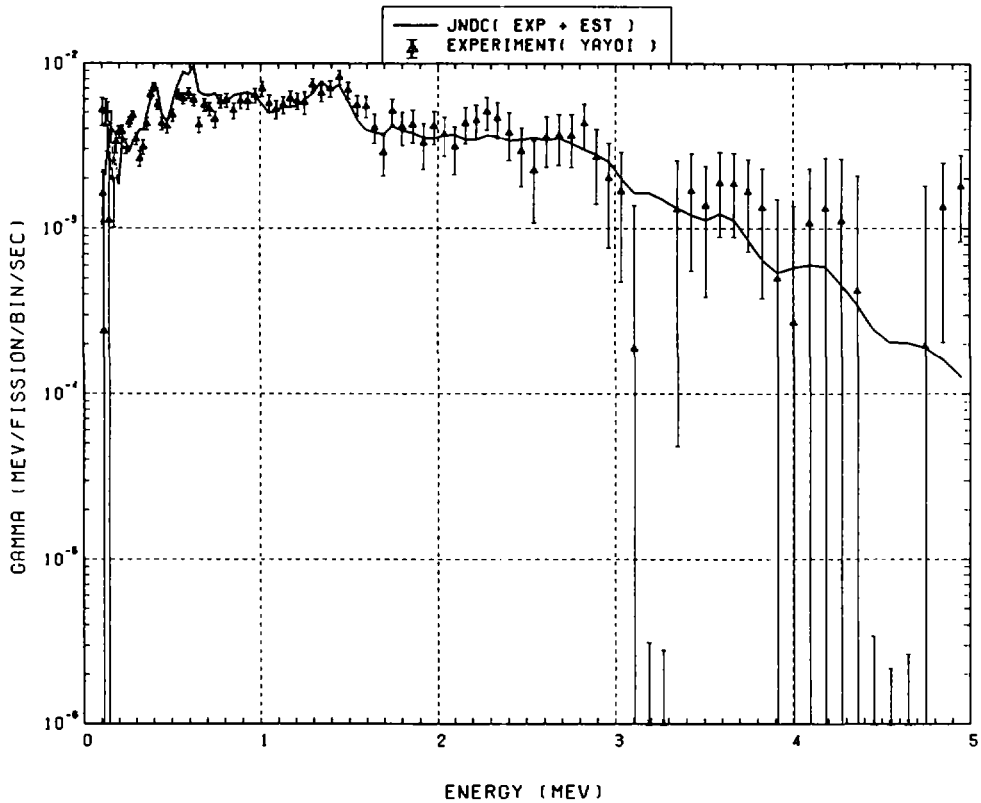

Fig. 125 Comparison of calculated gamma-ray energy spectrum with measured results at 35 seconds after fast neutron fission of ^{239}Pu. (t_{irrad} = 10 s, t_{wait} = 25 s, t_{count} = 10 s)

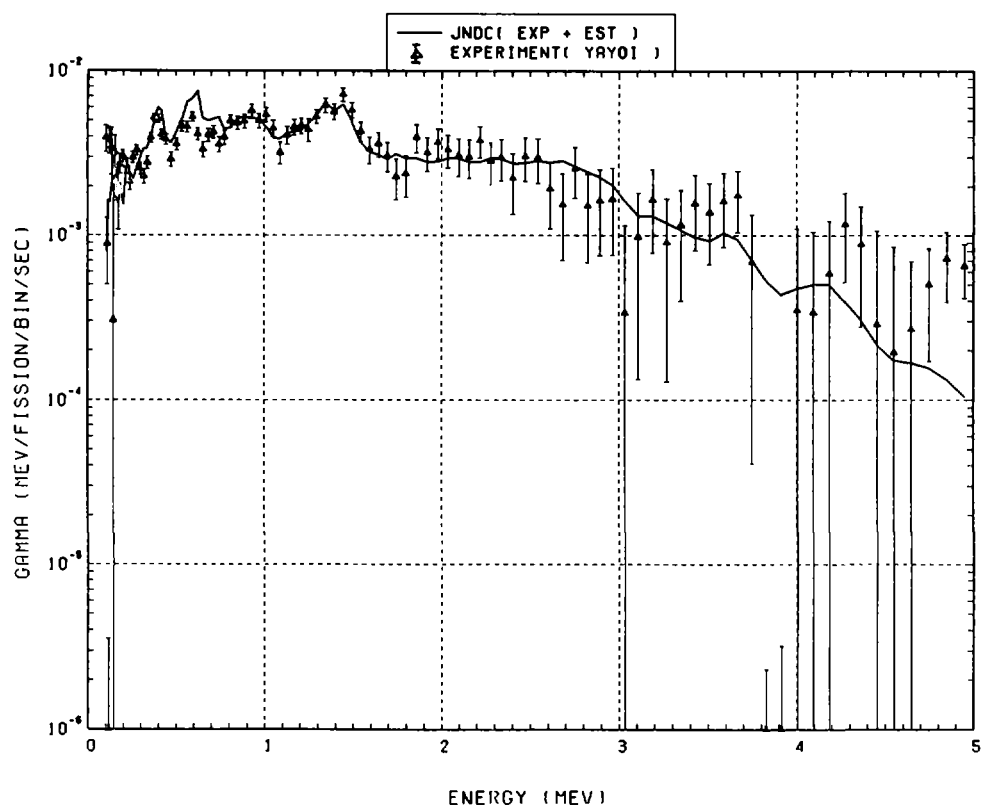

Fig. 126 Comparison of calculated gamma-ray energy spectrum with measured results at 45 seconds after fast neutron fission of ^{239}Pu. (t_{irrad} = 10 s, t_{wait} = 35 s, t_{count} = 10 s)

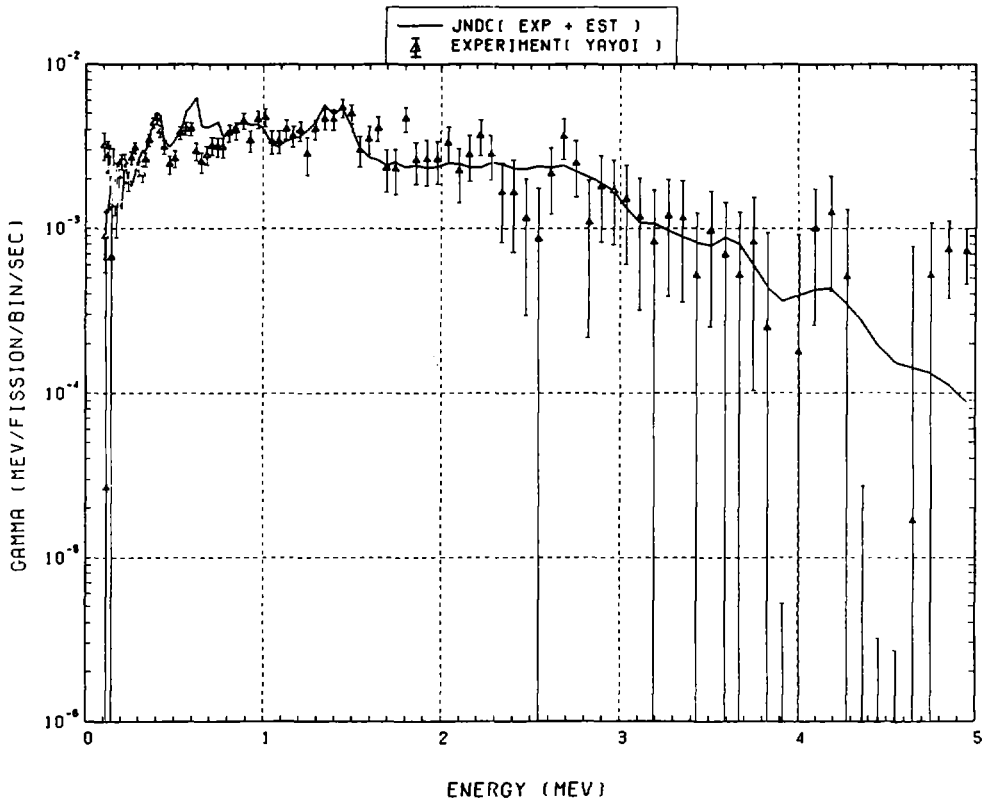

Fig. 127 Comparison of calculated gamma-ray energy spectrum with measured results at 55 seconds after fast neutron fission of ^{239}Pu. (t_{irrad} = 10 s, t_{wait} = 45 s, t_{count} = 10 s)

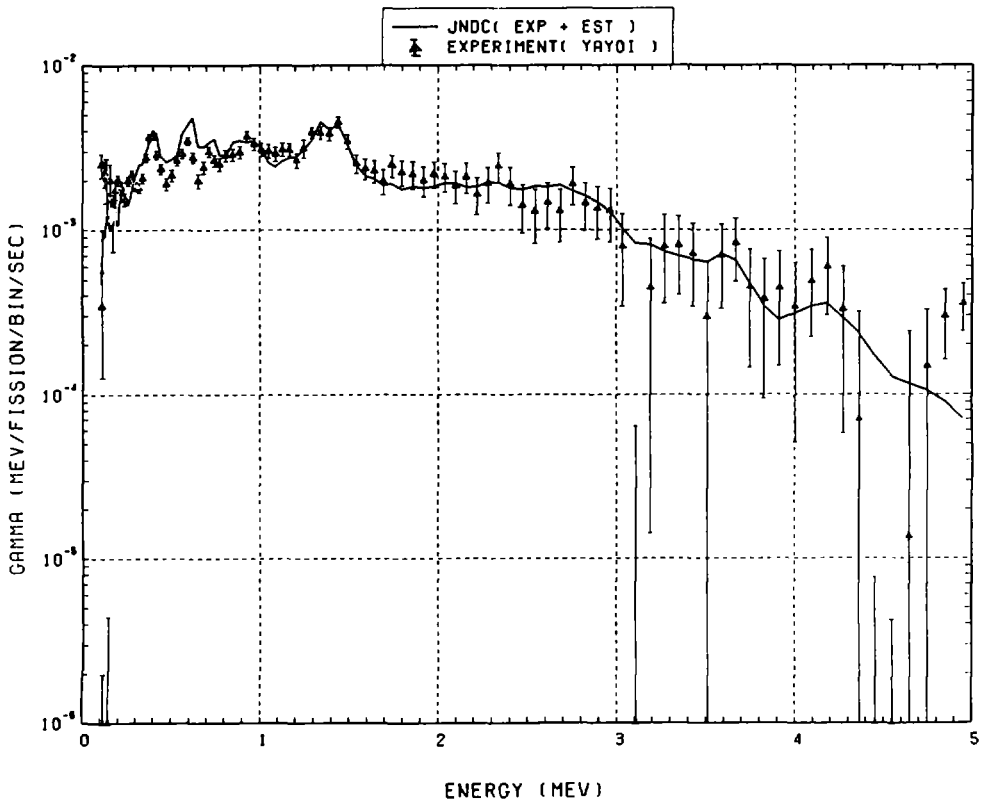

Fig. 128 Comparison of calculated gamma-ray energy spectrum with measured results at 70 seconds after fast neutron fission of ^{239}Pu. (t_{irrad} = 10 s, t_{wait} = 55 s, t_{count} = 20 s)

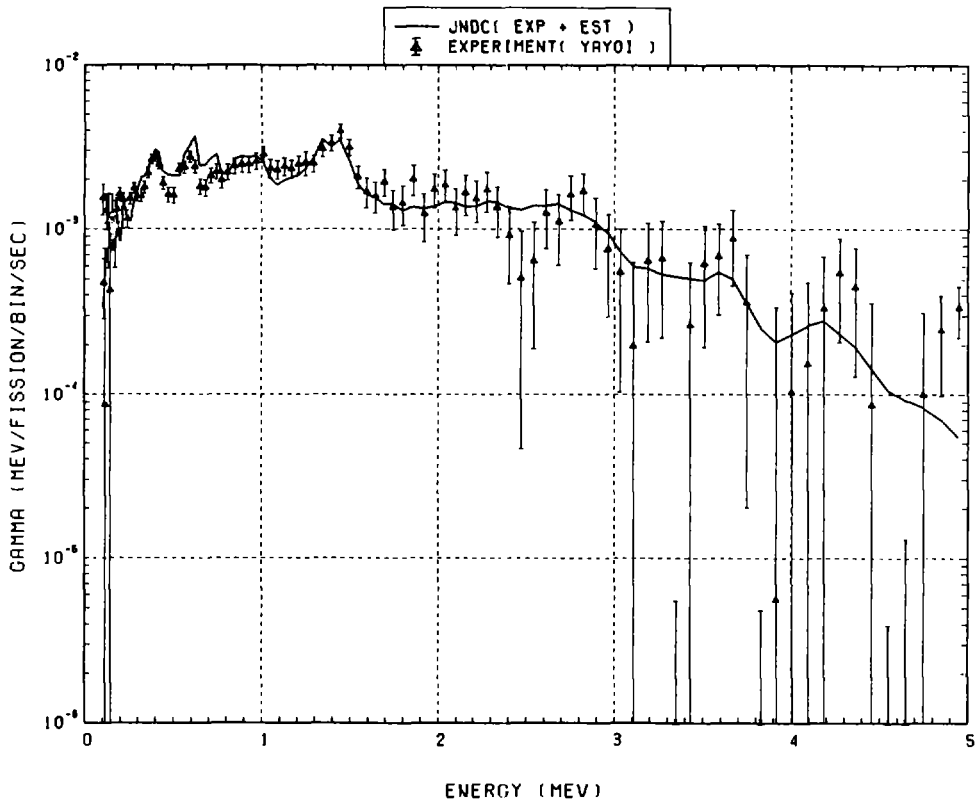

Fig. 129 Comparison of calculated gamma-ray energy spectrum with measured results at 90 seconds after fast neutron fission of ^{239}Pu. (t_{irrad} = 10 s, t_{wait} = 75 s, t_{count} = 20 s)

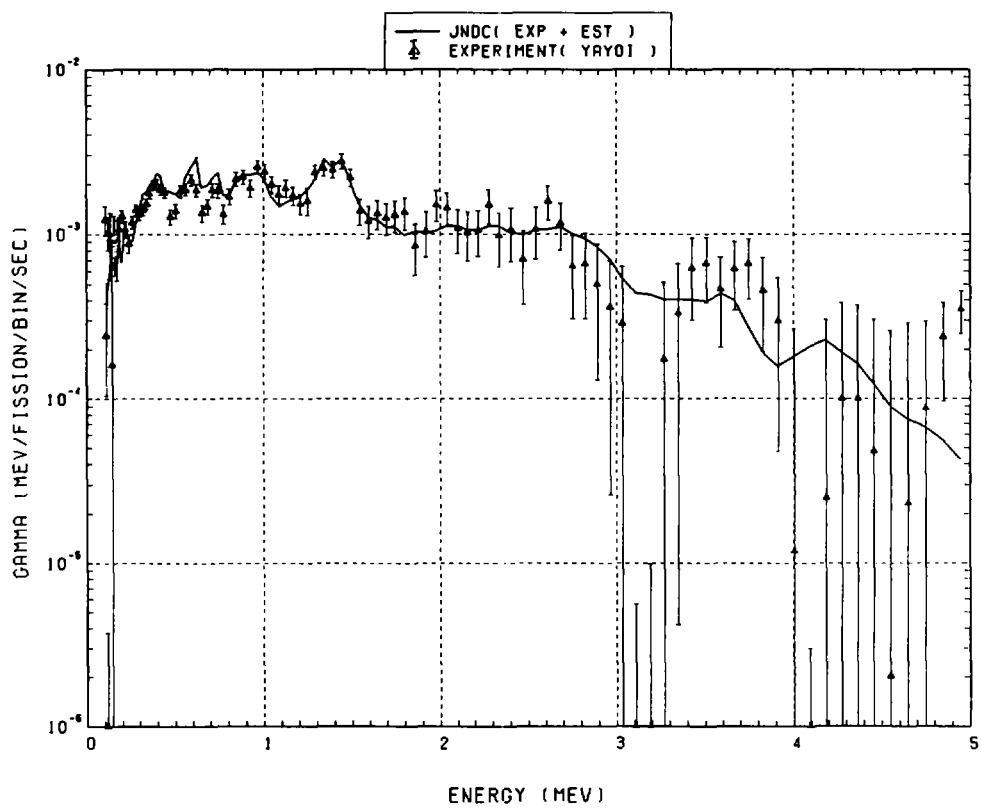

Fig. 130 Comparison of calculated gamma-ray energy spectrum with measured results at 110 seconds after fast neutron fission of ^{239}Pu. (t_{irrad} = 10 s, t_{wait} = 95 s, t_{count} = 20 s)

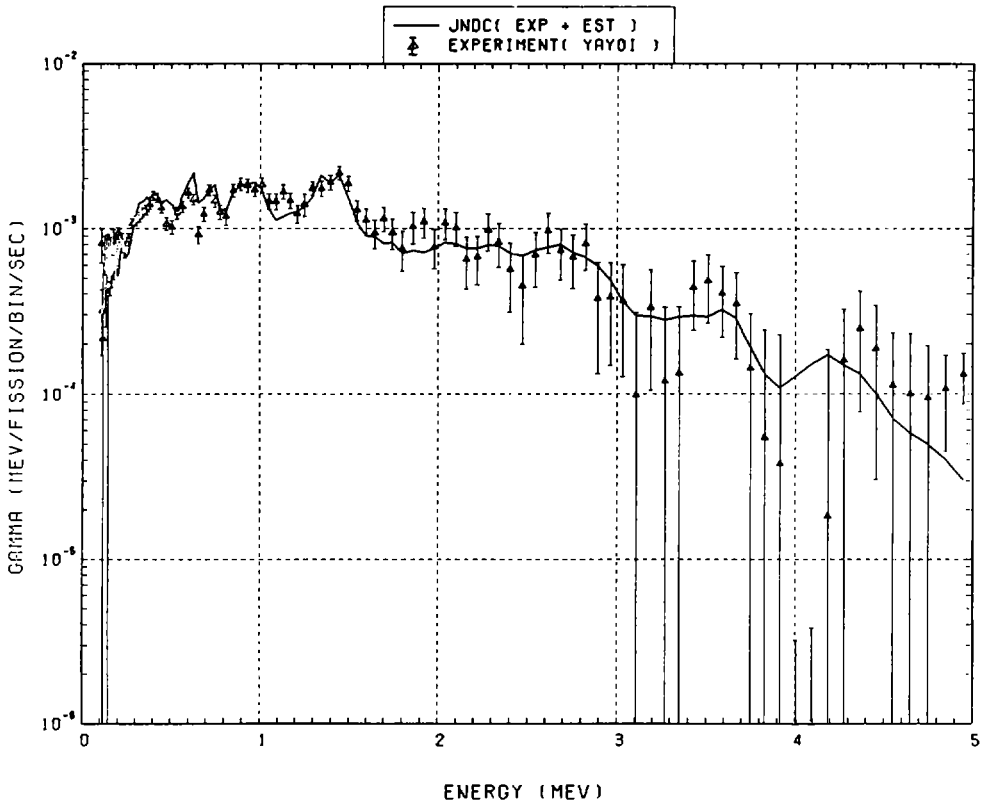

Fig. 131 Comparison of calculated gamma-ray energy spectrum with measured results at 140 seconds after fast neutron fission of ^{239}Pu. (t_{irrad} = 10 s, t_{wait} = 115 s, t_{count} = 40 s)

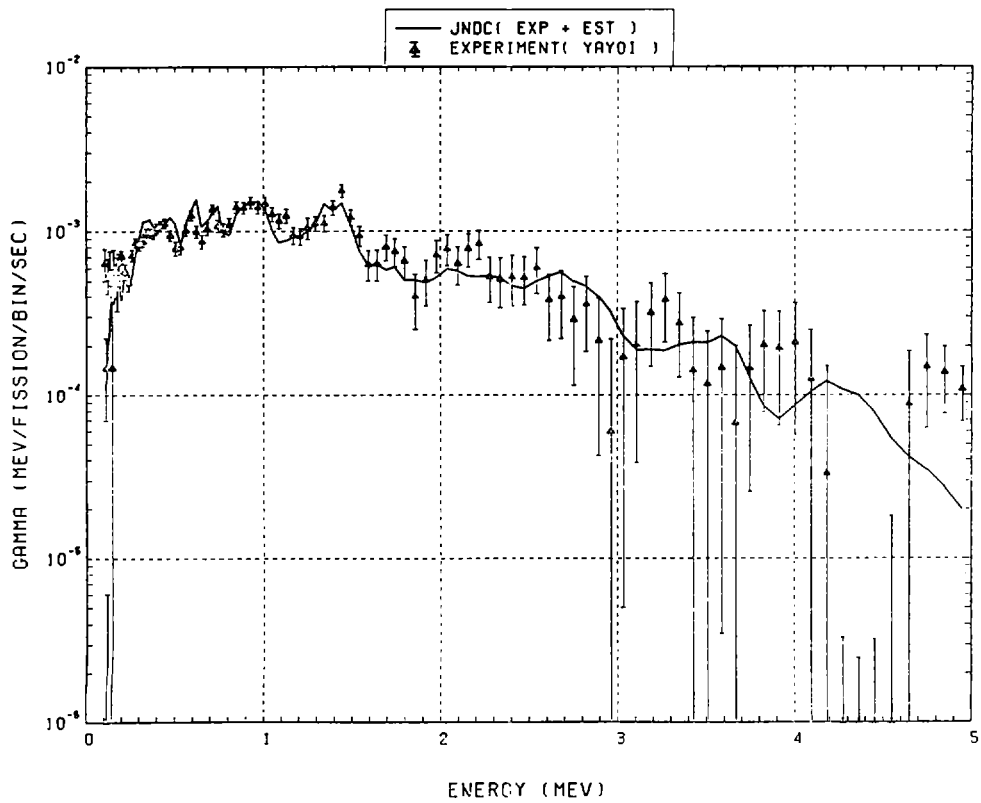

Fig. 132 Comparison of calculated gamma-ray energy spectrum with measured results at 180 seconds after fast neutron fission of ^{239}Pu. (t_{irrad} = 10 s, t_{wait} = 155 s, t_{count} = 40 s)

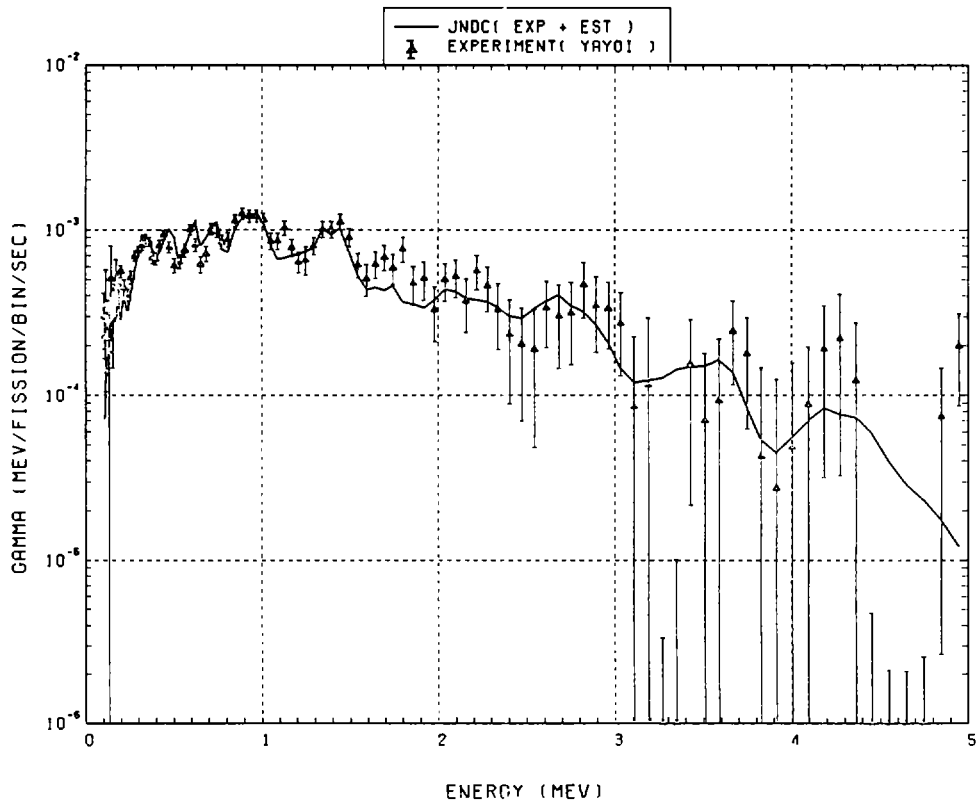

Fig. 133 Comparison of calculated gamma-ray energy spectrum with measured results at 230 seconds after fast neutron fission of ^{239}Pu. (t_{irrad} = 10 s, t_{wait} = 195 s, t_{count} = 60 s)

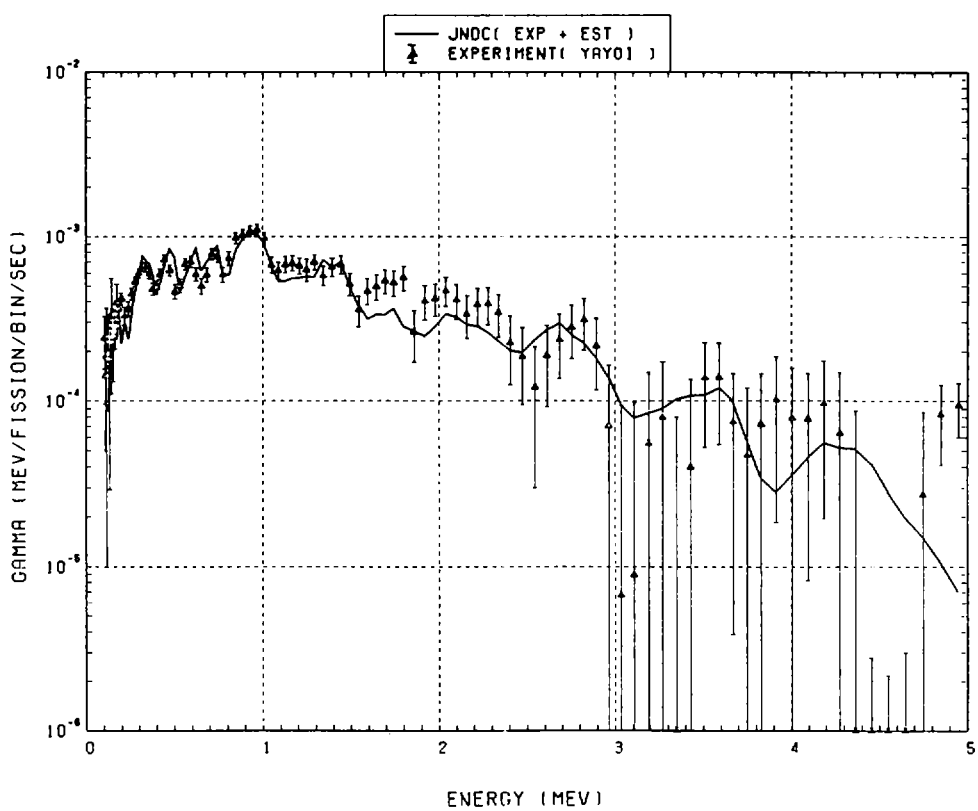

Fig. 134 Comparison of calculated gamma-ray energy spectrum with measured results at 290 seconds after fast neutron fission of ^{239}Pu. (t_{irrad} = 10 s, t_{wait} = 255 s, t_{count} = 60 s)

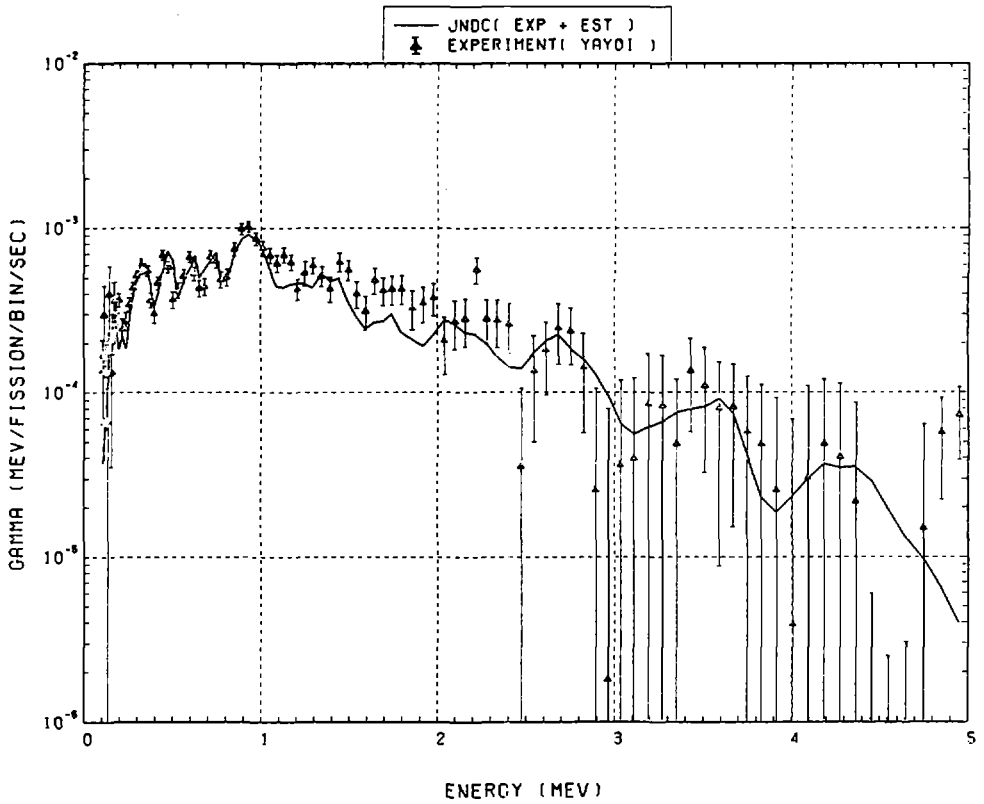

Fig. 135 Comparison of calculated gamma-ray energy spectrum with measured results at 360 seconds after fast neutron fission of ^{239}Pu. (t_{irrad} = 10 s, t_{wait} = 315 s, t_{count} = 80 s)

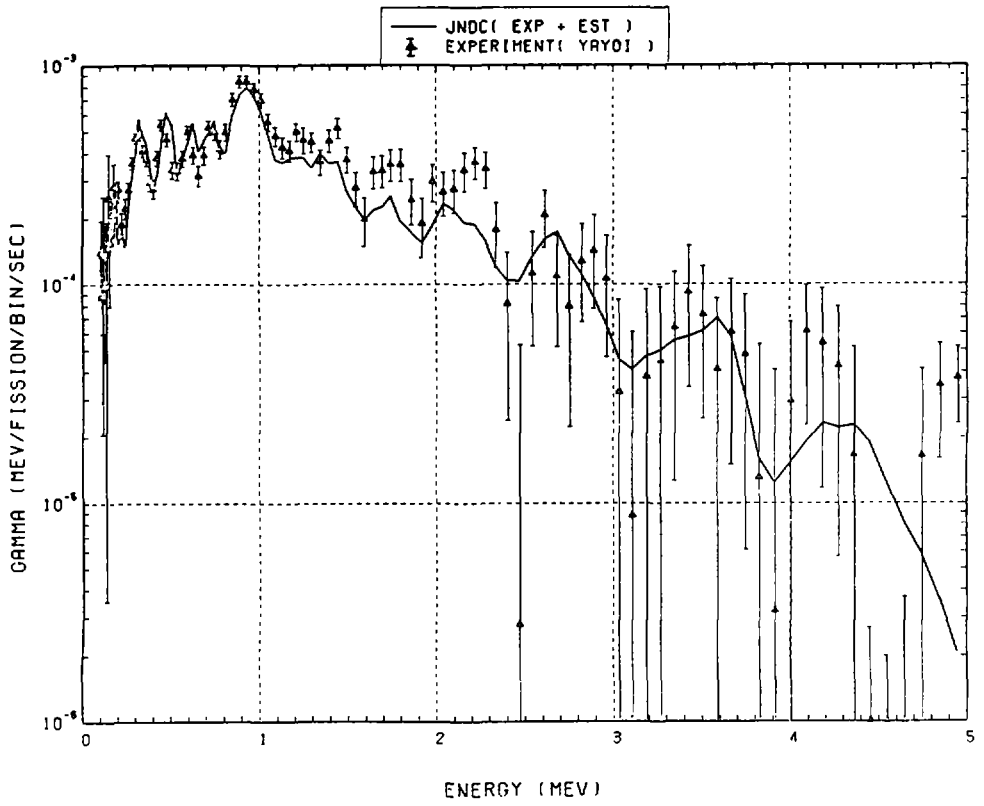

Fig. 136 Comparison of calculated gamma-ray energy spectrum with measured results at 450 seconds after fast neutron fission of ^{239}Pu. (t_{irrad} = 10 s, t_{wait} = 395 s, t_{count} = 100 s)

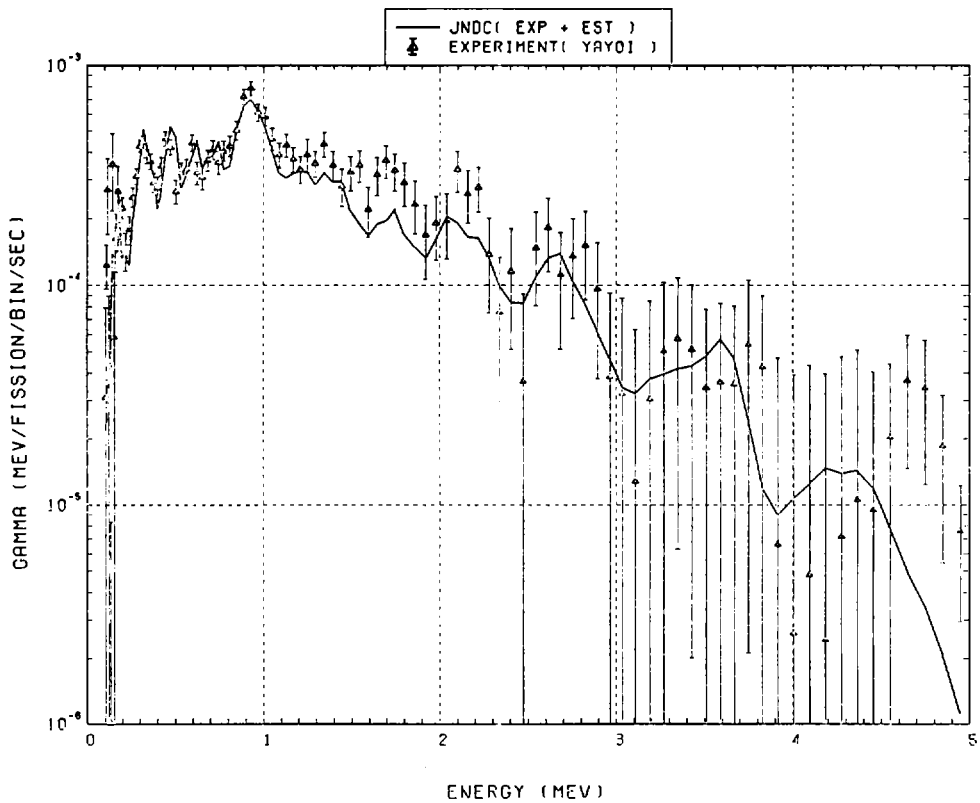

Fig. 137 Comparison of calculated gamma-ray energy spectrum with measured results at 550 seconds after fast neutron fission of ^{239}Pu. (t_{irrad} = 10 s, t_{wait} = 495 s, t_{count} = 100 s)

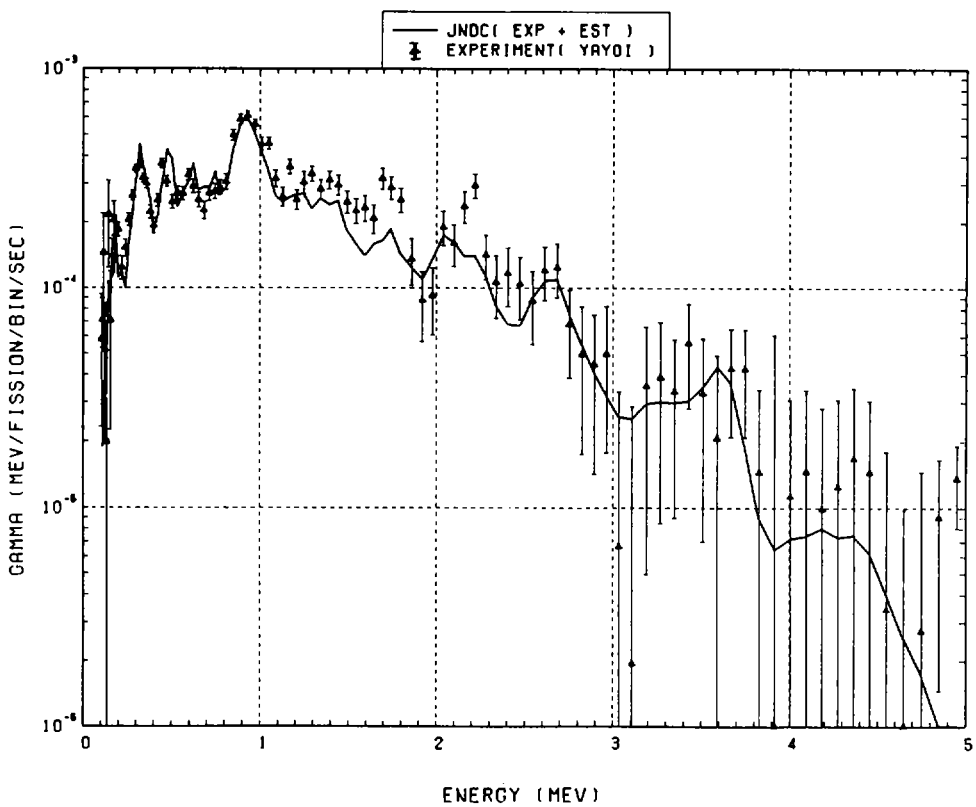

Fig. 138 Comparison of calculated gamma-ray energy spectrum with measured results at 700 seconds after fast neutron fission of ^{239}Pu. (t_{irrad} = 10 s, t_{wait} = 595 s, t_{count} = 200 s)

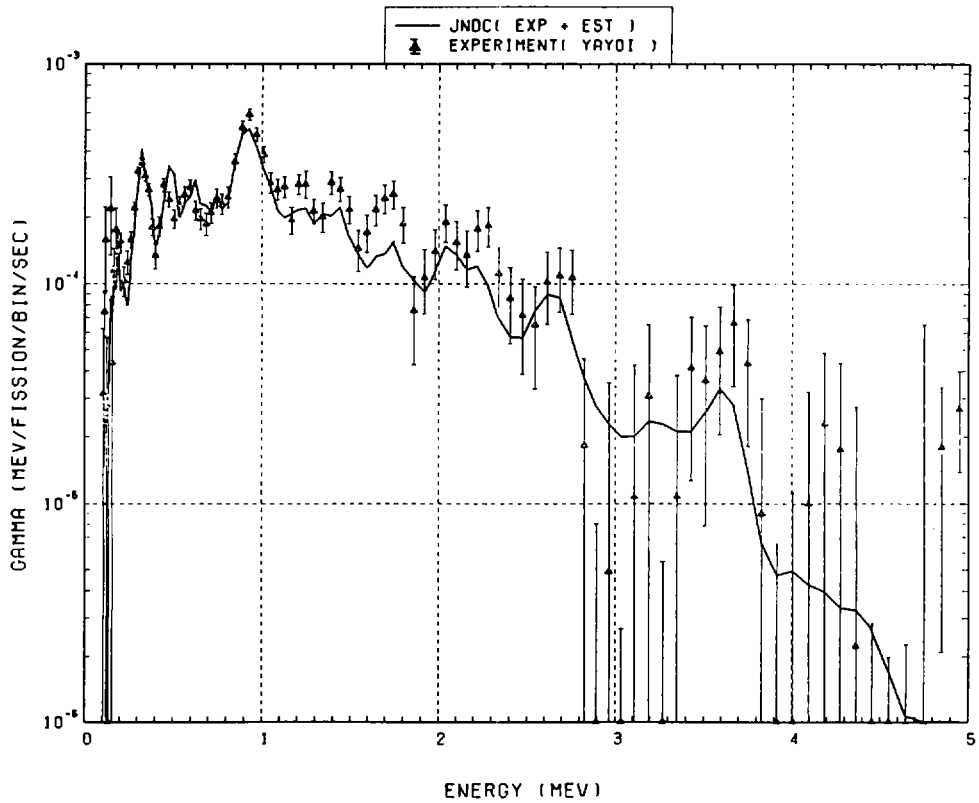

Fig. 139 Comparison of calculated gamma-ray energy spectrum with measured results at 900 seconds after fast neutron fission of ^{239}Pu. (t_{irrad} = 10 s, t_{wait} = 795 s, t_{count} = 200 s)

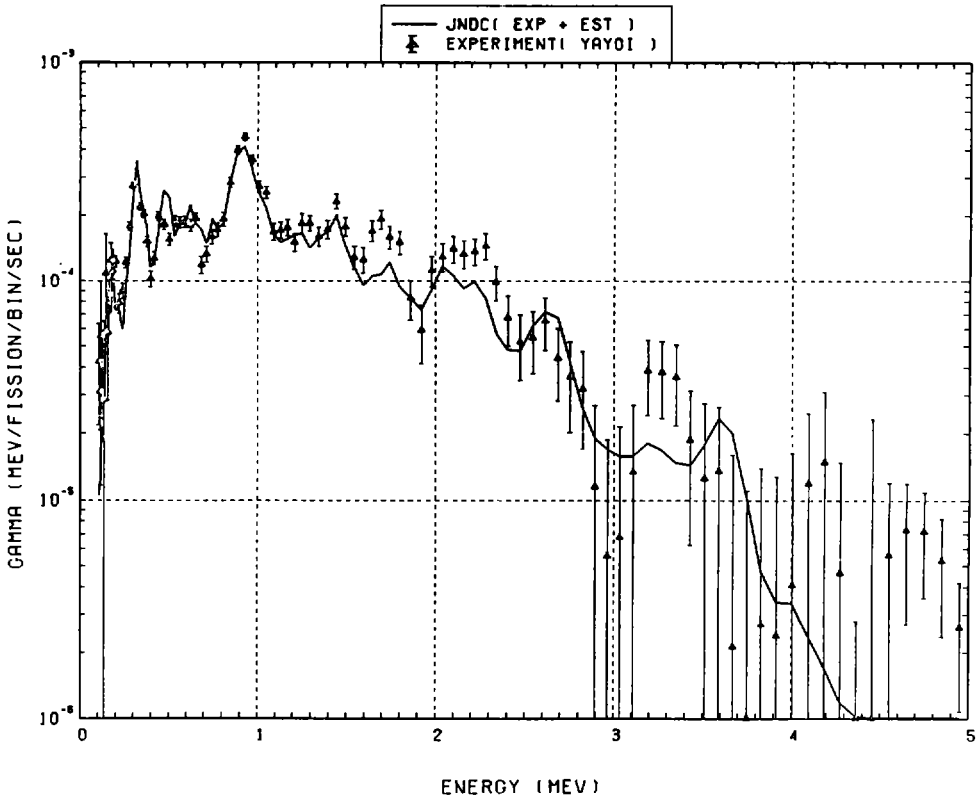

Fig. 140 Comparison of calculated gamma-ray energy spectrum with measured results at 1200 seconds after fast neutron fission of ^{239}Pu. (t_{irrad} = 10 s, t_{wait} = 995 s, t_{count} = 400 s)

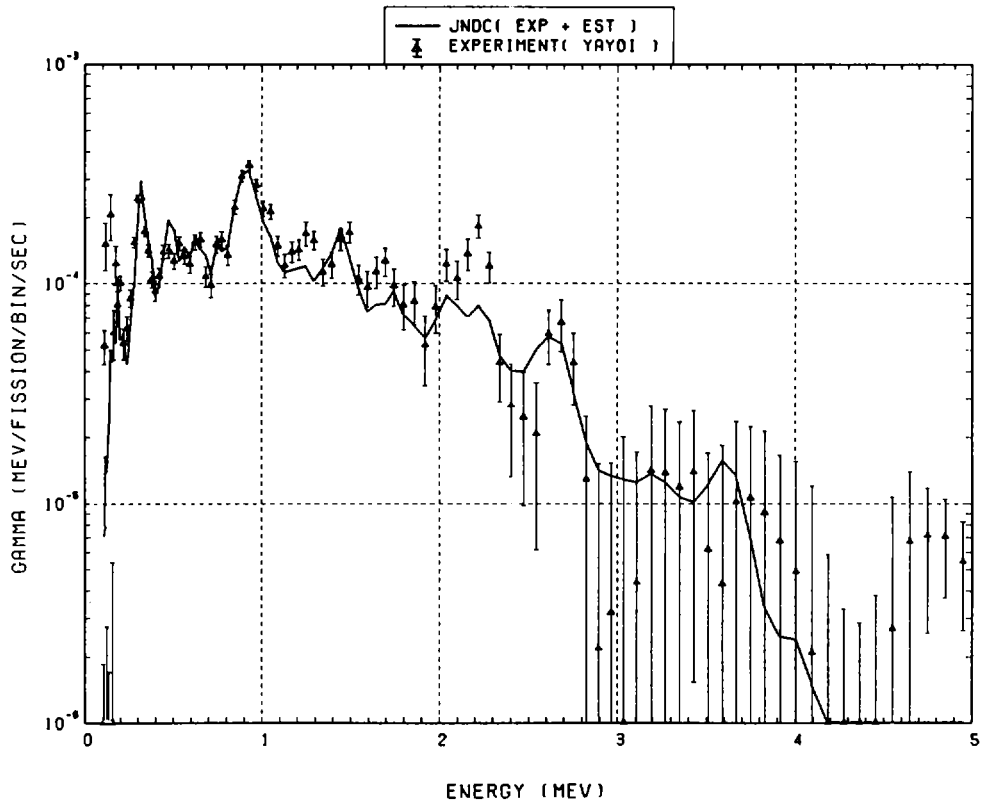

Fig. 141 Comparison of calculated gamma-ray energy spectrum with measured results at 1600 seconds after fast neutron fission of ^{239}Pu. (t_{irrad} = 10 s, t_{wait} = 1395 s, t_{count} = 400 s)

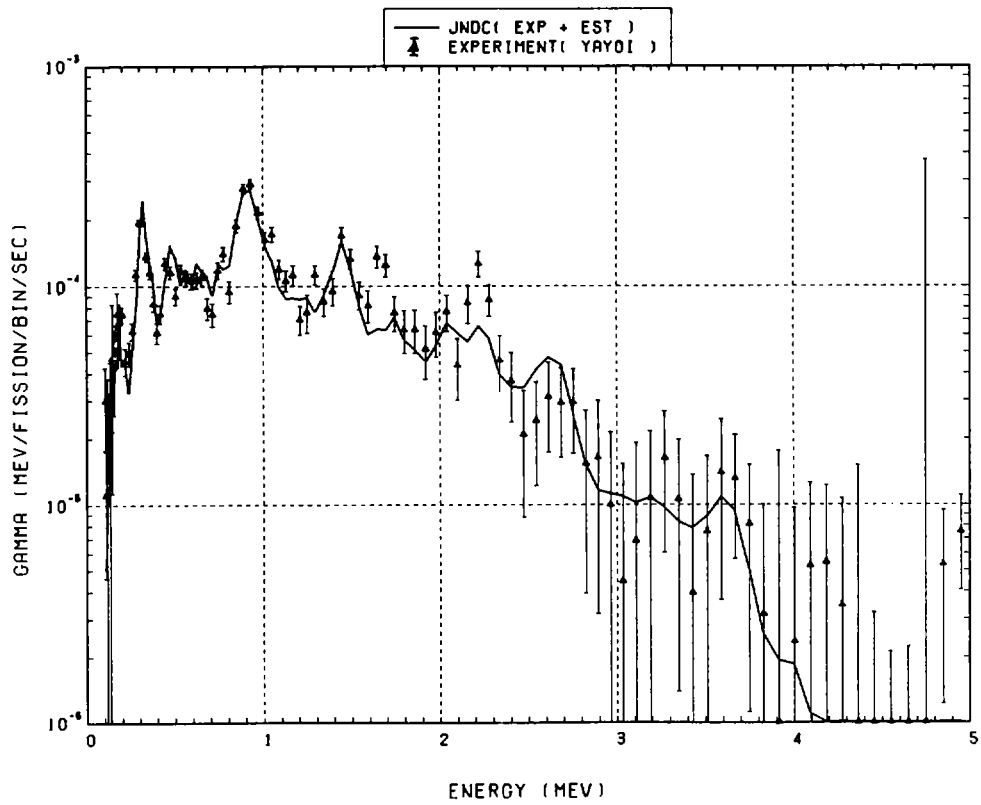

Fig. 142 Comparison of calculated gamma-ray energy spectrum with measured results at 2000 seconds after fast neutron fission of ^{239}Pu. (t_{irrad} = 10 s, t_{wait} = 1795 s, t_{count} = 400 s)

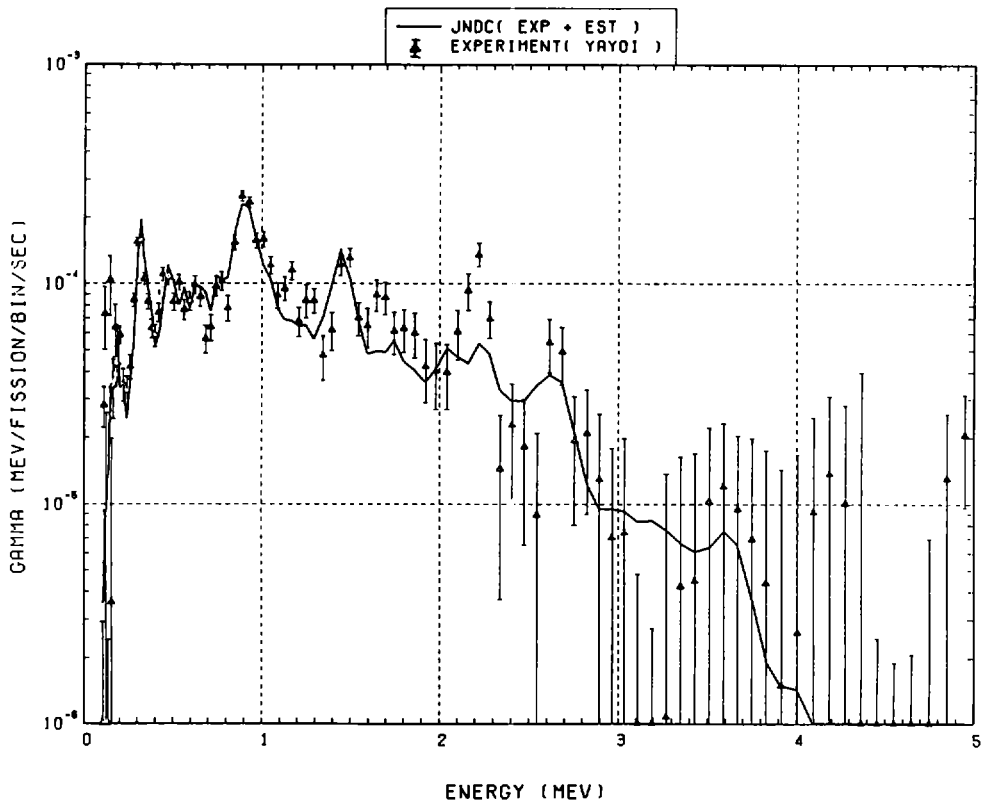

Fig. 143 Comparison of calculated gamma-ray energy spectrum with measured results at 2450 seconds after fast neutron fission of ^{239}Pu. (t_{irrad} = 10 s, t_{wait} = 2195 s, t_{count} = 500 s)

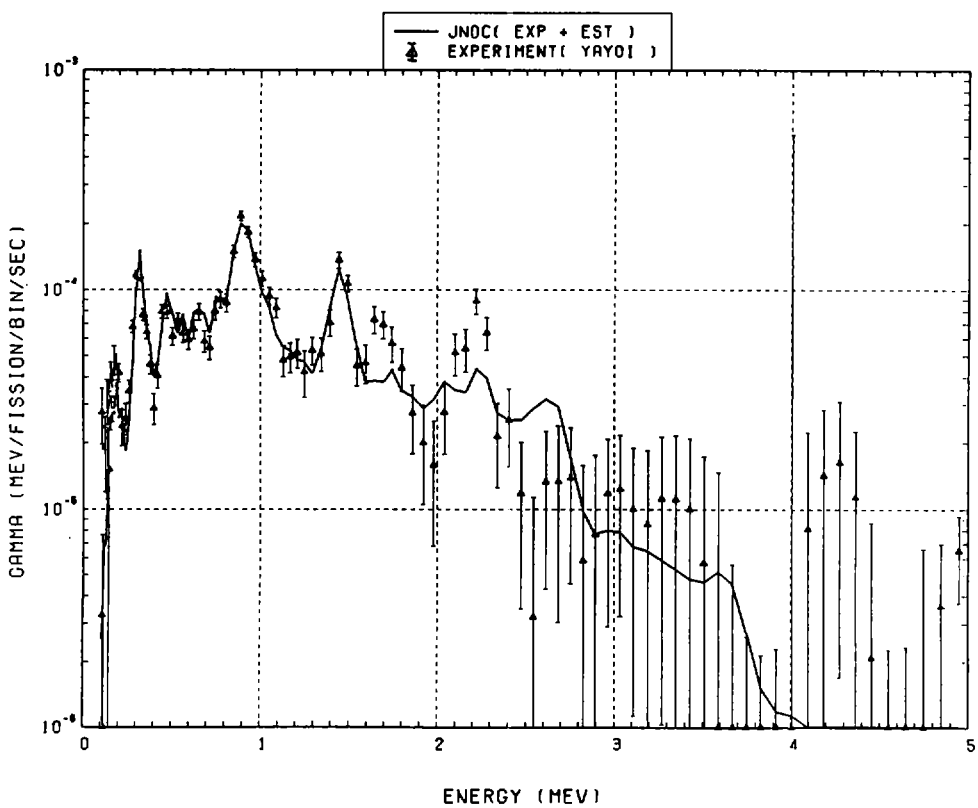

Fig. 144 Comparison of calculated gamma-ray energy spectrum with measured results at 2950 seconds after fast neutron fission of ^{239}Pu. (t_{irrad} = 10 s, t_{wait} = 2695 s, t_{count} = 500 s)

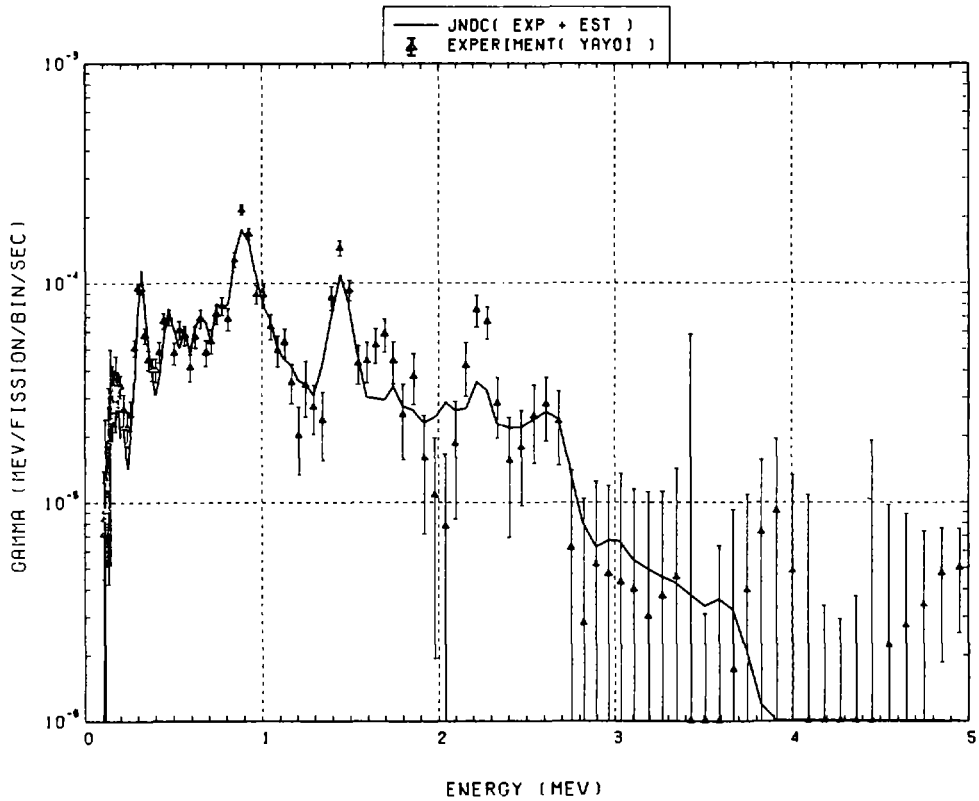

Fig. 145 Comparison of calculated gamma-ray energy spectrum with measured results at 3500 seconds after fast neutron fission of ^{239}Pu. (t_{irrad} = 10 s, t_{wait} = 3195 s, t_{count} = 600 s)

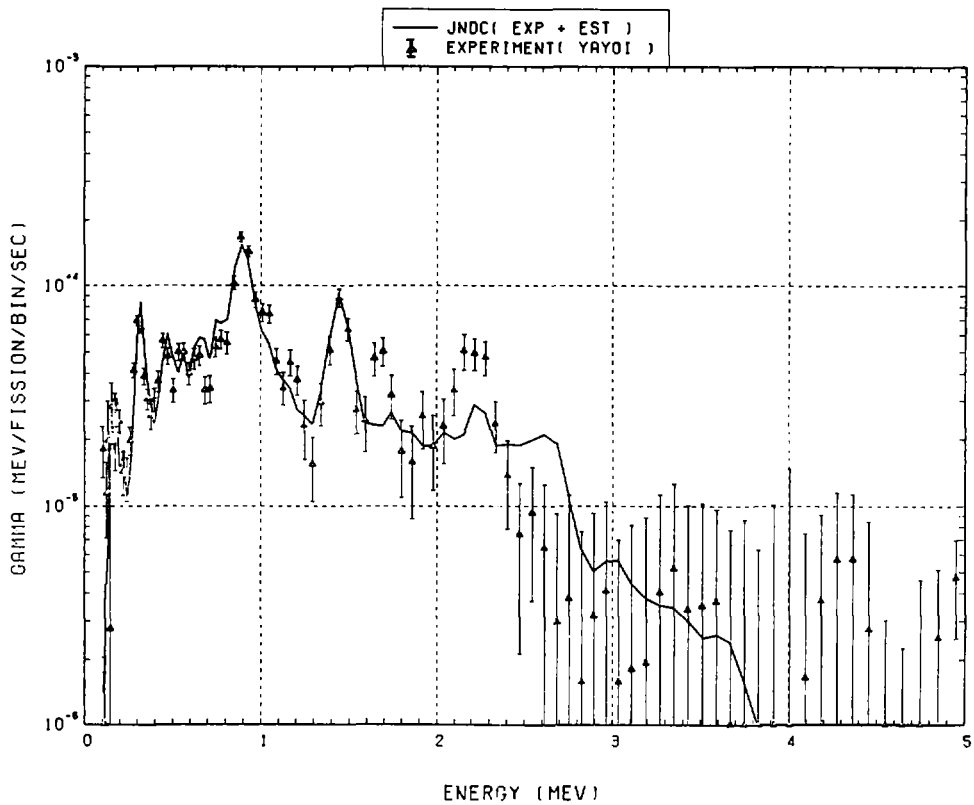

Fig. 146 Comparison of calculated gamma-ray energy spectrum with measured results at 4100 seconds after fast neutron fission of ^{239}Pu. (t_{irrad} = 10 s, t_{wait} = 3795 s, t_{count} = 600 s)

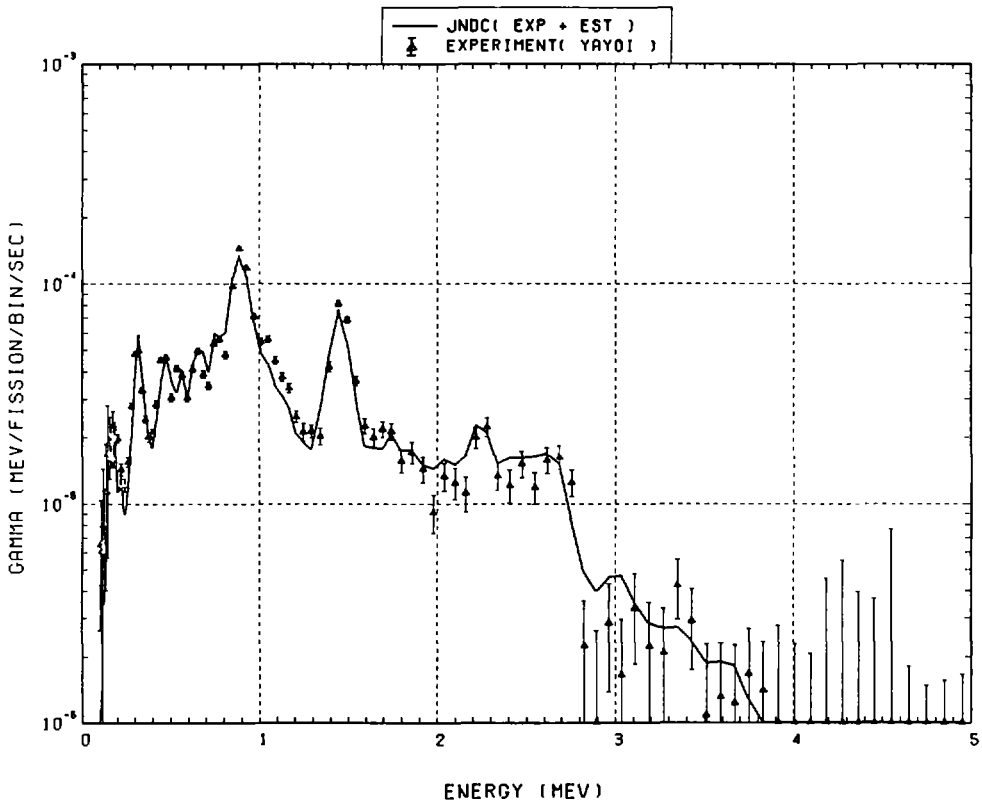

Fig. 147 Comparison of calculated gamma-ray energy spectrum with measured results at 4800 seconds after fast neutron fission of ^{239}Pu. (t_{irrad} = 100 s, t_{wait} = 4350 s, t_{count} = 800 s)

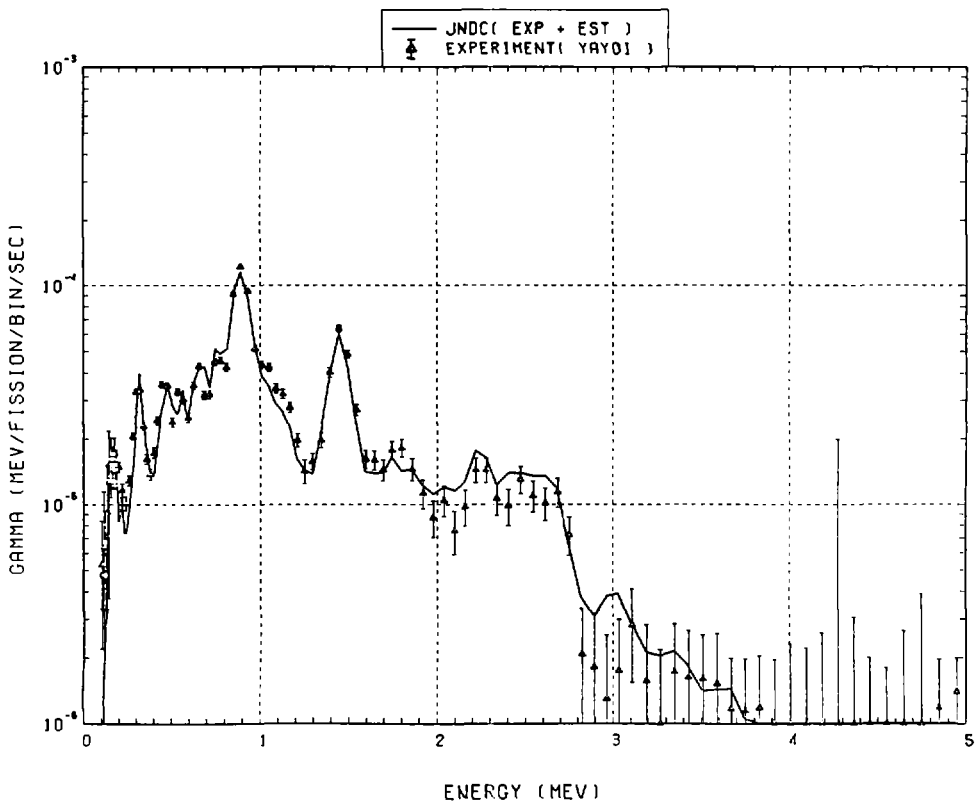

Fig. 148 Comparison of calculated gamma-ray energy spectrum with measured results at 5600 seconds after fast neutron fission of ^{239}Pu. (t_{irrad} = 100 s, t_{wait} = 5150 s, t_{count} = 800 s)

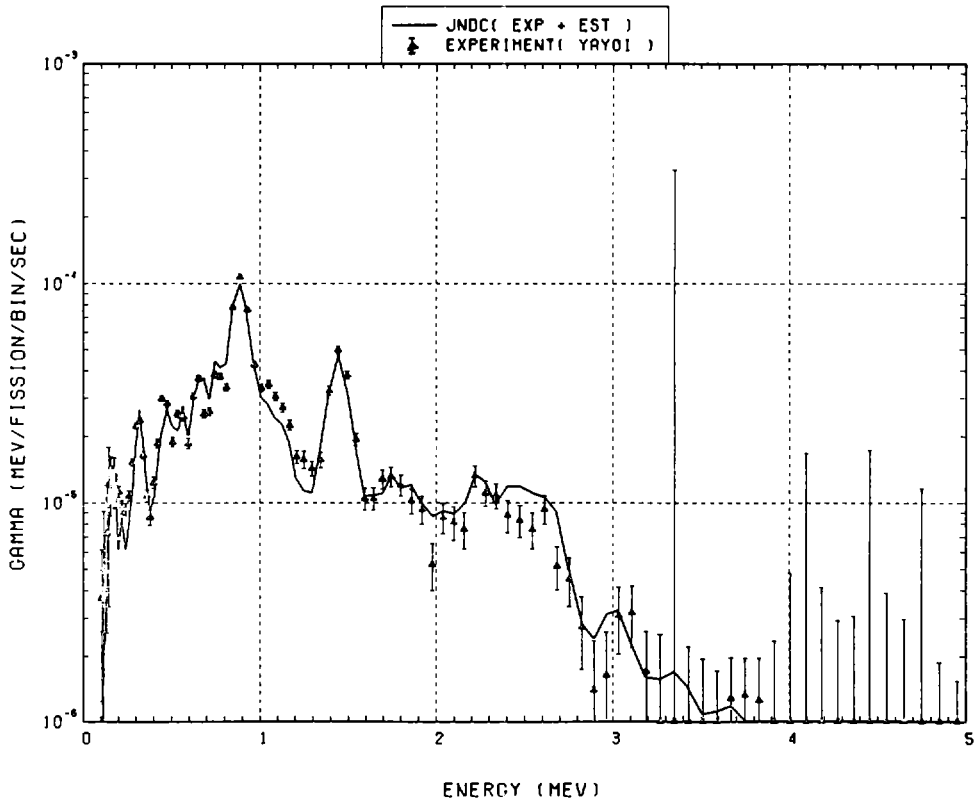

Fig. 149 Comparison of calculated gamma-ray energy spectrum with measured results at 6500 seconds after fast neutron fission of ^{239}Pu. (t_{irrad} = 100 s, t_{wait} = 5950 s, t_{count} = 1000 s)

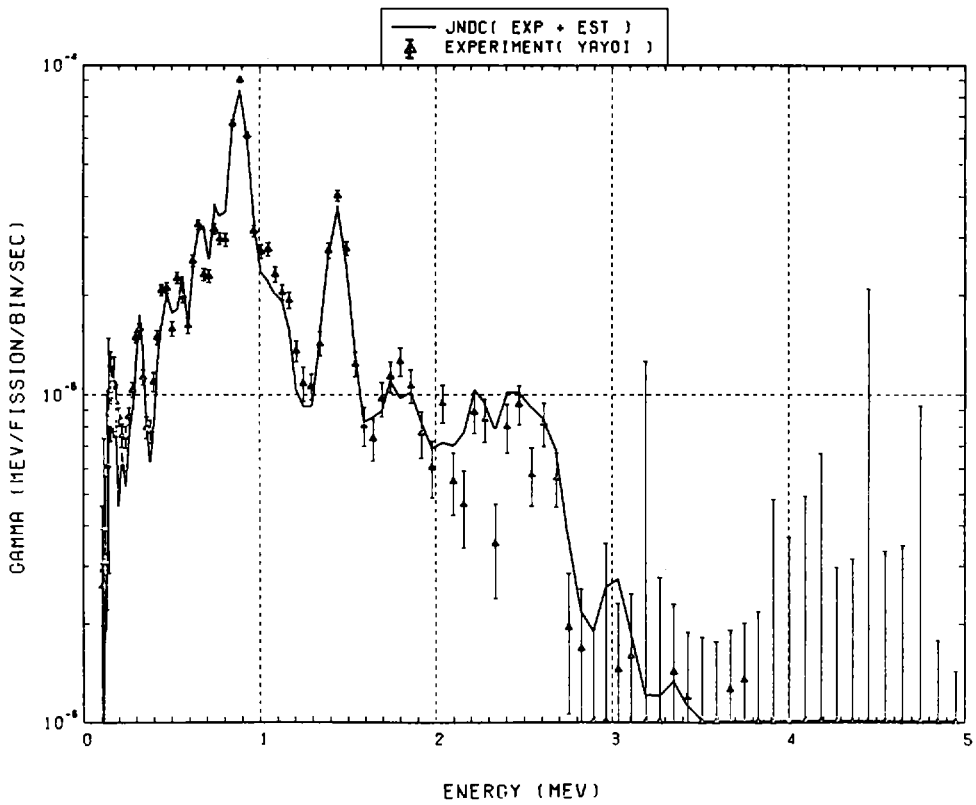

Fig. 150 Comparison of calculated gamma-ray energy spectrum with measured results at 7500 seconds after fast neutron fission of ^{239}Pu. (t_{irrad} = 100 s, t_{wait} = 6950 s, t_{count} = 1000 s)

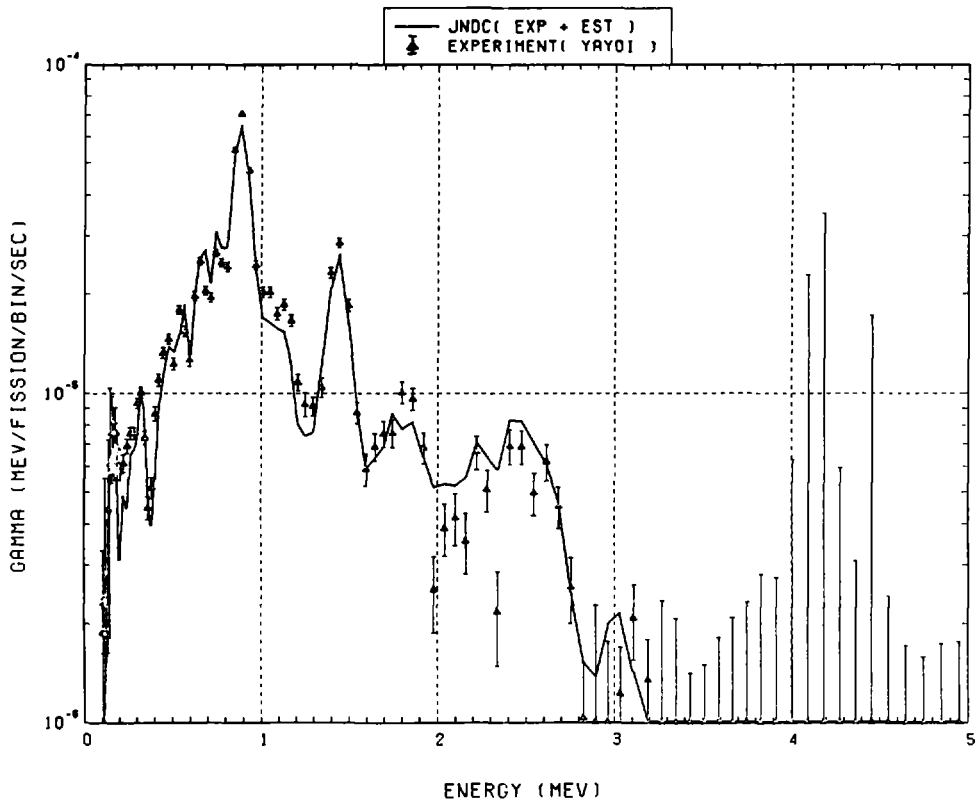

Fig. 151 Comparison of calculated gamma-ray energy spectrum with measured results at 9000 seconds after fast neutron fission of ^{239}Pu. (t_{irrad} = 100 s, t_{wait} = 7950 s, t_{count} = 2000 s)

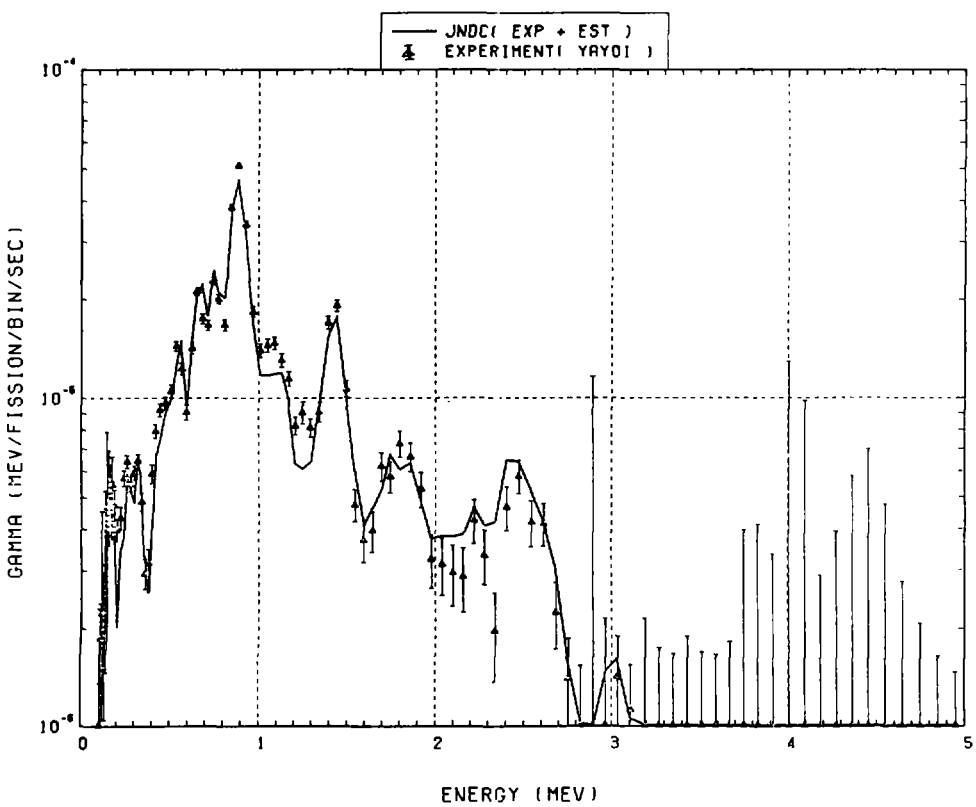

Fig. 152 Comparison of calculated gamma-ray energy spectrum with measured results at 11000 seconds after fast neutron fission of ^{239}Pu. (t_{irrad} = 100 s, t_{wait} = 9950 s, t_{count} = 2000 s)

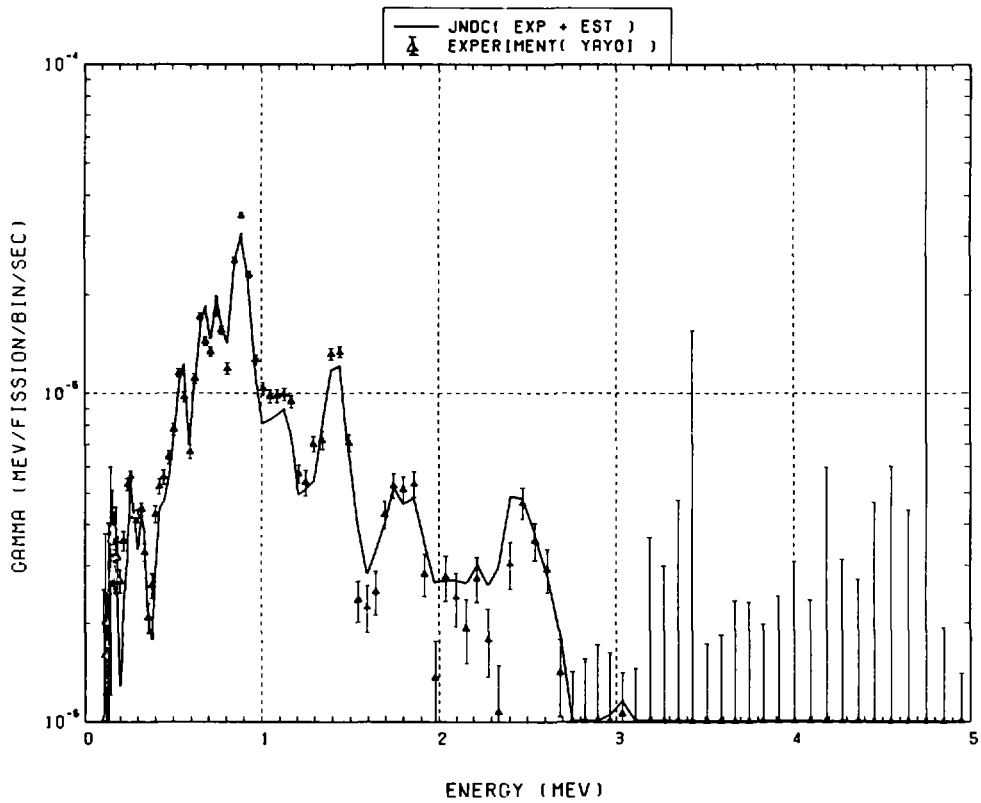

Fig. 153 Comparison of calculated gamma-ray energy spectrum with measured results at 13500 seconds after fast neutron fission of ^{239}Pu. (t_{irrad} = 100 s, t_{wait} = 11950 s, t_{count} = 3000 s)

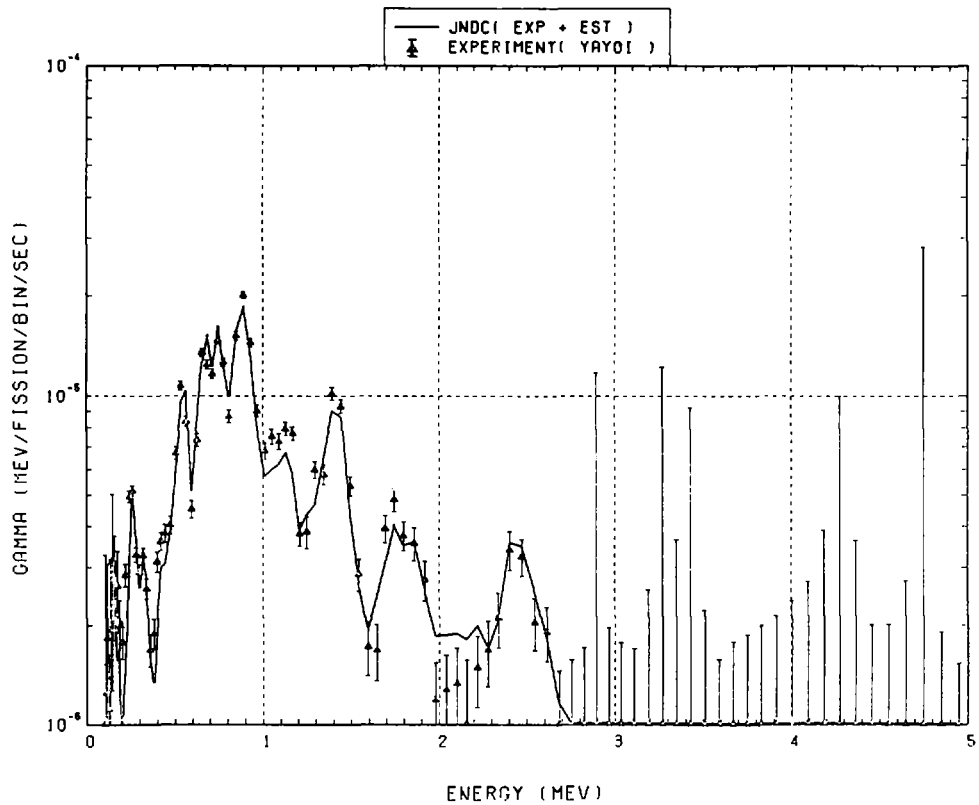

Fig. 154 Comparison of calculated gamma-ray energy spectrum with measured results at 16500 seconds after fast neutron fission of ^{239}Pu. (t_{irrad} = 100 s, t_{wait} = 14950 s, t_{count} = 3000 s)

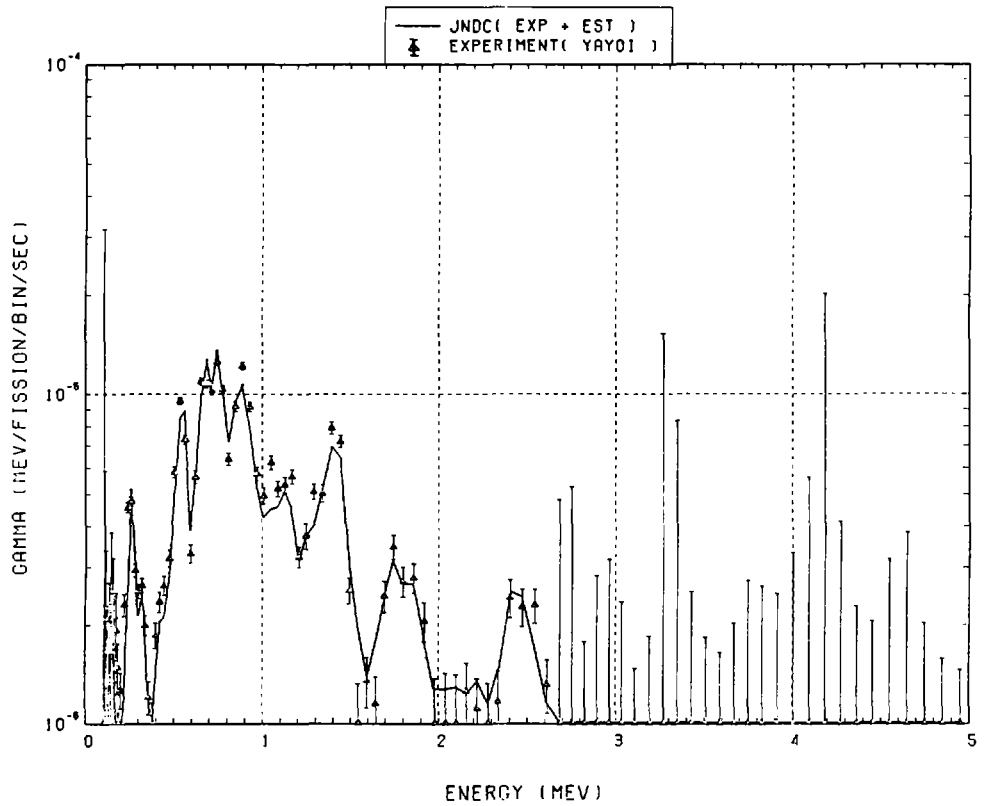

Fig. 155 Comparison of calculated gamma-ray energy spectrum with measured results at 20000 seconds after fast neutron fission of ^{239}Pu. (t_{irrad} = 100 s, t_{wait} = 17950 s, t_{count} = 4000 s)

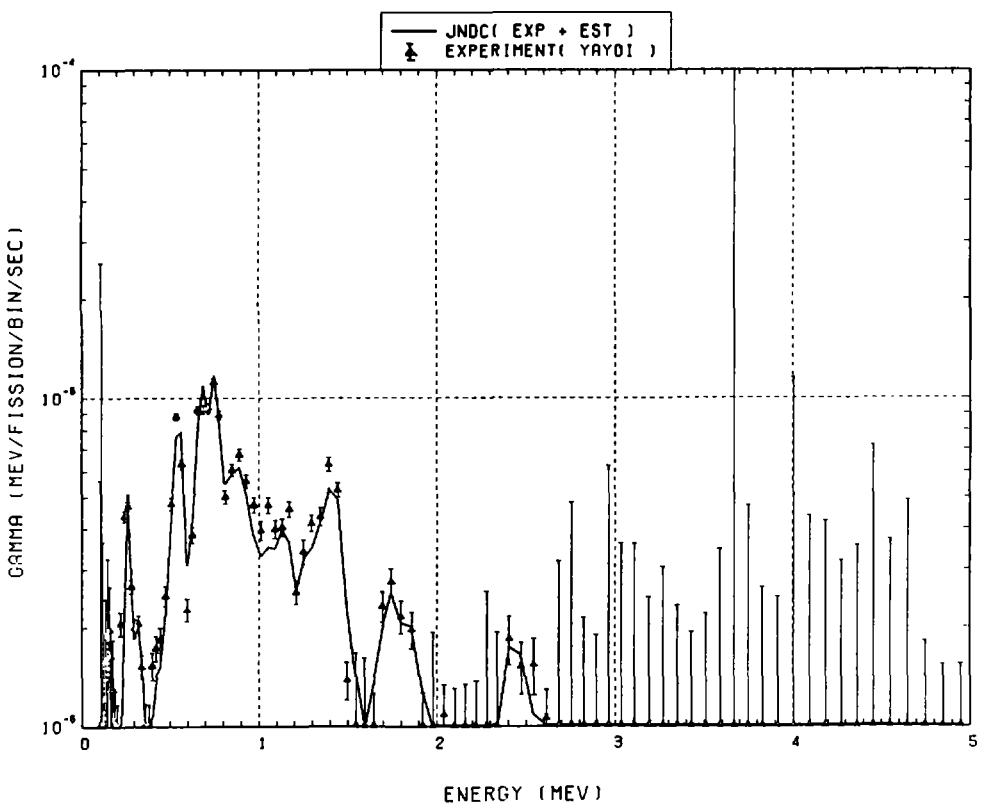

Fig. 156 Comparison of calculated gamma-ray energy spectrum with measured results at 24000 seconds after fast neutron fission of ^{239}Pu. (t_{irrad} = 100 s, t_{wait} = 21950 s, t_{count} = 4000 s)

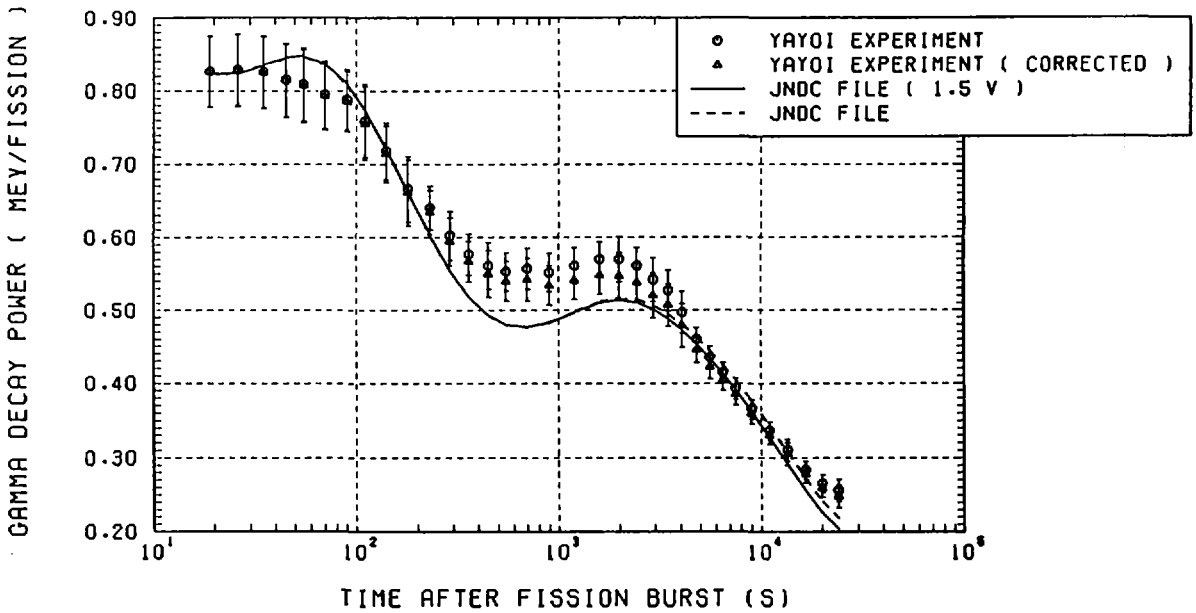

Fig. 157 Comparison of calculated gamma-decay heat with measured results at YAYOI for fast neutron fission of ^{238}U.

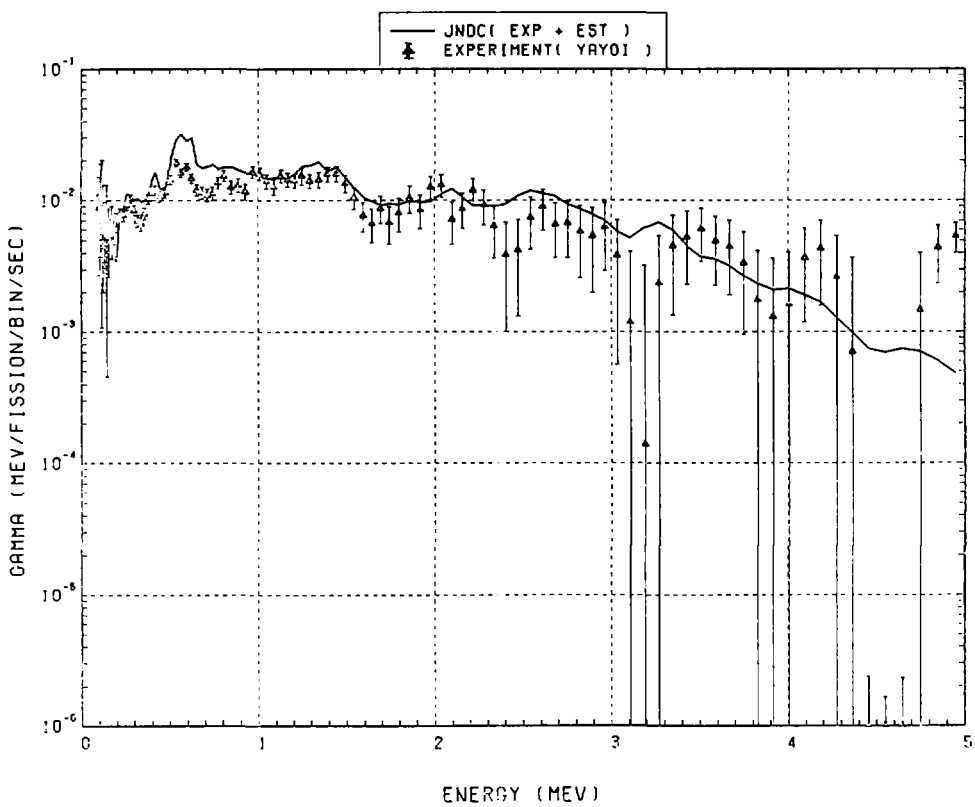

Fig. 158 Comparison of calculated gamma-ray energy spectrum with measured results at 19 seconds after fast neutron fission of ^{238}U. (t_{irrad} = 10 s, t_{wait} = 11 s, t_{count} = 6 s)

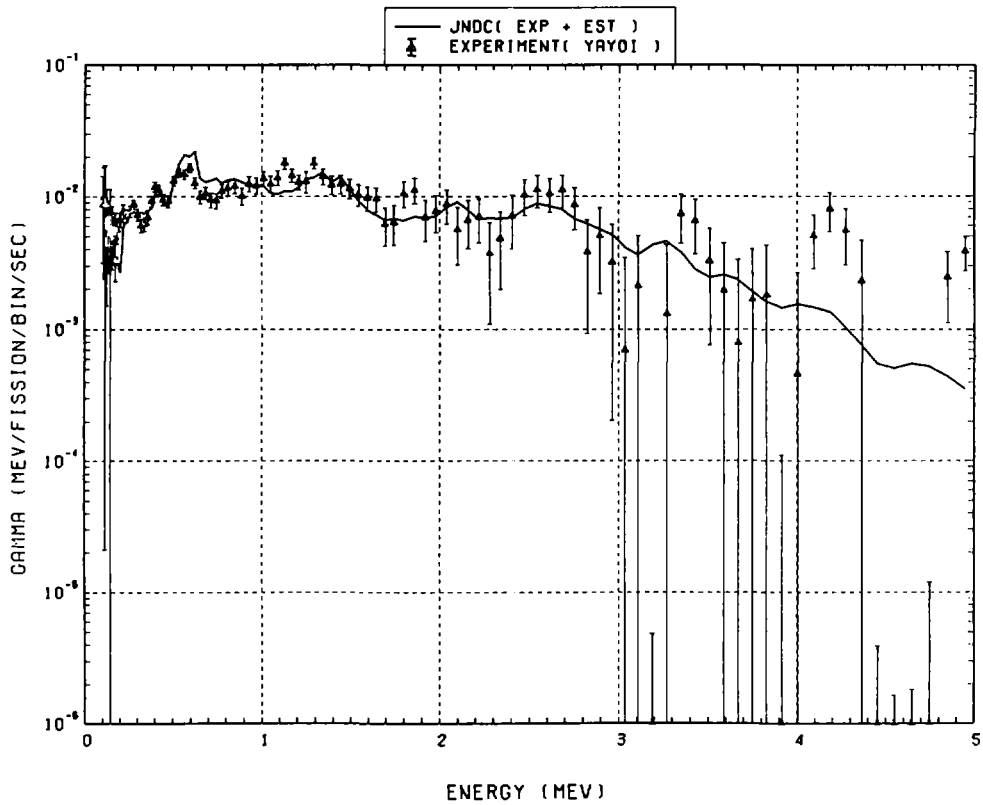

Fig. 159 Comparison of calculated gamma-ray energy spectrum with measured results at 26 seconds after fast neutron fission of ^{238}U. (t_{irrad} = 10 s, t_{wait} = 17 s, t_{count} = 8 s)

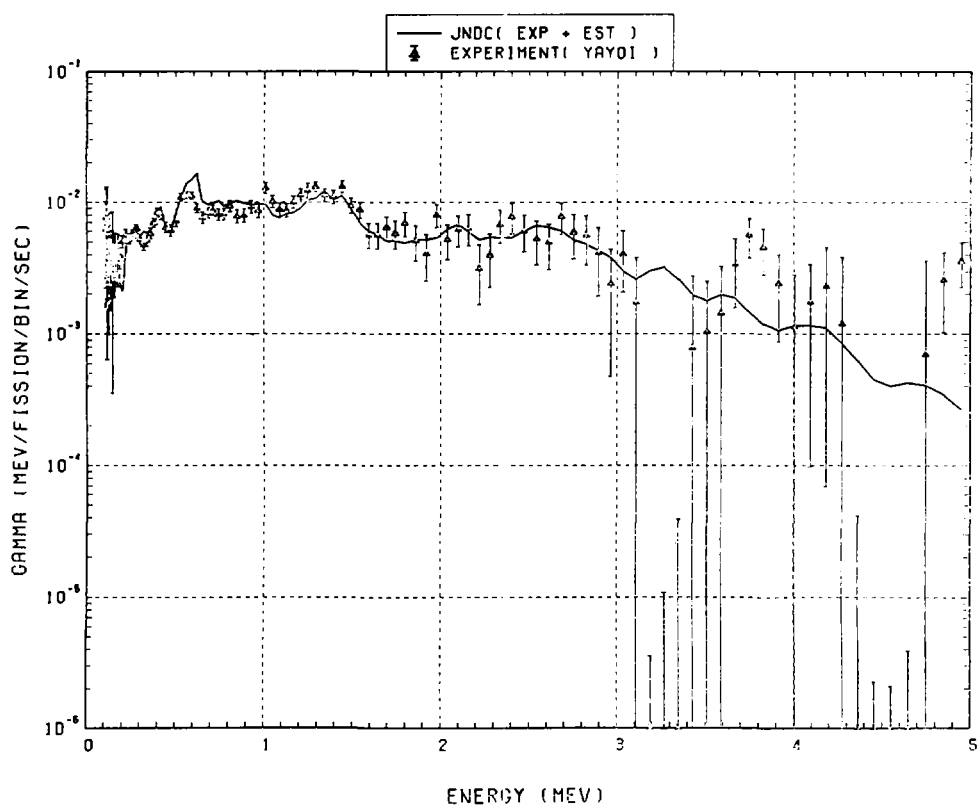

Fig. 160 Comparison of calculated gamma-ray energy spectrum with measured results at 35 seconds after fast neutron fission of ^{238}U. (t_{irrad} = 10 s, t_{wait} = 25 s, t_{count} = 10 s)

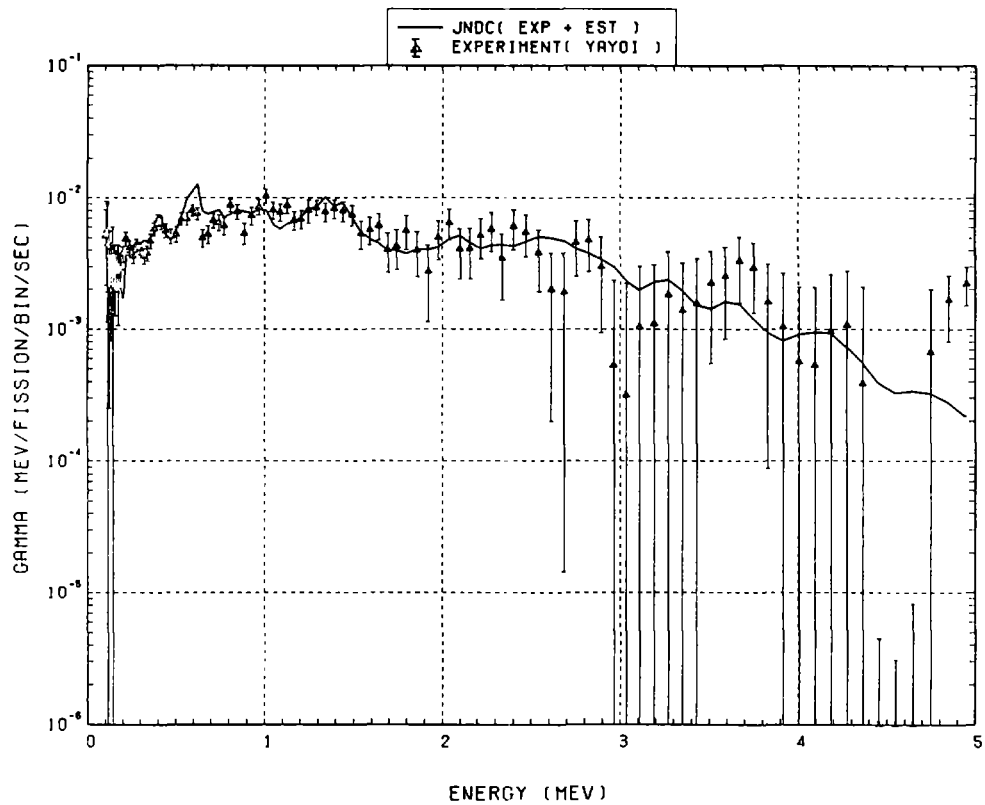

Fig. 161 Comparison of calculated gamma-ray energy spectrum with measured results at 45 seconds after fast neutron fission of ^{238}U. (t_{irrad} = 10 s, t_{wait} = 35 s, t_{count} = 10 s)

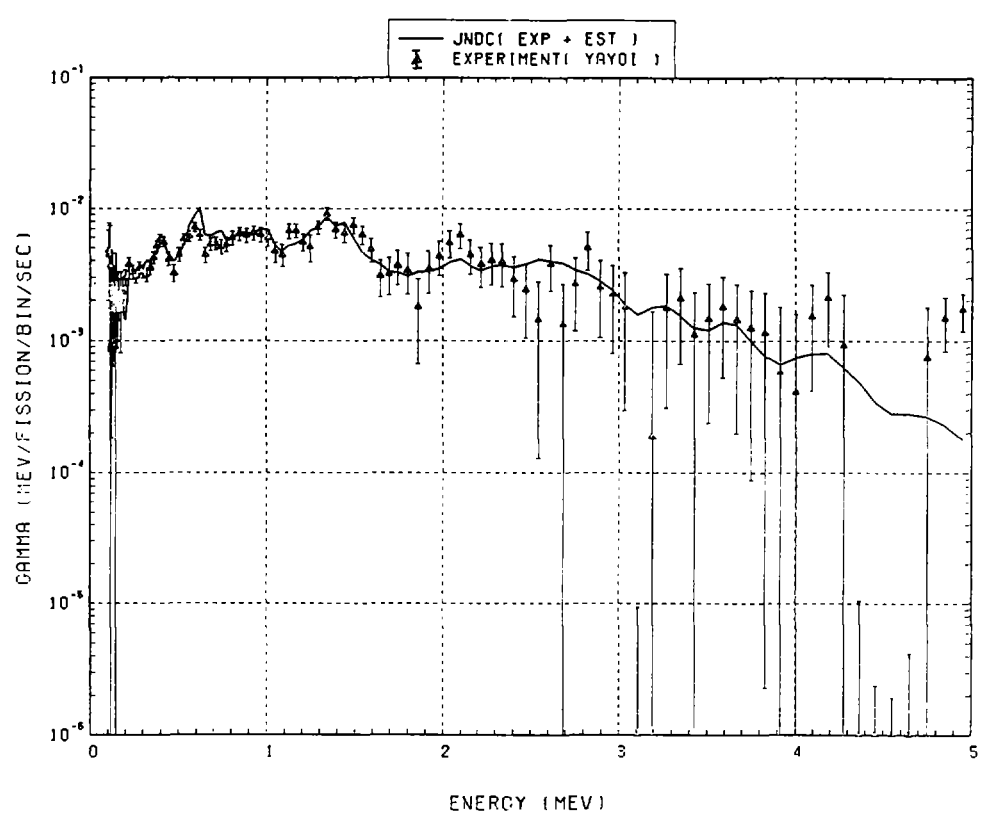

Fig. 162 Comparison of calculated gamma-ray energy spectrum with measured results at 55 seconds after fast neutron fission of ^{238}U. (t_{irrad} = 10 s, t_{wait} = 45 s, t_{count} = 10 s)

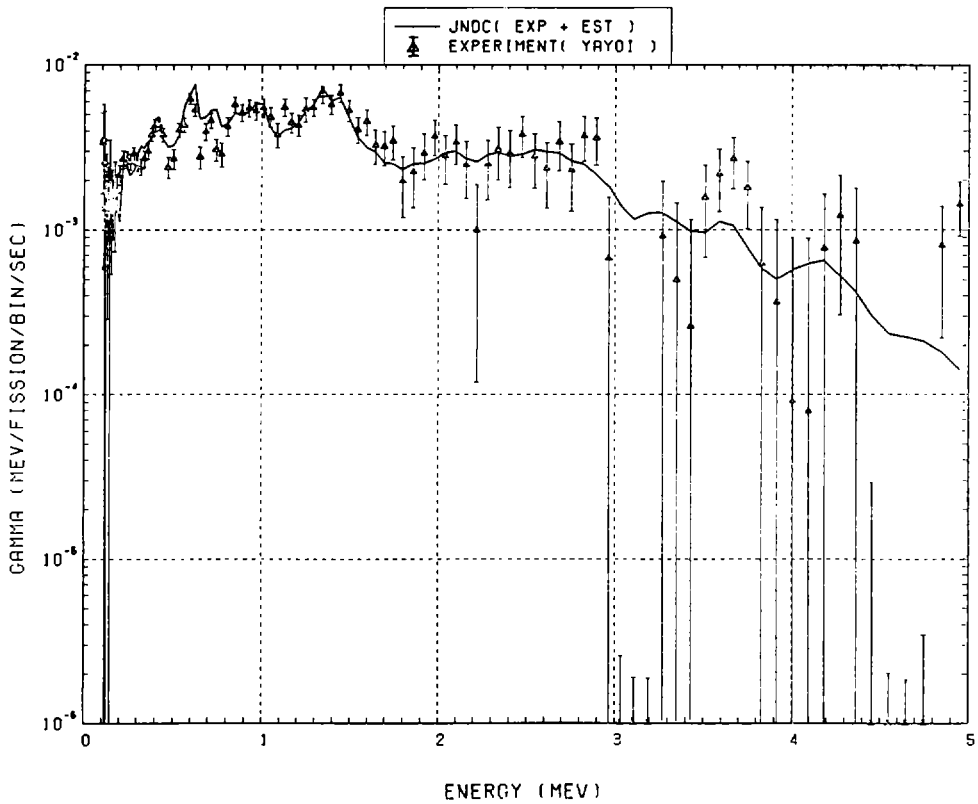

Fig. 163 Comparison of calculated gamma-ray energy spectrum with measured results at 70 seconds after fast neutron fission of ^{238}U. (t_{irrad} = 10 s, t_{wait} = 55 s, t_{count} = 20 s)

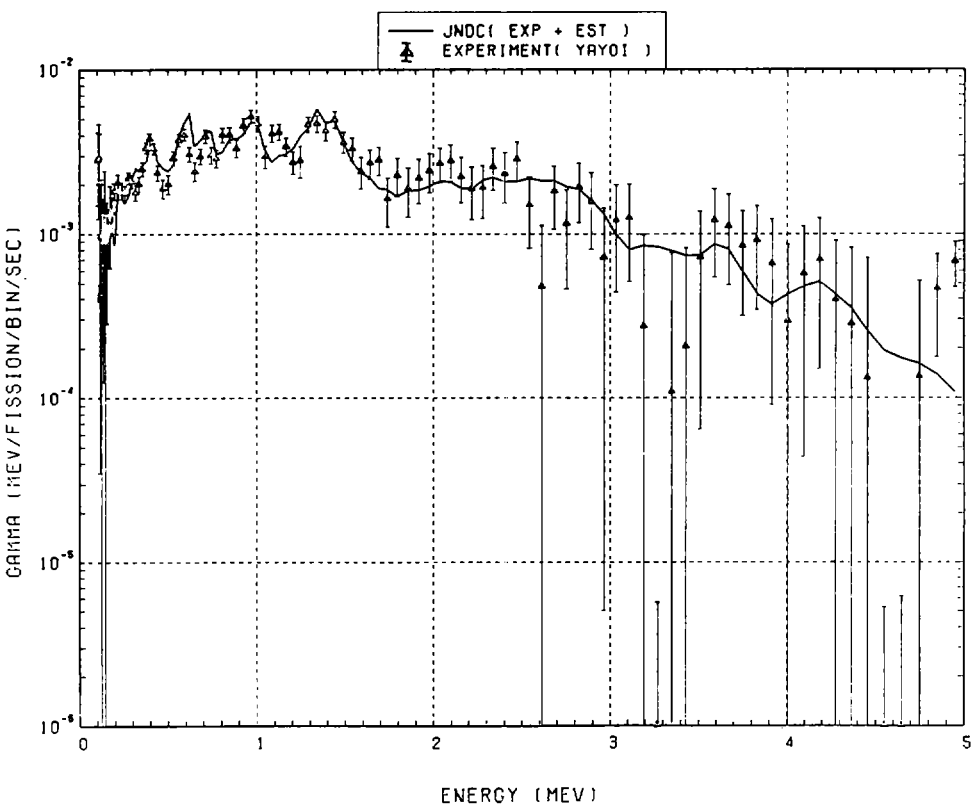

Fig. 164 Comparison of calculated gamma-ray energy spectrum with measured results at 90 seconds after fast neutron fission of ^{238}U. (t_{irrad} = 10 s, t_{wait} = 75 s, t_{count} = 20 s)

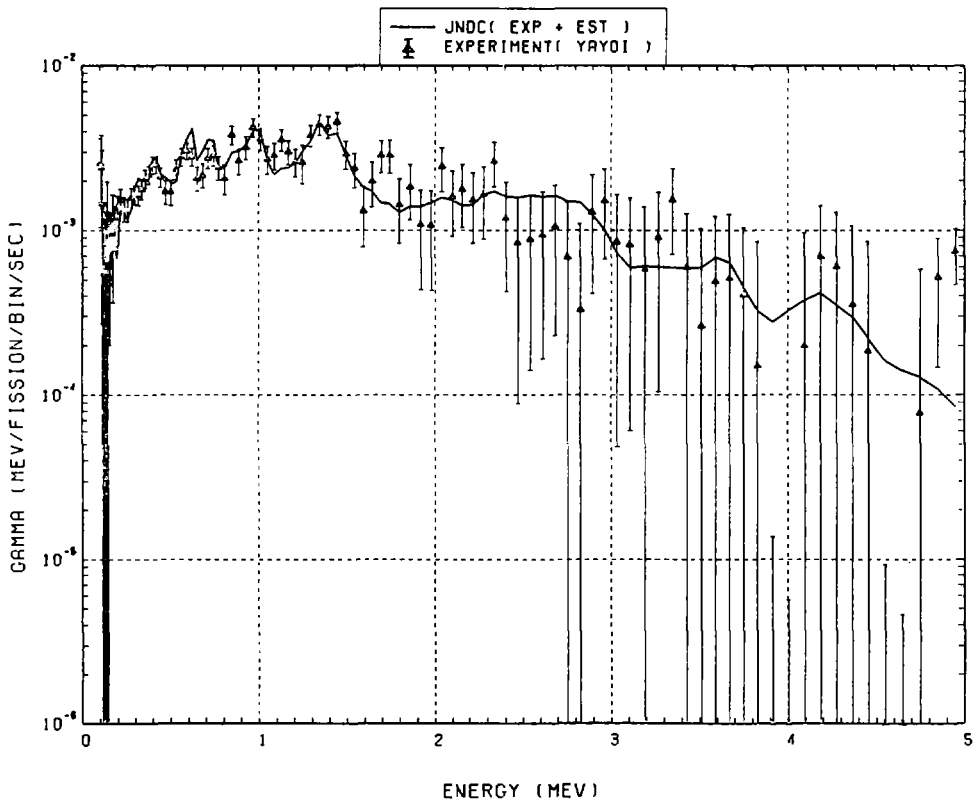

Fig. 165 Comparison of calculated gamma-ray energy spectrum with measured results at 110 seconds after fast neutron fission of ^{238}U. (t_{irrad} = 10 s, t_{wait} = 95 s, t_{count} = 20 s)

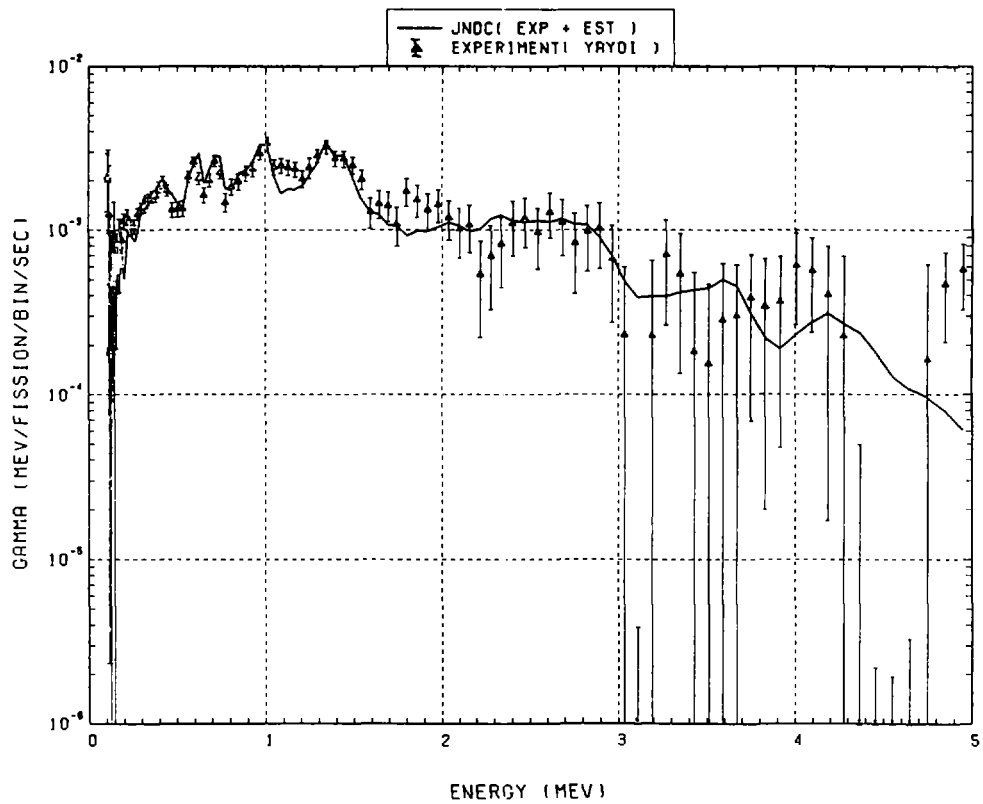

Fig. 166 Comparison of calculated gamma-ray energy spectrum with measured results at 140 seconds after fast neutron fission of ^{238}U. (t_{irrad} = 10 s, t_{wait} = 115 s, t_{count} = 40 s)

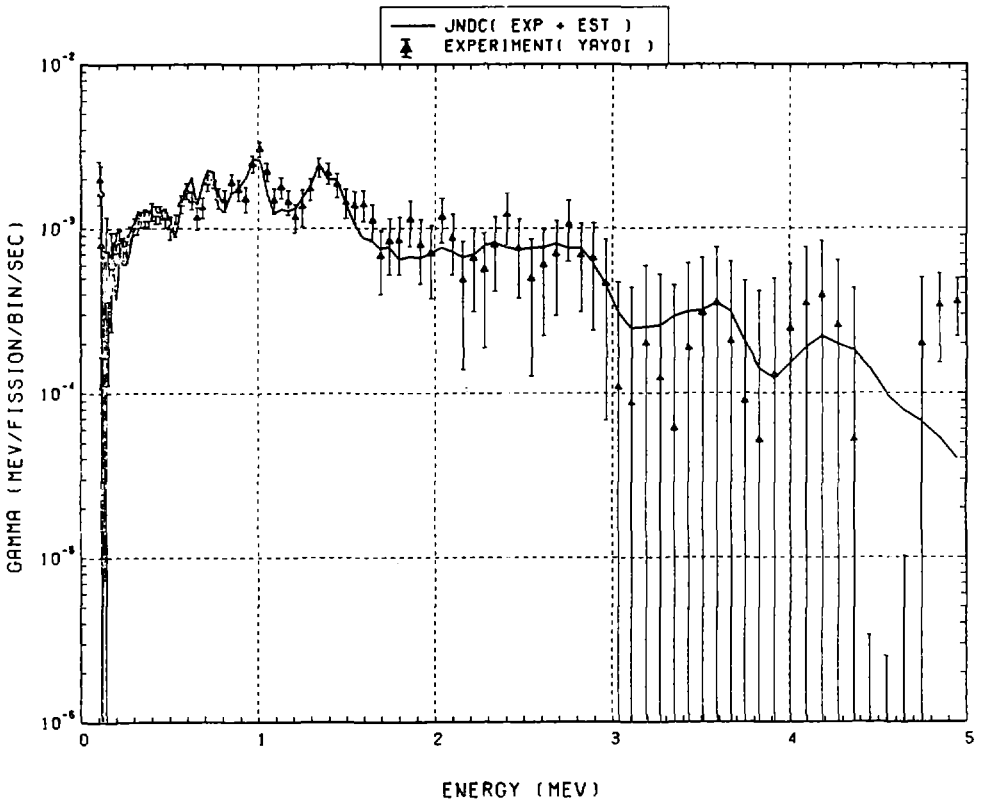

Fig. 167 Comparison of calculated gamma-ray energy spectrum with measured results at 180 seconds after fast neutron fission of ^{238}U. (t_{irrad} = 10 s, t_{wait} = 150 s, t_{count} = 40 s)

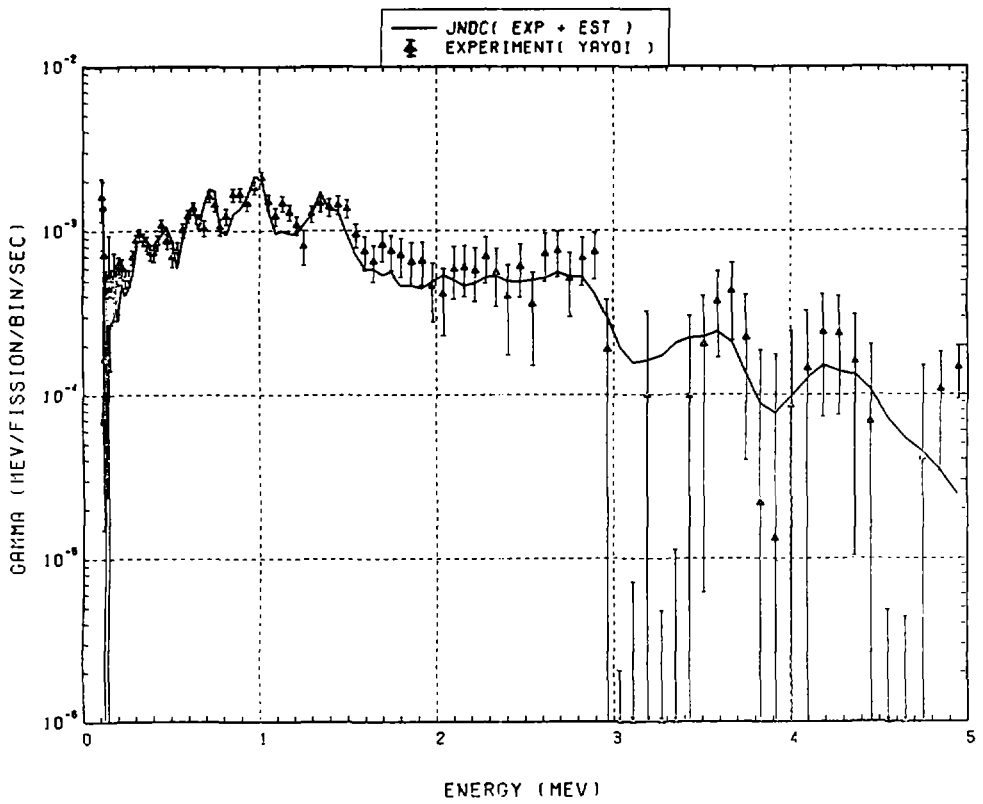

Fig. 168 Comparison of calculated gamma-ray energy spectrum with measured results at 230 seconds after fast neutron fission of ^{238}U. (t_{irrad} = 10 s, t_{wait} = 195 s, t_{count} = 60 s)

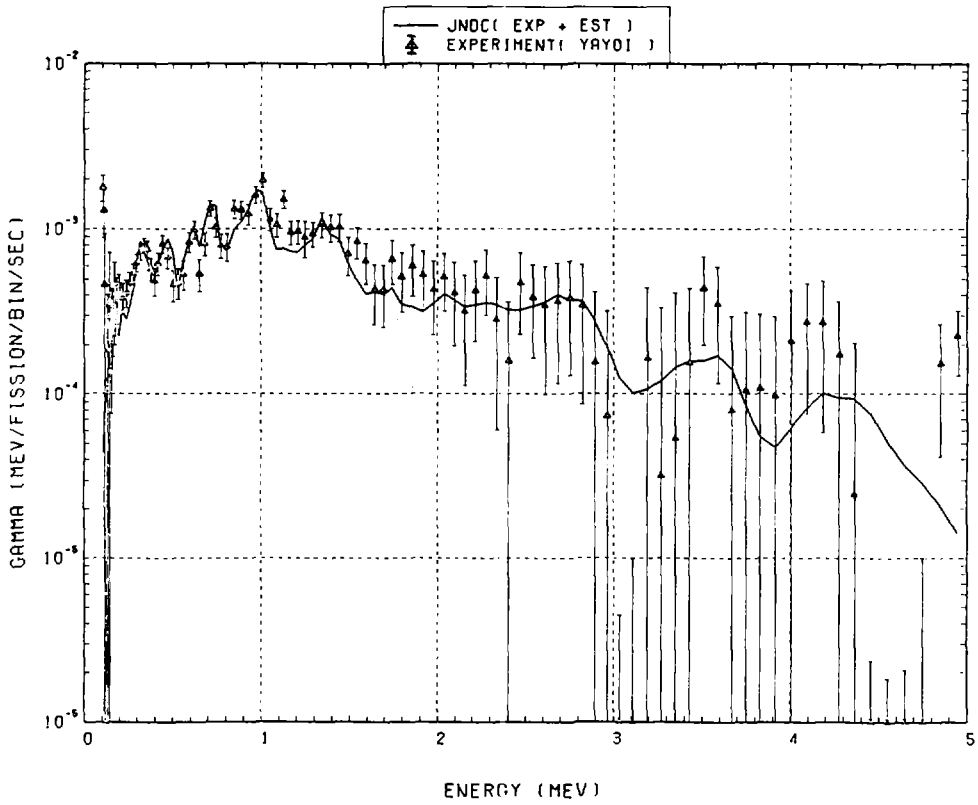

Fig. 169 Comparison of calculated gamma-ray energy spectrum with measured results at 290 seconds after fast neutron fission of ^{238}U. (t_{irrad} = 10 s, t_{wait} = 255 s, t_{count} = 60 s)

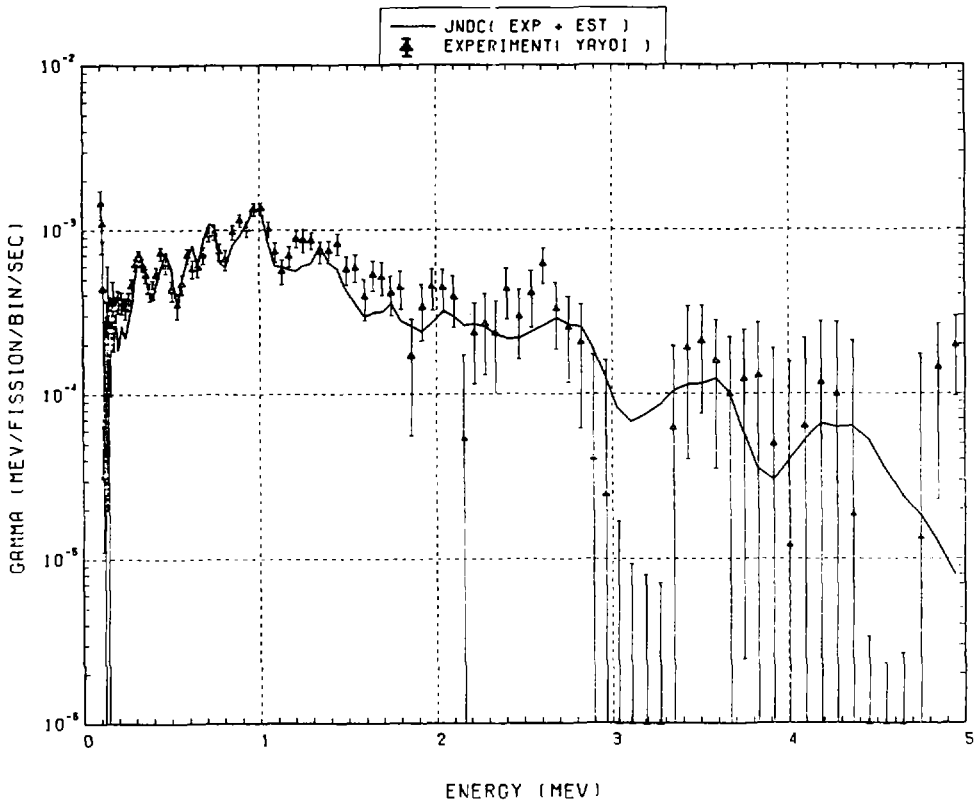

Fig. 170 Comparison of calculated gamma-ray energy spectrum with measured results at 360 seconds after fast neutron fission of ^{238}U. (t_{irrad} = 10 s, t_{wait} = 315 s, t_{count} = 80 s)

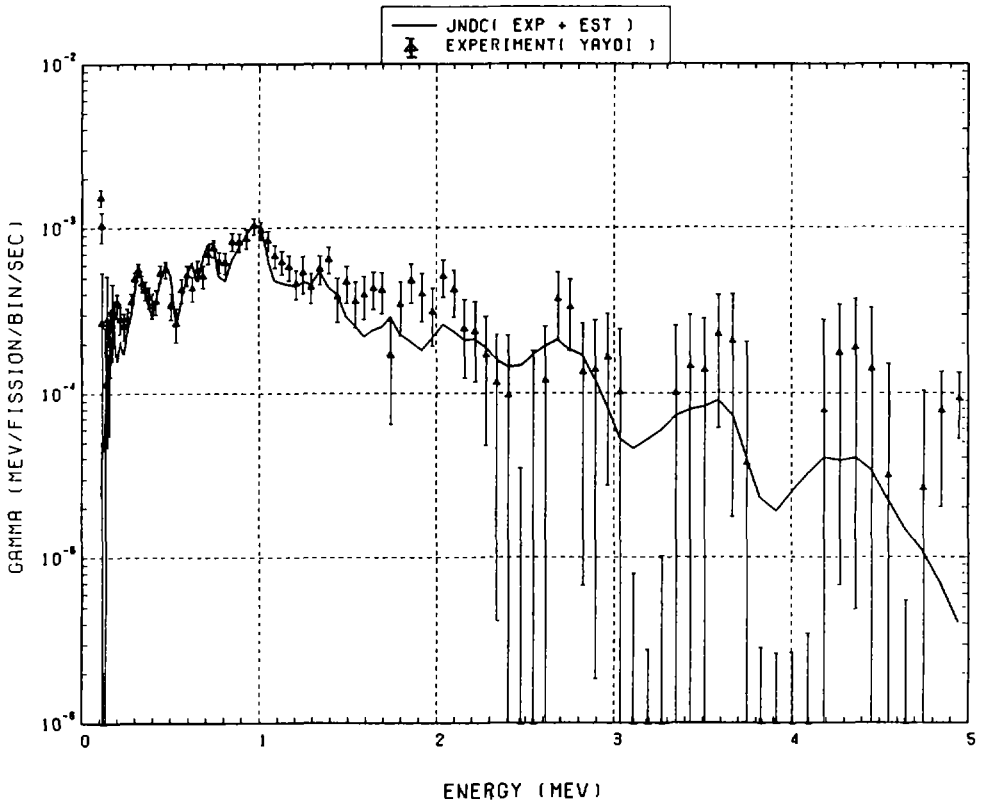

Fig. 171 Comparison of calculated gamma-ray energy spectrum with measured results at 450 seconds after fast neutron fission of ^{238}U. (t_{irrad} = 10 s, t_{wait} = 395 s, t_{count} = 100 s)

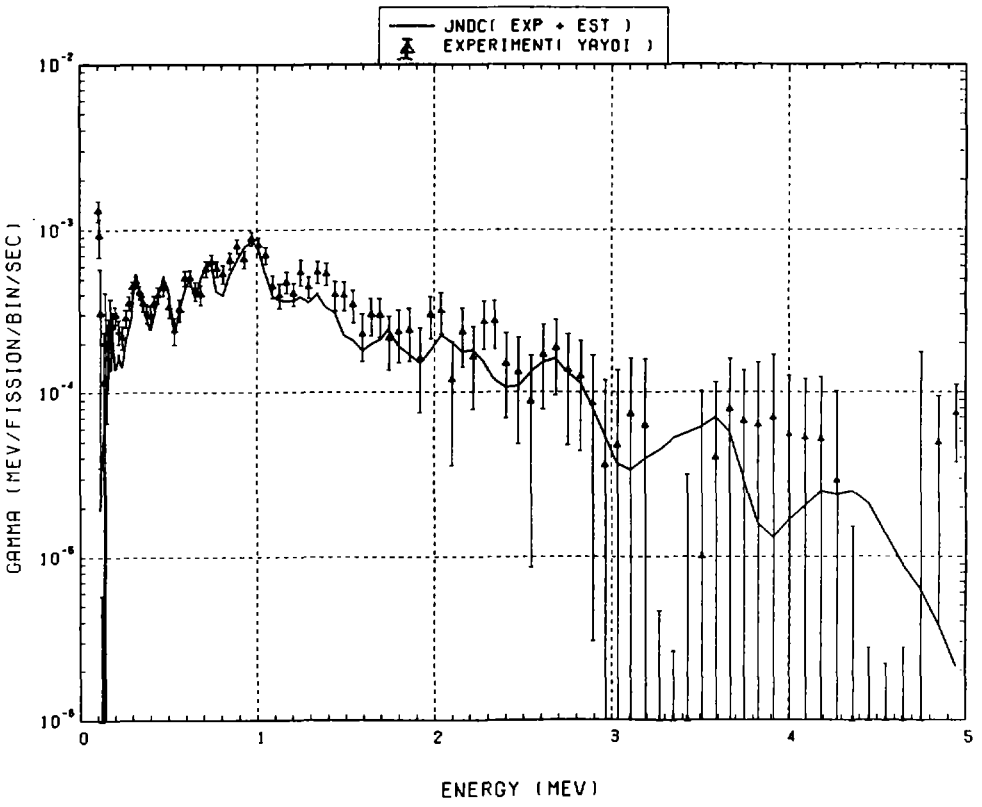

Fig. 172 Comparison of calculated gamma-ray energy spectrum with measured results at 550 seconds after fast neutron fission of ^{238}U. (t_{irrad} = 10 s, t_{wait} = 495 s, t_{count} = 100 s)

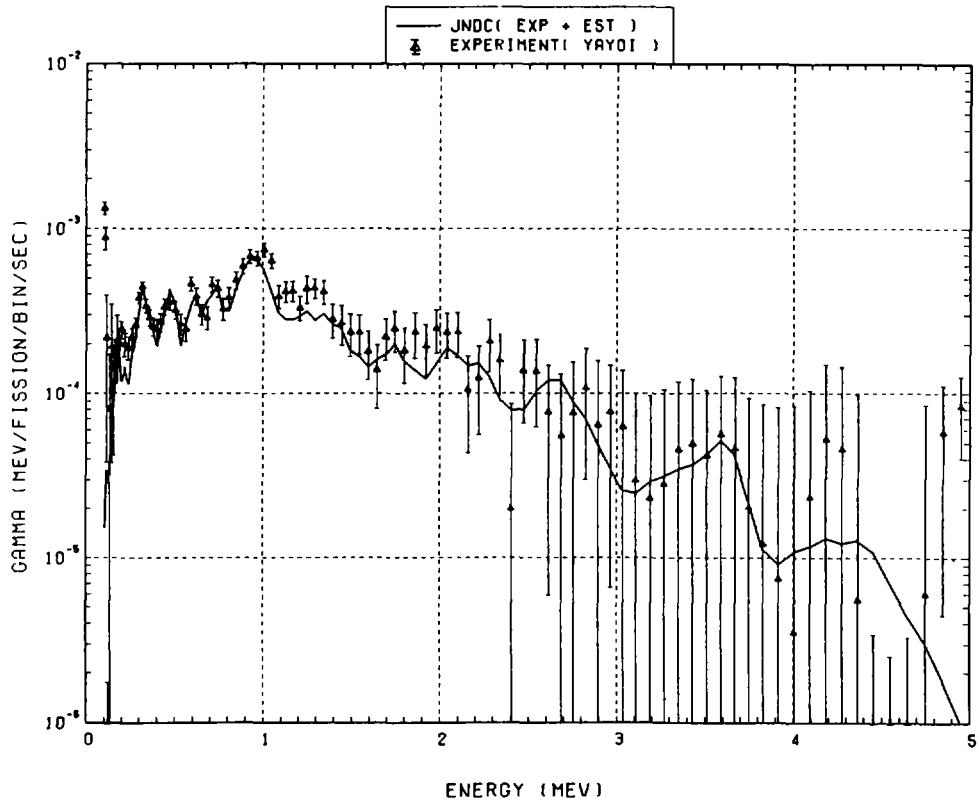

Fig. 173 Comparison of calculated gamma-ray energy spectrum with measured results at 700 seconds after fast neutron fission of ^{238}U. (t_{irrad} = 10 s, t_{wait} = 595 s, t_{count} = 200 s)

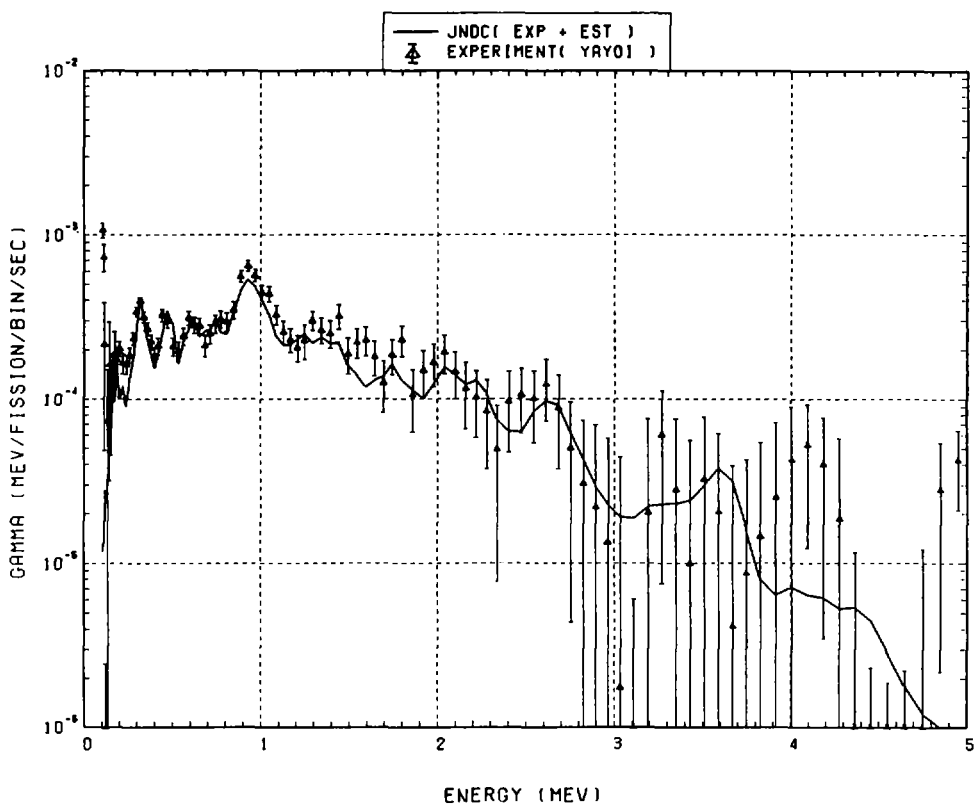

Fig. 174 Comparison of calculated gamma-ray energy spectrum with measured results at 900 seconds after fast neutron fission of ^{238}U. (t_{irrad} = 10 s, t_{wait} = 795 s. t_{count} = 200 s)

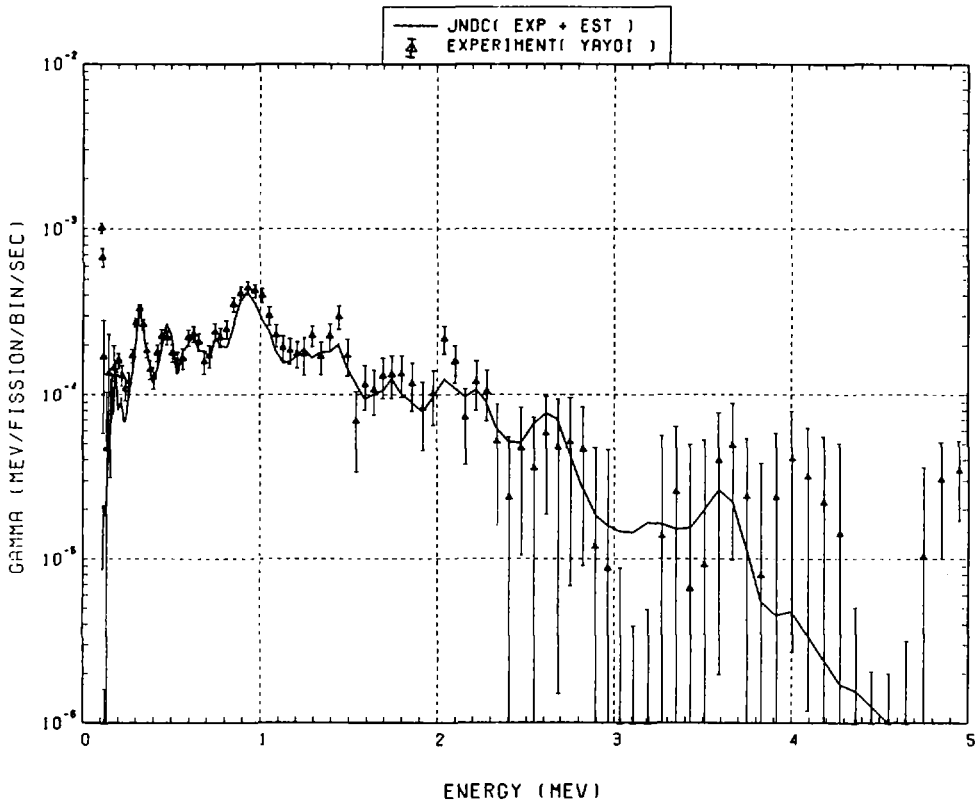

Fig. 175 Comparison of calculated gamma-ray energy spectrum with measured results at 1200 seconds after fast neutron fission of ^{238}U. (t_{irrad} = 10 s, t_{wait} = 995 s, t_{count} = 440 s)

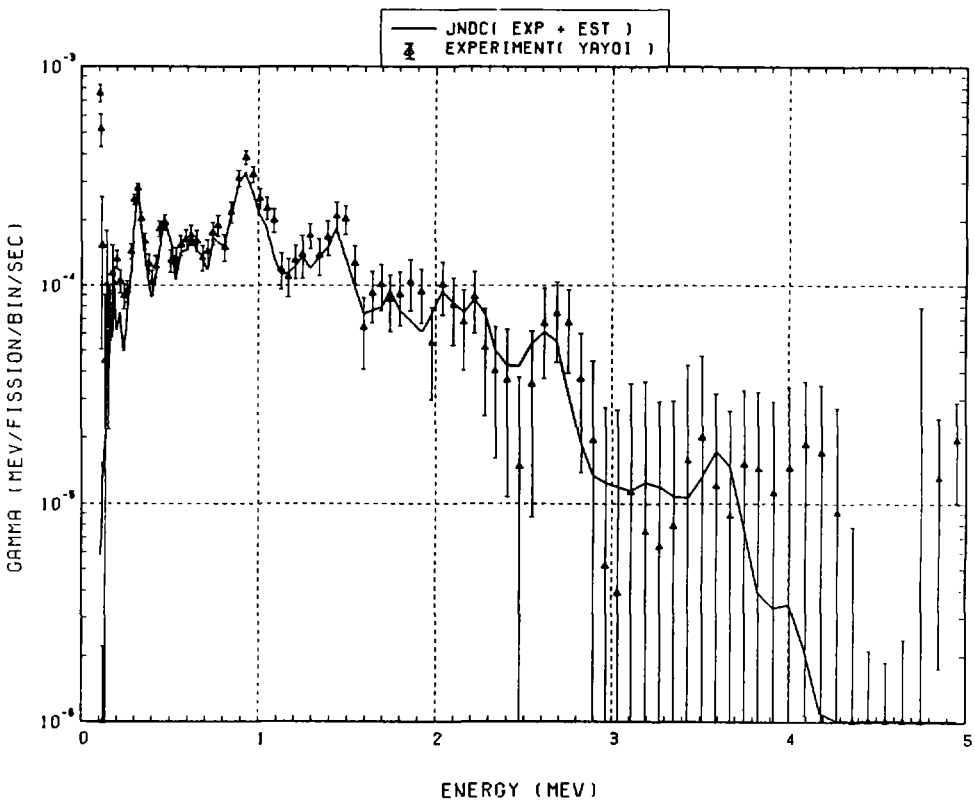

Fig. 176 Comparison of calculated gamma-ray energy spectrum with measured results at 1600 seconds after fast neutron fission of ^{238}U. (t_{irrad} = 10 s, t_{wait} = 1395 s, t_{count} = 400 s)

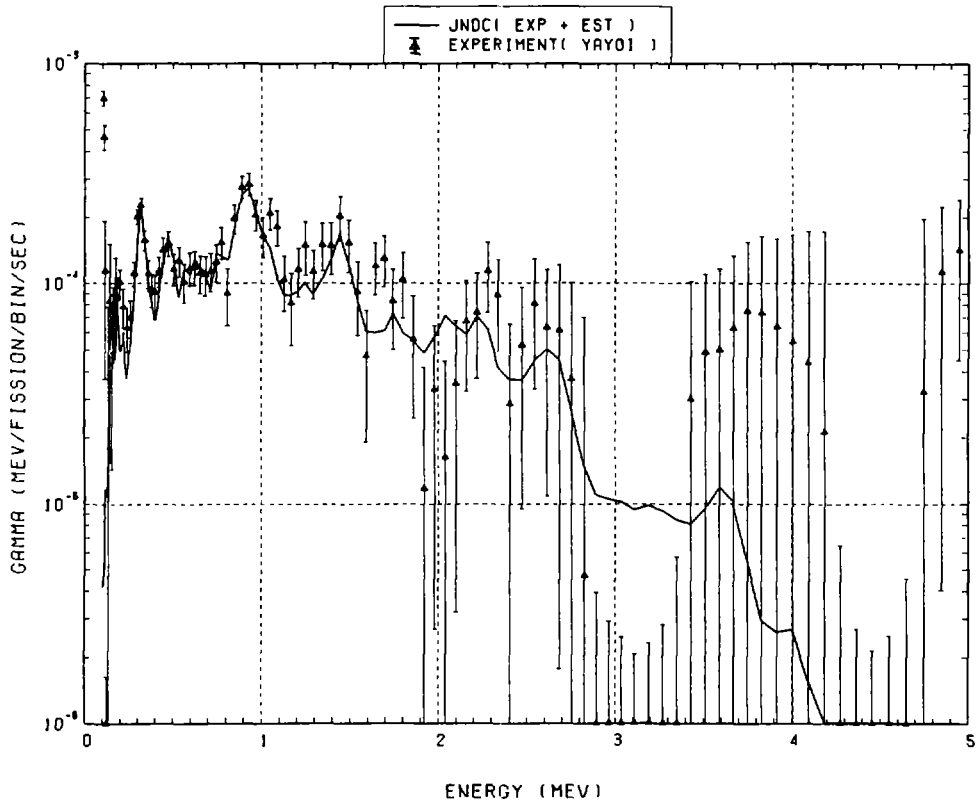

Fig. 177 Comparison of calculated gamma-ray energy spectrum with measured results at 2000 seconds after fast neutron fission of ^{238}U. (t_{irrad} = 10 s, t_{wait} = 1795 s, t_{count} = 400 s)

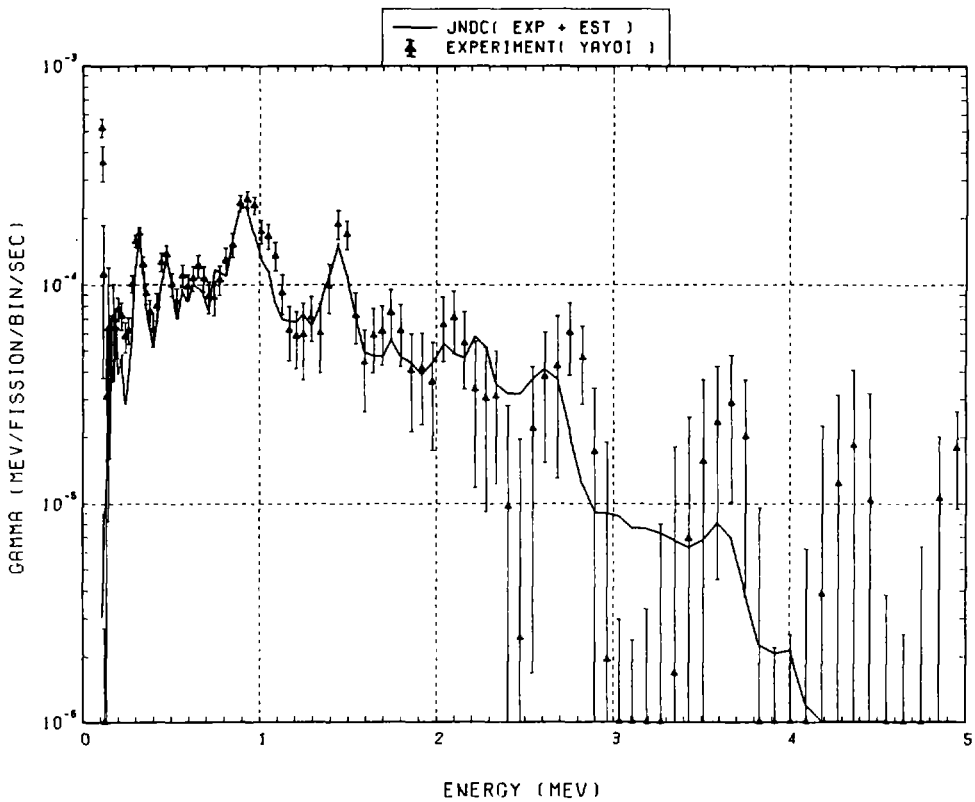

Fig. 178 Comparison of calculated gamma-ray energy spectrum with measured results at 2450 seconds after fast neutron fission of ^{238}U. (t_{irrad} = 10 s, t_{wait} = 2195 s, t_{count} = 500 s)

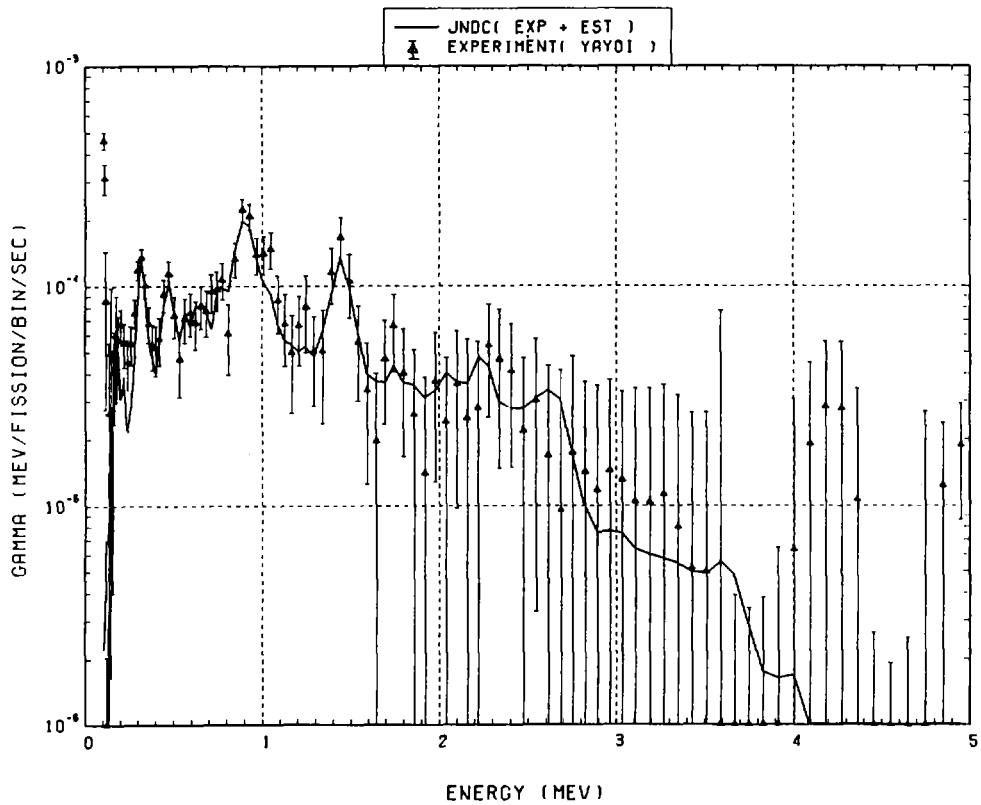

Fig. 179 Comparison of calculated gamma-ray energy spectrum with measured results at 2950 seconds after fast neutron fission of ^{238}U. (t_{irrad} = 10 s, t_{wait} = 2695 s, t_{count} = 500 s)

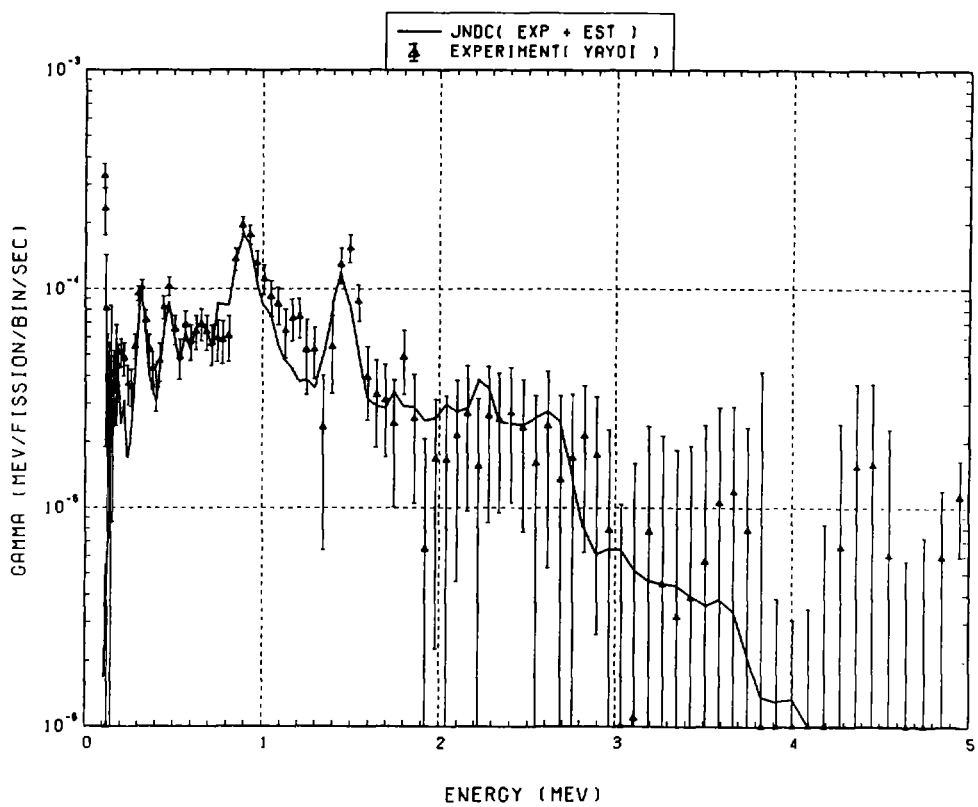

Fig. 180 Comparison of calculated gamma-ray energy spectrum with measured results at 3500 seconds after fast neutron fission of ^{238}U. (t_{irrad} = 10 s, t_{wait} = 3195 s, t_{count} = 600 s)

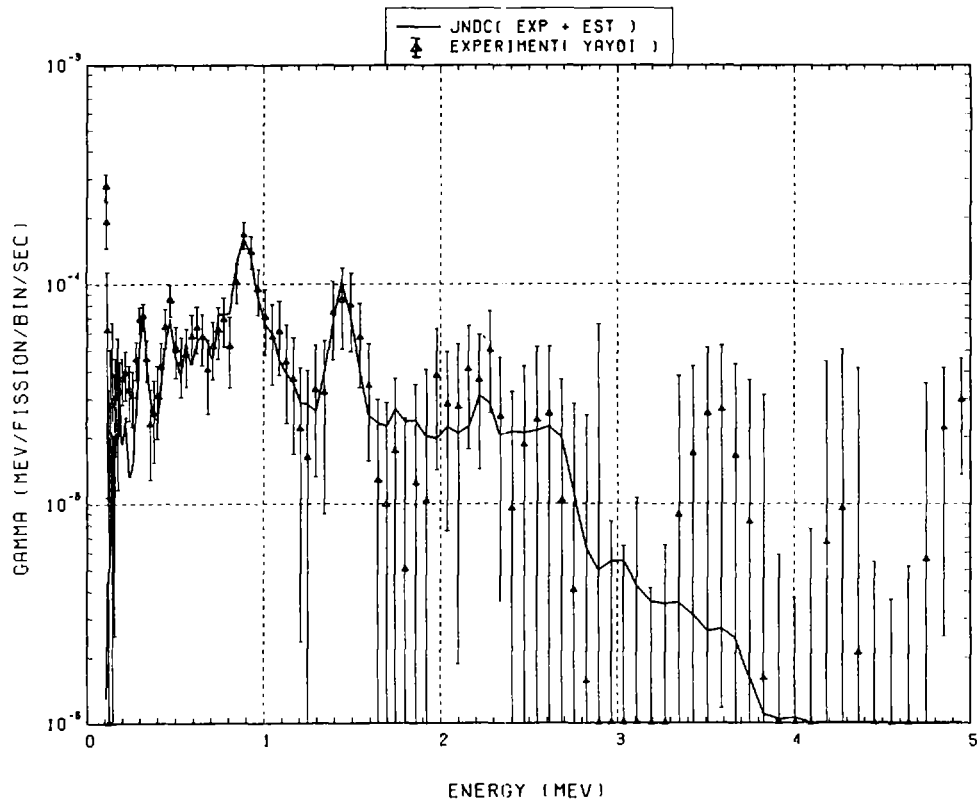

Fig. 181 Comparison of calculated gamma-ray energy spectrum with measured results at 4100 seconds after fast neutron fission of ^{238}U. (t_{irrad} = 10 s, t_{wait} = 3795 s, t_{count} = 600 s)

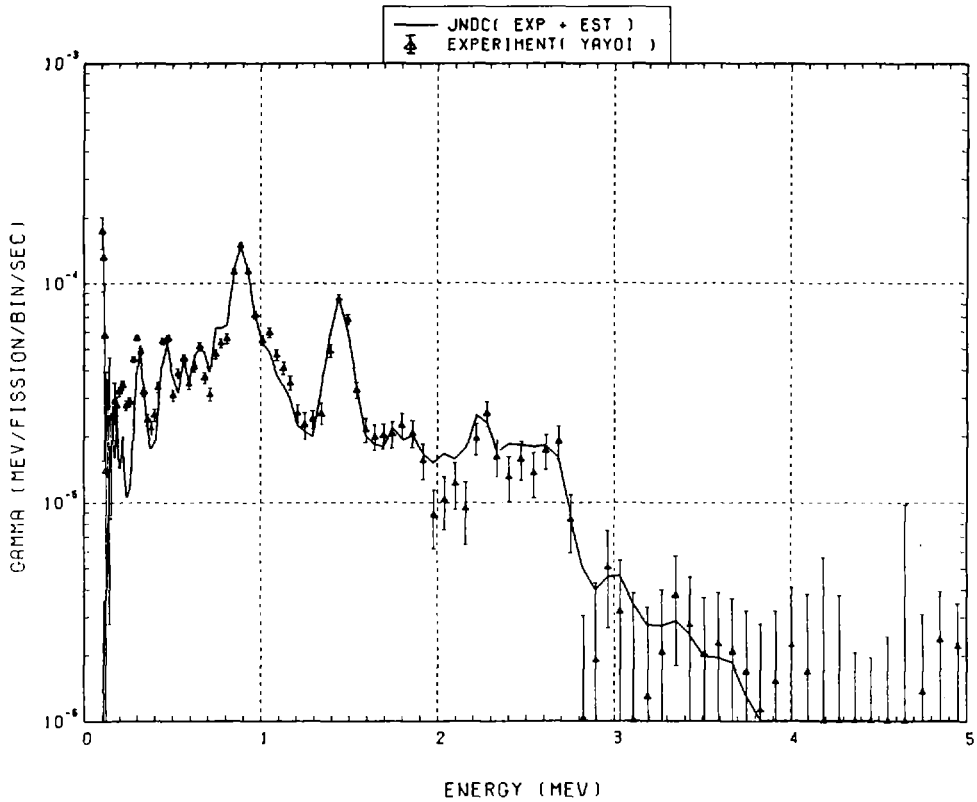

Fig. 182 Comparison of calculated gamma-ray energy spectrum with measured results at 4800 seconds after fast neutron fission of ^{238}U. (t_{irrad} = 100 s, t_{wait} = 4350 s, t_{count} = 800 s)

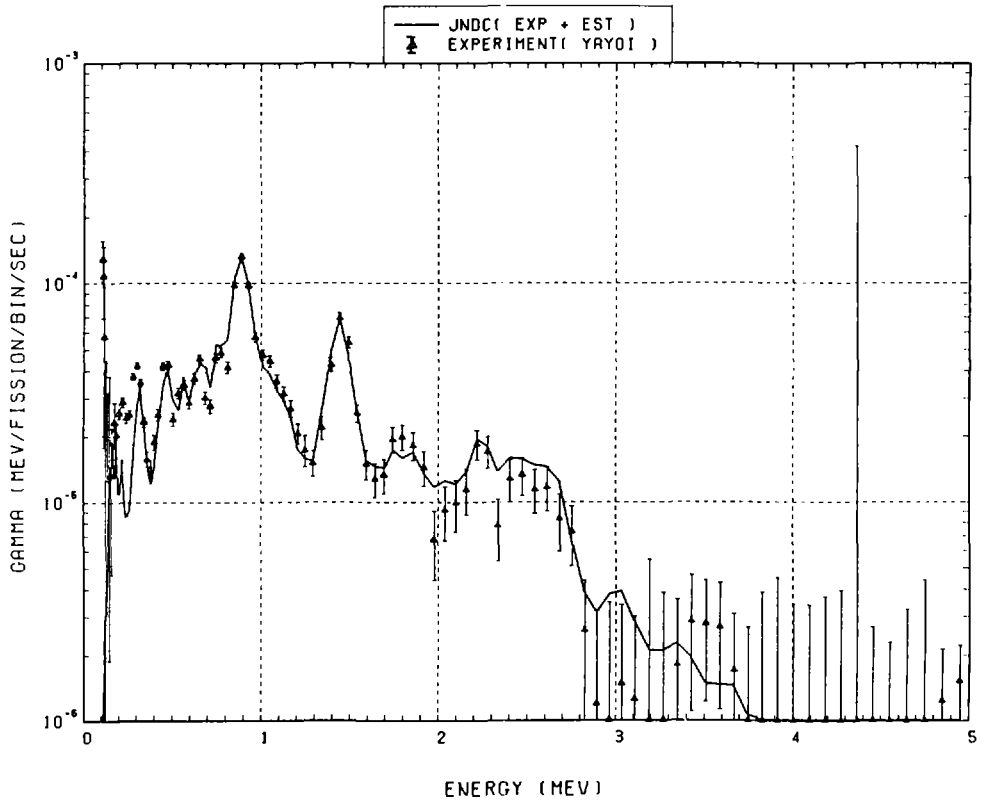

Fig. 183 Comparison of calculated gamma-ray energy spectrum with measured results at 5600 seconds after fast neutron fission of ^{238}U. (t_{irrad} = 100 s, t_{wait} = 5150 s, t_{count} = 800 s)

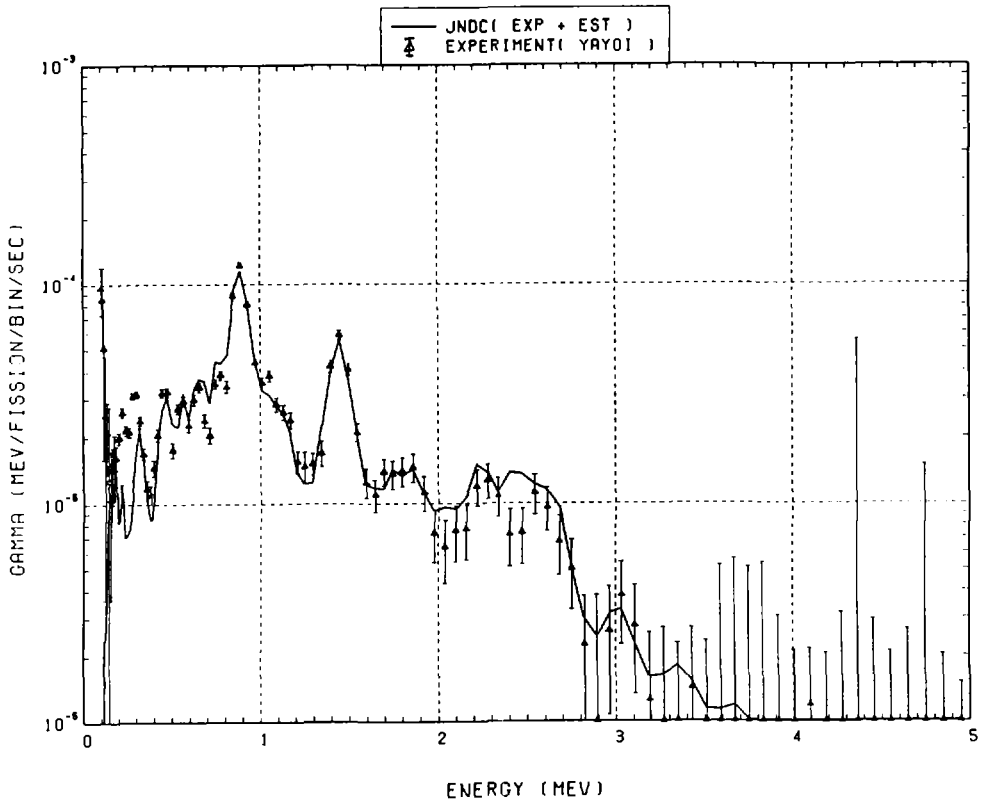

Fig. 184 Comparison of calculated gamma-ray energy spectrum with measured results at 6500 seconds after fast neutron fission of ^{238}U. (t_{irrad} = 100 s, t_{wait} = 5950 s, t_{count} = 1000 s)

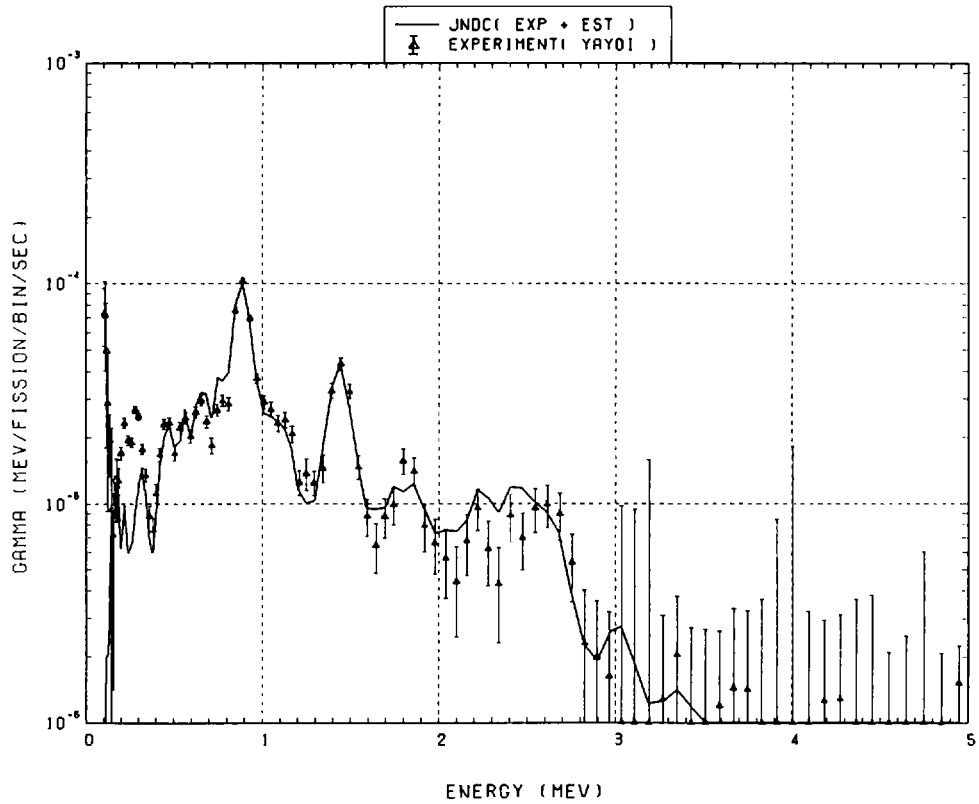

Fig. 185 Comparison of calculated gamma-ray energy spectrum with measured results at 7500 seconds after fast neutron fission of ^{238}U. (t_{irrad} = 100 s, t_{wait} = 6950 s, t_{count} = 1000 s)

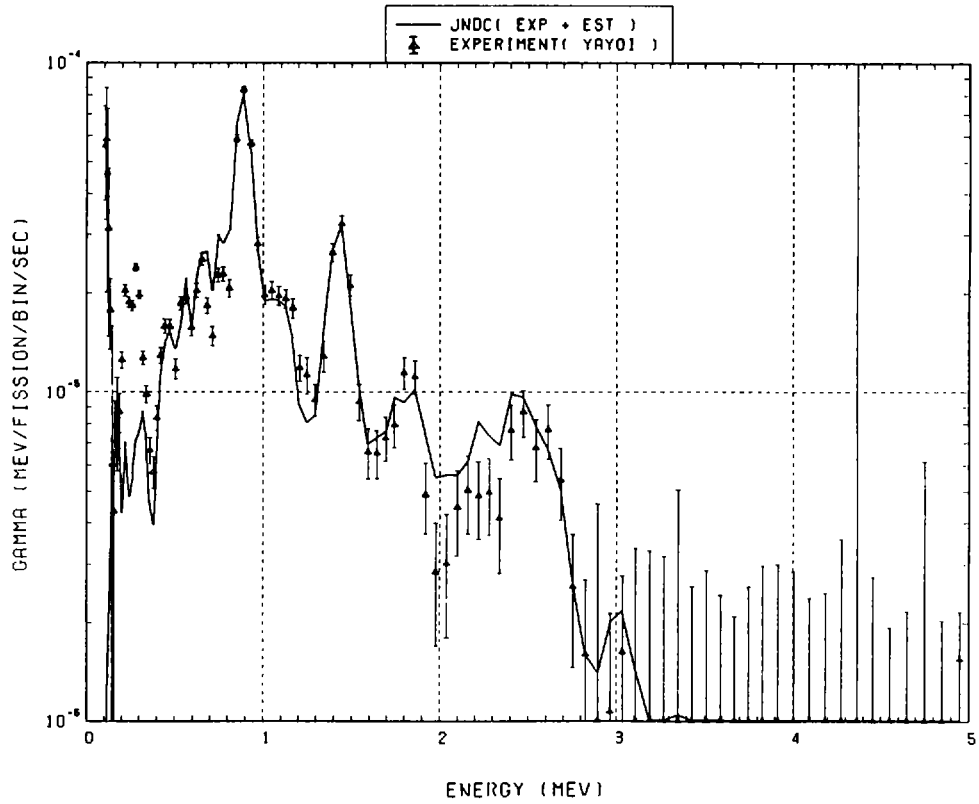

Fig. 186 Comparison of calculated gamma-ray energy spectrum with measured results at 9000 seconds after fast neutron fission of ^{238}U. (t_{irrad} = 100 s, t_{wait} = 7950 s, t_{count} = 2000 s)

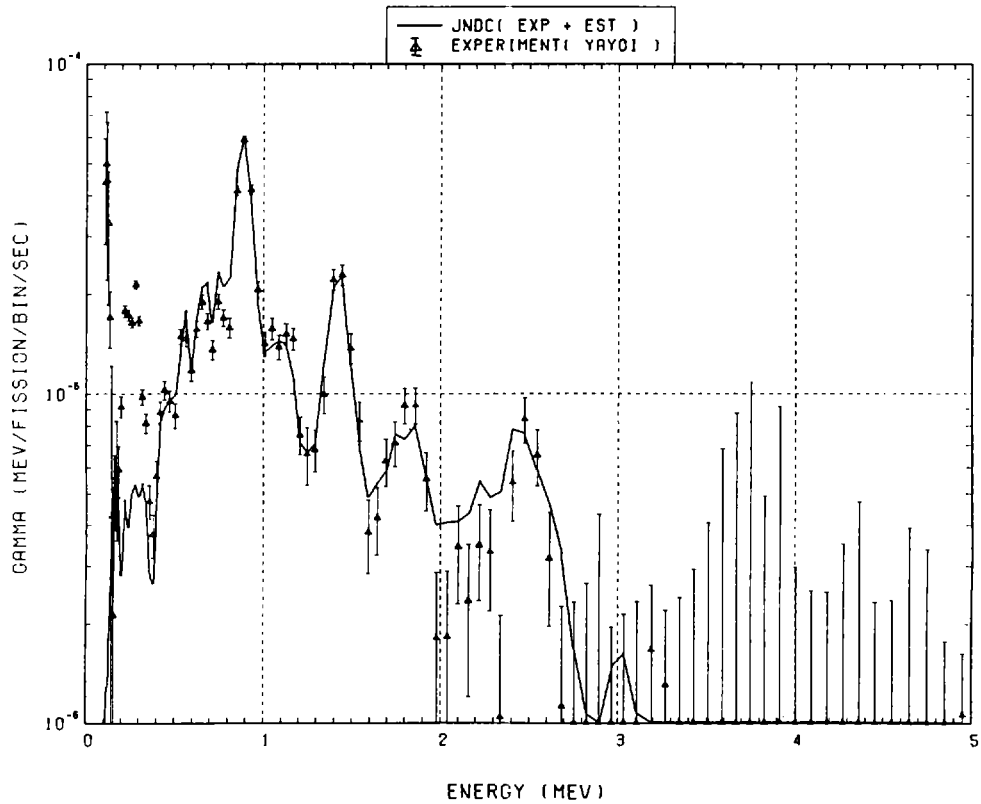

Fig. 187 Comparison of calculated gamma-ray energy spectrum with measured results at 11000 seconds after fast neutron fission of ^{238}U. (t_{irrad} = 100 s, t_{wait} = 9950 s, t_{count} = 2000 s)

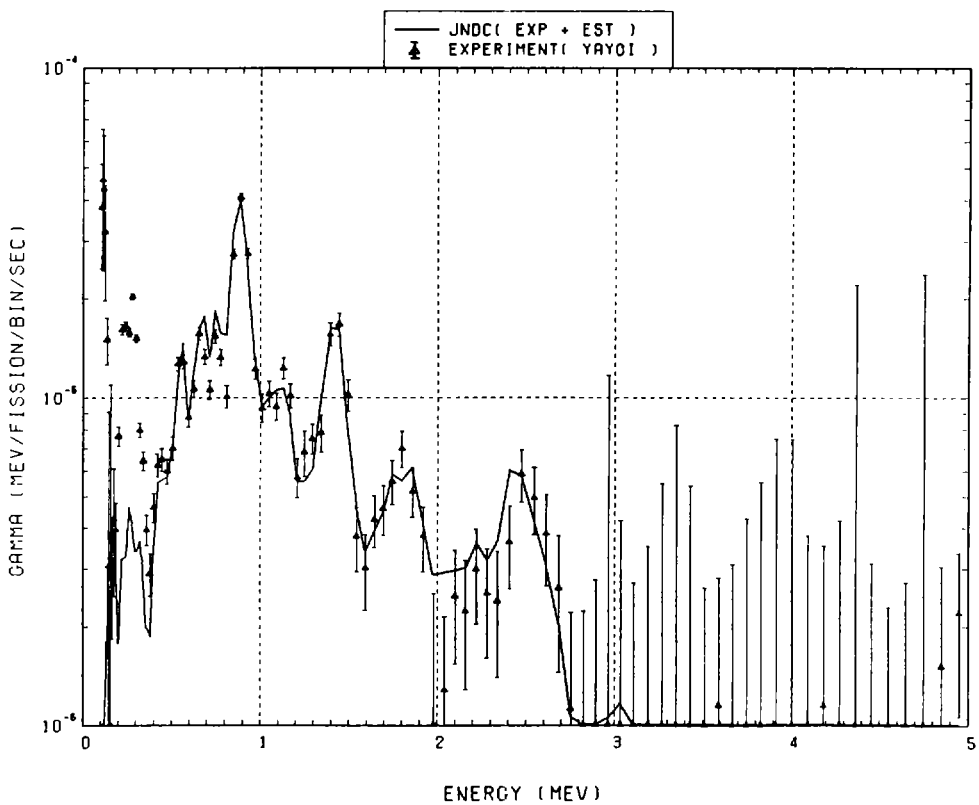

Fig. 188 Comparison of calculated gamma-ray energy spectrum with measured results at 13500 seconds after fast neutron fission of ^{238}U. (t_{irrad} = 100 s, t_{wait} = 11950 s, t_{count} = 3000 s)

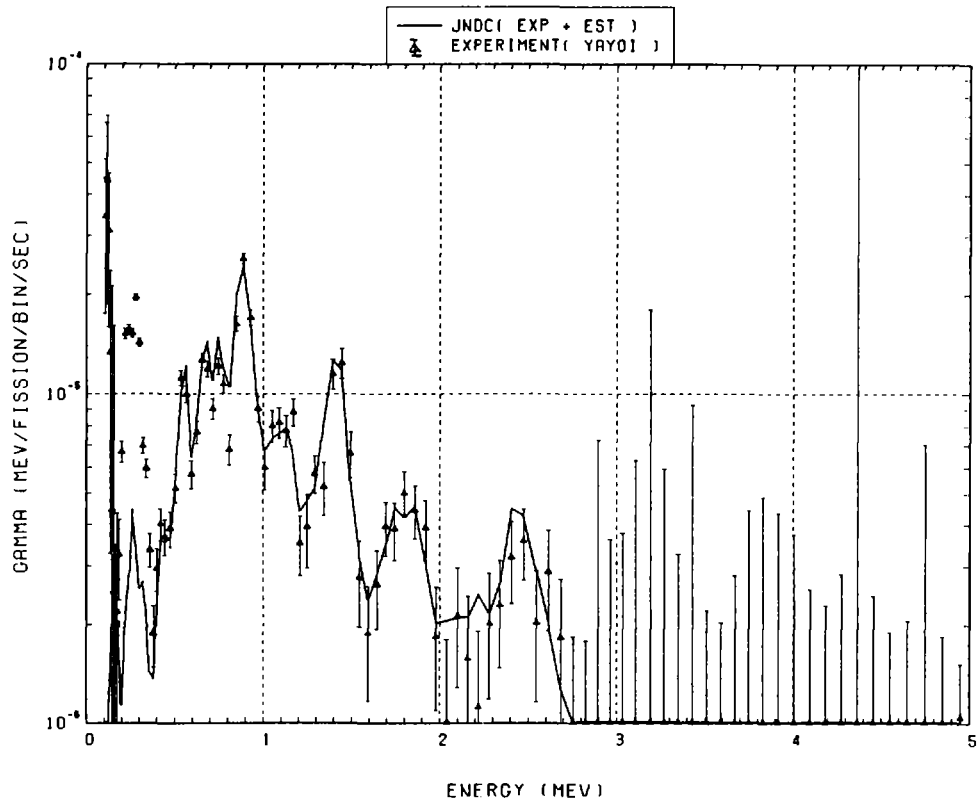

Fig. 189 Comparison of calculated gamma-ray energy spectrum with measured results at 16500 seconds after fast neutron fission of ^{238}U. (t_{irrad} = 100 s, t_{wait} = 14950 s, t_{count} = 3000 s)

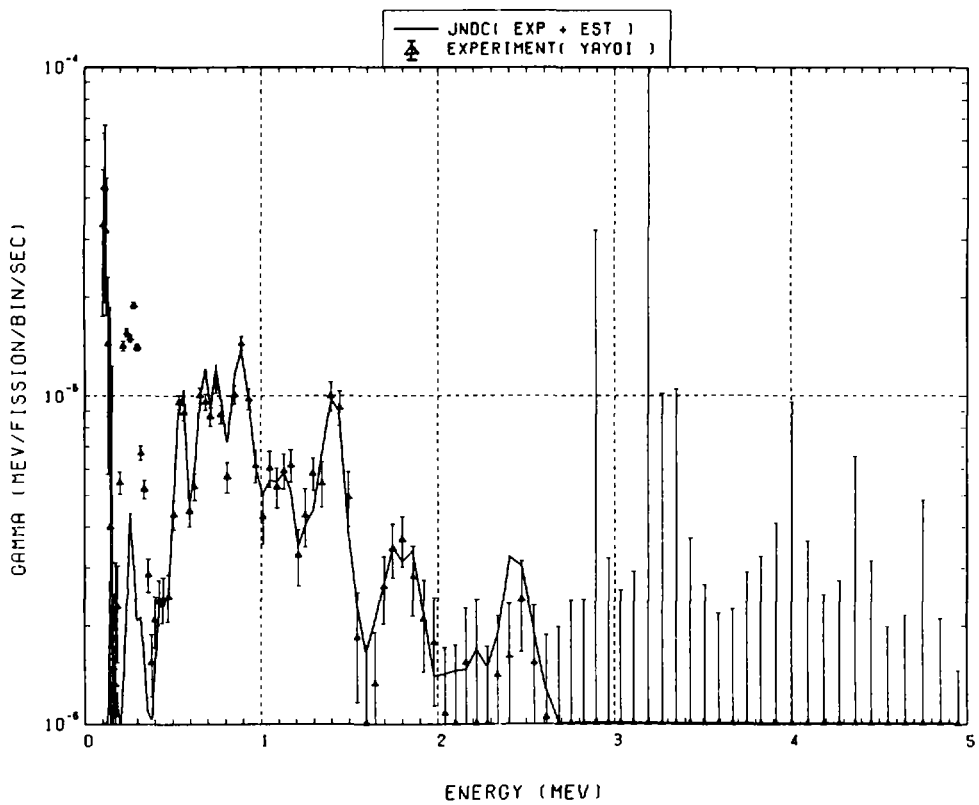

Fig. 190 Comparison of calculated gamma-ray energy spectrum with measured results at 20000 seconds after fast neutron fission of ^{238}U. (t_{irrad} = 100 s, t_{wait} = 17950 s, t_{count} = 4000 s)

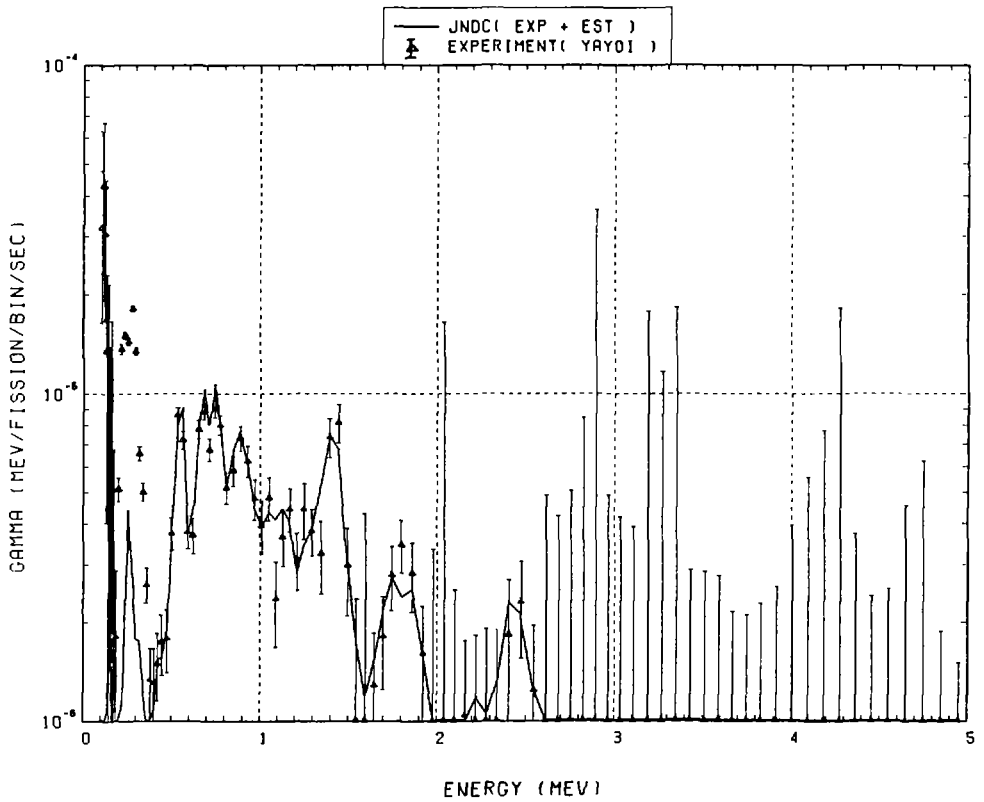

Fig. 191 Comparison of calculated gamma-ray energy spectrum with measured results at 24000 seconds after fast neutron fission of ^{238}U. (t_{irrad} = 100 s, t_{wait} = 21950 s, t_{count} = 4000 s)

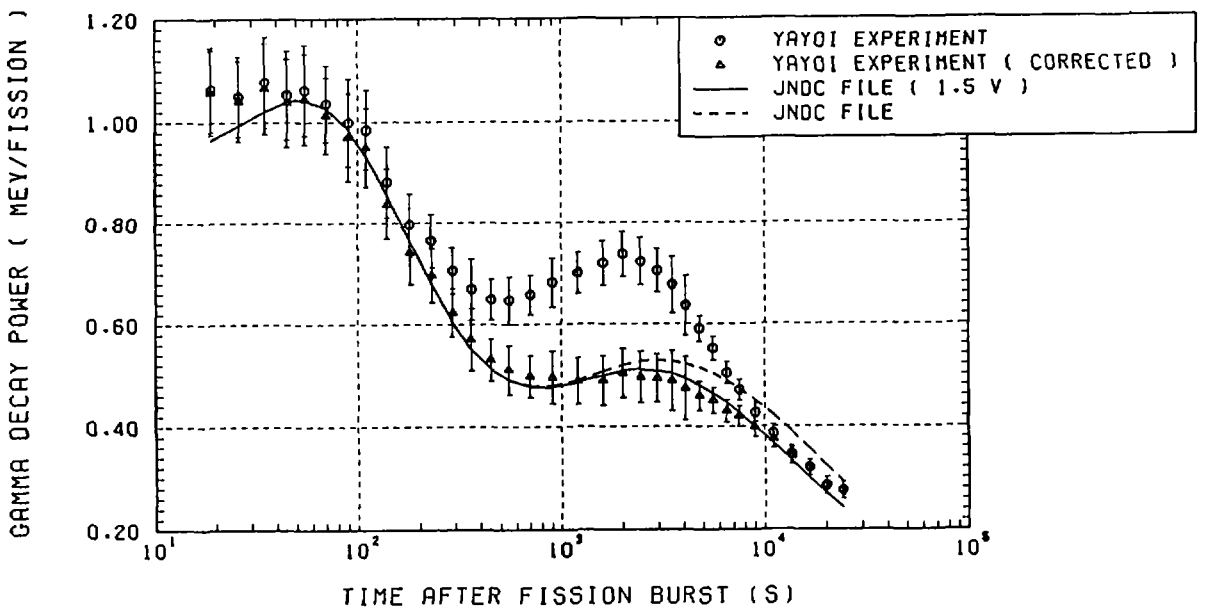

Fig. 192 Comparison of calculated gamma-decay heat with measured results at YAYOI for fast neutron fission of ^{232}Th.

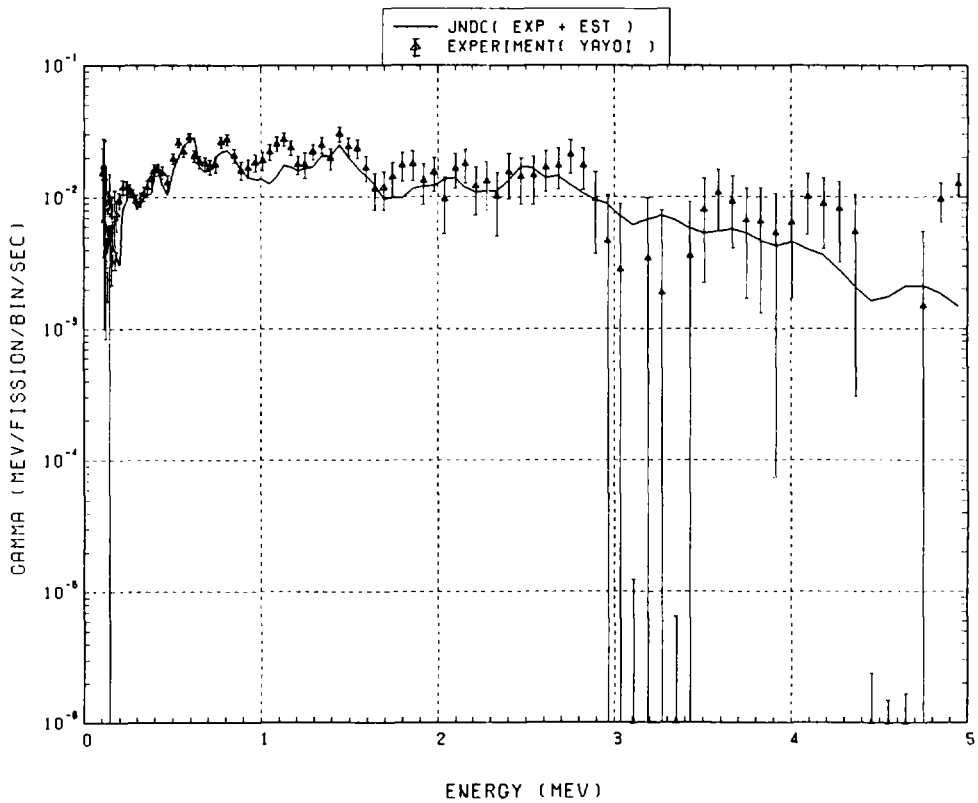

Fig. 193 Comparison of calculated gamma-ray energy spectrum with measured results at 19 seconds after fast neutron fission of ^{232}Th. (t_{irrad} = 10 s, t_{wait} = 11 s, t_{count} = 6 s)

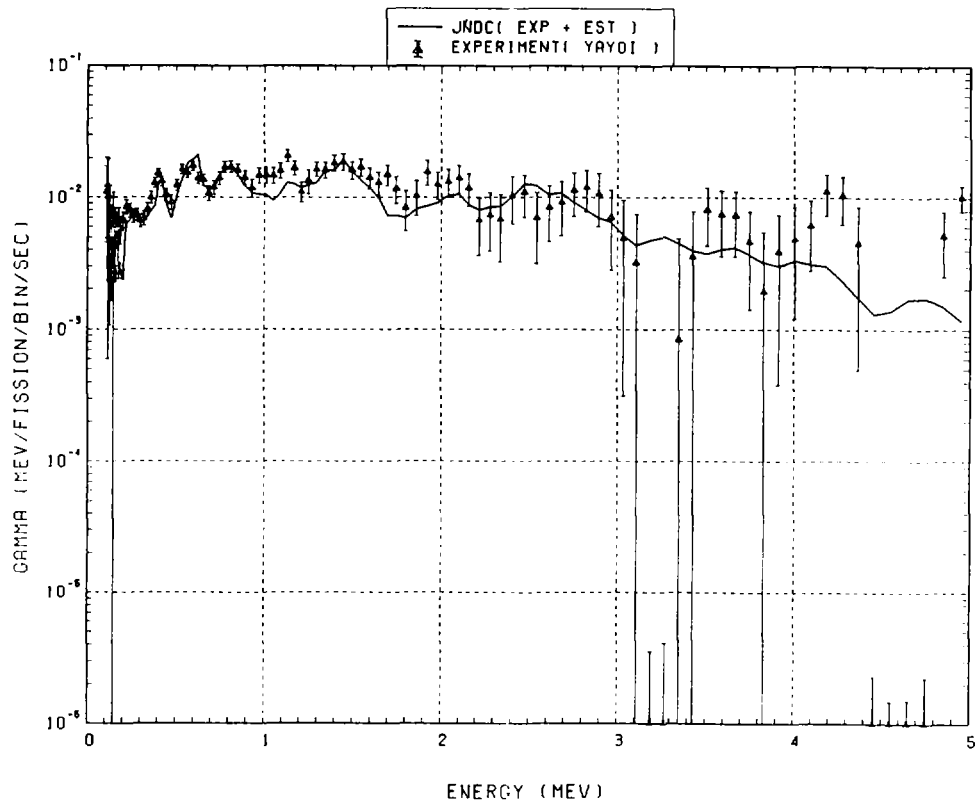

Fig. 194 Comparison of calculated gamma-ray energy spectrum with measured results at 26 seconds after fast neutron fission of ^{232}Th. (t_{irrad} = 10 s, t_{wait} = 17 s, t_{count} = 8 s)

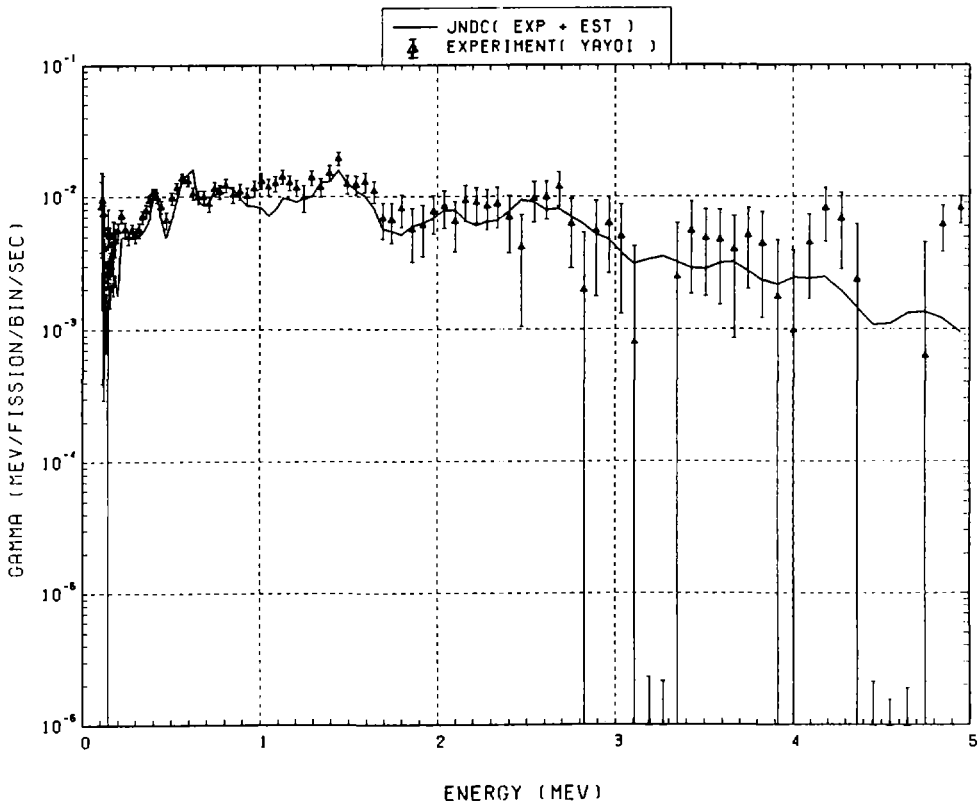

Fig. 195 Comparison of calculated gamma-ray energy spectrum with measured results at 35 seconds after fast neutron fission of ^{232}Th. (t_{irrad} = 10 s, t_{wait} = 25 s, t_{count} = 10 s)

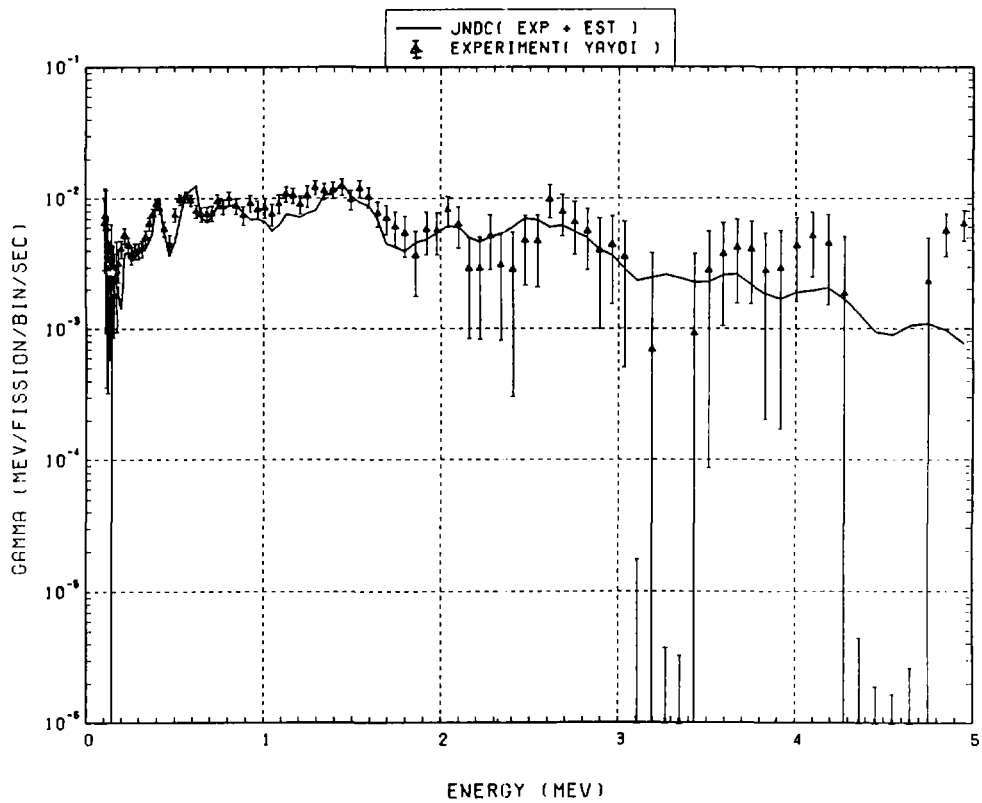

Fig. 196 Comparison of calculated gamma-ray energy spectrum with measured results at 45 seconds after fast neutron fission of ^{232}Th. (t_{irrad} = 10 s, t_{wait} = 35 s, t_{count} = 10 s)

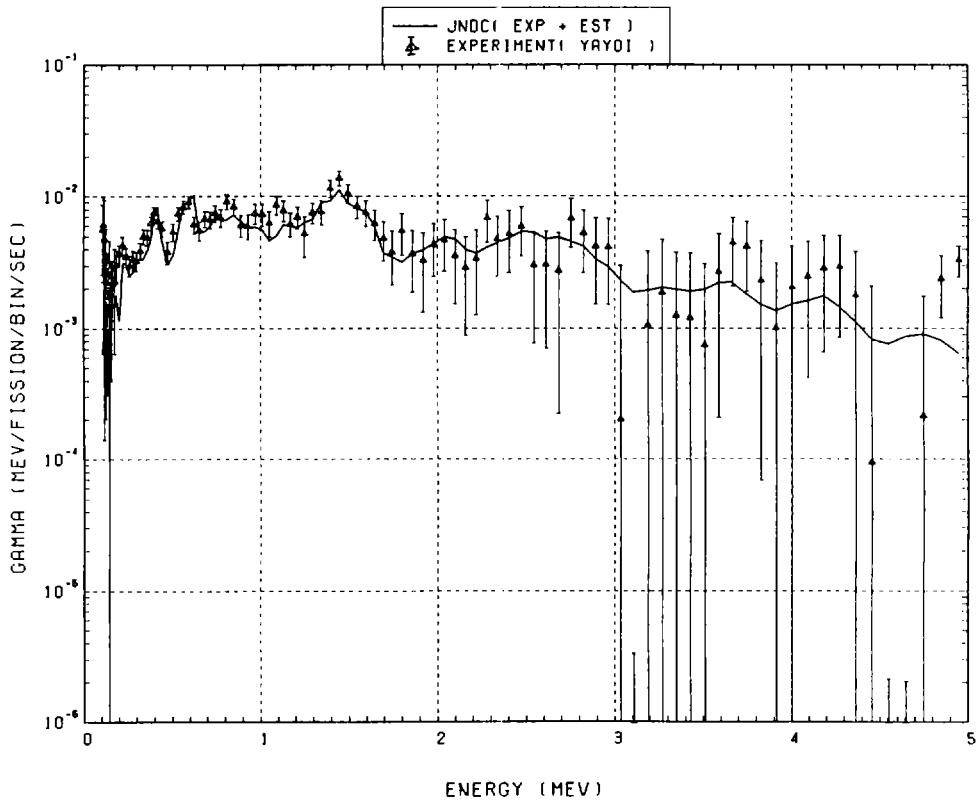

Fig. 197 Comparison of calculated gamma-ray energy spectrum with measured results at 55 seconds after fast neutron fission of ^{232}Th. (t_{irrad} = 10 s, t_{wait} = 45 s, t_{count} = 10 s)

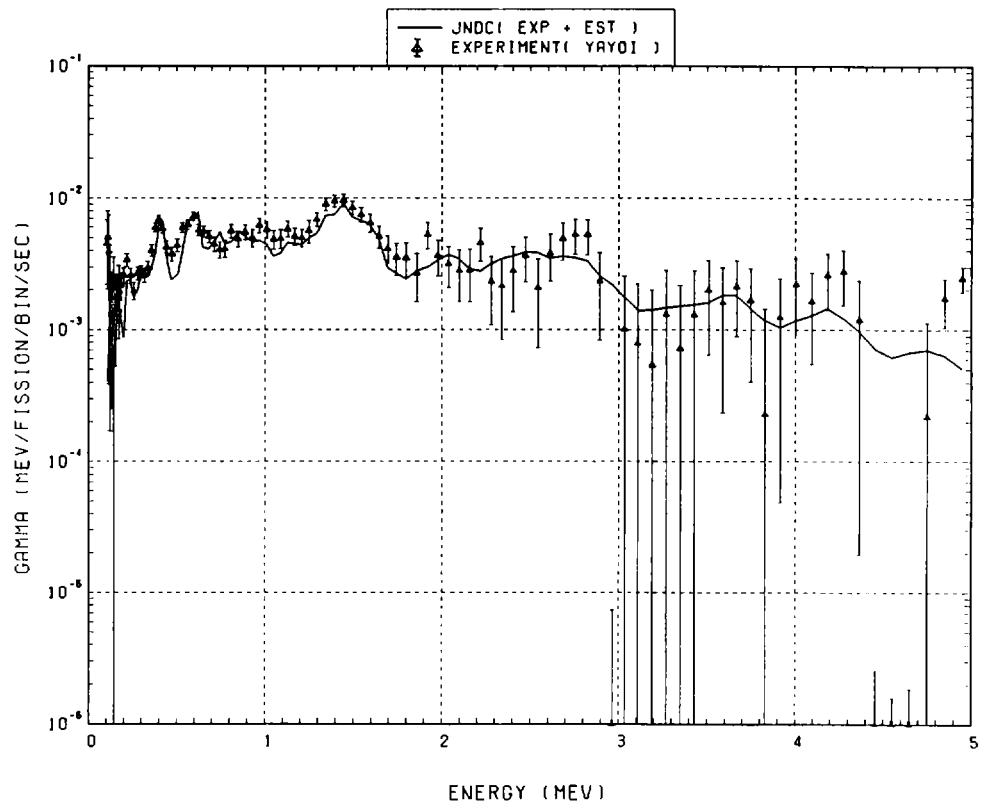

Fig. 198 Comparison of calculated gamma-ray energy spectrum with measured results at 70 seconds after fast neutron fission of ^{232}Th. (t_{irrad} = 10 s, t_{wait} = 55 s, t_{count} = 20 s)

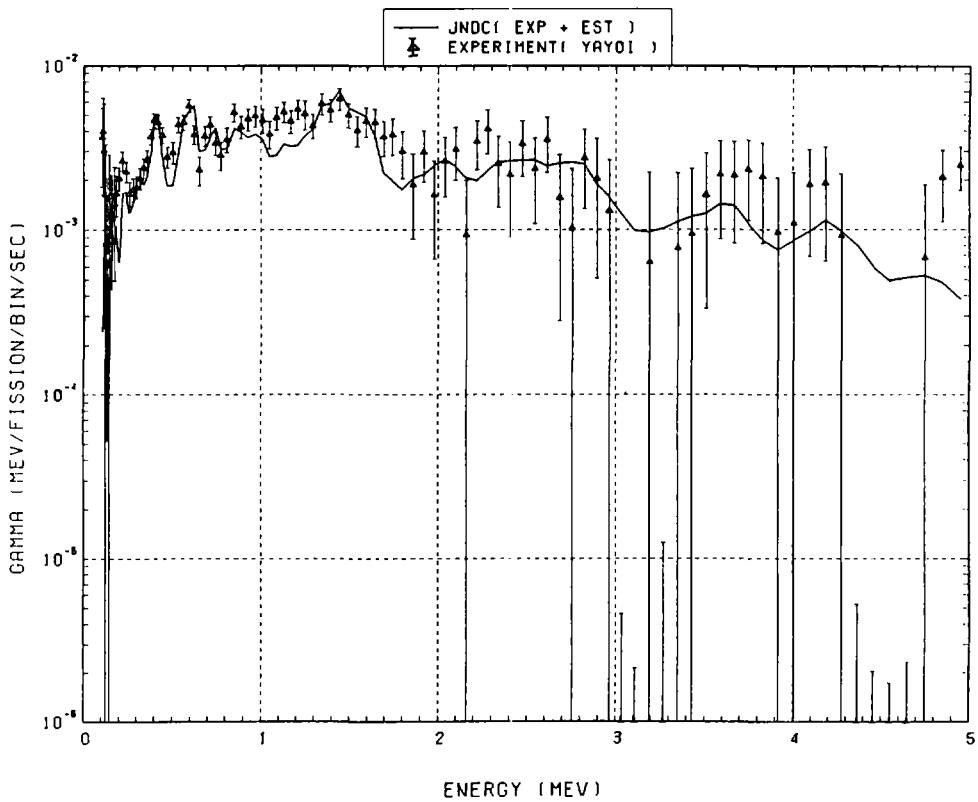

Fig. 199 Comparison of calculated gamma-ray energy spectrum with measured results at 90 seconds after fast neutron fission of ^{232}Th. (t_{irrad} = 10 s, t_{wait} = 75 s, t_{count} = 20 s)

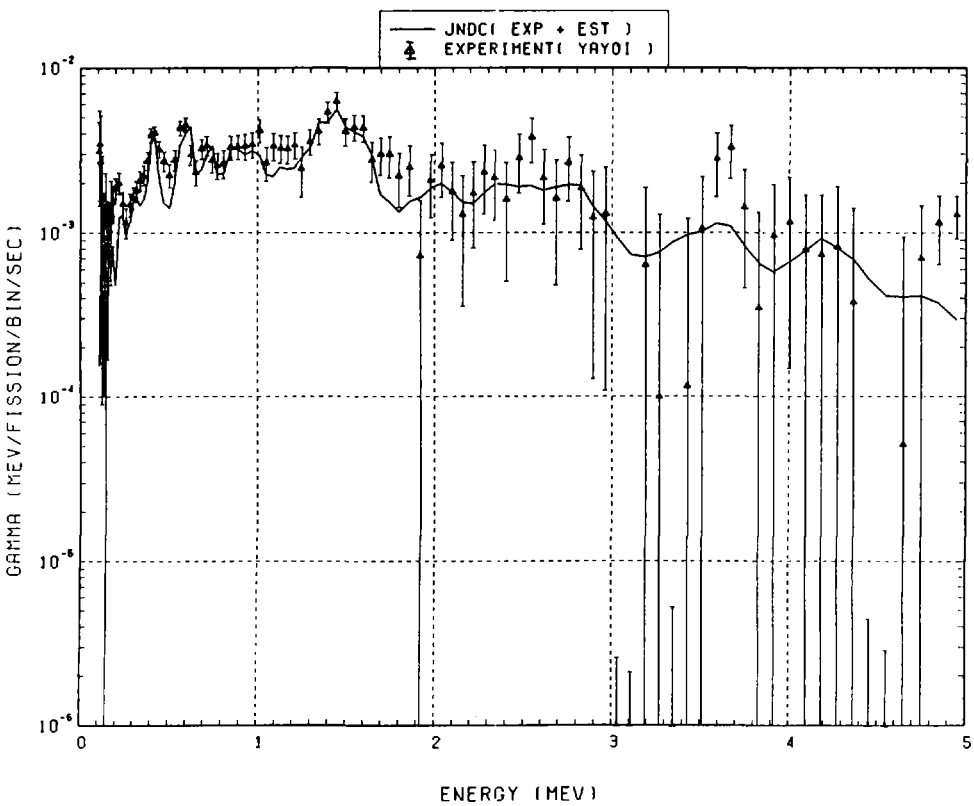

Fig. 200 Comparison of calculated gamma-ray energy spectrum with measured results at 110 seconds after fast neutron fission of ^{232}Th. (t_{irrad} = 10 s, t_{wait} = 95 s, t_{count} = 20 s)

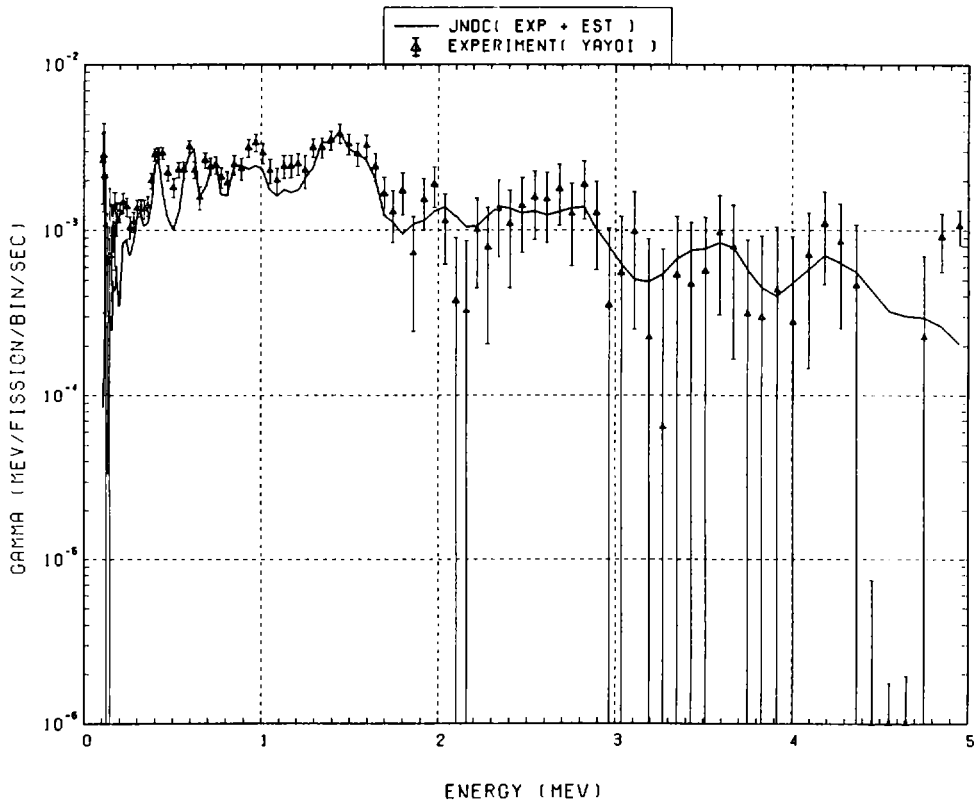

Fig. 201 Comparison of calculated gamma-ray energy spectrum with measured results at 140 seconds after fast neutron fission of ^{232}Th. (t_{irrad} = 10 s, t_{wait} = 115 s, t_{count} = 40 s)

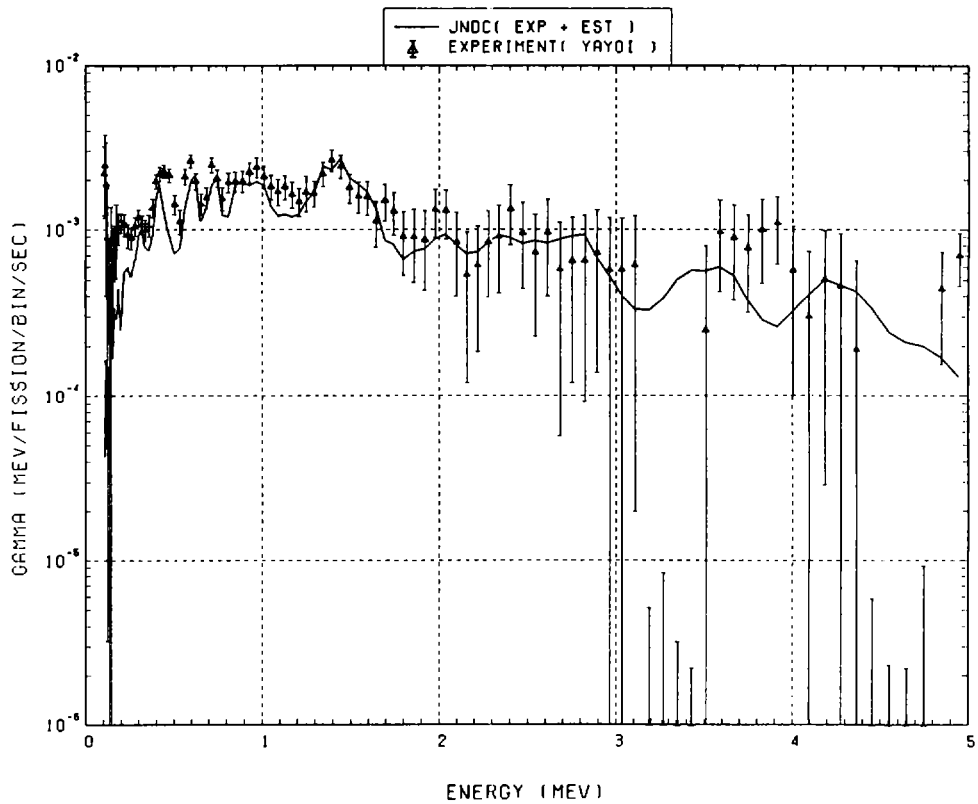

Fig. 202 Comparison of calculated gamma-ray energy spectrum with measured results at 180 seconds after fast neutron fission of ^{232}Th. (t_{irrad} = 10 s, t_{wait} = 155 s, t_{count} = 40 s)

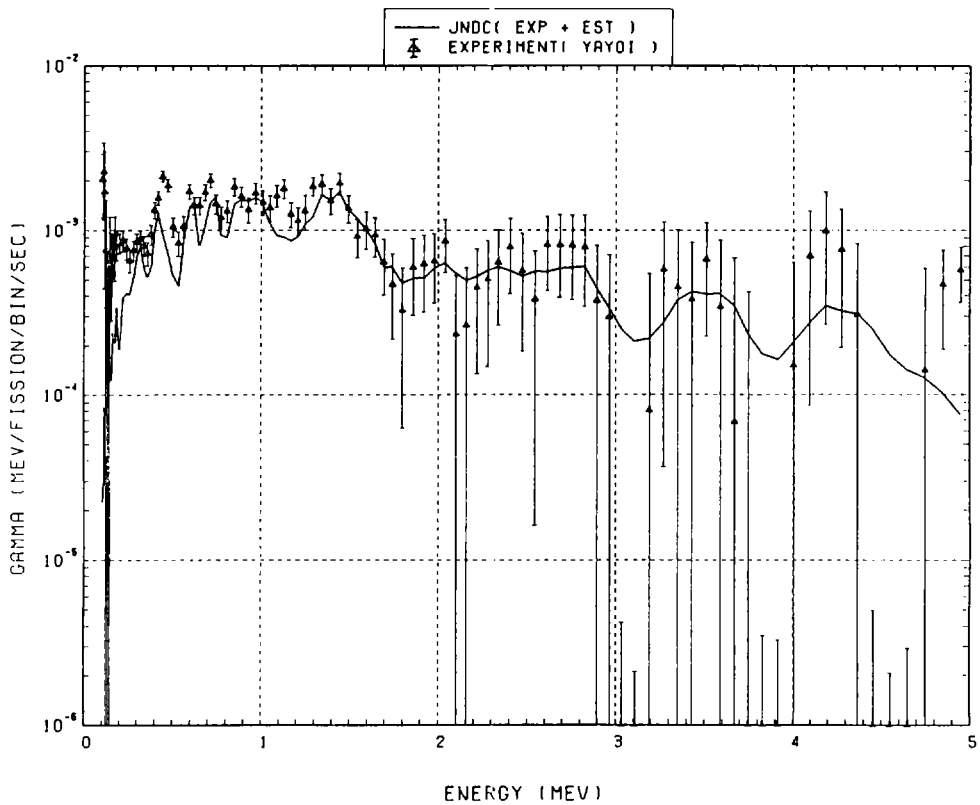

Fig. 203 Comparison of calculated gamma-ray energy spectrum with measured results at 230 seconds after fast neutron fission of ^{232}Th. (t_{irrad} = 10 s, t_{wait} = 195 s, t_{count} = 60 s)

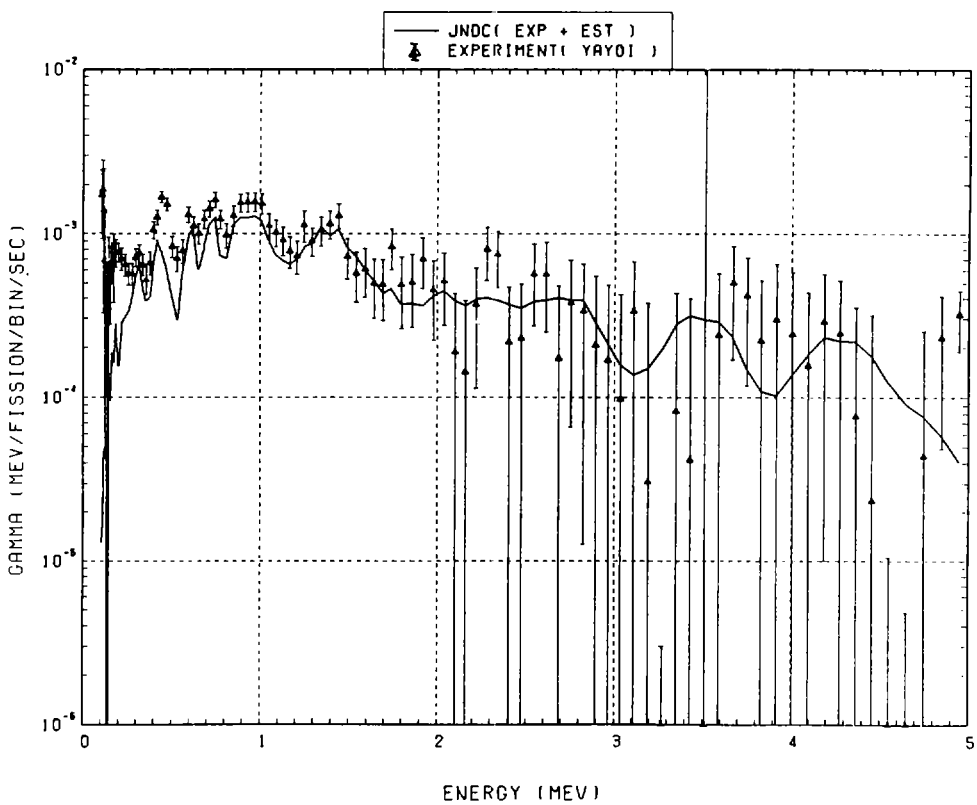

Fig. 204 Comparison of calculated gamma-ray energy spectrum with measured results at 290 seconds after fast neutron fission of ^{232}Th. (t_{irrad} = 10 s, t_{wait} = 255 s, t_{count} = 60 s)

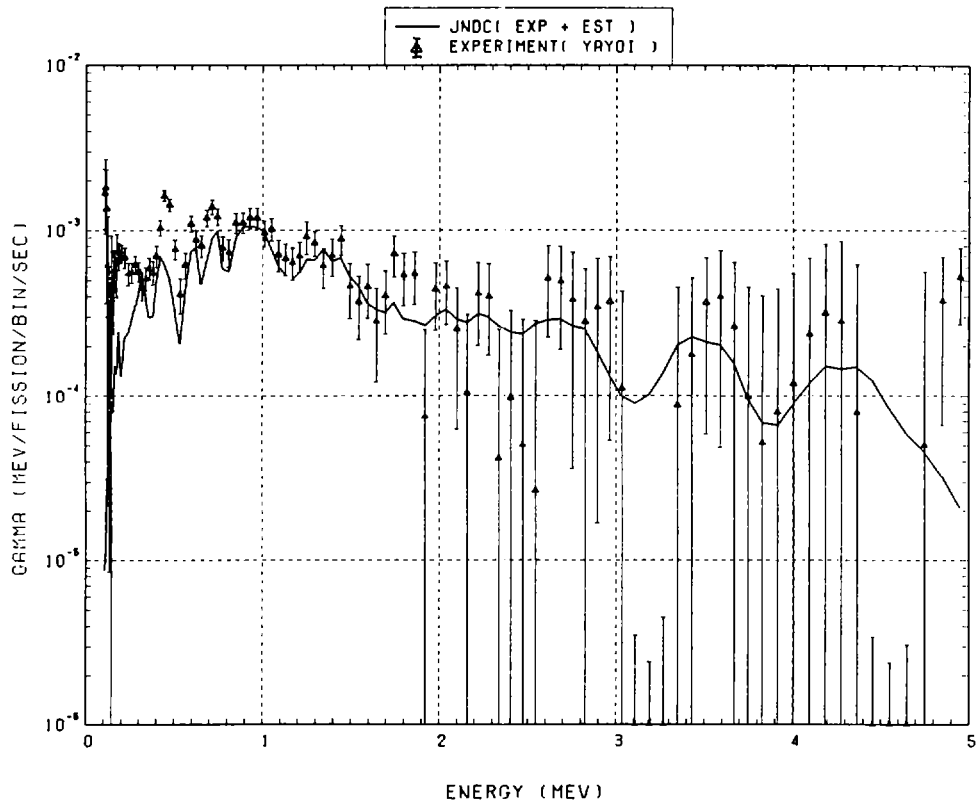

Fig. 205 Comparison of calculated gamma-ray energy spectrum with measured results at 360 seconds after fast neutron fission of ^{232}Th. (t_{irrad} = 10 s, t_{wait} = 315 s. t_{count} = 80 s)

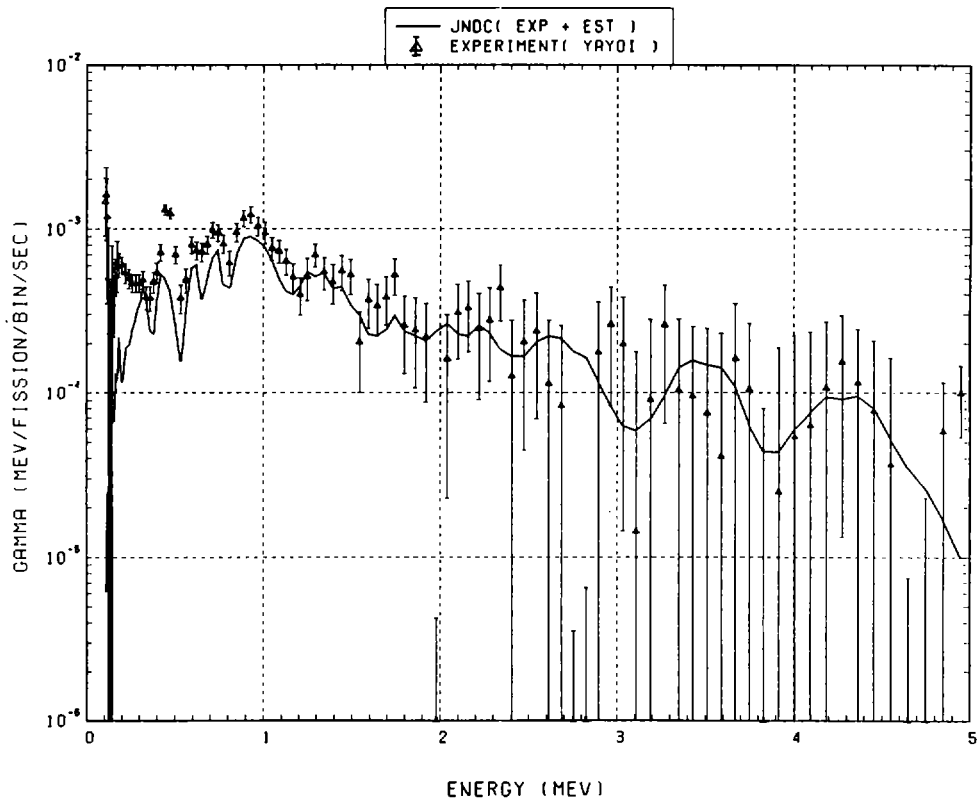

Fig. 206 Comparison of calculated gamma-ray energy spectrum with measured results at 450 seconds after fast neutron fission of ^{232}Th. (t_{irrad} = 10 s, t_{wait} = 395 s, t_{count} = 100 s)

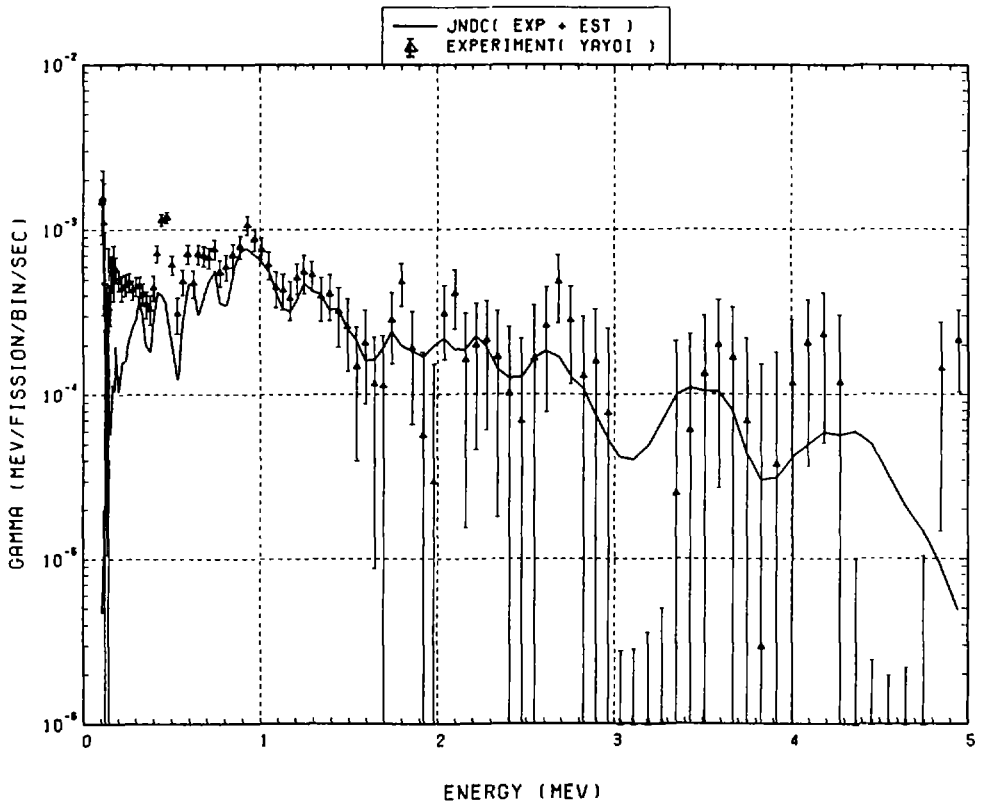

Fig. 207 Comparison of calculated gamma-ray energy spectrum with measured results at 550 seconds after fast neutron fission of ^{232}Th. (t_{irrad} = 10 s, t_{wait} = 495 s, t_{count} = 100 s)

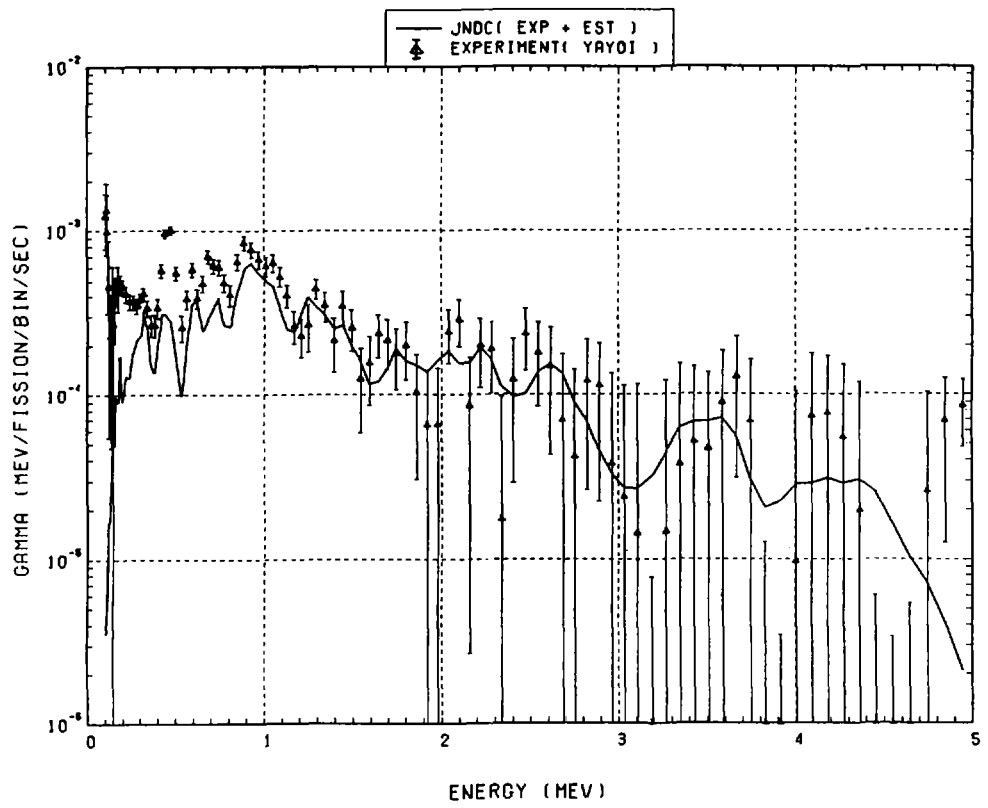

Fig. 208 Comparison of calculated gamma-ray energy spectrum with measured results at 700 seconds after fast neutron fission of ^{232}Th. (t_{irrad} = 10 s, t_{wait} = 595 s, t_{count} = 200 s)

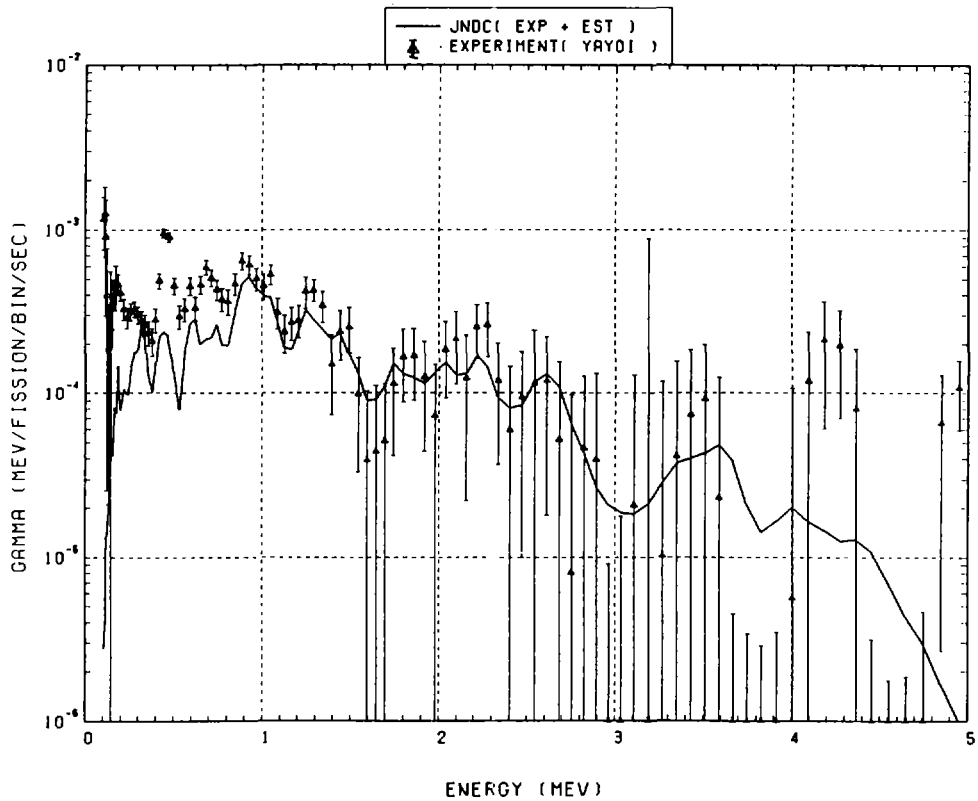

Fig. 209 Comparison of calculated gamma-ray energy spectrum with measured results at 900 seconds after fast neutron fission of ^{232}Th. (t_{irrad} = 10 s, t_{wait} = 795 s, t_{count} = 200 s)

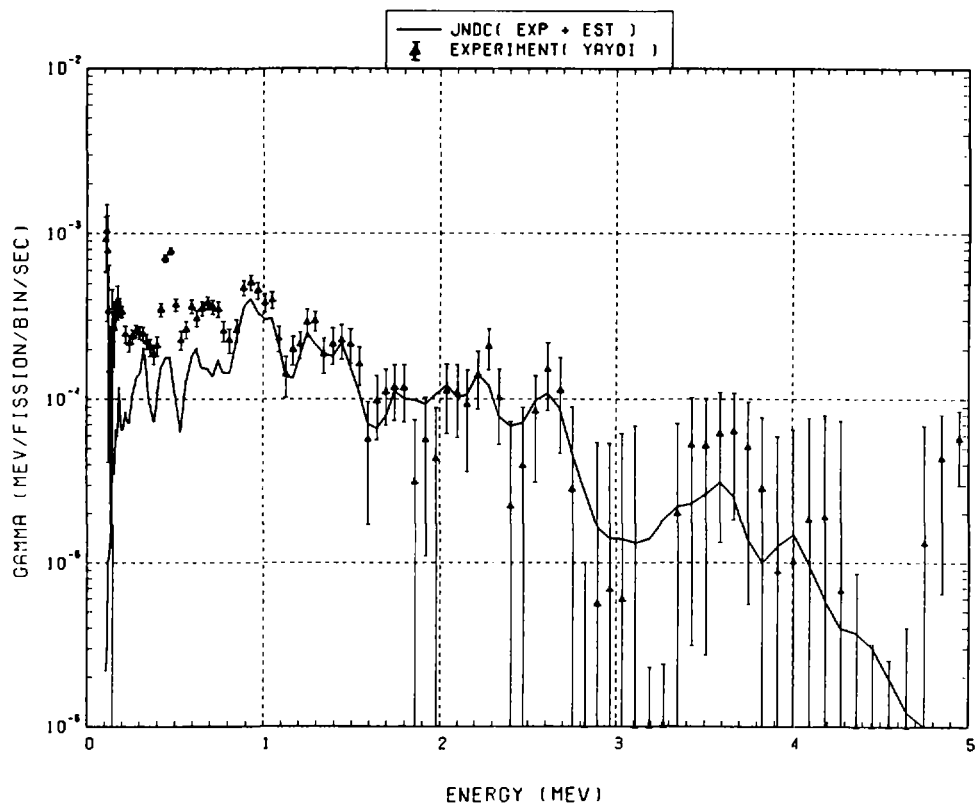

Fig. 210 Comparison of calculated gamma-ray energy spectrum with measured results at 1200 seconds after fast neutron fission of ^{232}Th. (t_{irrad} = 10 s, t_{wait} = 995 s, t_{count} = 400 s)

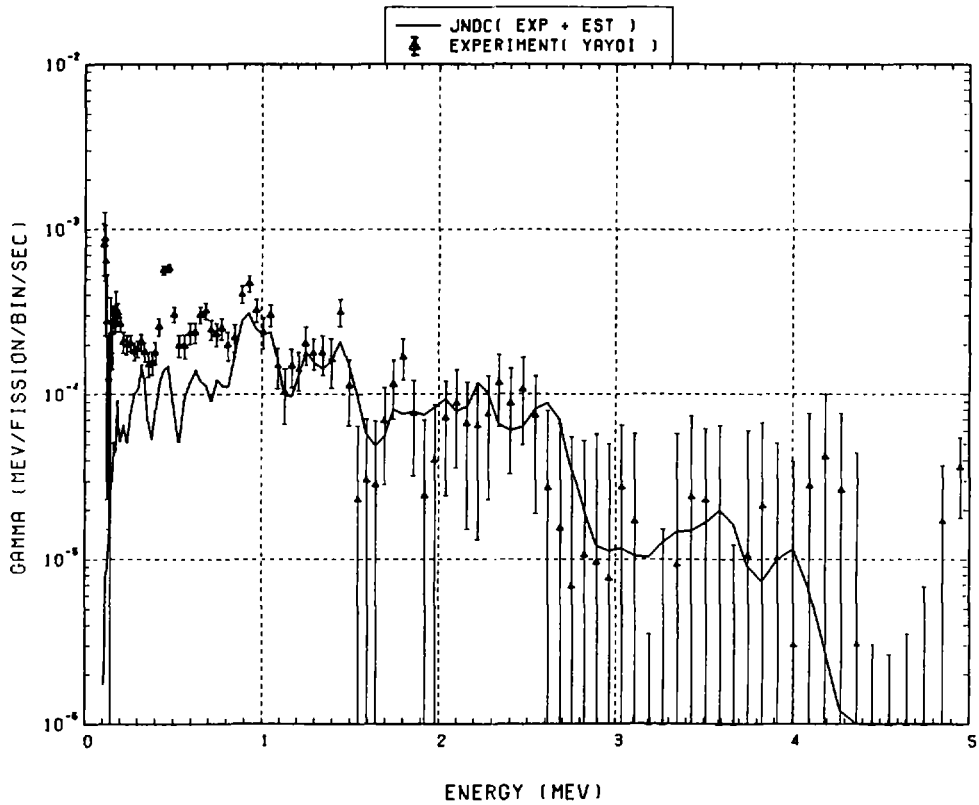

Fig. 211 Comparison of calculated gamma-ray energy spectrum with measured results at 1600 seconds after fast neutron fission of ^{232}Th. (t_{irrad} = 10 s, t_{wait} = 1395 s, t_{count} = 400 s)

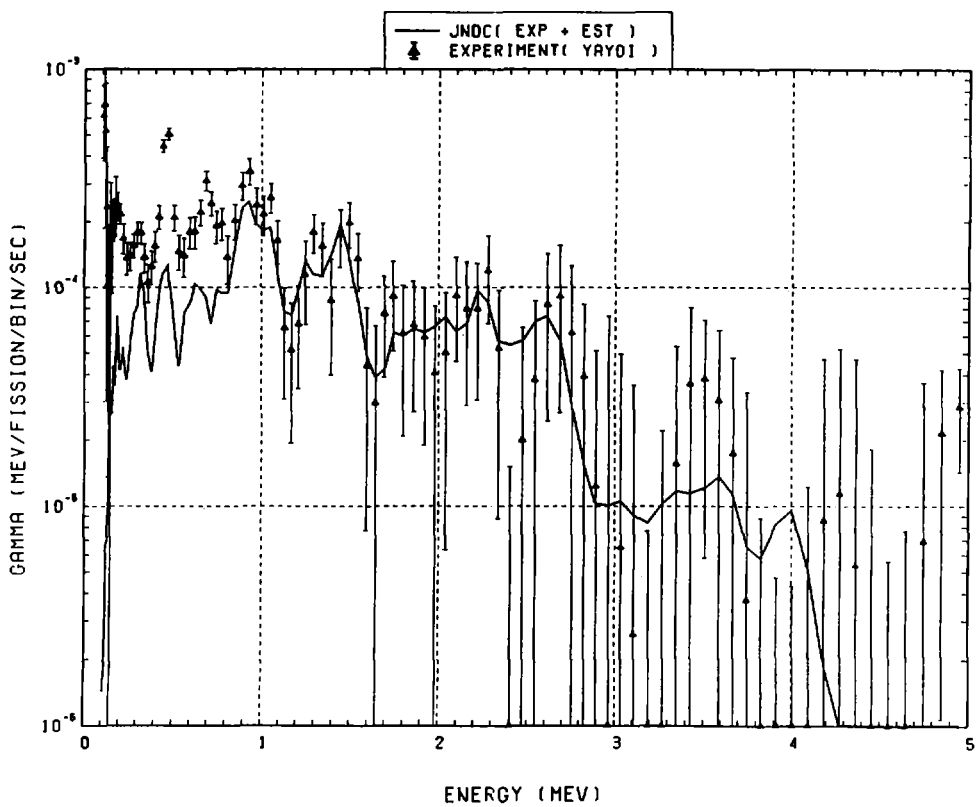

Fig. 212 Comparison of calculated gamma-ray energy spectrum with measured results at 2000 seconds after fast neutron fission of ^{232}Th. (t_{irrad} = 10 s, t_{wait} = 1795 s, t_{count} = 400 s)

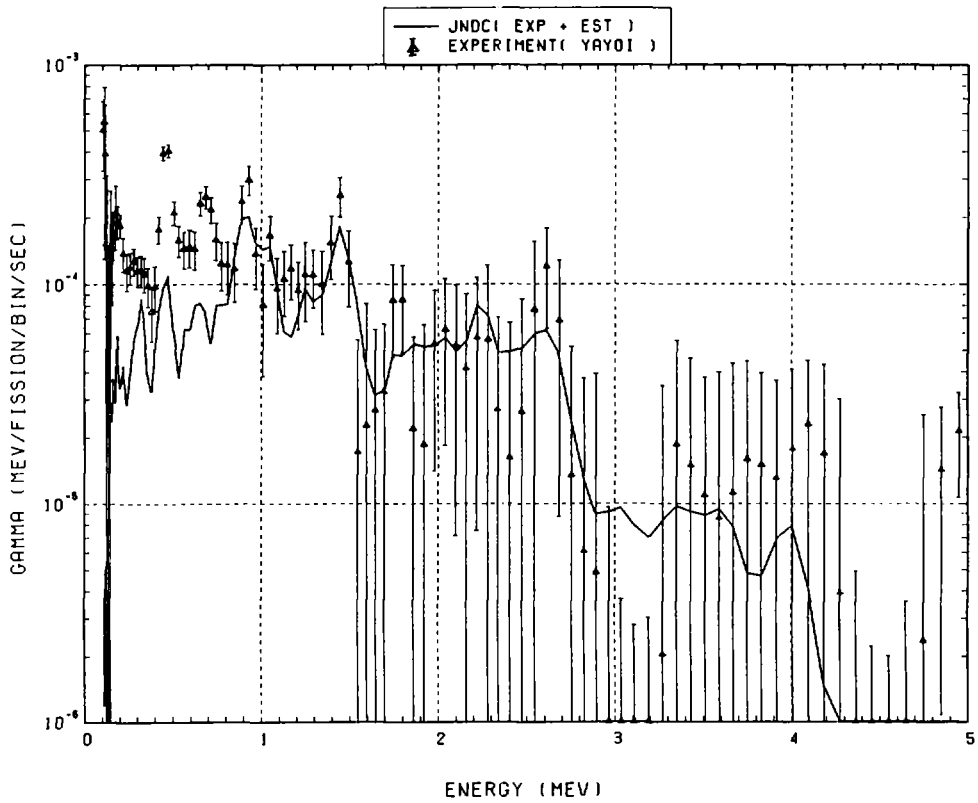

Fig. 213 Comparison of calculated gamma-ray energy spectrum with measured results at 2450 seconds after fast neutron fission of ^{232}Th. (t_{irrad} = 10 s, t_{wait} = 2195 s, t_{count} = 500 s)

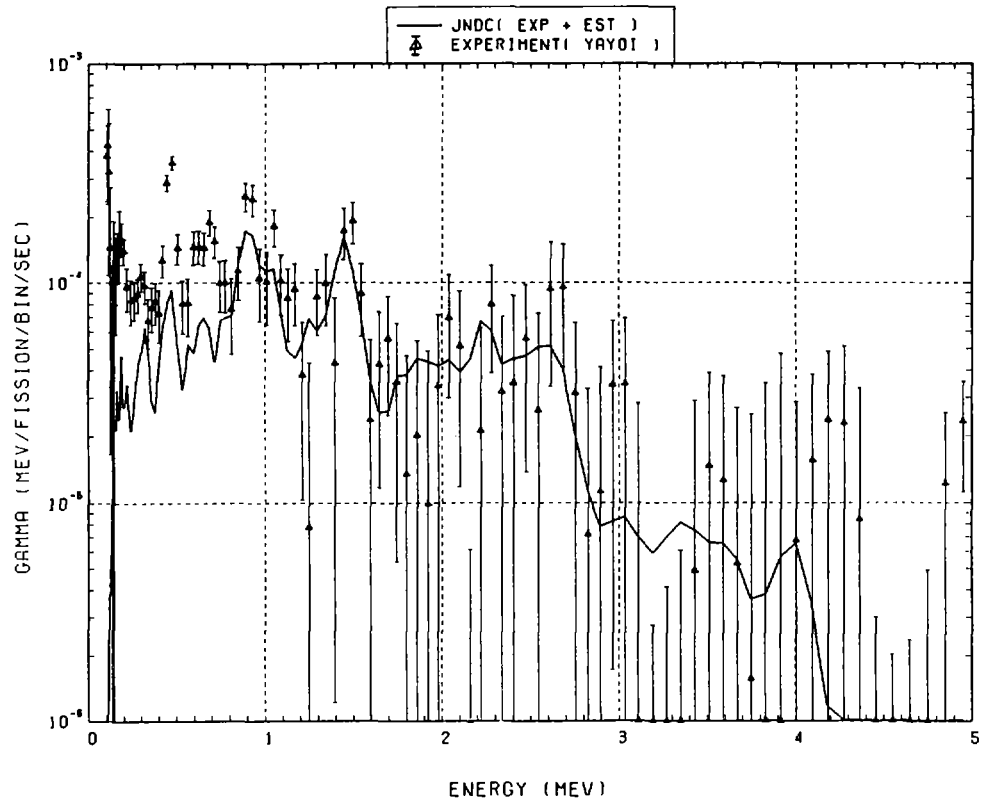

Fig. 214 Comparison of calculated gamma-ray energy spectrum with measured results at 2950 seconds after fast neutron fission of ^{232}Th. (t_{irrad} = 10 s, t_{wait} = 2695 s, t_{count} = 500 s)

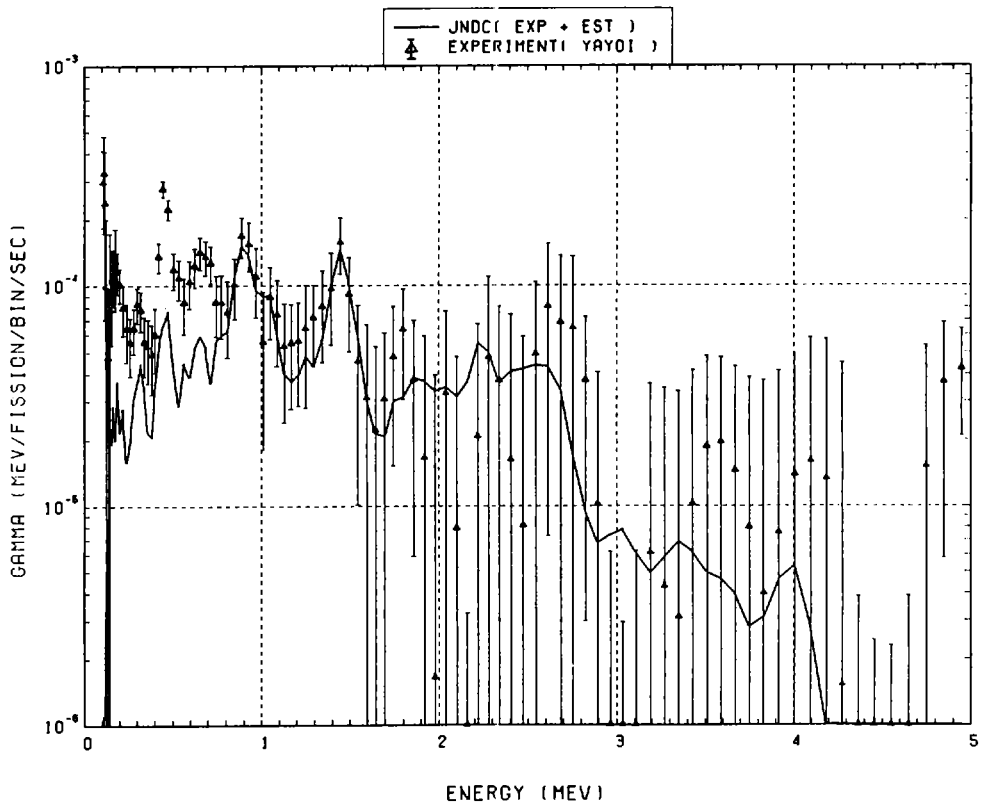

Fig. 215 Comparison of calculated gamma-ray energy spectrum with measured results at 3500 seconds after fast neutron fission of ^{232}Th. (t_{irrad} = 10 s, t_{wait} = 3195 s, t_{count} = 600 s)

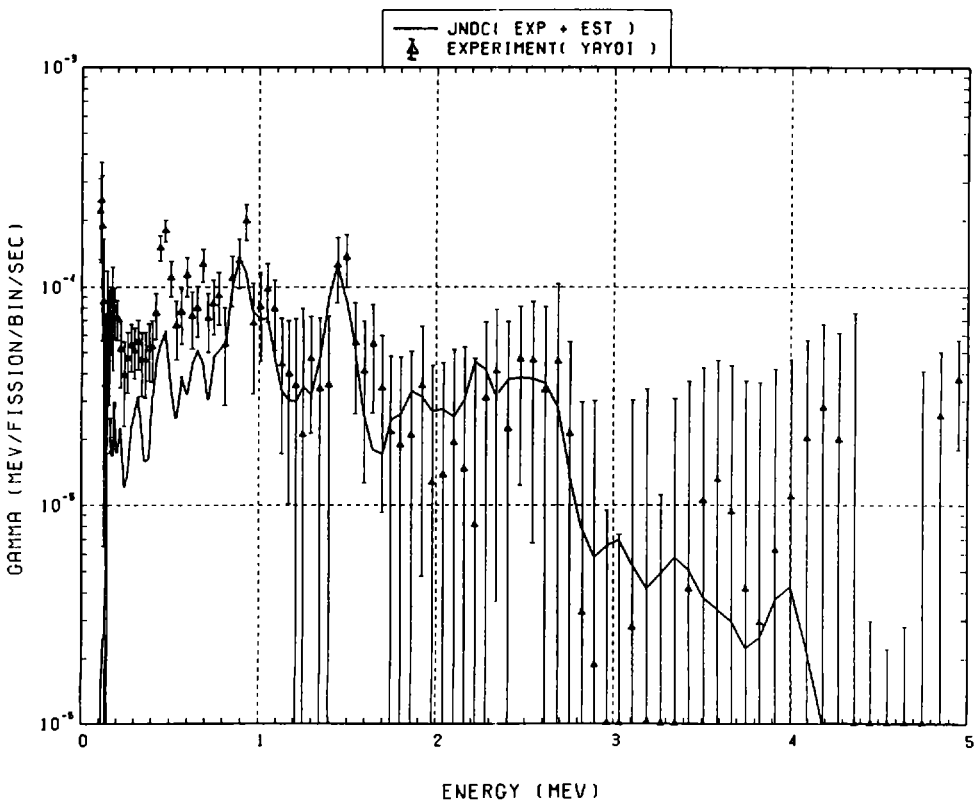

Fig. 216 Comparison of calculated gamma-ray energy spectrum with measured results at 4100 seconds after fast neutron fission of ^{232}Th. (t_{irrad} = 10 s, t_{wait} = 3795 s, t_{count} = 600 s)

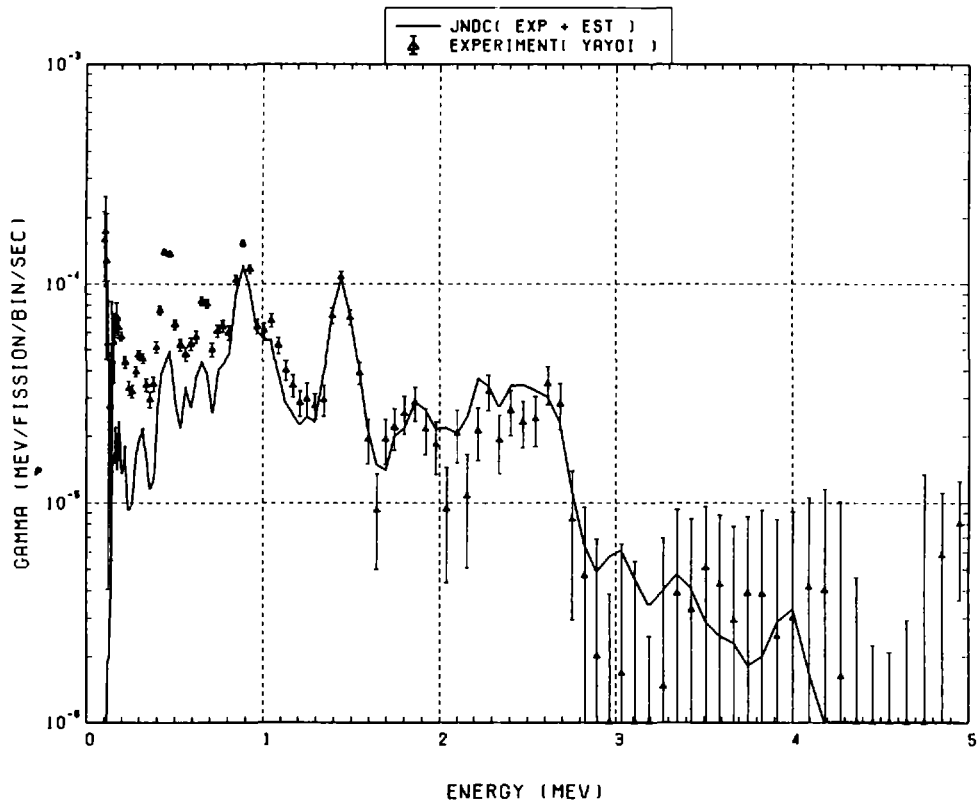

Fig. 217 Comparison of calculated gamma-ray energy spectrum with measured results at 4800 seconds after fast neutron fission of ^{232}Th. (t_{irrad} = 100 s, t_{wait} = 4350 s, t_{count} = 800 s)

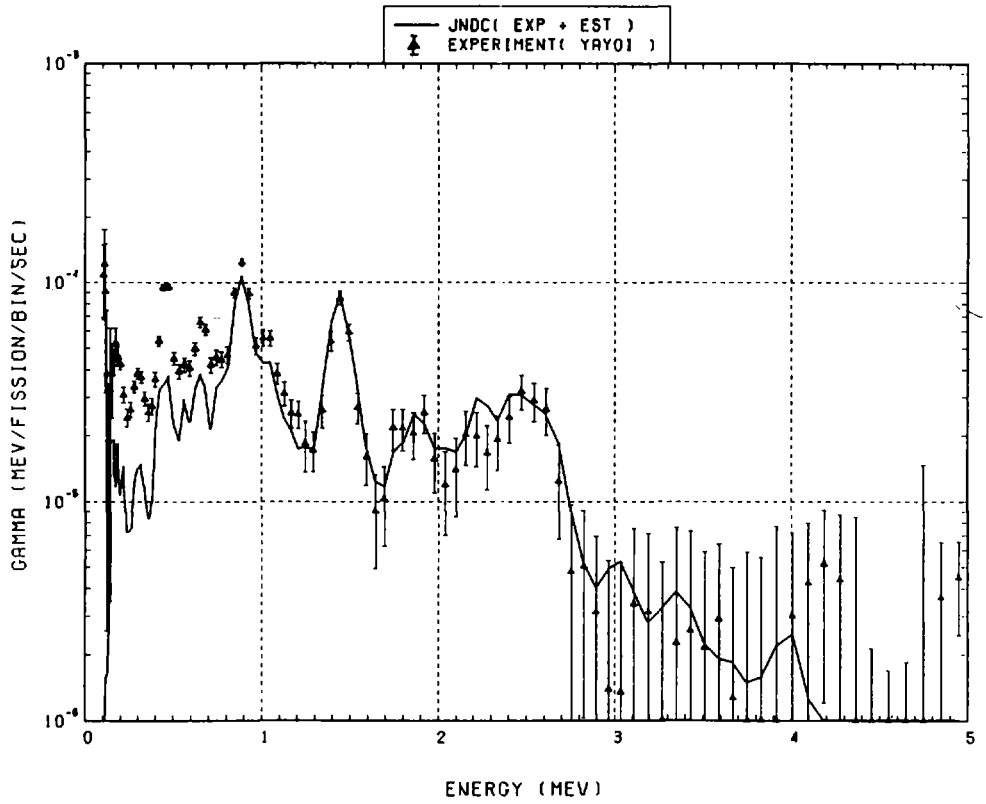

Fig. 218 Comparison of calculated gamma-ray energy spectrum with measured results at 5600 seconds after fast neutron fission of ^{232}Th. (t_{irrad} = 100 s, t_{wait} = 5150 s, t_{count} = 800 s)

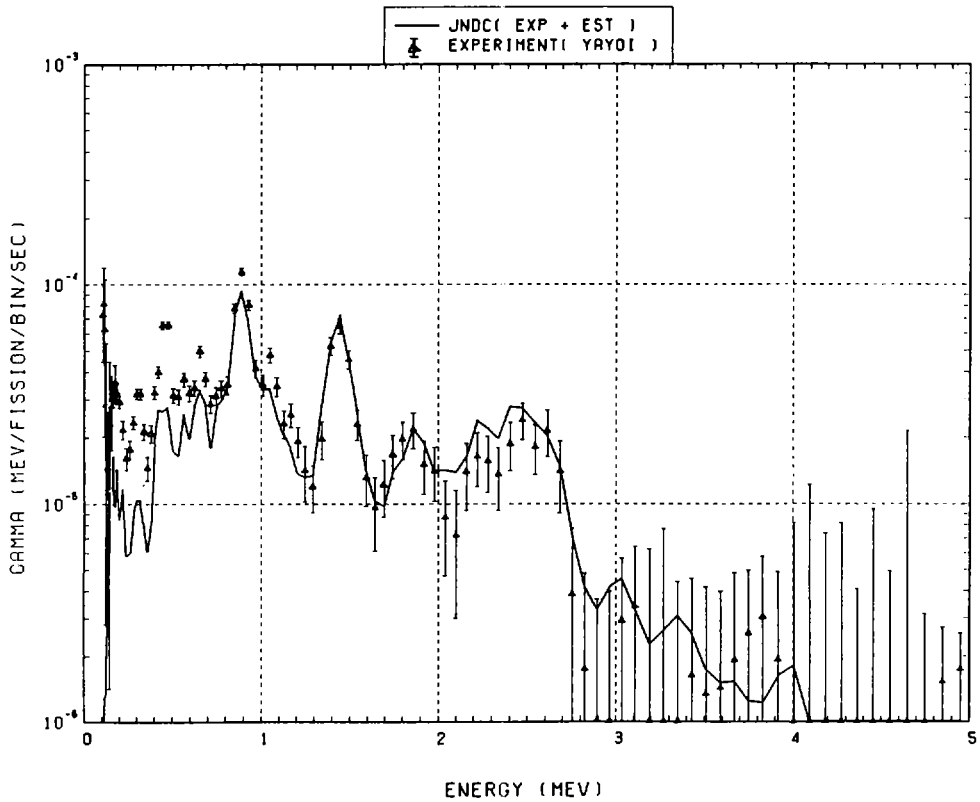

Fig. 219 Comparison of calculated gamma-ray energy spectrum with measured results at 6500 seconds after fast neutron fission of ^{232}Th. (t_{irrad} = 100 s, t_{wait} = 5950 s, t_{count} = 1000 s)

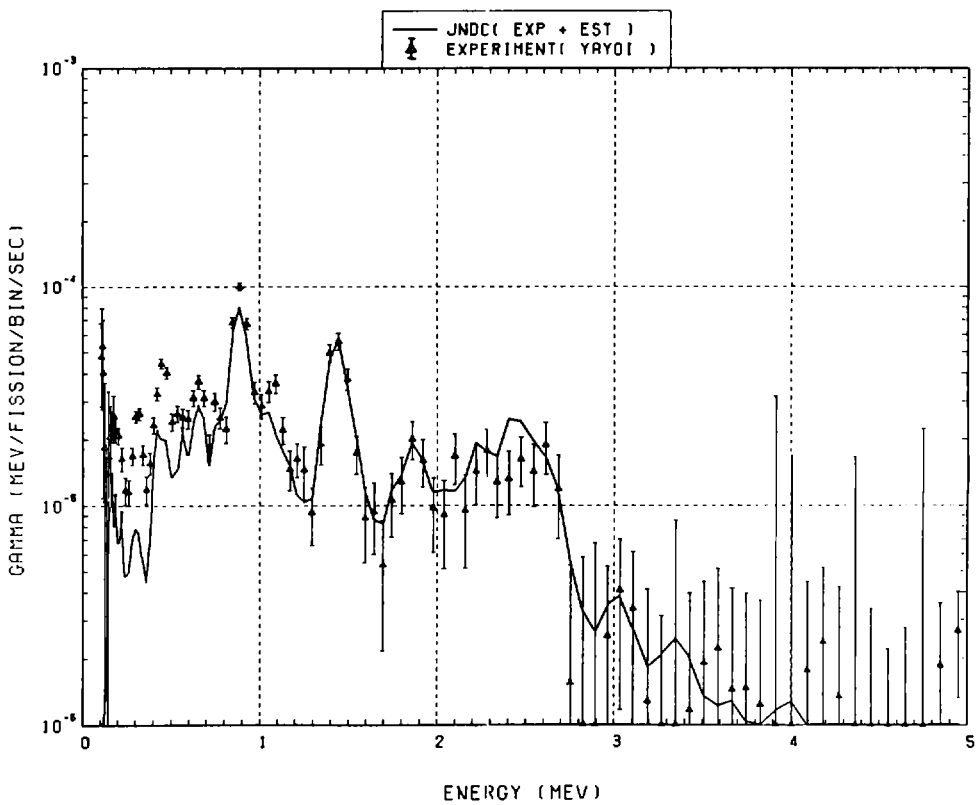

Fig. 220 Comparison of calculated gamma-ray energy spectrum with measured results at 7500 seconds after fast neutron fission of ^{232}Th. (t_{irrad} = 100 s, t_{wait} = 6950 s, t_{count} = 1000 s)

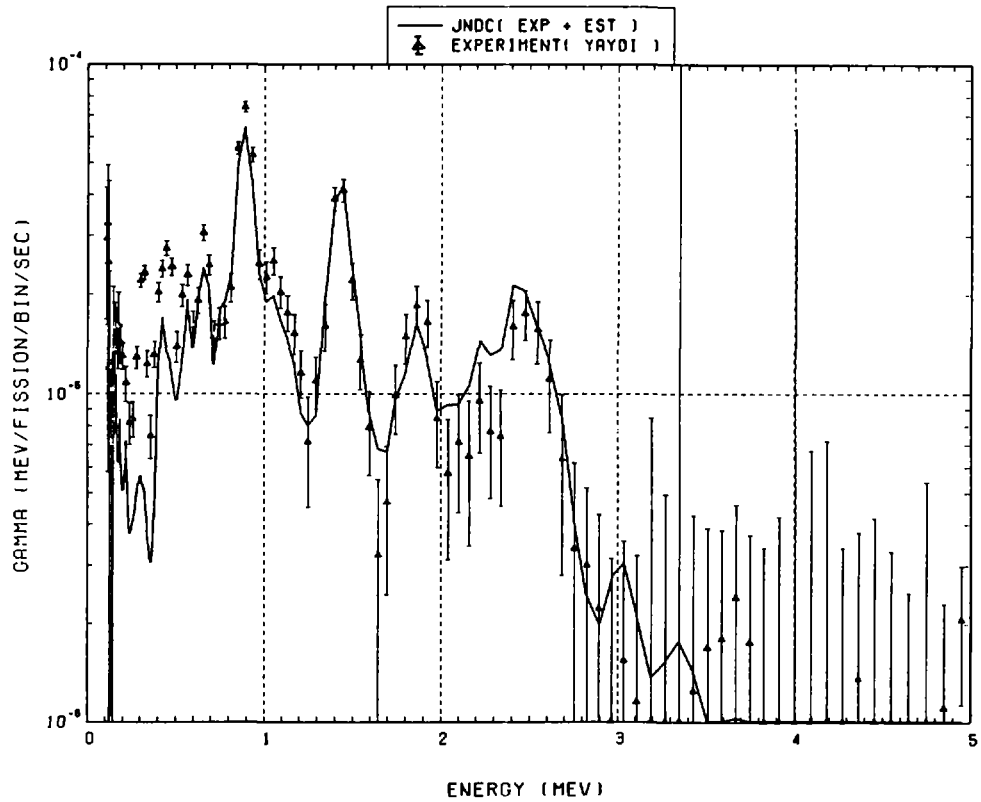

Fig. 221 Comparison of calculated gamma-ray energy spectrum with measured results at 9000 seconds after fast neutron fission of ^{232}Th. (t_{irrad} = 100 s, t_{wait} = 7950 s, t_{count} = 2000 s)

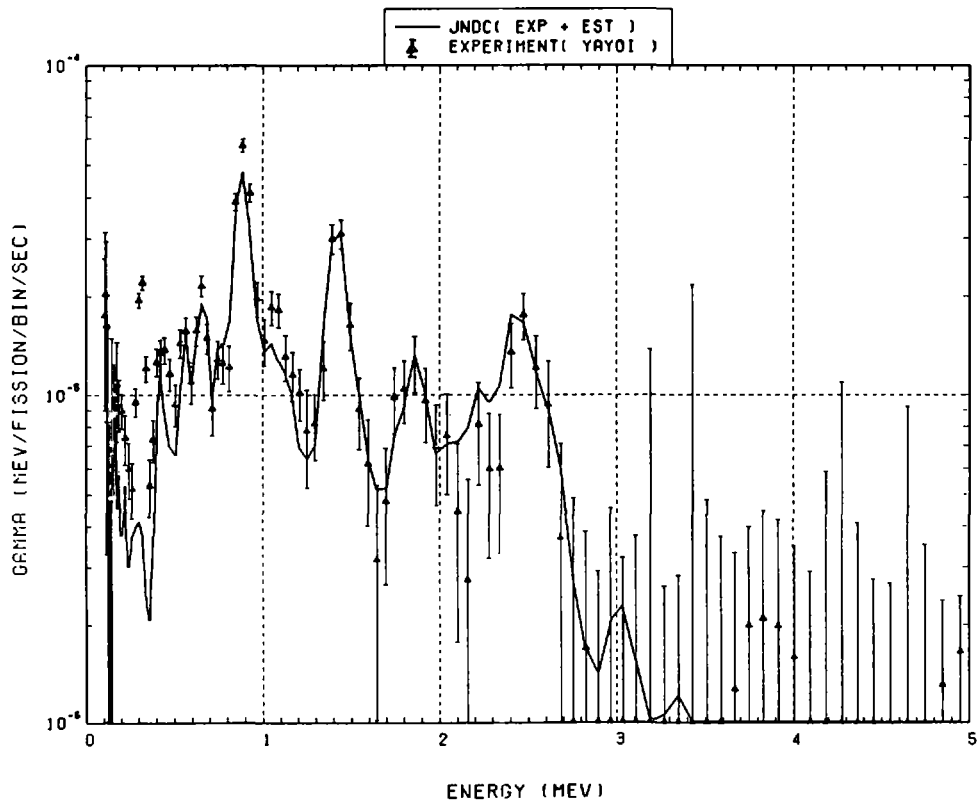

Fig. 222 Comparison of calculated gamma-ray energy spectrum with measured results at 11000 seconds after fast neutron fission of ^{232}Th. (t_{irrad} = 100 s, t_{wait} = 9950 s, t_{count} = 2000 s)

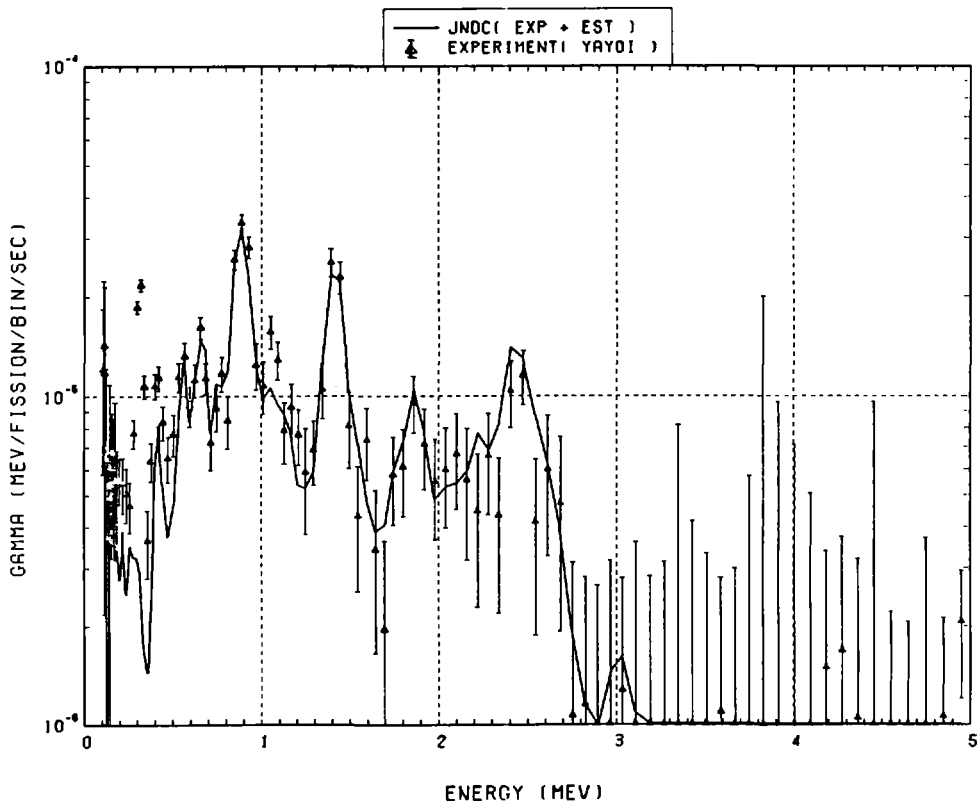

Fig. 223 Comparison of calculated gamma-ray energy spectrum with measured results at 13500 seconds after fast neutron fission of ^{232}Th. (t_{irrad} = 100 s, t_{wait} = 11950 s, t_{count} = 3000 s)

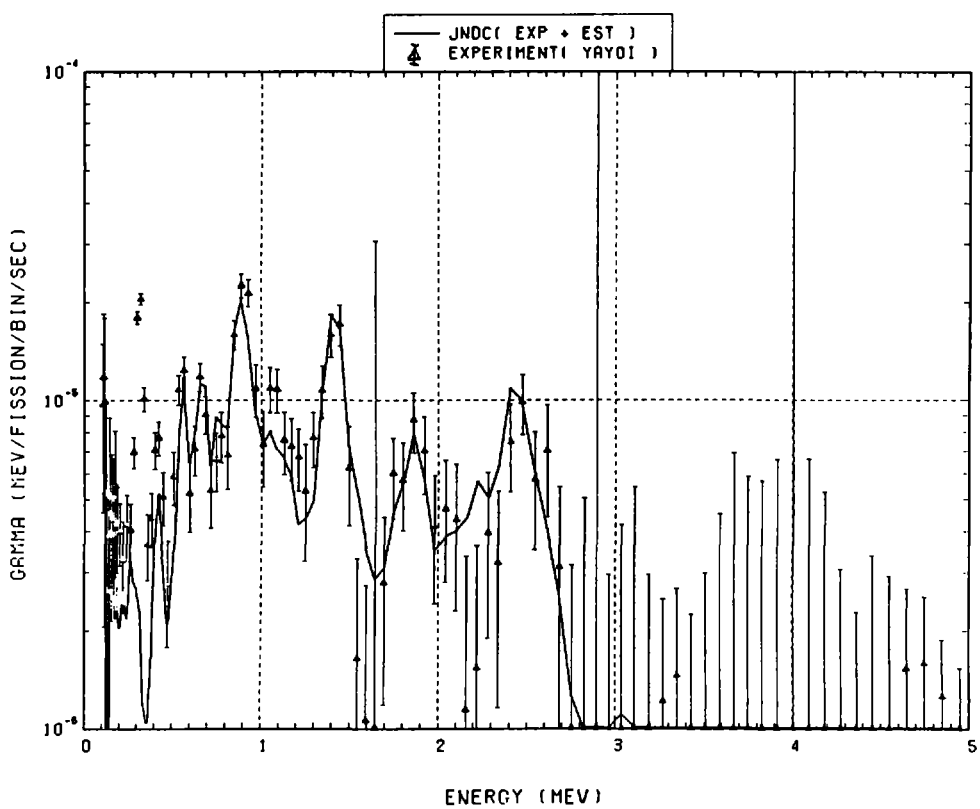

Fig. 224 Comparison of calculated gamma-ray energy spectrum with measured results at 16500 seconds after fast neutron fission of ^{232}Th. (t_{irrad} = 100 s, t_{wait} = 14950 s, t_{count} = 3000 s)

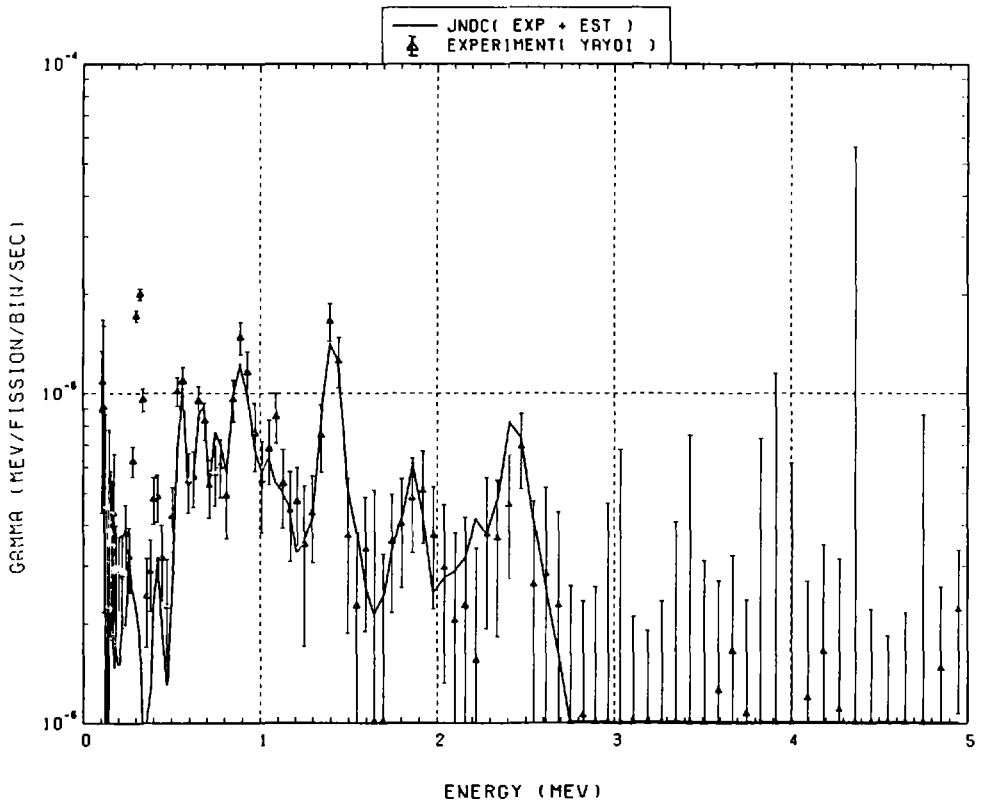

Fig. 225 Comparison of calculated gamma-ray energy spectrum with measured results at 20000 seconds after fast neutron fission of ^{232}Th. (t_{irrad} = 100 s, t_{wait} = 17950 s, t_{count} = 4000 s)

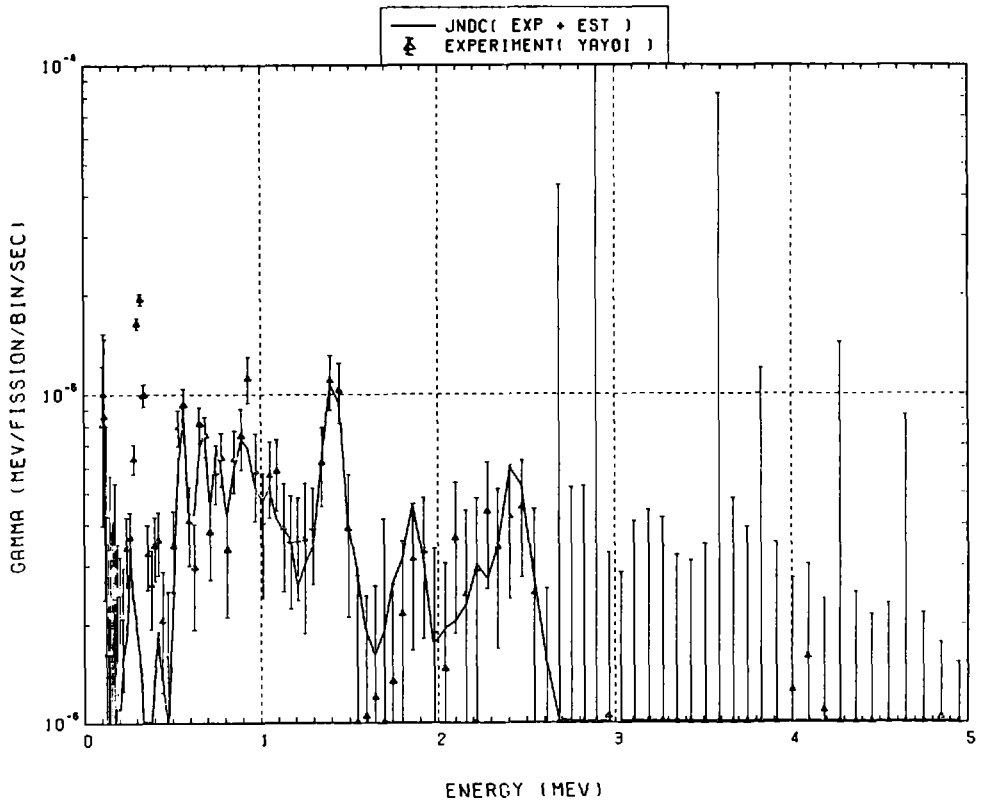

Fig. 226 Comparison of calculated gamma-ray energy spectrum with measured results at 24000 seconds after fast neutron fission of ^{232}Th. (t_{irrad} = 100 s, t_{wait} = 21950 s, t_{count} = 4000 s)

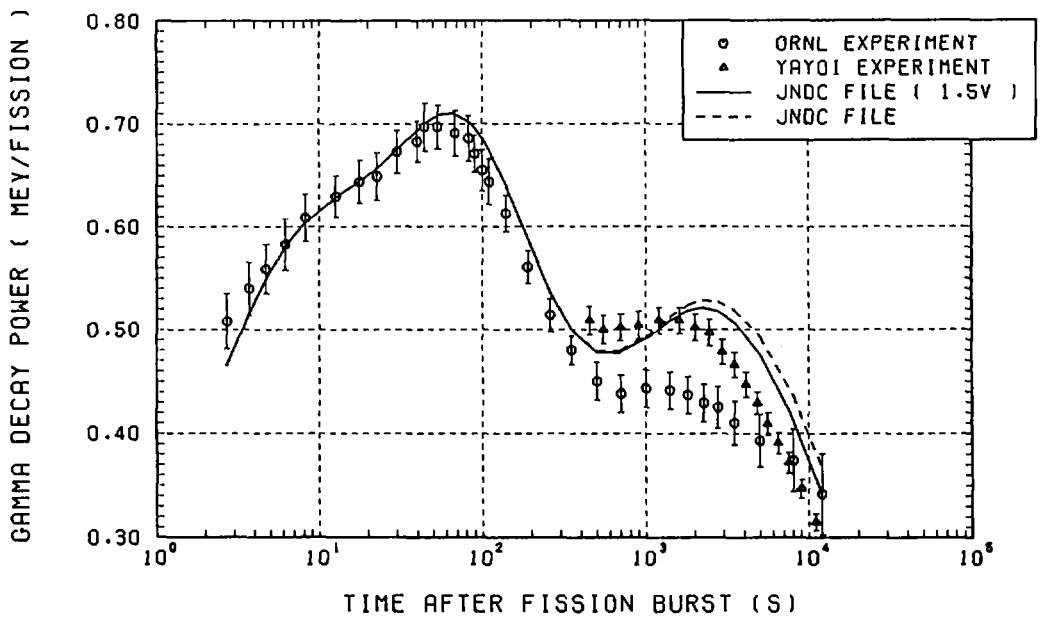

Fig. 227 Comparison of calculated gamma-decay heat with measured results at ORNL and at YAYOI for thermal neutron fission of ^{235}U.

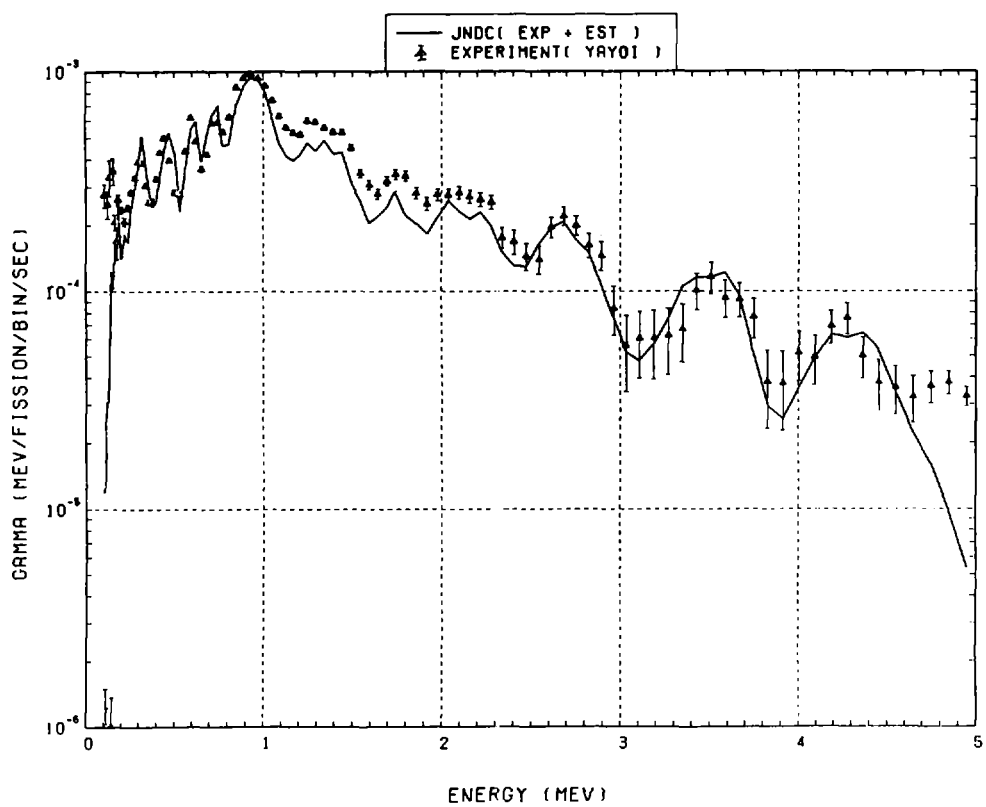

Fig. 228 Comparison of calculated gamma-ray energy spectrum with measured results at 450 seconds after thermal neutron fission of ^{235}U (YAYOI). (t_{irrad} = 100 s, t_{wait} = 355 s, t_{count} = 90 s)

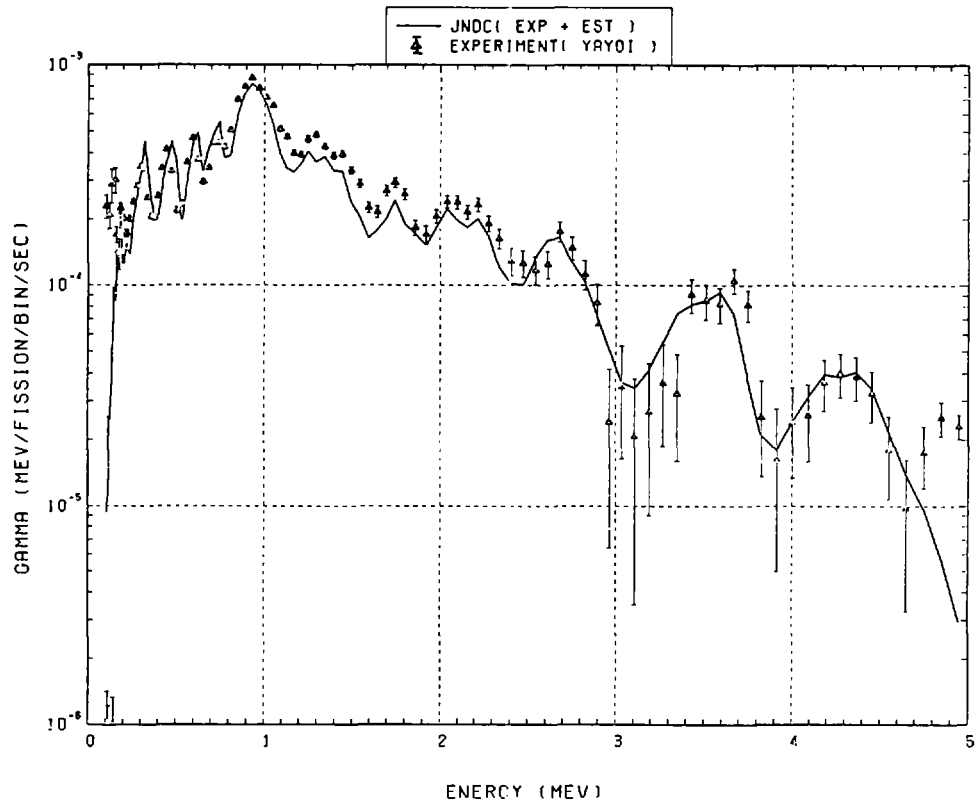

Fig. 229 Comparison of calculated gamma-ray energy spectrum with measured results at 550 seconds after thermal neutron fission of ^{235}U (YAYOI). (t_{irrad} = 100 s, t_{wait} = 450 s, t_{count} = 100 s)

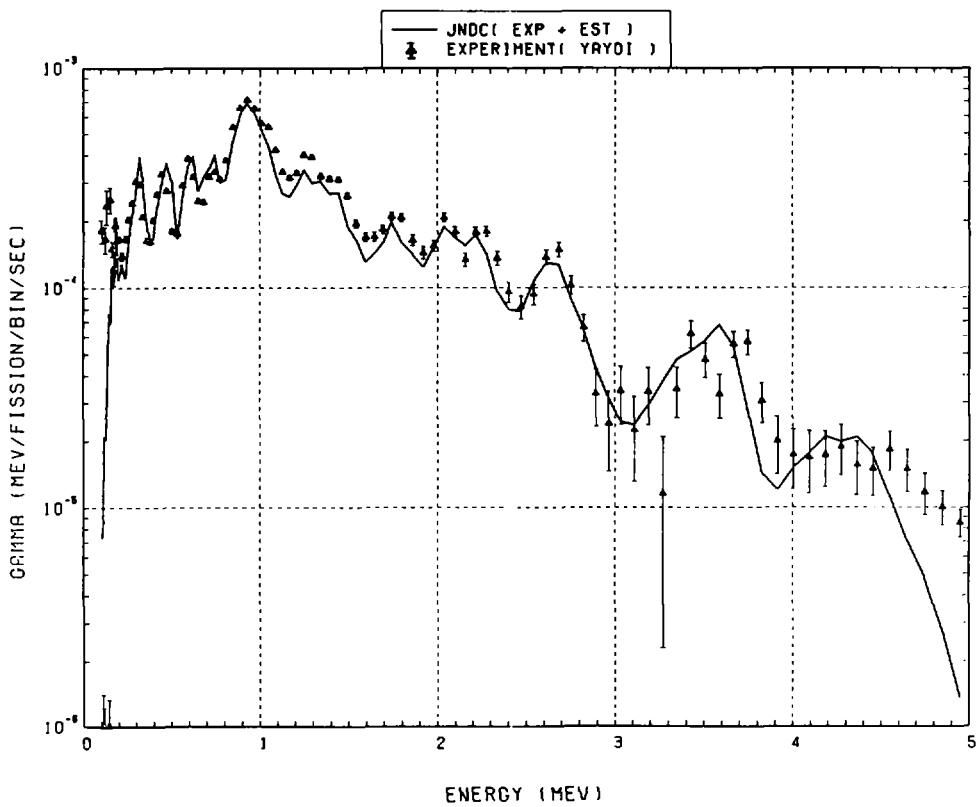

Fig. 230 Comparison of calculated gamma-ray energy spectrum with measured results at 700 seconds after thermal neutron fission of ^{235}U (YAYOI). (t_{irrad} = 100 s, t_{wait} = 550 s, t_{count} = 200 s)

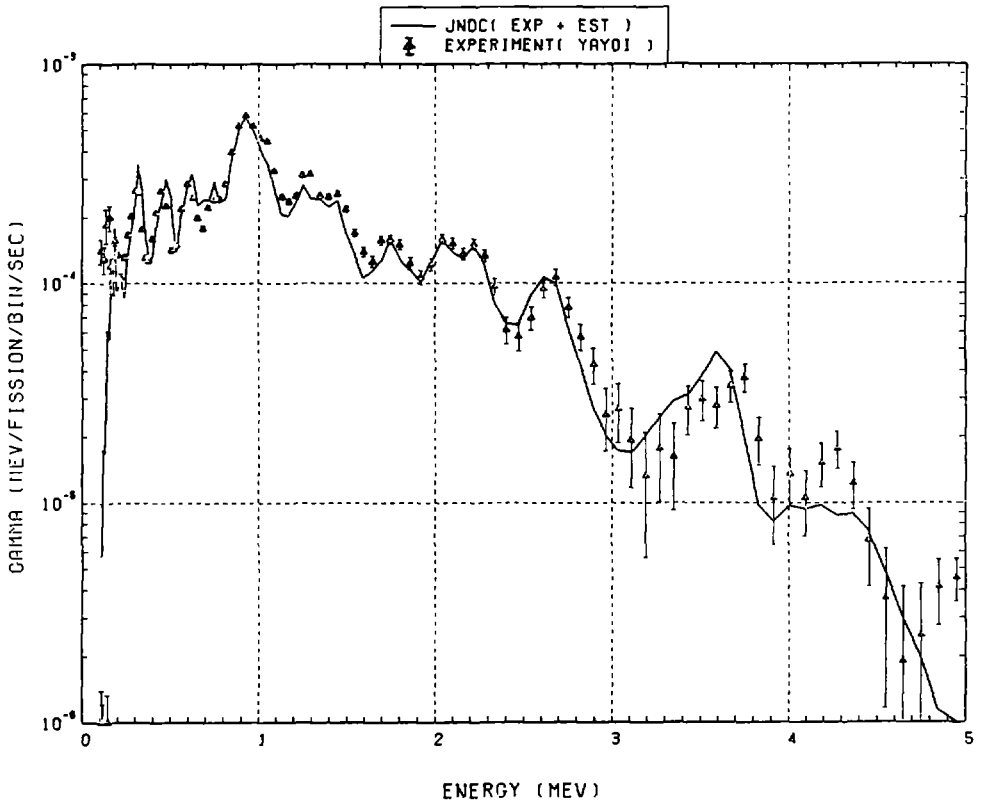

Fig. 231 Comparison of calculated gamma-ray energy spectrum with measured results at 900 seconds after thermal neutron fission of ^{235}U (YAYOI). (t_{irrad} = 100 s, t_{wait} = 750 s, t_{count} = 200 s)

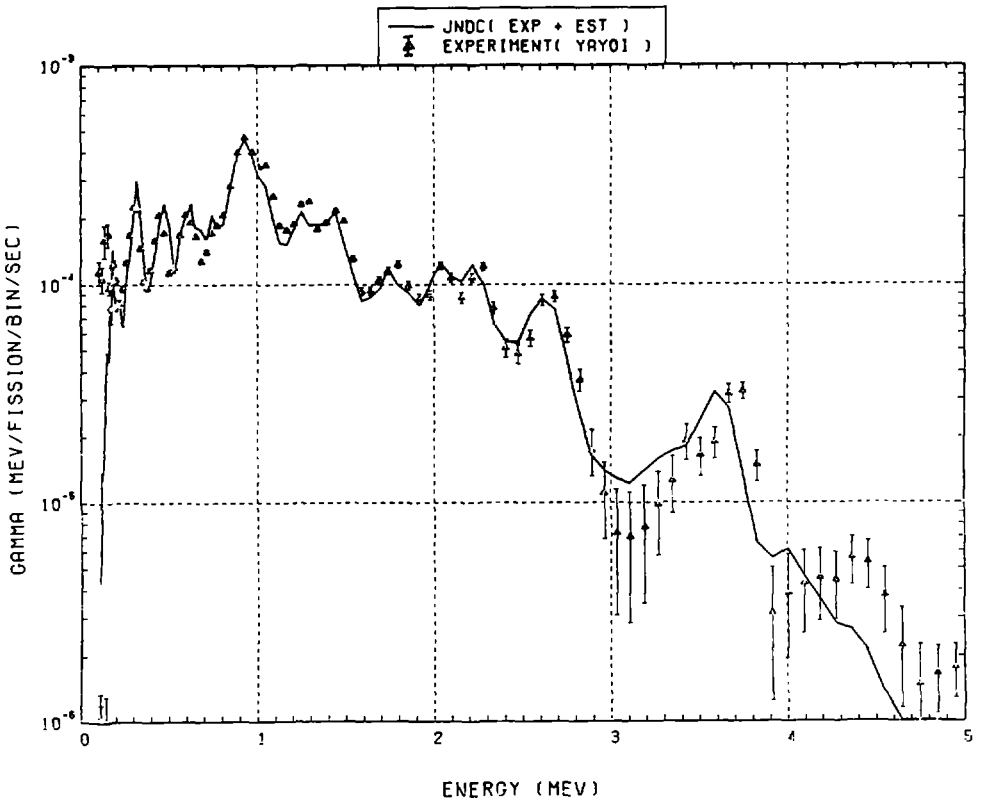

Fig. 232 Comparison of calculated gamma-ray energy spectrum with measured results at 1200 seconds after thermal neutron fission of ^{235}U (YAYOI). (t_{irrad} = 100 s, t_{wait} = 950 s, t_{count} = 400 s)

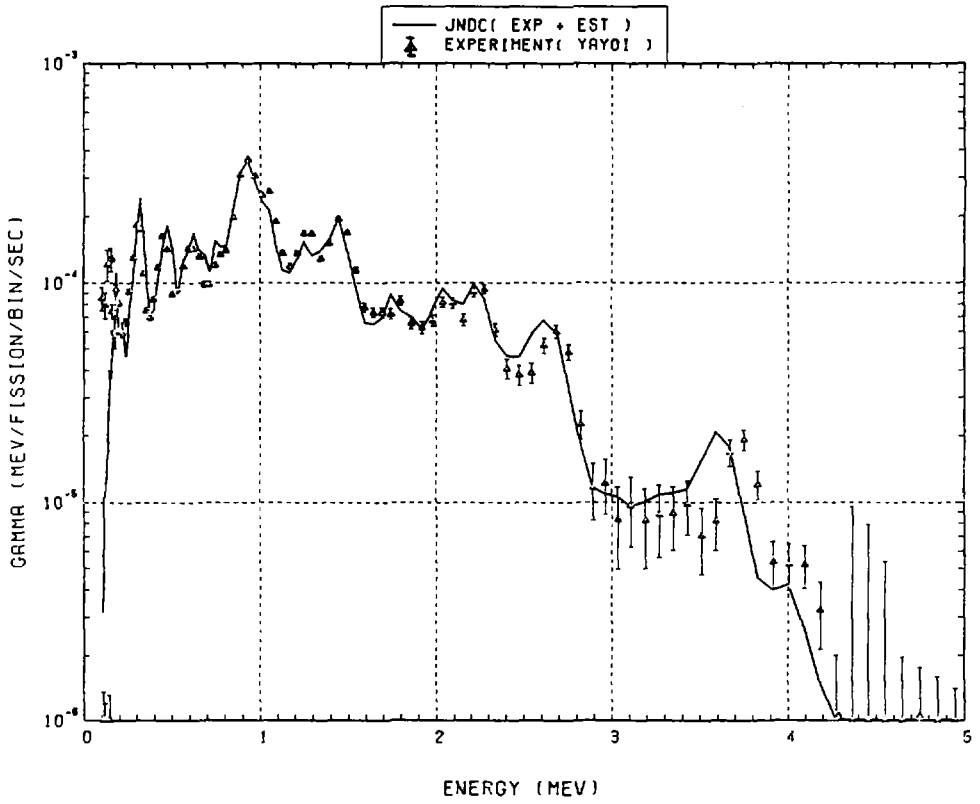

Fig. 233 Comparison of calculated gamma-ray energy spectrum with measured results at 1600 seconds after thermal neutron fission of ^{235}U (YAYOI). (t_{irrad} = 100 s, t_{wait} = 1350 s, t_{count} = 400 s)

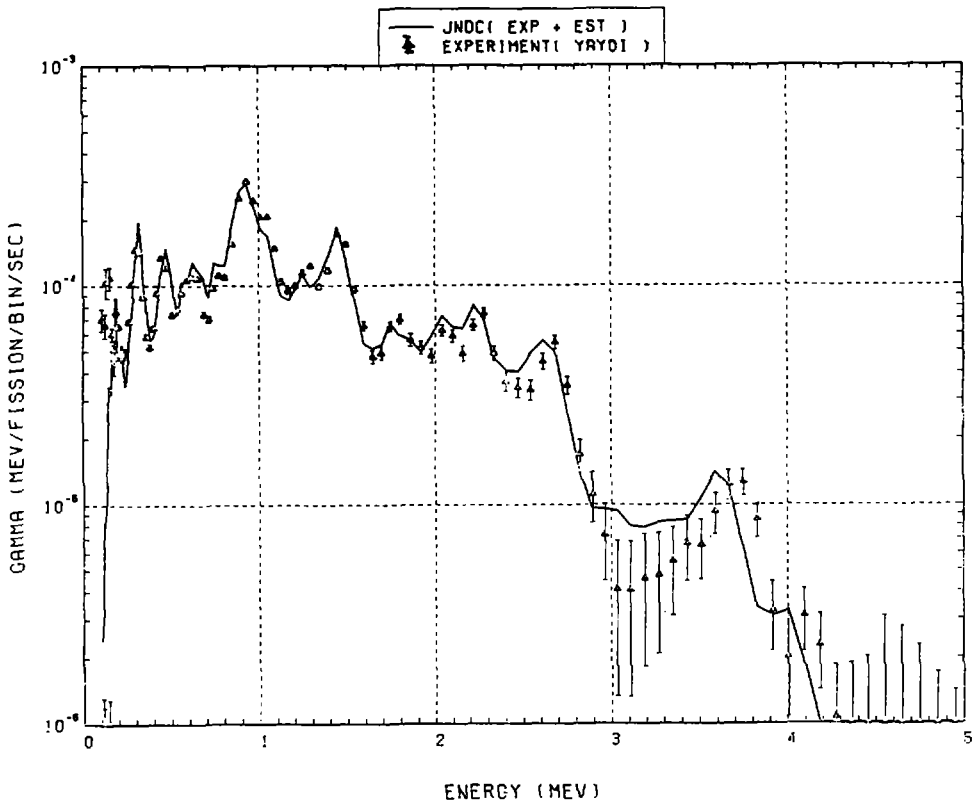

Fig. 234 Comparison of calculated gamma-ray energy spectrum with measured results at 2000 seconds after thermal neutron fission of ^{235}U (YAYOI). (t_{irrad} = 100 s, t_{wait} = 1750 s, t_{count} = 400 s)

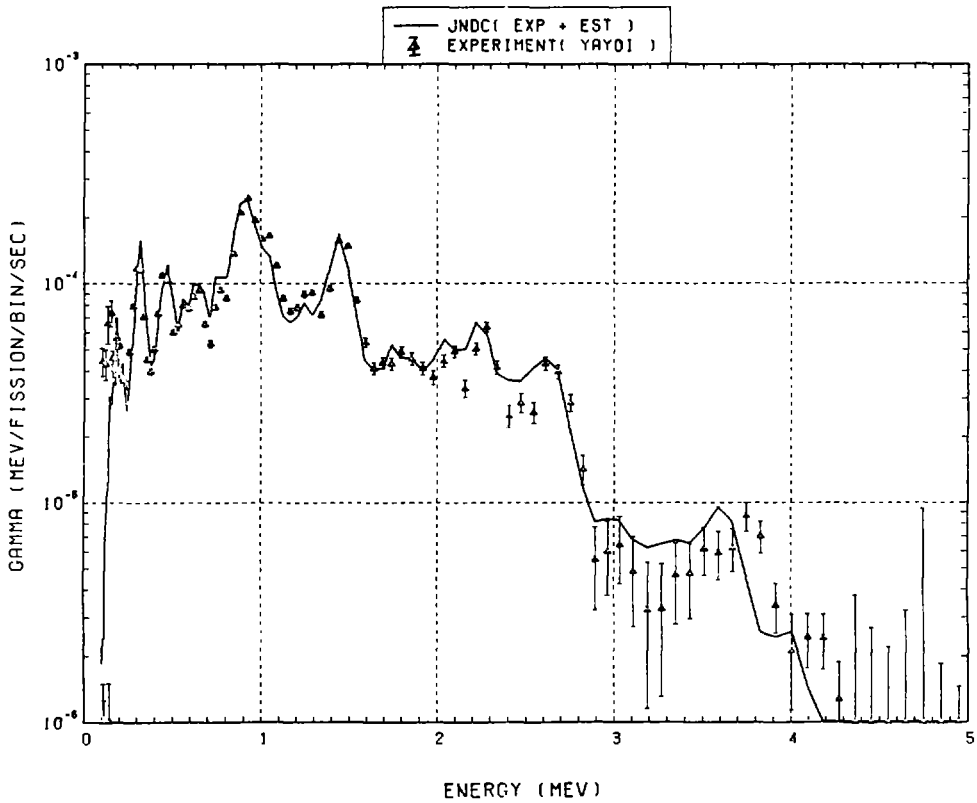

Fig. 235 Comparison of calculated gamma-ray energy spectrum with measured results at 2450 seconds after thermal neutron fission of ^{235}U (YAYOI). (t_{irrad} = 100 s, t_{wait} = 2150 s, t_{count} = 500 s)

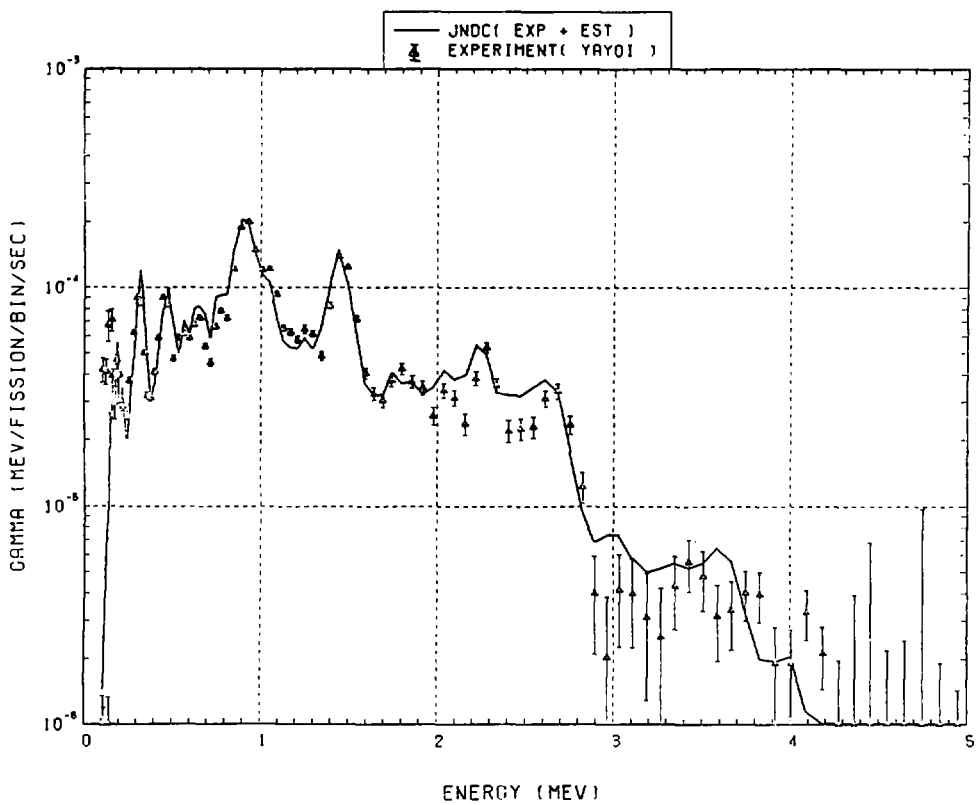

Fig. 236 Comparison of calculated gamma-ray energy spectrum with measured results at 2950 seconds after thermal neutron fission of ^{235}U (YAYOI). (t_{irrad} = 100 s, t_{wait} = 2650 s, t_{count} = 500 s)

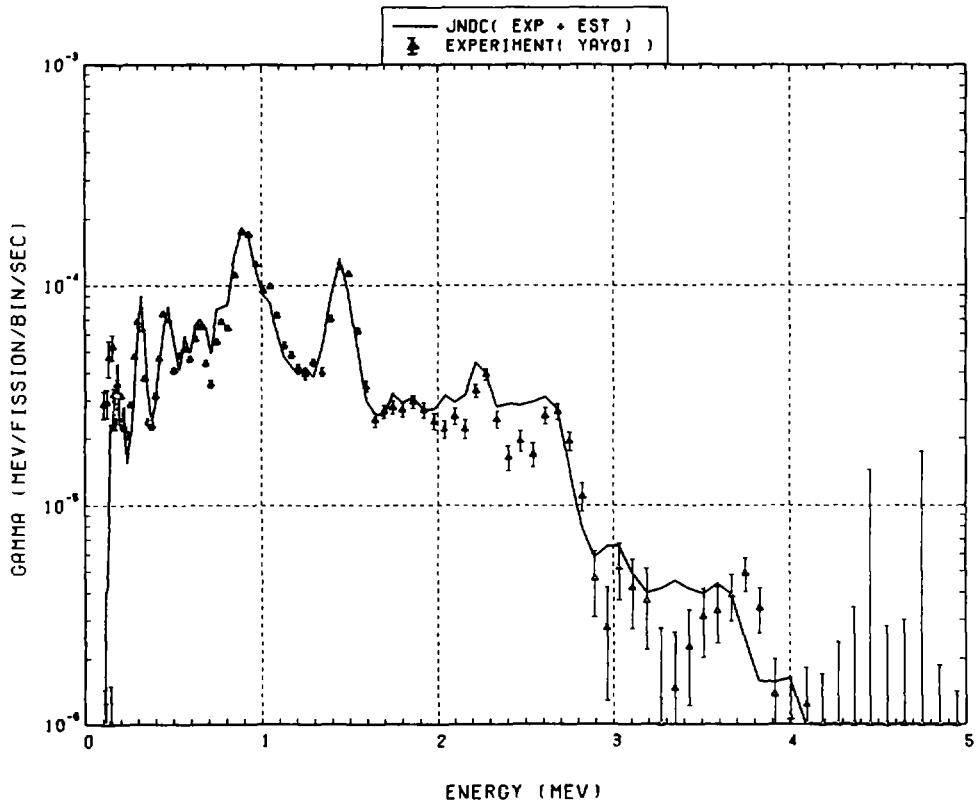

Fig. 237 Comparison of calculated gamma-ray energy spectrum with measured results at 3500 seconds after thermal neutron fission of ^{235}U (YAYOI). (t_{irrad} = 100 s, t_{wait} = 3150 s, t_{count} = 600 s)

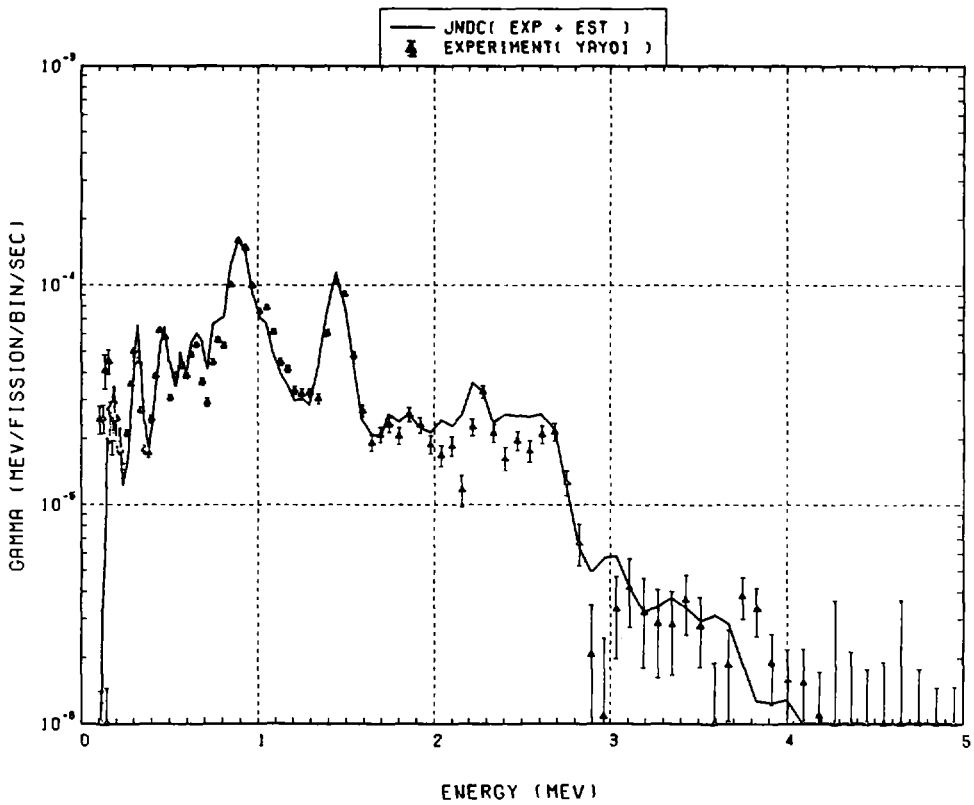

Fig. 238 Comparison of calculated gamma-ray energy spectrum with measured results at 4100 seconds after thermal neutron fission of ^{235}U (YAYOI). (t_{irrad} = 100 s, t_{wait} = 3750 s, t_{count} = 600 s)

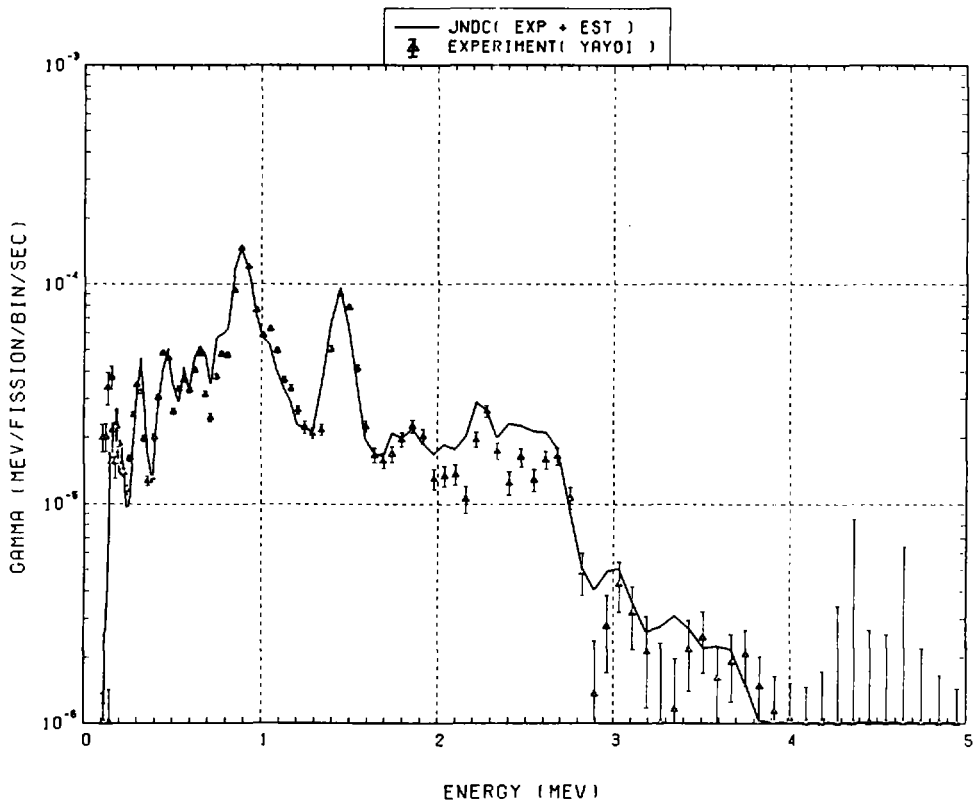

Fig. 239 Comparison of calculated gamma-ray energy spectrum with measured results at 4800 seconds after thermal neutron fission of ^{235}U (YAYOI). (t_{irrad} = 100 s, t_{wait} = 4350 s, t_{count} = 800 s)

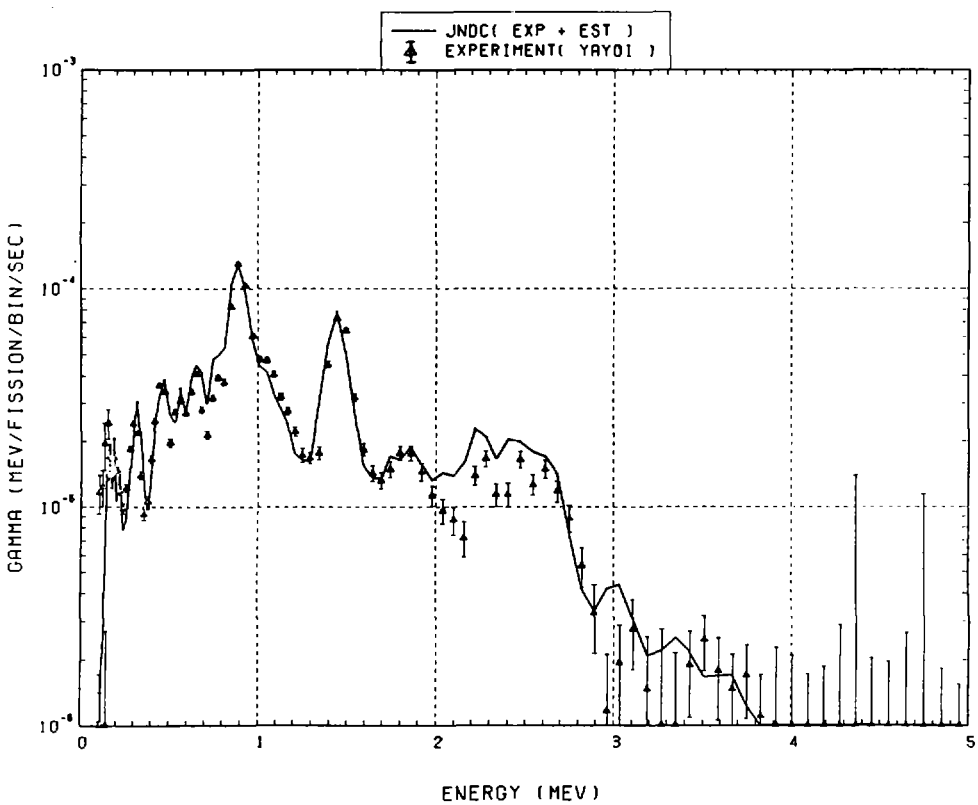

Fig. 240 Comparison of calculated gamma-ray energy spectrum with measured results at 5600 seconds after thermal neutron fission of ^{235}U (YAYOI). (t_{irrad} = 100 s, t_{wait} = 5150 s, t_{count} = 800 s)

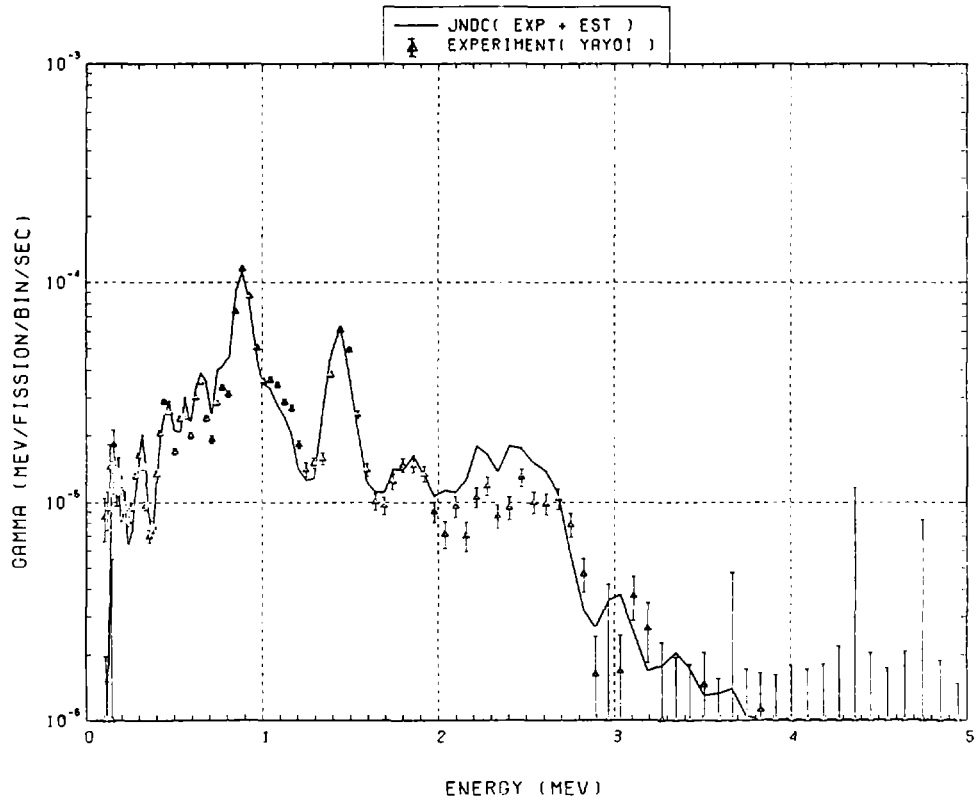

Fig. 241 Comparison of calculated gamma-ray energy spectrum with measured results at 6500 seconds after thermal neutron fission of ^{235}U (YAYOI). (t_{irrad} = 100 s, t_{wait} = 5950 s, t_{count} = 1000 s)

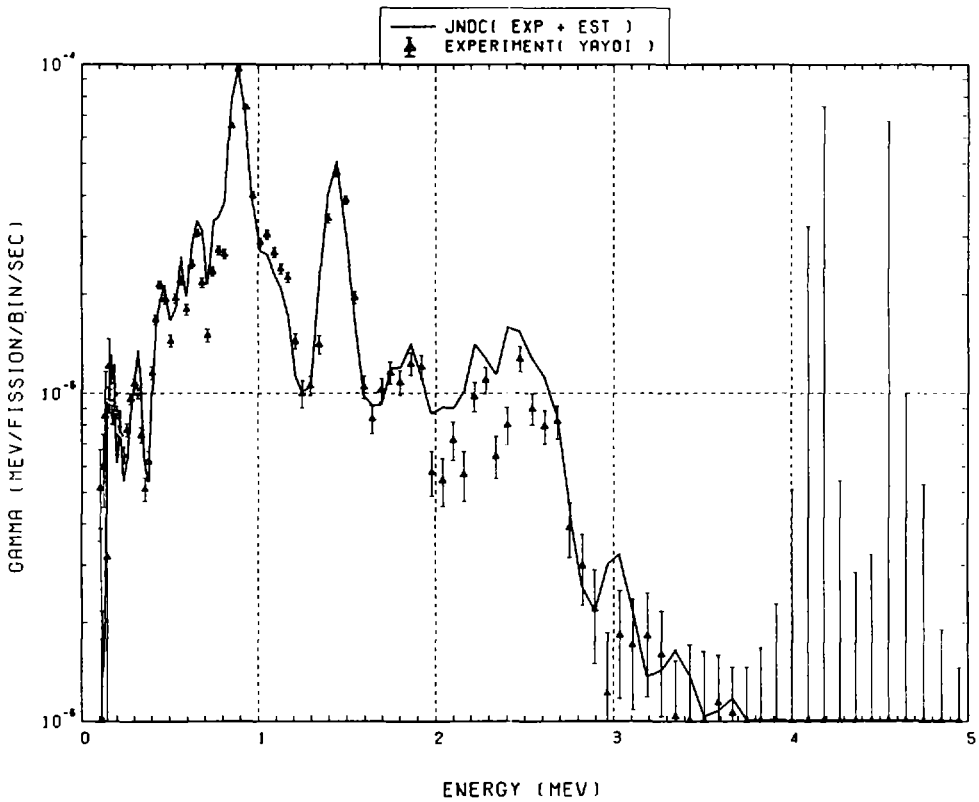

Fig. 242 Comparison of calculated gamma-ray energy spectrum with measured results at 7500 seconds after thermal neutron fission of ^{235}U (YAYOI). (t_{irrad} = 100 s, t_{wait} = 6950 s, t_{count} = 1000 s)

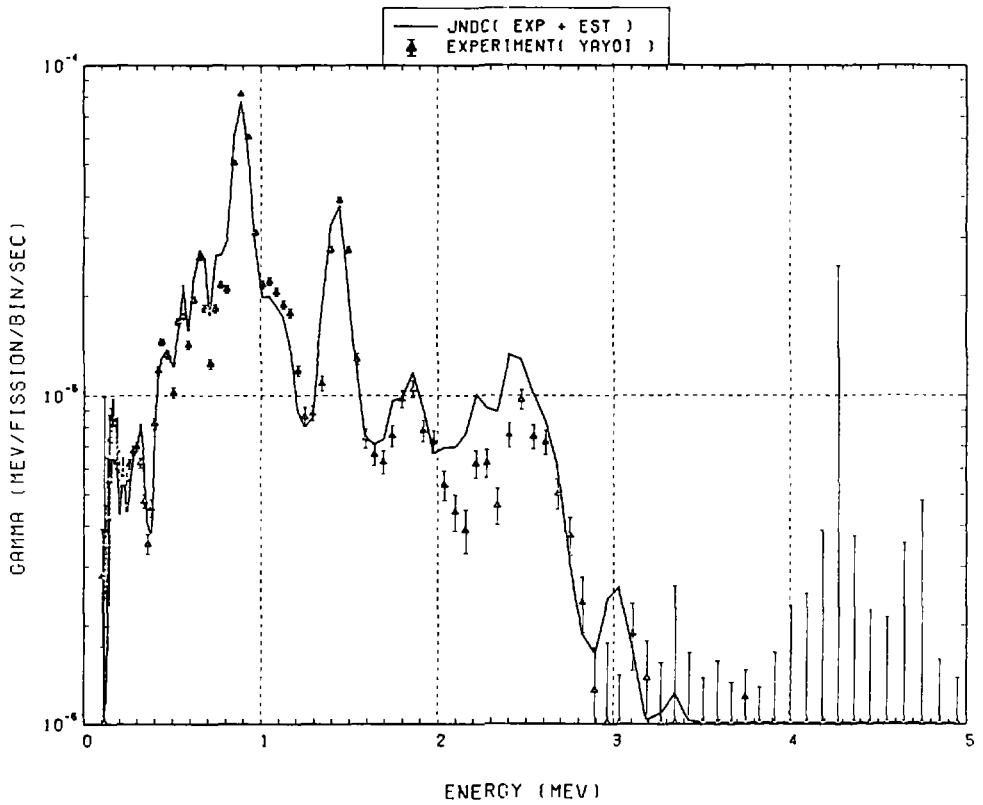

Fig. 243 Comparison of calculated gamma-ray energy spectrum with measured results at 9000 seconds after thermal neutron fission of ^{235}U (YAYOI). (t_{irrad} = 100 s, t_{wait} = 7950 s, t_{count} = 2000 s)

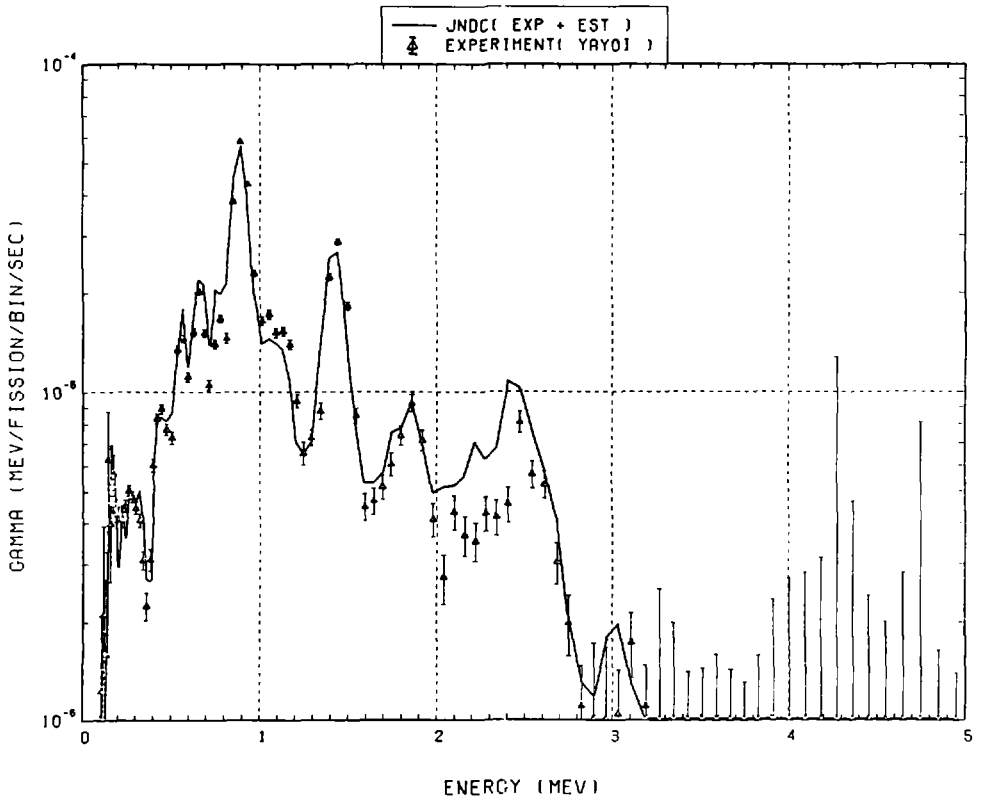

Fig. 244 Comparison of calculated gamma-ray energy spectrum with measured results at 11000 seconds after thermal neutron fission of ^{235}U (YAYOI).
(t_{irrad} = 100 s, t_{wait} = 9950 s, t_{count} = 2000 s)

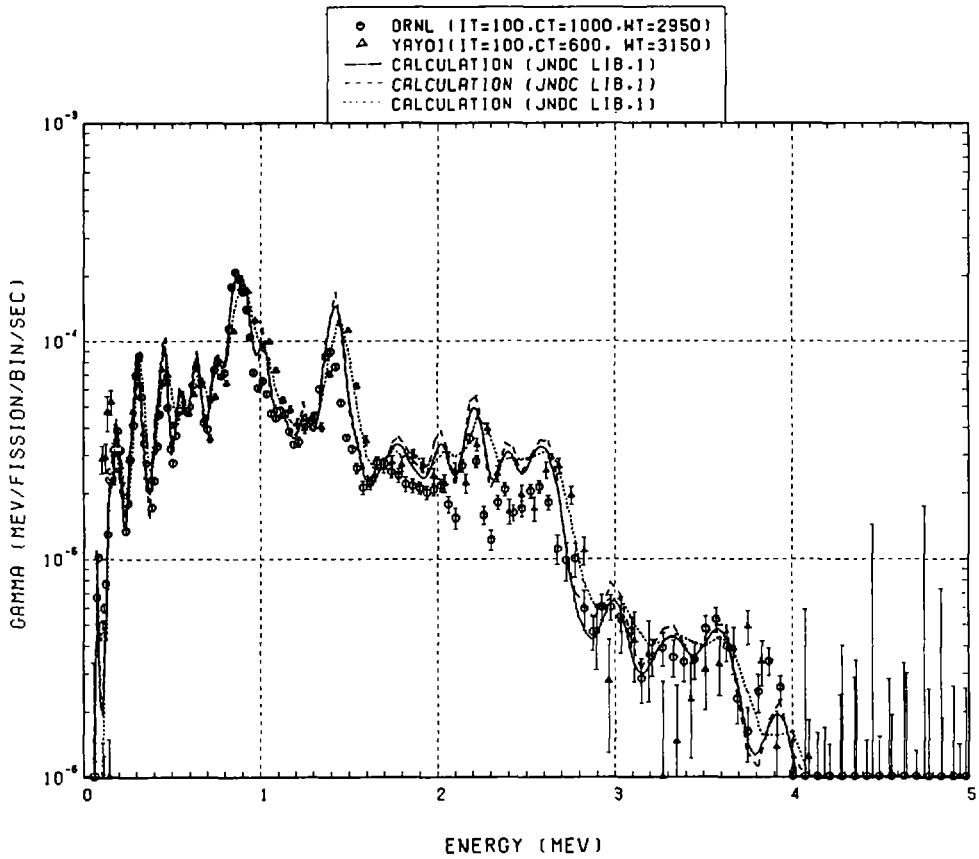

Fig. 245 Comparison between measurements at same cooling time 3500 (= $t_{wait} + \frac{1}{2}(t_{irrad} + t_{count})$). Open circles indicate the ORNL measurements and triangles are the YAYOI measurements. Solid line is the calculation with very fine energy group structure (about 1300 energy groups below 5 MeV) and with the same detector response as that of the ORNL measurement. Dashed line indicates the calculation with the same energy group structure and the same detector response as those of the ORNL measurement. Dotted line shows the calculation with the same energy group structure and the same detector response as those of the YAYOI measurement.

国際単位系 (SI) と換算表

表 1　SI 基本単位および補助単位

量	名称	記号
長さ	メートル	m
質量	キログラム	kg
時間	秒	s
電流	アンペア	A
熱力学温度	ケルビン	K
物質量	モル	mol
光度	カンデラ	cd
平面角	ラジアン	rad
立体角	ステラジアン	sr

表 2　SI と併用される単位

名称	記号
分，時，日	min，h，d
度，分，秒	°，′，″
リットル	l，L
トン	t
電子ボルト	eV
原子質量単位	u

$1\ \mathrm{eV} = 1.60218 \times 10^{-19}\ \mathrm{J}$

$1\ \mathrm{u} = 1.66054 \times 10^{-27}\ \mathrm{kg}$

表 5　SI 接頭語

倍数	接頭語	記号
10^{18}	エクサ	E
10^{15}	ペタ	P
10^{12}	テラ	T
10^{9}	ギガ	G
10^{6}	メガ	M
10^{3}	キロ	k
10^{2}	ヘクト	h
10^{1}	デカ	da
10^{-1}	デシ	d
10^{-2}	センチ	c
10^{-3}	ミリ	m
10^{-6}	マイクロ	μ
10^{-9}	ナノ	n
10^{-12}	ピコ	p
10^{-15}	フェムト	f
10^{-18}	アト	a

表 3　固有の名称をもつ SI 組立単位

量	名称	記号	他の SI 単位による表現
周波数	ヘルツ	Hz	s^{-1}
力	ニュートン	N	$m \cdot kg/s^2$
圧力，応力	パスカル	Pa	N/m^2
エネルギー，仕事，熱量	ジュール	J	N·m
工率，放射束	ワット	W	J/s
電気量，電荷	クーロン	C	A·s
電位，電圧，起電力	ボルト	V	W/A
静電容量	ファラド	F	C/V
電気抵抗	オーム	Ω	V/A
コンダクタンス	ジーメンス	S	A/V
磁束	ウェーバ	Wb	V·s
磁束密度	テスラ	T	Wb/m^2
インダクタンス	ヘンリー	H	Wb/A
セルシウス温度	セルシウス度	℃	
光束	ルーメン	lm	cd·sr
照度	ルクス	lx	lm/m^2
放射能	ベクレル	Bq	s^{-1}
吸収線量	グレイ	Gy	J/kg
線量当量	シーベルト	Sv	J/kg

表 4　SI と共に暫定的に維持される単位

名称	記号
オングストローム	Å
バーン	b
バール	bar
ガル	Gal
キュリー	Ci
レントゲン	R
ラド	rad
レム	rem

$1\ \text{Å} = 0.1\ \mathrm{nm} = 10^{-10}\ \mathrm{m}$

$1\ \mathrm{b} = 100\ \mathrm{fm}^2 = 10^{-28}\ \mathrm{m}^2$

$1\ \mathrm{bar} = 0.1\ \mathrm{MPa} = 10^5\ \mathrm{Pa}$

$1\ \mathrm{Gal} = 1\ \mathrm{cm/s}^2 = 10^{-2}\ \mathrm{m/s}^2$

$1\ \mathrm{Ci} = 3.7 \times 10^{10}\ \mathrm{Bq}$

$1\ \mathrm{R} = 2.58 \times 10^{-4}\ \mathrm{C/kg}$

$1\ \mathrm{rad} = 1\ \mathrm{cGy} = 10^{-2}\ \mathrm{Gy}$

$1\ \mathrm{rem} = 1\ \mathrm{cSv} = 10^{-2}\ \mathrm{Sv}$

（注）

1. 表 1 ― 5 は「国際単位系」第 5 版，国際度量衡局 1985 年刊行による。ただし，1 eV および 1 u の値は CODATA の 1986 年推奨値によった。
2. 表 4 には海里，ノット，アール，ヘクタールも含まれているが日常の単位なのでここでは省略した。
3. bar は，JIS では流体の圧力を表わす場合に限り表 2 のカテゴリーに分類されている。
4. EC 閣僚理事会指令では bar，barn および「血圧の単位」mmHg を表 2 のカテゴリーに入れている。

換　算　表

力	N(=10^5dyn)	kgf	lbf
	1	0.101972	0.224809
	9.80665	1	2.20462
	4.44822	0.453592	1

粘　度　1 Pa·s(N·s/m^2)=10 P(ポアズ)(g/(cm·s))

動粘度　1 m^2/s=10^4St(ストークス)(cm^2/s)

圧力	MPa(=10 bar)	kgf/cm^2	atm	mmHg(Torr)	lbf/in^2(psi)
	1	10.1972	9.86923	7.50062×10^3	145.038
	0.0980665	1	0.967841	735.559	14.2233
	0.101325	1.03323	1	760	14.6959
	1.33322×10^{-4}	1.35951×10^{-3}	1.31579×10^{-3}	1	1.93368×10^{-2}
	6.89476×10^{-3}	7.03070×10^{-2}	6.80460×10^{-2}	51.7149	1

エネルギー・仕事・熱量	J(=10^7erg)	kgf·m	kW·h	cal(計量法)	Btu	ft·lbf	eV
	1	0.101972	2.77778×10^{-7}	0.238889	9.47813×10^{-4}	0.737562	6.24150×10^{18}
	9.80665	1	2.72407×10^{-6}	2.34270	9.29487×10^{-3}	7.23301	6.12082×10^{19}
	3.6×10^6	3.67098×10^5	1	8.59999×10^5	3412.13	2.65522×10^6	2.24694×10^{25}
	4.18605	0.426858	1.16279×10^{-6}	1	3.96759×10^{-3}	3.08747	2.61272×10^{19}
	1055.06	107.586	2.93072×10^{-4}	252.042	1	778.172	6.58515×10^{21}
	1.35582	0.138255	3.76616×10^{-7}	0.323890	1.28506×10^{-3}	1	8.46233×10^{18}
	1.60218×10^{-19}	1.63377×10^{-20}	4.45050×10^{-26}	3.82743×10^{-20}	1.51857×10^{-22}	1.18171×10^{-19}	1

1 cal = 4.18605 J（計量法）

= 4.184 J　（熱化学）

= 4.1855 J　（15 °C）

= 4.1868 J（国際蒸気表）

仕事率　1 PS（仏馬力）

= 75 kgf·m/s

= 735.499 W

放射能	Bq	Ci
	1	2.70270×10^{-11}
	3.7×10^{10}	1

吸収線量	Gy	rad
	1	100
	0.01	1

照射線量	C/kg	R
	1	3876
	2.58×10^{-4}	1

線量当量	Sv	rem
	1	100
	0.01	1

（86 年 12 月 26 日現在）